

University of Dundee

DOCTOR OF PHILOSOPHY

Pharmacokinetics and Biological Mechanisms of Drug Outcomes in Type 2 Diabetes Mellitus

Mccreight, Laura

Award date:
2019

[Link to publication](#)

General rights

Copyright and moral rights for the publications made accessible in the public portal are retained by the authors and/or other copyright owners and it is a condition of accessing publications that users recognise and abide by the legal requirements associated with these rights.

- Users may download and print one copy of any publication from the public portal for the purpose of private study or research.
- You may not further distribute the material or use it for any profit-making activity or commercial gain
- You may freely distribute the URL identifying the publication in the public portal

Take down policy

If you believe that this document breaches copyright please contact us providing details, and we will remove access to the work immediately and investigate your claim.



University of Dundee

**Pharmacokinetics and Biological Mechanisms of Drug
Outcomes in Type 2 Diabetes Mellitus**

Dr. Laura Joan McCreight

Doctor of Philosophy (PhD)
University of Dundee
June 2019

Contents

Table of Figures	12
Acknowledgements	19
Declaration.....	20
Abstract.....	21
Introduction	23
Type 2 diabetes.....	23
Metformin	24
History of metformin	24
Pharmacokinetics of metformin	27
Administration	27
Absorption.....	27
Distribution and Metabolism.....	32
Excretion.....	33
Pharmacokinetics of metformin intolerance	33
Pharmacodynamics of metformin	34
Main evidence for clinical benefit.....	34
Mechanism of action.....	38
Effect on hepatic gluconeogenesis	38
Other effects: Anti-cancer, anti-aging, anti-inflammatory	44
Relationship with the gastrointestinal tract.....	48
Pharmacogenetics of metformin.....	58
Intolerance.....	58
Response.....	59

Thesis Aims	62
Methods: Bioinformatics resources	63
Diabetes REsearCh on patient sTratification (DIRECT)	63
Genetics of Diabetes Audit and Research in Tayside Scotland (GoDARTS)	63
Genetics of Scottish Health Research Register (GoSHARE)	64
Generation Scotland: Scottish Family Health Study (GS:SFHS)	65
Health Informatics Centre (HIC)	65
Methods: Pharmacokinetics	66
Pharmacokinetics – overview	66
Absorption.....	66
Distribution.....	67
Metabolism	67
Excretion.....	67
Pharmacokinetic modelling.....	68
Pharmacokinetic study of metformin intolerance	69
Pharmacokinetic parameters and their calculation	70
Bioavailability (F)	70
T _{max}	71
C _{max}	71
AUC	71
Volume of distribution	72
T $\frac{1}{2}$ life.....	72
Clearance	73
Methods: Recruit-by-Genotype (RBG) studies.....	74

Genetics and stratified medicine	74
Recruit-by-Genotype Study Design	74
Statistical power in RBG	75
Benefits of Recruit-by-Genotype studies	76
Limitations of Recruit-by-Genotype Studies	77
Ethics of Recruit-by-Genotype Studies.....	78
Methods: Glucose Tracer Modelling	80
Steady state	81
Non-steady state, single compartment model and Steele's equation	83
Two-compartment modelling	86
Circulatory model	87
Methods: Mass Spectrometry	90
POMI Study	90
RAMP Study.....	90
Method	90
Glucose Quantification.....	94
Methods: Beta cell modelling	95
Background	95
β -cell modelling	98
Application.....	101
Methods: Indirect Calorimetry	102
Theory	102
Energy expenditure	103
Calculation.....	103

Respiratory Quotient	103
Application.....	104
RAMP study	105
Methods: MRI Assessment of Adipose Distribution	106
Adipose volume and distribution.....	106
Liver fat and iron.....	107
Methods: Modelling Insulin Sensitivity	109
Homeostatic model assessment (HOMA)	109
Matsuda Index.....	110
Insulinogenic Index.....	111
Oral Glucose Insulin Sensitivity (OGIS) index	111
Disposition index and oral disposition index.....	112
Pharmacokinetics of metformin intolerance (POMI) study	113
Contributions:	113
Introduction.....	114
Pharmacokinetics of metformin.....	114
Metformin and the gastrointestinal tract.....	115
Hypothesis.....	118
Aims	118
Materials and Methods	119
Recruitment	119
Study design and interventions.....	120
Outcomes	120
Statistical methods.....	121

Results	123
Recruitment	123
Baseline characteristics	124
Effect of acute metformin dosing	125
Metformin pharmacokinetics in intolerant and tolerant individuals	126
Serum lactate and metformin intolerance	128
Plasma Serotonin, histamine and bile acid concentrations	129
Discussion	133
Limitations.....	136
Conclusion	137
Impact of OCT1 genotype and OCT1 inhibiting drugs on an individual's metformin tolerance (ImpOCT) study.....	138
Contributions:	138
Introduction.....	139
Hypothesis and Aims.....	149
Materials and Methods	149
Study design	149
Recruitment	151
Intervention and sampling schedule	155
Randomisation.....	157
Symptom severity score and dose titration	158
Statistical methods.....	161
Results	164
Recruitment flow chart.....	164

Baseline characteristics	167
Visualisation of the data.....	167
Statistical analysis	171
Mixed effects model – gene-drug interaction	175
Discussion	178
Hypothesis Review	178
Study Design	179
Primary analysis: No effect of OCT1 genotype on metformin tolerance ..	179
Secondary analysis – Gender, Age and BMI.	182
Limitations.....	182
Conclusion.....	185
Response of individuals with Ataxia-Telangiectasia to Metformin and Pioglitazone (RAMP) study.....	186
Contributions:	186
Introduction.....	187
GWAS of glycaemic response to metformin	187
ATM gene and encoded protein kinase	188
Ataxia-Telangiectasia	191
Ataxia-telangiectasia and insulin resistance	192
ATM deficiency and response to metformin.....	194
ATM and adipocyte function	194
Pioglitazone	195
Response of individuals with Ataxia-telangiectasia to Metformin and Pioglitazone (RAMP) study.....	197
Hypothesis and Aims.....	198

Materials and Methods:	199
Ethics and funding	199
Study design	199
Recruitment	201
Inclusion and exclusion criteria	202
Intervention and sampling schedule	204
Tracer studies of glucose metabolism	205
Outcomes	206
MRI studies of fat distribution.....	206
Statistical methods.....	208
Results:	210
Recruitment	210
Baseline characteristics	212
Individuals with A-T are insulin resistant.....	215
Response to metformin.....	220
Response to pioglitazone.....	229
Metformin versus pioglitazone	235
Adipocytes in A-T.....	237
Discussion	242
Metabolic phenotype in A-T	243
A-T is not associated with improved insulin sensitivity in response to metformin.....	244
Response to metformin in controls	245
Pioglitazone improves insulin sensitivity in A-T.....	247

Pioglitazone in the management of diabetes in A-T.....	248
Adipocyte dysfunction in A-T	249
Limitations.....	250
Conclusion.....	252
Conclusions	254
What have we learned?.....	254
Pharmacokinetics of Metformin Intolerance.....	254
Impact of OCT1 genotype and OCT1 inhibiting drugs on an individual's metformin tolerance	255
Response of individuals with Ataxia-Telangiectasia to Metformin and Pioglitazone	257
Conclusion.....	259
Appendix 1: POMI sample analysis methods.....	260
Determination of metformin concentrations in plasma and urine samples. .	260
Determination of histamine, serotonin and bile acid concentrations.....	260
Determination of plasma lactate concentrations	263
Appendix 2 : Questionnaire to Assess Character and Severity of Metformin Intolerance.....	264
Appendix 3: OCT1 inhibiting drugs	267
Appendix 4: ImpOCT Analysis	269
McNemar Test R code and Output:.....	269
OCT1 wild type:	269
OCT1 Null:.....	269
Cochran-Mantel-Haenszel test.....	270
Cumulative linked mixed models	271

Generalised Linear Mixed Models	276
Generalised linear models.....	280
Discussion	284
Sub- analyses – the Impact of Age	284
Appendix 5 Tracer Timeline	286
Appendix 6: RAMP analysis.....	291
Individuals with A-T are insulin resistant	291
HOMA.....	291
Response to metformin	297
Response to pioglitazone	302
Metformin mixed effects models.....	305
BMI	305
Fasting active GLP1	306
Mean active GLP1	306
Fasting total GLP1	307
Mean total GLP1.....	307
Mean glucagon	308
Fasting EGP	308
Mean EGP	309
Fasting Clearance.....	309
Mean Clearance	310
Appendix 7: Summary table RAMP results	311
Appendix 8: Assays	319
Lactate	319

Glucose.....	319
NEFA	319
Glucagon	319
Total GLP-1	319
Active GLP-1.....	320
Leptin	320
Adiponectin	320
Insulin	320
C-peptide	320
Paracetamol.....	321
U+E and LFTs	321
References	322

Table of Figures

Figure 1 Excerpt from the algorithm for blood glucose lowering therapy in adults with type 2 diabetes, as per the NICE guidelines.....	23
Figure 2 Timeline of metformin's development	26
Figure 3 Metformin transport into the enterocyte is transporter dependent, using OCT1, PMAT and SERT	29
Figure 4 Actions of AMPK, Jeon et al	39
Figure 5 Mechanisms by which metformin effects hepatic glucose metabolism are clearly summarised in this diagram from Rena et al	43
Figure 6 Pathways via which metformin may exert anti-cancer effects, reproduced with permission from Morales et al (93)	45
Figure 7 Anti-inflammatory actions of metformin, reproduced with permission from Saisho (104).....	47
Figure 8 Metformin's actions in the gastrointestinal tract	49
Figure 9 Relative abundance of microbiome species with and without metformin treatment, reproduced with permission from Karlsson et al (159).....	57
Figure 10 An example of a concentration time curve, with some of the commonly measured PK parameters identified. Solid line represents measured data, dotted line is extrapolation.	70
Figure 11 Log-transformed drug concentration is plotted against time. The terminal slope of the curve can be used in the calculation of the $t_{1/2}$ life of the drug.....	72
Figure 12 Methyloxime penta-trimethylsilyl (MOX-TMS) glucose.....	91
Figure 13 MOX-TMS glucose fragments between C2 and C3. The major fragment of D-glucose (left) has an m/z of 319, whereas D2-glucose (right) has he m/z 321.	93

Figure 14 Data from a hyperglycaemic clamp, demonstrating insulin concentration at baseline and elevated glucose concentrations, with a simplified β -cell dose-response curve below. Reproduced with permission from Natali et al (5).	96
Figure 15 Time course of insulin during OGTT or MMT, demonstrating the dose-response curve, exaggerated response in the early phase, and prolonged response secondary to potentiation. These three components of insulin response are modelled in the beta cell model by Mari et al described below. Figure reproduced with permission from Mari et al (222).	97
Figure 16 Illustration of the insulin secretion model, and its output. The model consists of three components - early secretion, dose-response, and potentiation. Reproduced with permission from Mari et al (222).	98
Figure 17 Axial slice at the level of the kidneys, showing visceral adipose tissue (VAT) in red, and subcutaneous adipose tissue (SAT) in green.	107
Figure 18 Recruitment flow diagram for the Pharmacokinetics of Metformin Intolerance (POMI) study.	123
Figure 19 Symptoms of metformin intolerance by phenotype, following a single dose of metformin, 500mg.	125
Figure 20 Plasma concentration of metformin over time, following a single dose of 500mg given at time 0 hr. Data points are mean \pm SEM.	127
Figure 21 Mean lactate concentration over time, following a single dose of metformin, 500mg at time 0 hr. Data points are mean \pm SEM.	129
Figure 22 Mean serotonin concentration over time, following a single dose of metformin, 500mg at time 0hr. Data points are mean \pm SEM.	130
Figure 23 Metformin uptake in stably transfected HEK293 cells expressing OCT1 and its variants. Reproduced with permission from Shu et al.	141
Figure 24 Metformin response in HEK293 cells, transfected with OCT1 and its variants. There is an associated reduction in phosphorylation of AMPK and ACC	

with all OCT1 variants, except M408V. Reproduced with permission from Shu et al.	142
Figure 25 Labelling and over-encapsulation used to maintain blinding of the treatment order for the concurrent medication.	150
Figure 26 Infographic of the participant journey through the ImpOCT study... ..	151
Figure 27 Screenshot of the HIC recruitment tracker used in the ImpOCT study	153
Figure 28 Decision aid for metformin dose titration in the ImpOCT study	159
Figure 29 MISSS scores from participants of the POMI study. Data shown as mean with 95% confidence intervals.	161
Figure 30 Flow chart of participant recruitment, from three bio-resources	165
Figure 31 Breakdown of study population according to genotype and treatment order. Genotype A = OCT1 Wild Type; Genotype B = OCT1 Reduced Function; treatment order 1 = omeprazole followed by placebo; treatment order 2 = placebo followed by omeprazole.	166
Figure 32 Actual maximum tolerated dose of metformin whilst taking placebo versus omeprazole for the OCT1 wild type group. Bubble size indicates number of individuals.	168
Figure 33 Direction of tolerance of OCT1 wild type individuals. Data have been "jittered" around the data point to reveal overlapping data.	169
Figure 34 Actual maximum tolerated dose of metformin whilst taking placebo versus omeprazole for the OCT1 RF group. Bubble size indicates number of individuals.	170
Figure 35 Direction of tolerance of OCT1 RF individuals. Data have been "jittered" around the data point to reveal overlapping data.	170
Figure 36 Odds ratios of intolerance from commonly prescribed OCT1 inhibiting drugs, as demonstrated by Dujic et al. Reproduced with permission.	184

Figure 37 OGTT data from A-T (solid line) and healthy controls (dashed line). Reproduced with permission from Connelly et al (330).....	193
Figure 38 Area under the glucose concentration time curve from glucose tolerance testing in wild type (WT) and ATM heterozygote (ATM) mice, with and without metformin (MET). Reproduced with permission, from Gallagher et al, unpublished data.....	194
Figure 39 Flow diagram of the participant journey through the RAMP study ..	200
Figure 40 Images obtained from MRI for adipose distribution and VAT:SAT calculation. Subcutaneous fat is coloured green, and visceral fat is red. Image on left is a male with A-T, while the image on the right is a female control.	207
Figure 41 A composite 3D image obtained from MRI. Participant is a male with A- T.....	207
Figure 42 Sample size calculations for varying ΔEGP_{MET} with SD = 0.1, power 80% and two-sided alpha of 0.05.....	208
Figure 43 Recruitment flow diagram for the RAMP study	211
Figure 44 Paracetamol concentration over time. Data are mean (SEM).....	214
Figure 45 HOMA-IR at baseline (A), with A-T subdivided into classic and variant (B). Data are median (IQR).....	215
Figure 46 Plasma glucose (A) and plasma insulin (B) concentration during baseline MMT. Data are median (IQR).	216
Figure 47 ISR plotted against Matsuda index, showing the typical hyperbolic relationship of the disposition index.	218
Figure 48 Meal mean (AUC / time) glucose (A) and insulin (B) post-metformin. Data are median (IQR).....	221
Figure 49 Fasting glucose clearance (A) and endogenous glucose production (EGP) (B) and meal mean glucose clearance (C) and EGP (D) at all visits for both genotypes. Data are median (IQR).	222

Figure 50 Active GLP1 over the MMT at baseline and post-metformin in the A-T (A) and control (B) group	224
Figure 51 Total GLP1 over the MMT at baseline and post-metformin, in the A-T (A) and control (B) groups. Data are median (IQR).	224
Figure 52 Fasting and meal mean glucagon at baseline and post-metformin for both genotypes. Data are median (IQR).	225
Figure 53 Glucose (A) and insulin (B) over the duration of the MMT post-pioglitazone. Data are median (IQR).....	230
Figure 54 Fasting insulin (A) and glucose (B) and meal mean insulin (C) and glucose (D) at all visits, both genotypes. Data are median (IQR).....	231
Figure 55 Serum adiponectin (A) and leptin (B) concentrations at baseline, post-metformin and post-pioglitazone in A-T and Control groups. Data are median (IQR).	238
Figure 56 Basal and meal mean (AUC / time) plasma NEFA at each visit. Median (IQR).	240
Figure 57 Predicted probability of each maximum tolerated dose, according to group.....	274
Figure 58 Predicted probabilities of each MTD across groups.....	275
Figure 59 Mixed model (glmmPQL) predicted probability of MTD with genotype and treatment.....	278
Figure 60 Predicted MTD on Omeprazole, from Genotype and MTD on placebo	280
Figure 61 Predicted MTD on Omeprazole in 40 year olds, modelled using Im3	282
Figure 62 Predicted MTD on Omeprazole in 50 year olds, modelled using Im3	282

Figure 63 Predicted MTD on Omeprazole in 60 year olds, modelled using Im3	283
Figure 64 Predicted MTD on Omeprazole in 70 year olds, modelled using Im3	283
Figure 65 Comparison of calculated insulin sensitivity (HOMA%S) and beta cell function (HOMA%B) at baseline.	291
Figure 66 Dose-response curve at baseline. Data are mean (SEM).....	292
Figure 67 Potentiation factor over the first 120 minutes of the MMT. The lesser gradient of the A-T slope is in-keeping with impaired glucose tolerance. Data are mean (SEM).....	293
Figure 68 Insulinogenic index (IGI) plotted against the Matsuda insulin sensitivity index results in the rectangular inverse hyperbola associated with the disposition index. As beta cell function reduces the hyperbola moves closer to the origin.	294
Figure 69 Proof of hyperbolic relationship between IGI and Matsuda index. When log values of the indices are plotted, there should be a negative linear relationship, with slope =-1.....	294
Figure 70 ISR plotted against Matsuda index, showing the typical hyperbolic relationship.	295
Figure 71 Log ISR plotted against log Matsuda has a slope of -1.....	296
Figure 72 HOMA-IR after metformin treatment. Data are median (IQR).	297
Figure 73 HOMA%B compared to HOMA%S post-metformin.	298
Figure 74 Dose-response curve of insulin secretion according to glucose concentrations post-metformin. Data are mean (SEM).....	299
Figure 75 Potentiation factor post-metformin up to 120 minutes post-meal. Again, A-T group have a flatter profile, and loss of the initial potentiation post-meal. Data are mean (SEM).....	300

Figure 76 Comparison of the Matsuda index and ISR as an oral disposition index.	301
Figure 77 Oral disposition – log (Matsuda) against log (ISR) with the slope of -1.	301
Figure 78 HOMA-IR after pioglitazone treatment. Data are median (IQR).	302
Figure 79 HOMA%B compared to HOMA%S while taking pioglitazone. The axes scales have been kept constant for each study visit, to demonstrate the left shift of the hyperbola.	302
Figure 80 Dose-response curve following pioglitazone treatment. Data are mean (SEM).	303
Figure 81 Potentiation factor post-pioglitazone. Flatter profile persists despite improved glucose tolerance in the A-T group, lending support to the theory that there is a reduced incretin effect in these individuals. Data are mean (SEM).	304
Figure 82 Comparison of Matsuda index and ISR as an oral disposition index.	304
Figure 83 Oral DI: log (Matsuda) plotted against log (ISR). The green dashed line represents a gradient of -1, inkeeping with the inverse hyperbolic relationship between sensitivy and secretion.	305

Acknowledgements

I would like to thank my supervisor Professor Ewan Pearson, my co-authors, collaborators and colleagues for their support, guidance and enthusiasm throughout. Acknowledgement of individual collaborators is given at the beginning of each chapter.

Thanks to all of the study participants and their families, for their time, effort and determination, without which these studies would not have been possible.

Declaration

I declare that I am the sole author of this thesis.

All references cited have been consulted, unless otherwise stated. The nature and extent of my individual contribution is clearly documented at the beginning of each chapter, where the work detailed has involved collaboration with others.

This thesis has not been previously accepted for a higher degree.

Signed: _____

Date: 1st February 2019

Abstract

This thesis focuses on metformin – a drug commonly used in type 2 diabetes. Despite being a sexagenarian, metformin continues to intrigue researchers. This is due, in part, to: the variability in response to and tolerance of metformin; the uncertainty regarding its mechanism of action; and the potential for re-purposing metformin out-with diabetes. While metformin is the common theme, this thesis details three distinct clinical studies, each intended to further the understanding of the variability in response to and tolerance of metformin.

Firstly, an open label pharmacokinetic study of the potential mechanisms of metformin intolerance, including: altered uptake; increased lactate production; and alterations in serotonin uptake or bile acid pool, demonstrated that despite evidence of severe intolerance in our cohort, there was no significant difference in the pharmacokinetics of metformin, nor in systemic lactate, serotonin or bile acids. These results suggest that intolerance may be attributable to local factors within the lumen or enterocyte.

Secondly, a recruit-by-genotype, double-blind, randomised, placebo-controlled, crossover study to determine the impact of OCT1 genotype and the use of OCT1 inhibiting drugs on metformin intolerance, has identified a significant gene*drug interaction between OCT1, metformin and omeprazole. The study data show that individuals with OCT1 wild type have improved tolerance of metformin whilst taking omeprazole, compared to placebo. However, this benefit is lost in those with reduced OCT1 function.

Finally, to further investigate a GWAS-identified SNP associated with metformin response, an open label, crossover study of individuals with Ataxia-Telangiectasia (A-T) and healthy controls, employed dual-tracer mixed meal tests to assess their response to metformin and pioglitazone. Although unable to validate the GWAS result, the study data show that pioglitazone improves the insulin resistance and adipocyte dysfunction associated with A-T, and suggests

that pioglitazone, rather than metformin, should be considered in the management of diabetes associated with A-T.

Introduction

Type 2 diabetes

Type 2 diabetes is the most common form of diabetes worldwide. It accounts for approximately 90% of all cases of diabetes (1), and this proportion is increasing. There are currently approximately 400 million people with type 2 diabetes worldwide, and a further 352 million people at risk of developing type 2 (1). There is significant cost associated with the treatment of diabetes and its complications, both to the individual and the health economy – a worldwide total of approximately 727 billion USD in 2017 (1).

Type 2 diabetes is characterised by insulin resistance and relative insulin deficiency. Management of type 2 diabetes starts with lifestyle and dietary advice, before the addition of oral anti-hyperglycaemic drugs, injectable therapies and finally, insulin. The algorithm below is an excerpt taken from the NICE guidelines, last updated April 2017 (2).

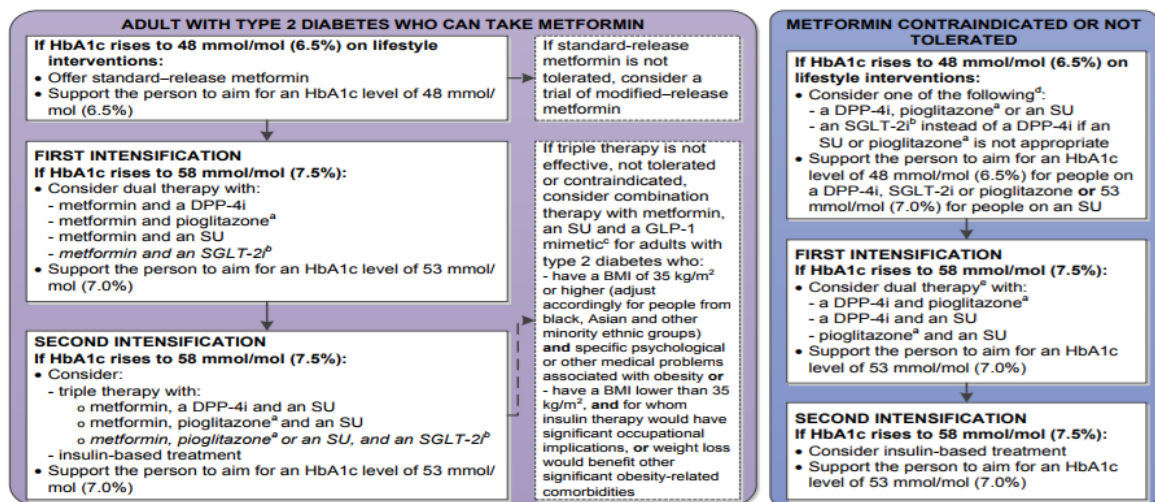


Figure 1 Excerpt from the algorithm for blood glucose lowering therapy in adults with type 2 diabetes, as per the NICE guidelines

Metformin is the first-line oral anti-hyperglycaemic agent, recommended for use in all of those who can tolerate it or in whom it is not contraindicated. When transitioning to insulin therapy, guidelines advise the continued use of metformin

for people without contraindications or intolerance, whereas the need for other blood glucose lowering therapies should be reviewed (2).

Metformin is a fascinating drug: with its roots in natural medicine; a tumultuous rise to fame; and continuing research into its potential applications, it continues to puzzle researchers due to its undefined mechanism of action, and the variability in response and tolerance seen in its clinical application. This thesis will examine some aspects of the variability in tolerance of and response to metformin.

Metformin

Metformin is the most commonly prescribed oral diabetes drug worldwide. It belongs to the biguanide class and is hailed as a benchmark for oral antihyperglycaemic agents. The ADA-EASD and NICE guidelines recommend metformin as first-line drug therapy in type 2 diabetes (3), based on decades of research which have repeatedly proven metformin's efficacy, safety and tolerability. It is proven to: improve glycaemic control; be cardio-protective; help with weight loss; and have no associated hypoglycaemic effects (3). It is also inexpensive – a very attractive quality in a strained health economy. Due to these qualities, there is increasing interest in the use of metformin for the prevention of progression of pre-diabetes to type 2 diabetes (4-6).

In fact, over the past 60 years of clinical use in type 2 diabetes, interest in metformin has come from many angles: as a treatment for polycystic ovarian syndrome (PCOS), as an anti-cancer agent, as an anti-inflammatory agent, in cardiac re-modelling, and longevity to name a few. However, metformin's rise to stardom was initially hindered by its association with the other biguanide drugs, and their causal relationship with lactic acidosis.

History of metformin

Metformin is manufactured from the *galega officinalis* plant (also known as French lilac, or goat's rue) (7). Identification of the glucose-lowering guanidine compound,

and latterly, the less toxic galegine, spawned multiple studies into these compounds in animals and latterly humans (8). Dr Jean Sterne, studying in France in the 1950s, recognised that dimethylbiguanide or “Glucophage” (literally ‘glucose eater’), was the most tolerable of the biguanides tested, with the best balance of potent activity and low toxicity in humans (9).

Around the same time, other groups in America and Germany were concurrently researching phenformin and buformin, respectively, as their biguanides of choice (10, 11). However, due to increasing reports of biguanide-associated lactic acidosis, the biguanide class fell out of favour, with phenformin and buformin being withdrawn from clinical use (12). Metformin was still available for clinical use, but was tarnished by the reputation of other biguanide drugs. Although metformin continued to be prescribed in Europe, it did not gain worldwide recognition as a safe and effective anti-hyperglycaemic medication until the 1990s, finally gaining FDA approval in 1994 (13), nearly 40 years after European approval. Since UKPDS published their UKPDS34 results in 1998 (14), showing a lower risk of premature death and fewer life-threatening complications, metformin has gone from strength to strength, and has been hailed as the benchmark for oral diabetes medications. The timeline of metformin’s botanical and commercial history is shown in Figure 1 (7, 13, 15).

Despite its long history of clinical use, and being the first-line treatment for type 2 diabetes as recommended by the ADA-EASD guidelines, many questions still exist around metformin’s mechanism of action, and the well documented variability in response and tolerance.

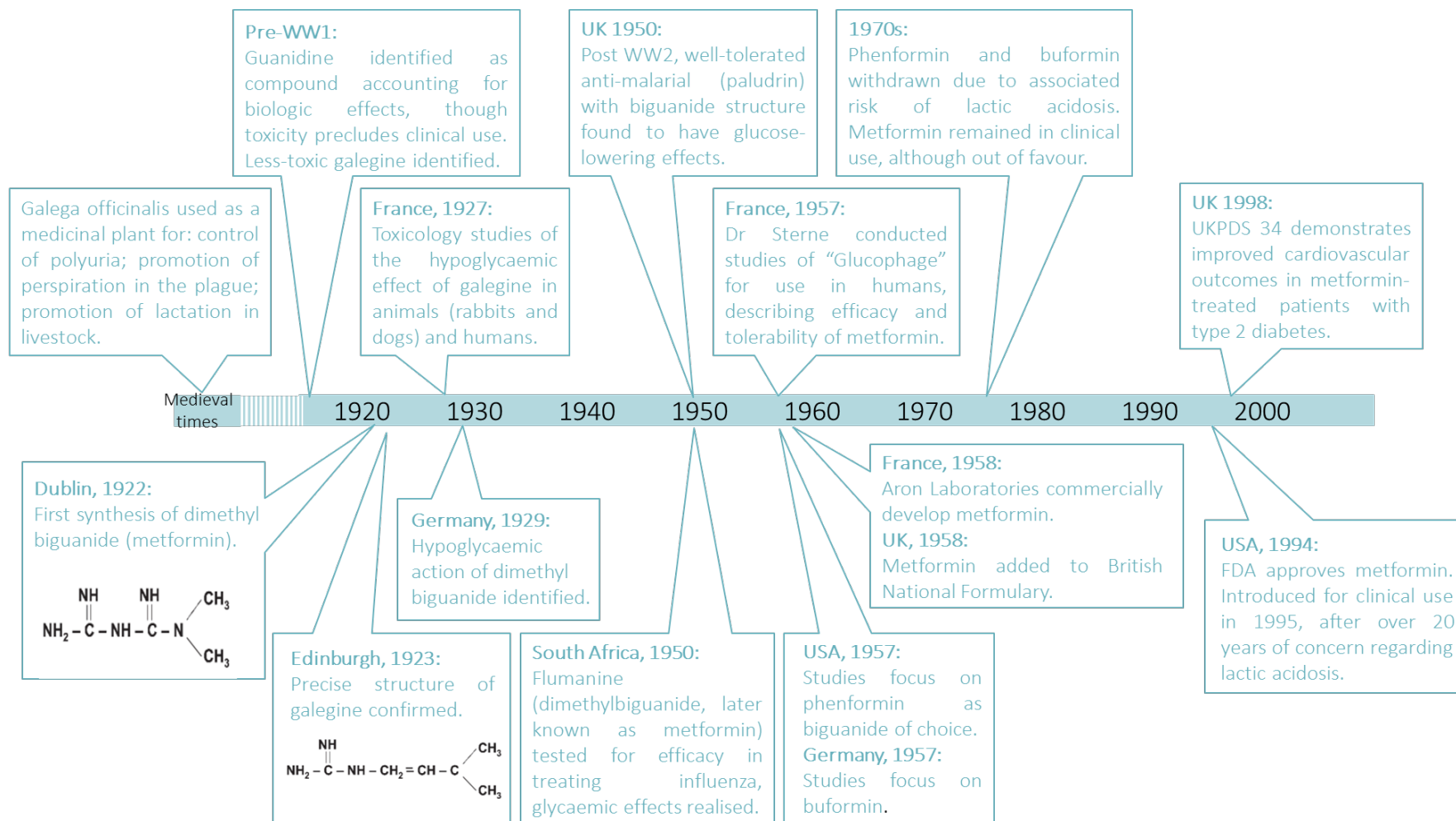


Figure 2 Timeline of metformin's development

Pharmacokinetics of metformin

Administration

Metformin is administered orally as a hydrochloride salt, in either tablet or solution formulation. At physiological pH, metformin exists as a hydrophilic cationic species, with less than 0.01% un-ionised in the blood, resulting in low lipophilicity and inability to diffuse passively through cell membranes (16).

Absorption

Absorption of immediate-release formulations of metformin is largely confined to the small intestine, with negligible absorption in the stomach or large intestine (16-18). In humans, intravenous administration of metformin results in rapid renal elimination, with little or no metformin detectable in the faeces (17), consistent with negligible biliary or GI secretion of metformin. However, in a mouse model of diabetes, intravenous administration of metformin does lead to accumulation of metformin in the enterocytes—most notably in the small intestine (19).

Oral bioavailability of metformin is approximately 70%, with approximately 30% dose recovery of unchanged metformin from faeces (20). Bioavailability is affected by gastric motility and may be reduced by high-fat meals (16). The metformin concentration in the jejunum peaks at 500 µg/g, 30–300 times greater than plasma concentrations (21), highlighting the small intestine as an important site of metformin uptake.

Metformin uptake is saturable and dose-dependent (17, 22), consistent with the theory that it is mostly transporter dependent. Studies in Caco-2 cell monolayers (a cellular model of human intestinal epithelium) have shown that metformin is efficiently taken up across the apical (luminal-facing) surface of enterocytes via bidirectional transporters, but that efflux across the basolateral surface of enterocytes is limited, resulting in the accumulation of metformin in the epithelium (22), possibly accounting for the greatly increased metformin concentration measured in these cells. To account for the presence of metformin in the portal

circulation, some paracellular uptake was postulated, with metformin diffusing passively.

Transporters

Several transporters, for which metformin is a likely substrate, have been identified, including organic cation transporter (OCT) 1–3, plasma membrane monoamine transporter (PMAT), multidrug and toxin extrusion protein (MATE) 1-2K, serotonin transporter (SERT) and high-affinity choline transporter (CHT).

To investigate which transporters are involved in the transport of metformin across the apical surface of enterocytes, Han et al used pharmacological inhibitors and knockdown studies in single transporter-expressing CHO (Chinese hamster ovary) cells and Caco-2 cell monolayers (23). They concluded that the main transporters of metformin are OCT1, PMAT, SERT and CHT, accounting for approximately 25%, 20%, 20% and 15% of apical metformin transport, respectively. However, comparison of the expression of these transporters in Caco-2 cells vs human jejunum using western blot analysis revealed that the expression of all four proteins was significantly higher in Caco-2 cells, with the expression of CHT in human jejunum barely detectable (23). Therefore, direct evidence of the in vivo contribution of CHT to metformin uptake is still lacking, leaving only OCT1, PMAT and SERT as likely metformin transporters in the human intestine.

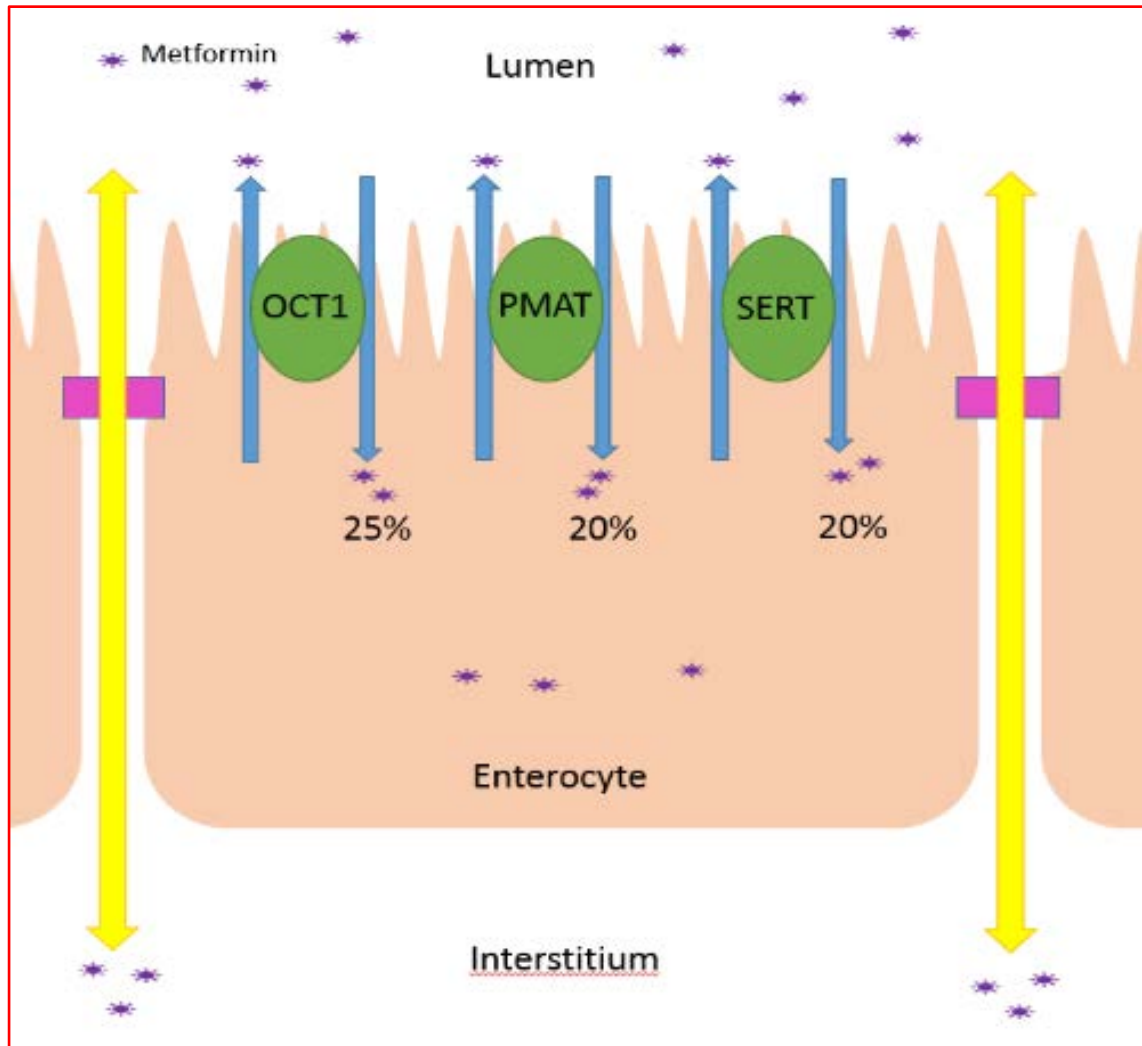


Figure 3 Metformin transport into the enterocyte is transporter dependent, using OCT1, PMAT and SERT

Organic Cation Transporters

Organic Cation Transporters (OCTs) are members of solute carrier family 22 (SLC22), initially described in 1994, and encoded on chromosome 6q26 (24). OCTs are expressed in several tissues, including the intestine, liver, kidney, brain, muscle and heart. OCT1 is predominantly expressed in the liver, but plays an important role in the transfer of cations, including metformin, from the gut lumen to the interstitium (25). Although initial reports localised OCT1 to the basolateral membrane (26), more recent reports place OCT1 on the apical surface of intestinal epithelial cells (23, 27). OCT2 is expressed mainly in the kidney and is

partly responsible for the renal excretion of metformin (25). OCT3 is mainly expressed in the skeletal muscle, but is also expressed in the gastrointestinal tract. Interestingly, OCT3 is associated with metformin uptake and efflux in the salivary glands, which may account for the dysgeusia associated with metformin treatment (28).

There are well-documented, relatively common loss-of function variants in human OCT1, and genetic variation in OCT1 has been investigated by a number of groups in relation to metformin pharmacokinetics, efficacy and GI intolerance (29-33). There is also the potential for drug-drug interactions due to the polyspecific nature of the OCT family.

As OCT1 is probably apically expressed (though this is still debated) it is most likely to influence local concentrations of metformin in the gut (lumen and enterocytes), rather than the transport of metformin into the systemic circulation. Consistent with this interpretation, a recent study concluded that OCT1 variants with loss of function do not alter metformin concentrations in healthy volunteers titrated to 1 g/day of metformin (31). However, Shu et al show that, following acute dosing with metformin the area under the plasma concentration–time curve (AUC) of metformin was significantly greater in those with OCT1 variants compared to those with wild type OCT1 (34). However, steady state pharmacokinetics of metformin appear to be independent of OCT1 genotype (31).

Plasma Membrane Monoamine Transporter

Plasma Membrane Monoamine Transporter (PMAT) was originally identified as a monoamine transporter from the equilibrative nucleoside transporter (ENT) family, found predominantly in the brain and central nervous system (35, 36). It was later recognised that PMAT was polyspecific and found in many tissues throughout the body, including the intestine, where it transports metformin with comparable affinity to the OCTs (37). PMAT is localised to the tips of the mucosal epithelial layer, suggesting that PMAT may have an integral role in metformin uptake (37).

To date, there are no established loss of function variants in PMAT. In one study by Christensen et al, a number of SNPs in PMAT, which were associated with reduced trough steady-state metformin concentrations, were significant to $p < 0.05$ level, however this result did not withstand multiple testing (32).

Serotonin Transporter

Serotonin Transporter (SERT, also known as 5-HTT), encoded by the SLC6A4 gene, is a member of the sodium:neurotransmitter symporter family (38, 39). Serotonin is primarily synthesised in the gastrointestinal tract from tryptophan, and released from enterochromaffin cells (40). It has a number of roles in the intestine, including modulation of gut motility, permeability and electrolyte absorption (41). SERT is highly expressed in the small intestine, more so than in the colon, localised on the apical and basolateral membranes of the enterocytes (42). Here, it plays a critical role in the uptake of serotonin from the gastrointestinal lumen to the systemic circulation.

Metformin has been identified as a substrate of SERT, implicating SERT in the uptake of metformin from gastrointestinal lumen, and its transport across the intestinal wall (23).

There have been a number of genetic variants of SERT identified. Most of these are not SNPs but variable number tandem repeats (VNTRs), which result in insertion / deletion polymorphisms (“long” and “short” alleles) of SERT (38, 39, 41, 43-46). One such polymorphism is the serotonin transporter-linked polymorphic region (5HTTLPR) variant, an insertion / deletion polymorphism in the promoter region, which modulates the expression of SERT. A recent observational cohort study (47) reported an increased odds ratio of metformin intolerance with low-expressing variants of 5HTTLPR. As yet, no in vivo studies have assessed the impact of genetic variation in SERT on the pharmacokinetics of metformin.

Multidrug and Toxin Extrusion Proteins

Multidrug and toxin extrusion proteins MATE1 and MATE2-K, encoded by the SLC47A1 and SLC47A2 genes respectively, belong to the MATE family of transporters, which excrete endogenous and exogenous toxic substrates (48). MATEs are primarily expressed in the liver and kidney, located on the luminal membrane of the renal tubule and bile canaliculi, where they work in conjunction with OCTs to eliminate organic cations, via the exchange of protons (H⁺ or Na⁺) (49). There is also high expression of MATE1 in the skeletal muscle, and to a lesser extent, the adrenals, testes and heart. MATE1 and MATE2-K are co-located on the apical (luminal) membrane of the proximal tubule and excrete metformin into the urine (16, 50).

There are well documented genetic variants of both MATE1 and MATE2K (51). A meta-analysis of the known SNPs in these, and other, metformin transporters did not identify any significant association between genetic variants and glycaemic response to metformin. However, drug-drug interactions and polymorphisms in SLC47A genes may affect renal excretion of metformin, which could lead to the occurrence of toxic side-effects (49). For example, concurrent use of ondansetron – a known substrate for OCTs and MATEs – results in increased exposure and decreased clearance of metformin (52).

Distribution and Metabolism

After absorption into the systemic circulation, metformin travels unbound to plasma proteins (16, 17). It is absorbed into other tissues, including the kidneys, liver, erythrocytes and, to a lesser extent, muscle, by transporters OCT1, OCT2, OCT3, MATE 1 + 2K, PMAT as demonstrated by a high volume of distribution (see Methods: Pharmacokinetics) (16). Metformin does not undergo metabolism, but is excreted unchanged in the urine (53). No metabolites of metformin are found in the urine (16, 17, 53).

Excretion

Metformin is excreted by the kidneys. In humans, negligible metformin has been found in the bowel or biliary tract after IV administration, indicating that metformin is almost exclusively excreted via the kidneys (16, 17). This is likely due to metformin's small molecular size and unbound state, allowing easy filtration through the glomerulus, or using transporters into the tubule.

OCT2 is found on the basolateral (blood) side of the renal tubule, while OCT1 is found on the apical (luminal) membrane of the tubules (25, 54-57). It is possible that metformin is taken up from the blood via OCT2, into the tubular cells, before secretion into urine via OCT1. MATE1 and 2K are found on the brush border (54, 58), and could transport metformin from the tubular cells into the urine. PMAT is also found in the podocytes of the glomerulus (59-61), therefore it is possible that it may transport metformin from the blood into the urine. Due to its low lipophilicity, it is unlikely that metformin would be passively resorbed from the tubules, although the presence of OCT1 on the apical membranes has raised the possibility of transporter dependent resorption (57, 62).

Pharmacokinetics of metformin intolerance

While there has been significant research into the impact of pharmacokinetics on metformin response, no previous research into the pharmacokinetics of metformin intolerance has been completed. Chapter 3 of this thesis, details the first of the three clinical trials undertaken as part of this PhD. In this study, we compare the pharmacokinetics of metformin tolerant and intolerant individuals to assess if drug absorption or systemic exposure impact on an individual's tolerance of metformin.

Pharmacodynamics of metformin

Main evidence for clinical benefit

Metformin has been the subject of research for over 60 years. Thousands of studies into the safety, mechanism of action, efficacy and tolerability of metformin have been performed. Table 1, below, lists some of the major studies and their conclusions regarding metformin, which have changed how the medical community view and use metformin.

Study	Author	Year	Design	Conclusion	Glycaemia	Cardio-vascular	Weight	Hypo-glycaemia	Mortality
UKPDS	UK Prospective Diabetes Study Group	1998	Multi-centre, randomised, controlled, open-label intervention clinical trial, comparing intensive treatment with diet control.	<p>↓ All-cause mortality with metformin.</p> <p>↓ Myocardial infarction with metformin.</p> <p>↓ Any diabetes-related end point.</p>	Improvement in HbA1c.	Protective – reduced MI in metformin treated participants.	Reduction in weight when compared to insulin or SU therapy.	Fewer hypoglycaemic events compared to insulin / SU.	Reduced.
DPP	Diabetes Prevention Program Research Group	2002	Multi-centre, randomised, placebo-controlled, intervention clinical trial comparing metformin therapy to lifestyle intervention for diabetes prevention.	<p>↓ Incidence of diabetes in metformin arm compared to placebo.</p> <p>↓ Incidence of diabetes in lifestyle intervention compared to metformin.</p>	Reduction in FPG and HbA1c.	-	Weight loss compared to placebo.	-	-

Saskatchewan Health	Johnson et al	2002	Retrospective, observational cohort study.	<p>↓ All-cause mortality with metformin monotherapy compared to SU monotherapy.</p> <p>↓ CV mortality with metformin compared to SU therapy.</p>	-	-	-	-	Reduced.
PRESTO	Kao et al	2004	Retrospective analysis of large, randomised, interventional trial, to compare metformin with insulin +/- SU.	↓ Any clinical event, including death and MI.	-	-	-	-	Reduced.
DPPOS	Diabetes Prevention Program Research Group, Knowler et al	2009	Multi-centre, randomised trial as above, extended to 10 years follow-up, with placebo group commenced on lifestyle intervention.	↓ Incidence of diabetes with metformin therapy.	Reduction in FPG and HbA1c.	-	Weight loss with metformin was maintained.		

HOME	Kooy et al	2009	Multi-centre, randomised, placebo-controlled trial of insulin with metformin / placebo.	<p>↓ Macrovascular clinical events.</p> <p>No effect on primary end-points (aggregate of secondary macro and micro vascular).</p>	Reduced HbA1c with metformin therapy.	No change in BP / lipids with metformin. Improved secondary macrovascular outcomes, but no effect on microvascular outcomes.	Metformin prevented weight gain.	As in combination with insulin, metformin had no effect on hypoglycaemia.	-
-------------	------------	------	---	---	---------------------------------------	--	----------------------------------	---	---

Table 1 Evidence base for the use of metformin as first-line drug therapy for type 2 diabetes. (14, 63-67)

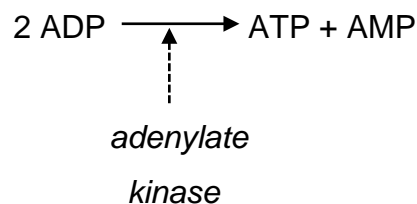
Mechanism of action

Metformin's mechanism of action is still the subject of much debate, despite having been in use for over 60 years (20, 68-76). As metformin was developed from a natural product used in herbal medicine, its safety and efficacy had been established before modern mechanistic studies were available. Therefore, it has sidestepped the now usual methods of drug development which target specific pathways or receptors (20).

Effect on hepatic gluconeogenesis

While it is widely agreed that metformin acts predominantly in the liver to reduce hepatic gluconeogenesis, there is increasing evidence that it has a multimodal mechanism of action, including effects on the gastrointestinal tract (77), which are discussed later in this chapter.

Metformin is taken into the hepatocyte via OCT1, where its positive charge results in it being taken into the mitochondrion (20). Within mitochondria, metformin inhibits complex 1 of the respiratory chain, resulting in a reduced oxidative phosphorylation of adenosine diphosphate (ADP) to adenosine triphosphate (ATP) (20, 72, 78). The subsequent build up of ADP, and increase in ADP:ATP ratio, stimulates conversion of ADP to adenosine monophosphate (AMP) catalyzed by adenylate kinase:



This increases the AMP:ATP ratio. The relative increase in AMP and ADP in relation to ATP has numerous knock-on effects, many of which are dependent upon the activation of adenosine monophosphate-activated protein kinase (AMPK) (20, 79). AMPK can be activated directly, by the change in ATP to ADP /

AMP, or indirectly via activation of LKB1. AMPK-dependent and -independent effects are considered below.

AMPK-dependent effects of metformin

AMPK is made of three subunits – α (a catalytic unit responsible for AMPK enzymatic activity), and the β and γ subunits which are regulatory (79). AMP, ADP and ATP all bind to the γ subunit, with ATP competitively inhibiting the binding of AMP or ADP. Only AMP and ADP can cause conformational change to expose the catalytic α subunit, and therefore activate the enzymatic activity of AMPK (79-81).

AMPK has numerous functions, controlling lipid metabolism, glucose metabolism, and protein synthesis. It also has a role in anti-aging, anti-inflammation and redox regulation. A summary of the many actions of AMPK is shown in the diagram below, reproduced with permission from Jeon et al (79):

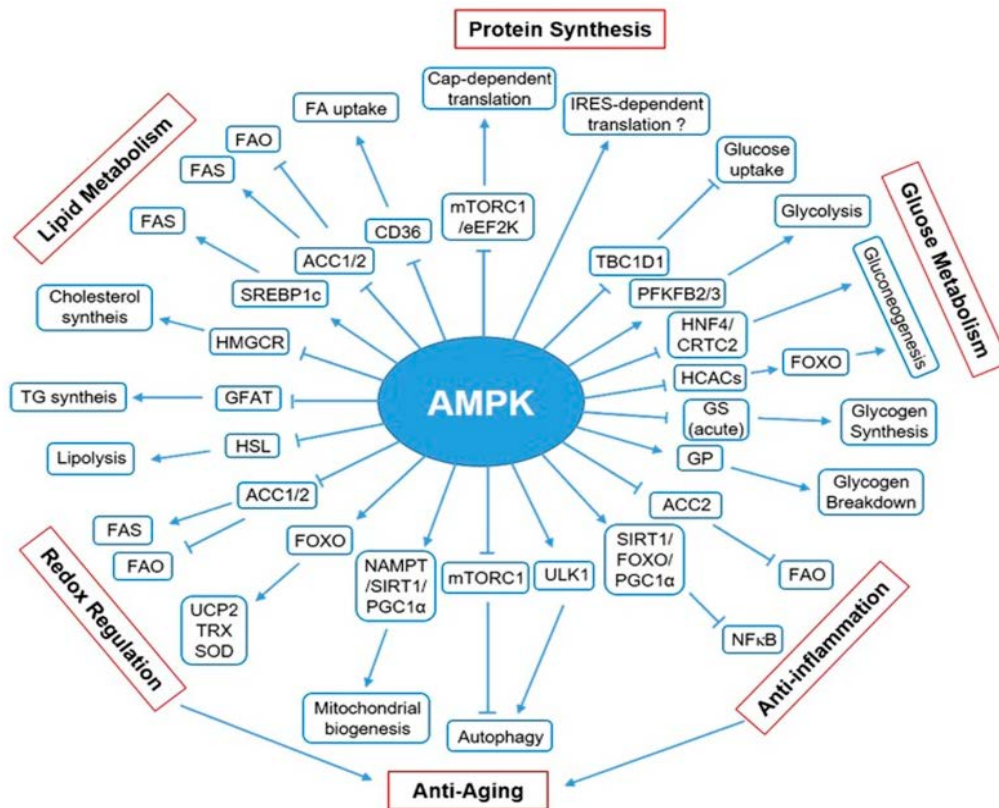


Figure 4 Actions of AMPK, Jeon et al

It has been reported for some time that metformin's mechanism of action partly depends on the activation of AMPK. There are controversies around this, as at physiological concentrations of metformin, there is little or no acute effect on ATP production, and subsequent AMPK activation (20, 78, 82). Cell and animal experiments often employ supraphysiological doses of metformin to obtain the observed effects. Others have shown inhibition of complex 1 of the respiratory chain by phenformin, metformin's predecessor (20, 72). However, lower concentrations of metformin do inhibit complex 1 in cell experiments, if left for a number of hours.

Activation of AMPK would explain some of metformin's clinical benefit (20, 72, 78, 79, 83-88):

1. **AMPK stimulates the translocation and insertion of GLUT4 to the plasma membrane in skeletal muscle and adipocytes**, which facilitates glucose uptake into the cytoplasm, thereby reducing systemic glucose concentrations.
2. **AMPK inhibits hepatic gluconeogenesis**, and therefore lowers blood glucose, by inhibiting transcription factors hepatocyte nuclear factor 4 (HNF4) and CREB-regulated transcription coactivator 2 (CRTC2). Both of these transcription factors promote the expression of gluconeogenic enzymes, phosphoenolpyruvate carboxykinase (PEP CK) and glucose-6-phosphatase (G6Pase). These important gluconeogenic enzymes are involved in the irreversible step of converting oxaloacetate into phosphoenolpyruvate and carbon dioxide, and hydrolysis of glucose-6-phosphate to free glucose, respectively. AMPK also indirectly inhibits the transcription factor FOXO, which is responsible for expression of gluconeogenic enzymes during fasting.

3. **AMPK drives glycolysis** by activating PFKFB enzymes, favouring production of fructose-2,6-bisphosphate which favours glycolysis to gluconeogenesis.
4. **AMPK lowers cAMP**, by activating the cAMP-specific 3',5'-cyclic phosphodiesterase 4B (PDE4B). The subsequent reduction in PKA switches off gluconeogenesis, by reducing gluconeogenic transcription factors, and increasing PFKFB1 as above.
5. **AMPK inhibits synthesis of fatty acids**, triglycerides and cholesterol, by inhibition of: acetyl-coA carboxylase 1 (ACC1) and sterol regulatory element-binding protein 1c (SREBP1c); glycerol-3-phosphate acyltransferase; and HMG-CoA reductase respectively. AMPK also activates lipid catabolism, by increasing fatty acid uptake into cells, where AMPK increases the β -oxidation of fatty acids by carnitine palmitoyltransferase-1 in the mitochondria. AMPK-mediated decreases in hepatic lipid content may serve to sensitize the liver to insulin, with increased suppression of gluconeogenic transcription.

AMPK-independent effects of metformin

The metformin-associated increase in AMP:ATP not only activates AMPK, but has other AMPK-independent effects on hepatic gluconeogenesis (20, 72), including:

1. **Direct inhibition of fructose-1,6-bisphosphatase (FBPase) (89)**, which catalyses the conversion by dephosphorylation of fructose 1,6-bisphosphate to fructose 6-phosphate – a key, rate-limiting step in gluconeogenesis. Therefore, an increase in AMP:ATP leads to acute inhibition of gluconeogenesis.

2. **Indirect inhibition of fructose-1,6-bisphosphatase (FBPase) (90)**, as a result of reduced cAMP production, due to the inhibition of adenylate cyclase. The subsequent reduction in protein kinase A (PKA) favours dephosphorylation and activation of PFKFB1, causing an increase in fructose-2,6-bisphosphate (F2,6BP), which activates phosphofructokinase (PFK) and inhibits fructose-1,6-bisphosphatase (FBPase), resulting in a drive towards glycolysis and, therefore, reduced gluconeogenesis.
3. **Indirect inhibition of fructose-1,6-bisphosphatase by AMP (91)**, a key rate-controlling enzyme in the gluconeogenic pathway. AMP concentration is a function of the energy status of the tissue and is involved in the regulation of hepatic gluconeogenesis. Inhibition of FBPase will result in an increase in fructose-1,6-bisphosphate, which will encourage glycolysis.
4. **Reduced transcription of gluconeogenic genes PEPCK and G6Pase (90)**, which is secondary to the reduction in PKA as described above. PKA phosphorylates the transcription factor cAMP response element binding protein (CREB), which induces transcription of PEPCK and G6Pase.

Out-with its effect on ATP production, metformin has recently been shown to inhibit endogenous glucose production by inhibition of mitochondrial glycerophosphate dehydrogenase (mGPD) – a redox shuttle enzyme, which modulates the cytosolic and mitochondrial redox state (82). Inhibition of mGPD limits the contribution of glycerol and lactate, but not alanine or pyruvate (92), to hepatic gluconeogenesis, by preventing conversion of glycerol to DHAP – necessary for gluconeogenesis, and by the accumulation of cytosolic NADH, which is unfavourable for conversion of lactate to pyruvate by lactate dehydrogenase (LDH) (82).

Some of the mechanisms by which metformin effects hepatic glucose metabolism as clearly summarised in the diagram below, reproduced with permission from Rena et al (20).

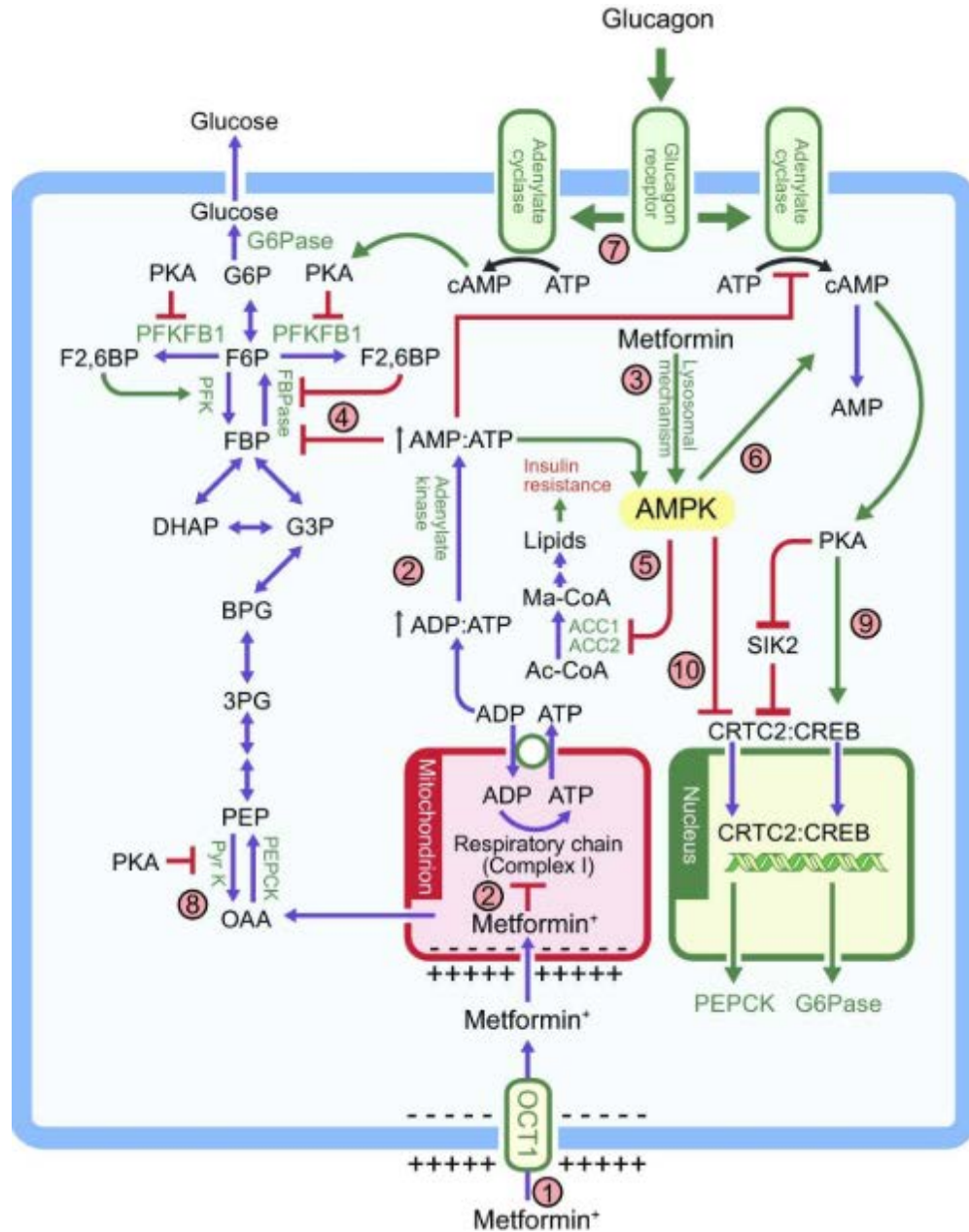


Figure 5 Mechanisms by which metformin effects hepatic glucose metabolism are clearly summarised in this diagram from Rena et al

Other effects: Anti-cancer, anti-aging, anti-inflammatory

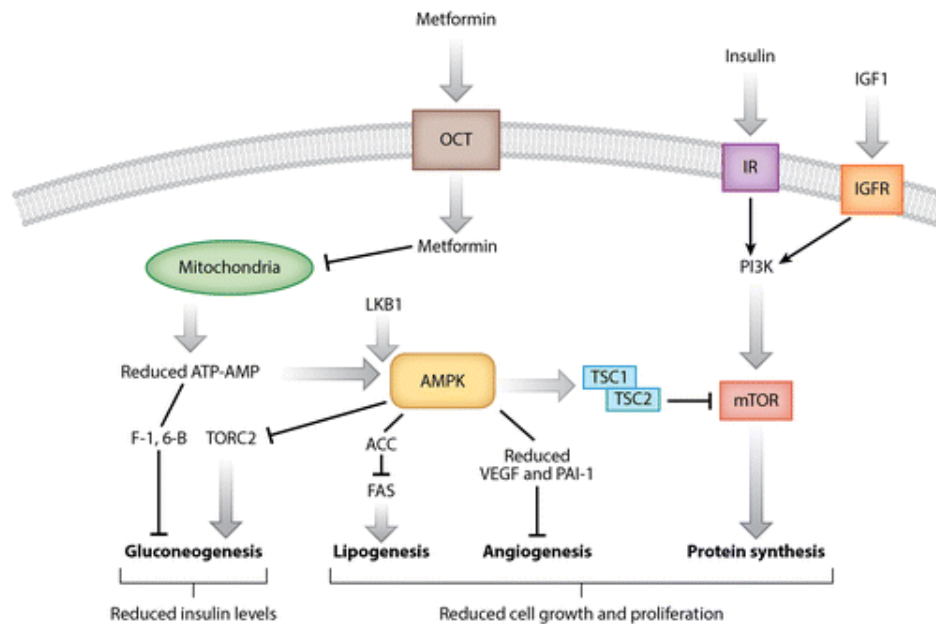
Anti-cancer

Type 2 diabetes is associated with an increased risk of certain cancers, including pancreatic, colorectal, hepatocellular and bladder cancers, as well as a worse prognosis (93, 94). Diabetes and cancer share common predisposing risk factors such as age, obesity and sedentary lifestyle, but the metabolic effects of type 2 diabetes may contribute to the development of cancer (93, 94). Hyperinsulinaemia may act as a growth factor by directly stimulating insulin receptor on cancer cells, or indirectly via insulin-like growth factors (IGFs), to stimulate cell proliferation and protect from apoptotic stimuli (93). Cancer cells have a high energy requirement and an increased glucose uptake, hence the hyperglycaemia of type 2 diabetes is likely a hospitable environment for their progression.

Metformin has been shown to exert an anti-cancer effect in both epidemiological, animal and cell studies (93-97). Observational research studies have reported a reduced cancer risk and improved mortality rates in people with type 2 diabetes on metformin (98, 99), however meta-analyses are less convincing. Metformin could impede cancer proliferation by reducing hyperglycaemia, and subsequently hyperinsulinaemia, or via insulin-independent pathways.

Reduction of hyperglycaemia will reduce the energy availability for cancer proliferation and reduce the Warburg effect – the phenomenon of aerobic glycolysis in cancer cells, producing large amounts of lactate regardless of oxygen availability (93, 98). The subsequent reduction in hyperinsulinaemia will also remove the direct stimulation of insulin- and IGF1-receptors on the cell surface, reducing activation of PI3K, and downstream, mechanistic target of rapamycin (mTOR), which is a major regulator of cell growth and proliferation (93, 94, 98).

Alternatively, the insulin-independent, metformin-associated activation of AMPK may reduce gluconeogenesis, lipogenesis, protein synthesis, and angiogenesis required for cell proliferation and tumour growth (94, 98). AMPK activation also inhibits the synthesis of pro-inflammatory cytokines, which are associated with cancer proliferation and progression (93). There is also potential insulin-independent, AMPK-independent inhibition of cyclin D1 by metformin, resulting in an up-regulation of apoptosis and autophagy (100).




 Morales DR, Morris AD. 2015.
Annu. Rev. Med. 66:17–29

Figure 6 Pathways via which metformin may exert anti-cancer effects, reproduced with permission from Morales et al (93)

Anti-aging

Metformin has been suggested to improve longevity and have anti-aging effects. Aging is thought to occur via two pathways – the accumulation of reactive oxygen species (ROS) with cumulative DNA damage, or by the mTOR pathway (101). The mTOR pathway is involved in protein and lipid biosynthesis, inhibition of autophagy, and regulation of mitochondrial function and glucose metabolism.

However, it also has a key role in geroconversion – the irreversible transition from cell cycle arrest to senescence – and is therefore involved in aging (102).

Metformin is known to reduce ROS (103), and to inhibit the mTOR pathway through AMPK activation. In doing so, metformin reduces cumulative DNA damage, inhibits geroconversion, and increases autophagy, the induction of which may extend the lifespan (101).

Anti-inflammatory

Metformin has been reported to have numerous anti-inflammatory effects, both direct and indirect i.e. due to the improvement in insulin sensitivity and hyperglycaemia (104). Clinical studies have reported lower C-reactive protein (CRP) (105-107), fibrinogen (108), IL-1 β , IL-2, IL-6, IL-8, monocyte chemoattractant protein-1 (MCP-1), interferon (IFN)- γ and TNF- α in metformin treated patients (106, 107).

The mechanisms by which metformin exerts its anti-inflammatory effects can be divided into AMPK-dependent and independent pathways (104). By activating AMPK, metformin can increase nitric oxide synthesis, inhibit poly [ADP ribose] polymerase 1 (PARP-1), inhibit the activation of NF κ B, and suppress the expression of the advanced glycation end-products (AGE) receptor. Independent of AMPK, metformin can reduce AGE formation, and also directly activate the PTEN pathway with subsequent inhibition of NF κ B. All of these mechanisms act to reduce the generation of reactive oxygen species (ROS) and inflammation (104). These potential anti-inflammatory actions of metformin are summarised in the diagram below.

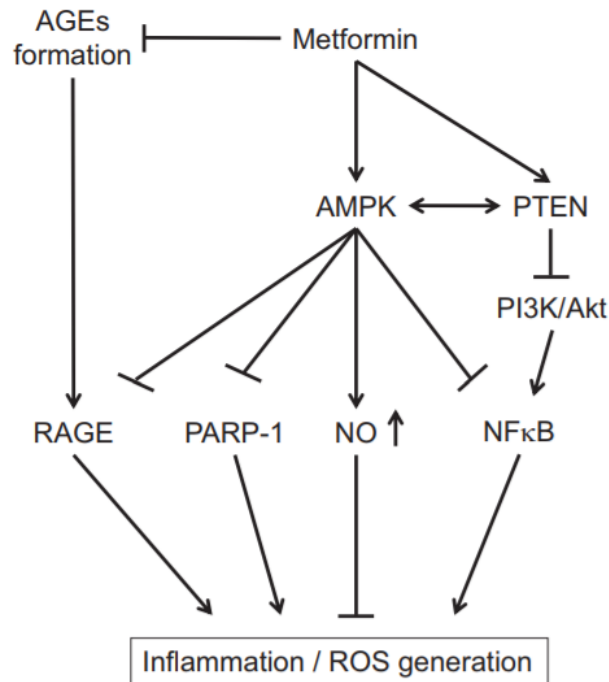


Figure 7 Anti-inflammatory actions of metformin, reproduced with permission from Saisho (104)

Anti-androgen

Polycystic Ovarian Syndrome (PCOS) is characterised by: oligomenorrhea; excess androgen and resultant hirsutism; and polycystic ovaries. Diagnosis requires only two of the three above, by the Rotterdam criteria. PCOS is often associated with insulin resistance, resultant hyperinsulinaemia and hyperandrogenism. Obesity increases the prevalence and severity of insulin resistance, and should be considered during the management of the condition (109).

In the ovary, the LH-stimulated thecal cells synthesise DHEA and androstenedione, most of which is converted to oestrogen by the granulosa cells, although the ovary does secrete androgens (testosterone and androstenedione) directly into the circulation (83). However, in PCOS, the androgen secretion from the ovary is increased, driven by the hyperinsulinaemia of insulin resistance. SHBG levels are negatively correlated with the circulating levels of insulin, which contributes to a high free testosterone level in women with PCOS (83).

By improving insulin sensitivity, metformin favours a reduction in thecal androgen production rate, a concurrent increase in SHBG and a resulting reduction in free androgen index (FAI) (83). Metformin's potentially positive impact on weight can also reduce the severity of insulin resistance and subsequently the severity of PCOS (83, 110-112).

Relationship with the gastrointestinal tract

Although much of the research into metformin's mechanism of action has centred on the hepatocyte and the pathways affecting hepatic gluconeogenesis, there is increasing interest in the relationship between metformin and the gastrointestinal tract. Buse et al demonstrated a dissociation of the glycaemic effect of metformin from systemic exposure, by comparing metformin DR (delayed release) to IR (immediate release) and XR (extended release) preparations (113). Despite a significant reduction in systemic exposure – measured as metformin AUC – with the DR preparation, the glucose-lowering efficacy was comparable to other preparations. This indicates that metformin exerts some of its glucose-lowering effects within the gut. The potential mechanisms via which metformin may act on the gastrointestinal tract are addressed below.

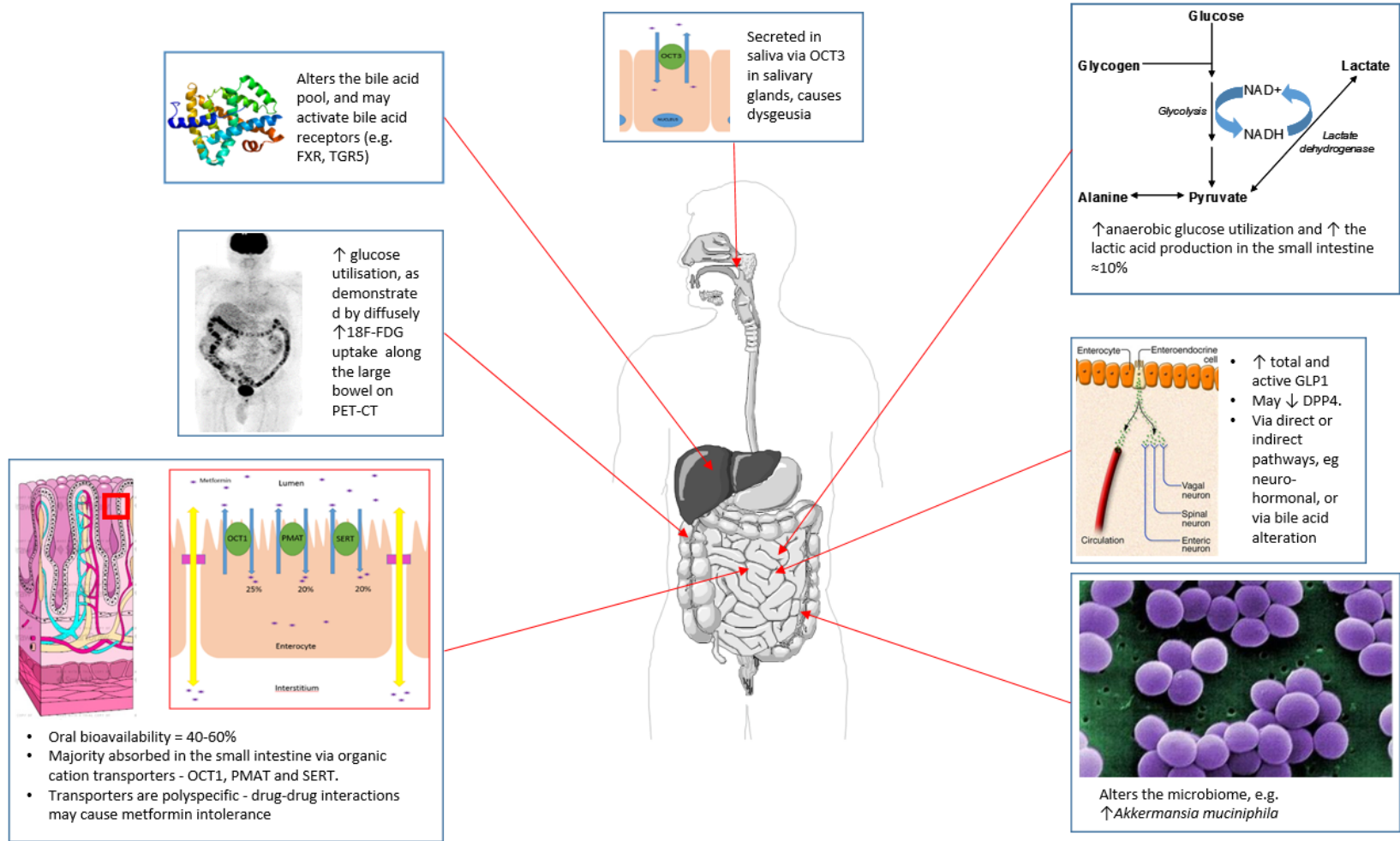


Figure 8 Metformin's actions in the gastrointestinal tract

Glucose uptake and utilisation

It has been known for some time that metformin increases glucose uptake and utilisation in the human intestine, resulting in an increase in lactate production in enterocytes (19, 21). Interestingly, the effect of metformin on gut glucose utilisation is well known to radiologists, as metformin use will interfere with imaging by positron emission tomography–computed tomography (PET-CT). This functional imaging technique uses positron-emitting 18F-fluorodeoxyglucose (18F-FDG) as a non-metabolised glucose analogue. The uptake of 18F-FDG is a marker of glucose uptake and, therefore, glucose utilisation, which is a measure of the metabolic activity of tissue. PET-CT is commonly used for the diagnosis, staging and monitoring of the response to treatment, of certain cancers (114). However, patients taking metformin have diffusely increased 18F-FDG uptake in the colon and small intestine on PET-CT (115-117), as can be seen in Fig. 1. This confirms that metformin causes increased glucose uptake in the gut. It also poses a significant risk of false-negative imaging results when assessing for colonic or genitourinary tumours. For this reason it is recommended that metformin be discontinued for at least 48 h prior to a PET-CT procedure/scan (115, 117).

The mechanism whereby metformin increases gut glucose uptake and utilisation remains unclear (118-122). In one study, metformin reduced the activity of sodium–glucose transporter 1 (SGLT1), but increased the recruitment of GLUT2 to the apical membrane of rat jejunum (120); a study assessing the response to 5'-AMP-activated protein kinase (AMPK) activators (5-aminoimidazole-4-carboxamide ribonucleotide [AICAR] and metformin) suggests GLUT2 localisation to the apical membrane is mediated via rapid AMPK phosphorylation (120, 121). The mechanism of glucose absorption and the role of GLUT2 in this process remains the subject of debate (122). However, in fasting lean rodents GLUT2 is located on the basolateral membrane and is only recruited to the apical membrane of the enterocyte following postprandial glucose stimulation of SGLT1 (123), whereas insulin results in the internalisation of GLUT2. Interestingly, fasting obese humans, unlike fasting lean individuals, have persistent GLUT2 abundance

in the apical membrane, signifying dysregulation of glucose sensing and transfer (123).

Lactate production

As metformin treatment increases the uptake and utilisation of glucose, there is a subsequent increase in plasma lactate. Both the gut and liver are implicated as the main sources of metformin-related lactate production. In the gut, metformin increases the uptake and anaerobic metabolism of glucose, contributing to the rise in lactate associated with metformin treatment (19, 21, 70, 82, 124-129). In rat hepatocytes, metformin inhibits mitochondrial glycerophosphate dehydrogenase, reducing the conversion of cytosolic lactate into pyruvate (82). This build-up of intracellular lactate results in its release into the plasma. Observational data indicate that metformin causes a rise in fasting and average lactate levels (124), with an average increase (adjusted for plasma glucose and BMI) of 0.16 mmol/l compared with diet or sulfonylurea treatment.

Several studies have attempted to localise the lactate production associated with metformin treatment (70, 125-129). Perhaps most convincingly, rat studies in which plasma glucose and lactate levels were measured in the inferior vena cava, hepatic vein, hepatic portal vein and the aorta demonstrated that the plasma lactate concentration peaks in the hepatic portal vein, with a corresponding drop in the plasma glucose concentration. This implicates the intestine as the main site of metformin-associated anaerobic glucose utilisation and lactate production (125). Ring biopsies taken from the jejunum and ileum of these rats after intrajejunal metformin infusion confirmed a 10% increase in intestinal lactate concentration (125). These findings were confirmed in humans by assessment of lactate concentrations in jejunal biopsies incubated with and without metformin (21). Cells incubated in solution with metformin had a higher lactate concentration (an increase of up to 35%) than those incubated in solution lacking metformin. These results provide corroborative evidence that metformin increases gut utilisation of glucose and subsequent lactate production. As a complementary

explanation, lactate production with metformin treatment may be due to its action on the gut microbiome (see later), by inhibition of glycerophosphate dehydrogenase, which is found in some colonic bacteria. This raises the question of local lactate concentrations contributing to the GI symptoms associated with metformin intolerance. As yet there is no clinical evidence to support this theory, but it warrants further investigation.

Gut-related peptides

Metformin and GLP-1

Metformin treatment has been shown to increase the glucagon-like peptide 1 (GLP-1) concentration in both mouse and human studies (130-143). GLP-1 is secreted from L cells, which are distributed throughout the intestine, but are highly concentrated in the ileum. GLP-1 is quickly degraded by dipeptidyl peptidase-4 (DPP4) in the intestinal mucosa and portal system. Metformin could potentially increase the GLP-1 concentration by increasing its secretion from L cells, and/or by reducing its breakdown by DPP4.

Several mouse and human in vivo studies have reported a metformin-associated reduction in DPP4 activity (130-137). However, in vitro studies have yet to find a direct effect of metformin on the activity of DPP4 (138), suggesting that any effect of metformin on DPP4 activity may be indirect, possibly by influencing hepatic production of DPP4 (136, 144). The results of a number of studies have suggested that any impact of metformin on DPP4 activity is likely to be small. First, metformin increases active GLP-1 levels in DPP4-deficient rats (139). Second, DPP4 degrades both GLP-1 and gastric inhibitory polypeptide (GIP), yet metformin treatment in humans only increases the GLP-1 concentration, whereas DPP4 inhibitors increase both GLP-1 and GIP concentrations (140, 141). Third, there is an additive effect on the GLP-1 concentration when metformin is added to the DPP4 inhibitor sitagliptin, suggesting a different mechanism of action of the two drugs (141).

Given that metformin is likely to have only a small impact on DPP4 activity, it is likely that the main impact of metformin on GLP-1 is to increase GLP-1 secretion. A study in mice reported that metformin increases the expression of precursor proteins such as preproglucagon and proglucagon in the large intestine, potentially increasing GLP-1 production and secretion (141). Whilst one study on L cell-like lines did not support a direct effect of metformin on L cells to mediate this effect (140), a more recent study has reported a direct effect of metformin on these cells, where an increase in the expression of the gene encoding proglucagon by metformin is mediated via a β -catenin–TCF7L2-mediated mechanism (143, 145).

Metformin could also act indirectly to stimulate GLP-1 secretion, via alterations in the bile acid pool. Metformin inhibits the farnesoid X receptor (FXR) via an AMPK-mediated mechanism, resulting in reduced sensing and ileal absorption of bile acids (146). The increase in the bile acid pool may then stimulate TGR5 bile acid receptors on the L cell (142, 147), causing an increase in GLP-1 secretion via mitochondrial oxidative phosphorylation and calcium influx (147).

Metformin, serotonin and histamine

Metformin has some structural similarities with selective agonists of the 5-HT₃ receptor and, as outlined earlier, is in part transported by SERT. Serotonin (5-HT) release from the intestine is associated with nausea, vomiting and diarrhoea—symptoms similar to those associated with metformin intolerance. Therefore, one possible mechanism for the GI intolerance associated with metformin may relate to altered transport of serotonin or to a direct serotonergic-like effect of metformin. Metformin stimulates the release of 5-HT from enterochromaffin cells collected by duodenal biopsy from metformin-naive individuals (148); however, this effect is not mediated via the 5-HT₃ receptor, as inhibition of the receptor does not alter the response. As an alternative explanation, it could be that metformin uptake via SERT or OCT1 results in reduced serotonin transport and resultant GI side-effects (149). Finally, a recent paper has identified a potential role for metformin

in inhibiting diamine oxidase, which is highly expressed in enterocytes and responsible for metabolism of histamine (149). Histamine, like serotonin, is also associated with increased gut motility. More studies are required to establish the likely mechanism for GI intolerance to metformin and, importantly, how this key side effect can be avoided or treated.

The gut–brain axis

A recent study in rats suggested that metformin influences the gut–brain axis (150). The effect of intraduodenal metformin infusion on duodenal mucosal AMPK production and subsequent hepatic glucose production was assessed. The rats required an increased rate of glucose infusion to maintain euglycaemia during clamp conditions within the first 60 min of intraduodenal metformin administration and had a lower hepatic glucose production. However, when metformin was infused into the hepatic portal vein, no increase in the glucose infusion rate was required, and there was no decrease in hepatic glucose production over the same timeframe (150). This indicates that duodenal metformin has a direct, pre-absorptive effect on glucose homeostasis in the rat. Based on this finding, it was hypothesised that metformin activates GLP-1 receptors to increase protein kinase A (PKA) activity on intestinal vagal afferents. It was envisaged that the afferents transmit to N-methyl-D-aspartate (NMDA) receptors in the nucleus of the solitary tract (NTS), with onward signalling to the efferent fibres of the hepatic vagal nerve, resulting in a reduction in hepatic glucose production. The pre-absorptive effect of metformin was lost when each part of this neuronal pathway was blocked using GLP-1 receptor antagonists or PKA inhibitors, tetracaine, the NMDA receptor blocker MK-801 and hepatic vagotomy. Although these studies were carried out in rat models, they once again highlight the small intestine as a site of action of metformin, and suggest a novel pathway through which metformin may be acting. This mechanism requires further investigation in humans.

Bile acids

Metformin increases the bile acid pool within the intestine (145, 151-155), predominantly through reduced ileal absorption (145, 152). This disruption of the enterohepatic circulation of bile salts has potential consequences for cholesterol homeostasis, entero-endocrine function and glucose homeostasis. It may also contribute to metformin intolerance through alterations in the microbiome and stool consistency. In addition, as discussed previously, the alteration in bile acid absorption may result in increased GLP-1 secretion, in a similar way to that observed with bile acid sequestrants such as colestevlam (156, 157).

Several studies have demonstrated reduced absorption of bile acids in patients receiving metformin treatment and shown this to be a direct effect of metformin on enterocytes (145, 152-155). Bile acid absorption in the jejunum is a passive, non-saturable and concentration-dependent process, whereas ileal absorption is mainly an active process (153). FXR is a bile acid sensor involved in ileal absorption of bile acids, as well as the synthesis and secretion of bile acids from the liver. AMPK binds directly to FXR and represses the receptor via direct phosphorylation, resulting in reduced FXR transcriptional activity and, subsequently, reduced bile acid absorption (145). As an AMPK activator, metformin could potentially exert effects on the bile acid pool via FXR.

A reduction in bile acid absorption has been suggested as a mechanism through which chronic metformin treatment can lower cholesterol (152, 153). It has also been suggested that an increased luminal bile salt concentration would have an osmotic effect, which could lead to the diarrhoea associated with metformin treatment (152).

The microbiome

The gut microbiome and the metagenome (the microbial genome) are areas receiving increasing research attention, and are now considered as environmental factors that contribute to the development of many diseases,

including obesity, the metabolic syndrome and type 2 diabetes (158-164). Large metagenome-wide studies in China and Europe have described gut microbial dysbiosis in association with obesity and type 2 diabetes. Although these two studies vary in the changes they identified, a common finding was a reduction in butyrate-producing bacteria and an increase in opportunistic pathogens (158, 161). More recently, data from these studies and the Danish MetaHIT project were analysed after controlling for metformin treatment (164). This identified the reduction in butyrate-producing taxa as a signature of gut microbiome shifts in type 2 diabetes.

Metformin alters the microbiome in both mice and humans, causing an overall decrease in the bacterial diversity of the mouse microbiome, which contrasts with the effect of a high-fat diet (165, 166). Studies in humans are more limited, but in a cross-sectional study of the microbiome in women with type 2 diabetes, those treated with metformin had a different microbiome compared with those not treated with the drug (see Fig. 8) (159). In particular, metformin treatment was accompanied by a marked increase in the bacterium *Akkermansia muciniphila* and an associated increase in mucin-producing goblet cells. In mice, treatment with oligofructose (resulting in an increase in *A. muciniphila*) or direct treatment with *A. muciniphila* has been reported to improve metabolic disorders, possibly by increasing endocannabinoids, which reduce inflammation, modify gut peptide secretion and improve the thickness of the gut mucous barrier (162). Administration of *A. muciniphila* to mice receiving a high-fat diet improved glucose tolerance (166), suggesting that the effect of metformin on abundance of this species within the microbiome may indirectly contribute to the glucose-lowering effect of metformin. It has been postulated that an increase in bacteria producing the short chain fatty acids butyrate and propionate may improve glycaemia (164). Butyrate and propionate increase intestinal gluconeogenesis. In rodents, increased intestinal gluconeogenesis results in a reduction in hepatic gluconeogenesis, appetite and weight, leading to improved glucose homeostasis.

An alteration in the microbiome by metformin may also be a potential cause of GI intolerance. Burton et al carried out a small open-label crossover study using a GI microbiome modulator (GIMM) or placebo in conjunction with metformin in metformin-intolerant patients with type 2 diabetes (167). They found that treatment with metformin in combination with GIMM resulted in lower fasting glucose levels, suggesting better tolerance of metformin therapy for longer or at a higher dosage. Therefore, metformin appears to affect the microbiome, and could potentially exert some of its chronic pharmacodynamic effects in this manner, and an individual's metformin tolerance may be influenced by their microbiome.

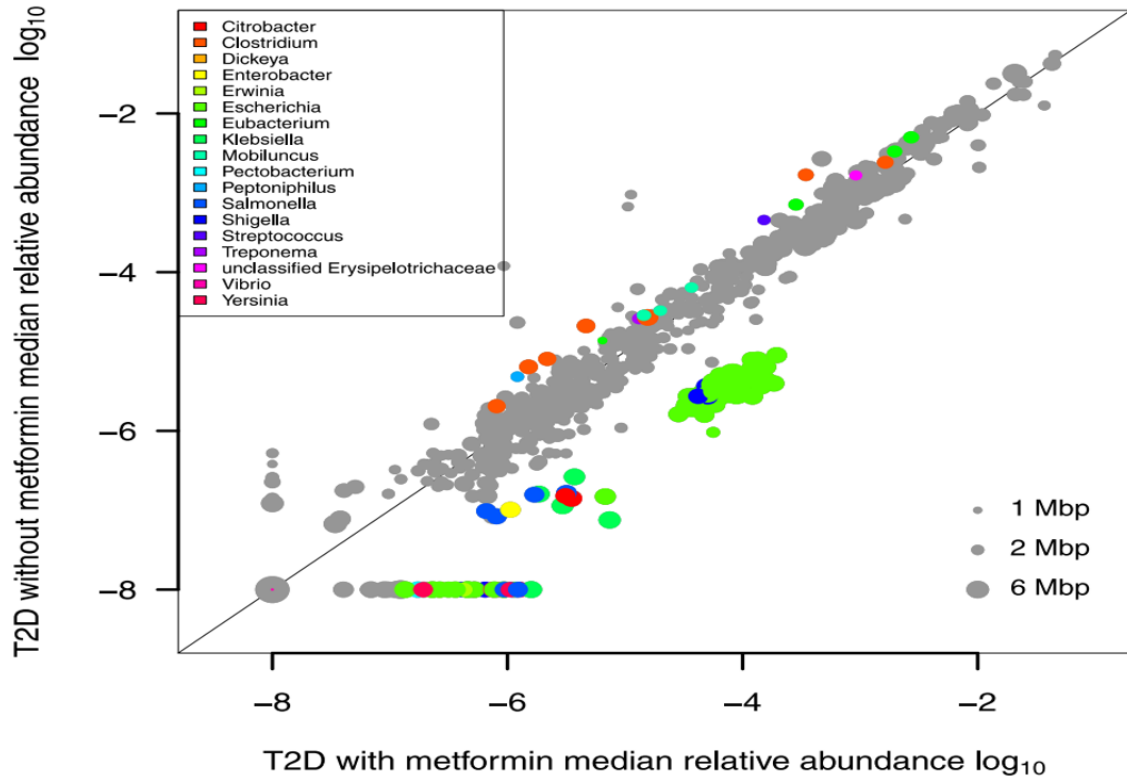


Figure 9 Relative abundance of microbiome species with and without metformin treatment, reproduced with permission from Karlsson et al (159).

Pharmacogenetics of metformin

Intolerance

Genetic studies have been employed to elucidate the cause of metformin intolerance as well as response. As already discussed, metformin intolerance affects up to 20% of those treated, with approximately 5% unable to take metformin. In an observational cohort study, Dujic et al used GoDARTS data to identify an increased odds ratio of metformin intolerance in the presence of two reduced function alleles of OCT1 (29). These individuals were more likely to develop intolerance. Concomitant use of OCT1 inhibiting drugs further increased the odds ratio of intolerance to >4 (29).

	OR (95% CI)	<i>p</i>
One or no reduced-function allele carriers not treated with OCT1 inhibiting drugs	1.00	
One or no reduced-function allele carriers treated with OCT1 inhibiting drugs	1.62 (1.16-2.26)	0.005
Two reduced-function alleles carriers not treated with OCT1 inhibiting drugs	2.27 (1.13-4.58)	0.022
Two reduced-function alleles carriers treated with OCT1 inhibiting drugs	4.13 (2.09-8.16)	<0.001

Table 2 Joint effects of OCT1 genotype and OCT1 interacting drugs on intolerance, reproduced with permission from Dujic et al (29)

Further investigation by Dujic et al into the effect of genetic variation in transporters on metformin tolerance, has also identified an increased risk of metformin intolerance in low-expressing SERT 5-HTTLPR variants (47). This study also highlighted a multiplicative interaction between OCT1 and SERT genotypes, but these results are yet to be replicated (47).

Impact of OCT1 on metformin tolerance

The observational results from Dujic et al (29) implicate OCT1 genotype in metformin intolerance. These results had been replicated, but not confirmed in clinical studies. Chapter 4 details the second clinical study of this project – “Impact of OCT1 Genotype and OCT1 inhibiting drugs on an individual’s tolerance of metformin” - the ImpOCT study. This recruit-by-genotype study employed a double-blind, randomised, placebo-controlled, crossover design to assess if OCT1 genotype or concurrent use of OCT1 inhibiting drugs impact on metformin tolerance.

Response

Understanding the variability in metformin response is difficult in the context of uncertain molecular mechanisms of action. There may be multiple factors affecting variability, including both genetic and environmental. Pharmacogenetic studies can be used to understand how genetics influence drug response. They can be used for patient stratification e.g. responders and non-responders, target identification or to characterise how the drug functions (168). Candidate gene analysis uses current biological knowledge to assess the impact of variation in specific genes, for example those encoding transporters of metformin, on metformin response. These studies can help to stratify patients and potentially predict those unlikely to respond to or develop intolerance of metformin. However, they will not identify new targets or pathways of metformin action. On the other hand, genome-wide association studies (GWAS) employ an open-minded, unbiased approach, to identify genes associated with a phenotype of interest, such as HbA1c reduction in metformin treatment. GWAS can therefore identify novel drug targets or clarify a drug’s mechanism of action.

The Genetics of Diabetes and Audit Research Tayside Study (GoDARTS) research group performed a GWAS study of metformin response, to assess the heritability of drug response. This demonstrated that between 20 and 34% of the variability in metformin response can be accounted for by genetic variation in

common variants (169). The heritability of response may be even greater if we were to consider less common variants. The extent of heritability of drug response confirms that pharmacogenetics studies of metformin response are worthwhile and may elucidate mechanism of action.

The GoDARTS group also identified a SNP rs11212617, associated with metformin treatment success, at a locus containing *ataxia telangiectasia mutated (ATM)* gene (170). This result was replicated in an independent patient group within GoDARTS and in UKPDS. However, the DPP, which studies pre-diabetes, did not replicate this finding, indicating that there may be a three-way interaction between drug, genetics and disease stage. *ATM* encodes the ATM protein kinase, which plays an important role in DNA repair. Homozygous loss of function of the *ATM* gene results in the development of a neurodegenerative condition called Ataxia Telangiectasia (A-T). As part of this multi-system disorder, patients develop insulin resistance, fatty liver and diabetes, therefore the GWAS association between *ATM* and metformin response presents an opportunity for treatment guidance in these individuals, as well as identification of a metformin target / pathway. A-T is discussed in greater detail later in this thesis.

Another genome-wide statistically significant association with metformin response was identified by the MetGen Consortium in a meta-analysis of over 10,000 individuals (171). SNP rs8192675 is an intronic SNP of *SLC2A2* gene, which encodes the glucose transporter, GLUT2 (172), and is associated with an improved response to metformin, i.e. greater on treatment reduction in HbA1c, controlling for baseline HbA1c. GLUT2 is expressed in hepatocytes and is thought to mediate hepatic glucose output, making it an excellent candidate for metformin mechanism of action. Of note, homozygous mutation in the *SLC2A2* gene causes the glycogen storage disease known as Fanconi Bickel syndrome, which is associated with hypoglycaemia between meals, and accumulation of glucose within the liver and kidneys.

Following on from candidate gene studies of metformin response, there has been significant research into the OCT1 transporter and its numerous coding missense SNPs. The four most common reduced-function variants are R61C, G401S, M420del and G465R. An initial report that OCT1 variants altered the glycaemic response to metformin in a clinical trial (32) was not confirmed in a recent re-analysis that took account of the baseline HbA1c level (33). This is consistent with the Genetics of Diabetes Audit and Research Tayside Study (GoDARTS) data, where Zhou et al found no effect of OCT1 genotype on the glycaemic response to metformin in a large population of patients with type 2 diabetes (173).

Other genetic variants associated with metformin response have been identified in the AMPK pathway, e.g. LKB/STK11 an upstream kinase, and in other transporters, e.g. MATE1-2 (51, 174). However, a recent meta-analysis of nine candidate polymorphisms in five transporter genes found no significant effect on the therapeutic response to metformin (51).

[Ataxia-Telangiectasia and metformin](#)

Using the GWAS results reported by Zhou et al (170), we developed the final study of this thesis. We hypothesised that individuals with A-T would demonstrate improved response to metformin compared to the general population. This could be of benefit in this patient population, due to their documented insulin resistance, chronic inflammatory state, and increased risk of cancer. Chapter 5 of this thesis details this open-label, recruit-by-genotype, crossover study, to compare the response to metformin and pioglitazone in individuals with A-T and healthy controls.

Thesis Aims

This thesis reports the results of three clinical trials which studied the variability in response to and tolerance of metformin.

Prior to the results chapters, the methods chapter details the variety of methods used throughout the three studies

Study 1: Pharmacokinetics of Metformin Intolerance (POMI)

Study 2: Impact of OCT1 genotype and OCT1 inhibiting drugs on an individual's tolerance of metformin (ImpOCT)

Study 3: Response of individuals with Ataxia-Telangiectasia to metformin and pioglitazone (RAMP)

Conclusions and ideas for future research are summarised in the final chapter, with additional or supplementary methods and data included in the appendices thereafter.

Methods: Bioinformatics resources

Throughout this thesis, the clinical studies have used bioinformatics resources to identify and recruit participants. The four main resources used are described below:

Diabetes REsearch on patient sTratification (DIRECT)

The DIRECT cohort was used for identification of metformin intolerant individuals for the “Pharmacokinetics of Metformin Intolerance” study.

DIRECT is a pan-European consortium, including academic institutions and pharmaceutical companies, whose aim is to study areas of heterogeneity within diabetes, such as the rate of onset or progression of diabetes, and the variation in response to therapeutic intervention (175).

This resource includes demographic, anthropometric, biochemical and prescribing data on individuals with diabetes. From this, we were able to identify individuals who had been exposed to, but were no longer taking metformin. Further inclusion criteria were applied (as per study protocol) to identify potential participants. These individuals were then individually matched for age, sex and BMI, to metformin tolerant individuals from the GoDARTS cohort.

Genetics of Diabetes Audit and Research in Tayside Scotland (GoDARTS)

Diabetes Audit and Research in Tayside Scotland (DARTS) began as a collaborative project between University of Dundee and Tayside Health Care Trusts. It is an electronic register which began in 1996, to identify patients with diabetes in the Tayside region of Scotland. From 1998, patients were invited to donate blood for DNA extraction and phenotypic data to the Genetics of DARTS (GoDARTS) study. From 2004 onwards, healthy controls have also been recruited. Currently, GoDARTS includes the genetic data from a total of 18306 individuals, of whom 10149 have type 2 diabetes. Recruitment is ongoing (176).

GoDARTS links genetic data to electronic health records via the community health index (CHI) number, including prescribing, diagnostic, and laboratory data. This provides up-to-date, anonymised longitudinal data (176).

Two of the clinical studies reported in this thesis used the GoDARTS cohort:

- 1) The “Pharmacokinetics of Metformin Intolerance (POMI)” study used the linked prescribing and anthropometric data to identify individuals with diabetes who were metformin tolerant, and matched the already recruited intolerant participants according to age, sex and BMI.
- 2) The “Impact of OCT1 genotype and OCT1 inhibiting drugs on an individual’s metformin tolerance (ImpOCT)” study used the linked genetic, prescribing, demographic and anthropometric data regarding the healthy controls of the GoDARTS cohort. Individuals with wild type or reduced function OCT1, who had never taken metformin, and were not using other OCT1 inhibiting medications were identified as potential participants, before considering the demographic data.

Genetics of Scottish Health Research Register (GoSHARE)

The Scottish Health Research Register (SHARE) was established as a register of people interested in participating in health research. Participants consent to SHARE accessing their electronic health record in an anonymised format, which can then be used in bioinformatics research, or to identify potential participants for upcoming clinical studies (177).

Genetics of SHARE (GoSHARE) is an extension of SHARE, where participants give consent to excess blood from routine samples being stored and used for genetic research (178).

The “Impact of OCT1 genotype and OCT1 inhibiting drugs on an individual’s metformin tolerance (ImpOCT)” study used the GoSHARE cohort, in conjunction

with GoDARTS, to identify non-diabetic people with specified OCT1 genotypes, who were metformin-naïve and not using other OCT1 inhibiting drugs.

Generation Scotland: Scottish Family Health Study (GS:SFHS)

The Scottish Family Health Study is a family-based genetic epidemiological study, linking DNA with demographic, clinical and lifestyle data (179). It includes almost 24,000 people with a wide variety of medical conditions.

The “Impact of OCT1 genotype and OCT1 inhibiting drugs on an individual’s metformin tolerance (ImpOCT)” study expanded recruitment to include the GS:SFHS. As with GoDARTS and GoSHARE, people with specified OCT1 genotypes were assessed for suitability according to the inclusion criteria.

Health Informatics Centre (HIC)

The Health Informatics Centre (HIC) at the University of Dundee act as the gatekeepers of sensitive electronic health data. They maintain a clinical data repository for linkage of health data, which can be used in medical research (180).

As the bioinformatics cohorts listed above anonymise data for analysis, HIC provide the link to the individual. Therefore, for identification of potential participants, HIC was utilised to search the database for those individuals meeting the inclusion criteria, before arranging mail-outs to appropriate individuals. The details of those who respond to the invitation letters are then uploaded to the HIC Recruitment Tracker, which provides researchers with a potential participant list for contacting.

Methods: Pharmacokinetics

Pharmacokinetics – overview

Pharmacokinetics (PK) is the study of the journey of a drug through the body, and can be considered in different stages (ADME) (181):

1. Absorption
2. Distribution
3. Metabolism
4. Excretion

Each stage is affected by a number of factors which can be patient- or drug-specific. Patient-specific factors include age, gender, BMI, renal function, liver function and genetics (e.g. genetic variants of transporters). Drug-specific factors include formulation, route of administration, molecular size and structure, pH (and pK_a – the acid dissociation constant), lipid solubility, and binding.

Absorption

Absorption is determined by the physicochemical properties of the drug, formulation and route of administration. In IV administration the drug enters the systemic circulation directly, whereas in other administration routes e.g. oral, buccal, intramuscular or subcutaneous, the drug potentially has to cross a number of membranes before reaching the systemic circulation. In oral administration, as considered in this thesis, the drug can be absorbed by passive diffusion, facilitated passive diffusion, active transport or pinocytosis.

Pharmacokinetic parameters pertaining to absorption include the maximum concentration of the drug achieved in the systemic circulation (C_{max}), the time at which the maximum concentration is achieved (T_{max}), and bioavailability (F). The bioavailability of a drug is the proportion of the drug dose which reaches the systemic circulation, and is determined by a number of factors including: the

chemical properties of the drug; its formulation; timing of administration e.g. with or without food; gastric emptying; gastrointestinal transporters; first-pass metabolism; and intestinal and hepatic health.

Distribution

On entering the systemic circulation, the drug is distributed to other tissues. Distribution is determined by blood flow and perfusion of the tissues, the extent of protein-binding of the drug in plasma, and lipid solubility.

The apparent volume of distribution (V_d) quantifies the extent of the distribution of the drug. It is a theoretical volume into which the dose would be uniformly distributed to achieve the current drug concentration in the plasma (181). Drugs that are protein bound and remain in plasma will have a similar volume of distribution to the circulating volume. Drugs which are lipophilic and distributed to other tissues including fat will have a much higher apparent volume of distribution.

Metabolism

Drug metabolism usually occurs in the liver, where there is a high concentration of metabolising enzymes, and can be divided into two phases – phase one which involves the cleavage of the drug, and phase two which is a conjugation process to aid excretion. Drug metabolites may be inactive, or in some cases may be the active form of the drug e.g. prodrugs which need to be cleaved to become active. The rate of drug metabolism can depend on drug concentration and on liver function. Some drugs are not metabolised – such as metformin – and are excreted unchanged.

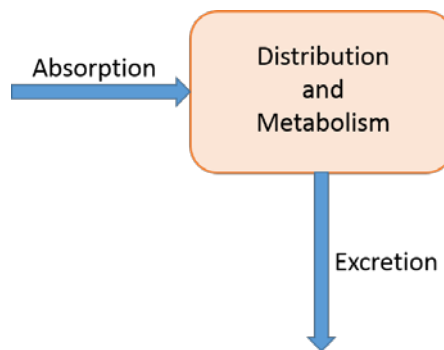
Excretion

While the kidneys are the main organ responsible for excretion of drugs and their metabolites, the biliary system, intestine (faeces), lungs, sweat and saliva can all contribute. Phase two metabolism increases with water solubility, making the drugs / metabolites more readily excreted via the kidneys. Most excretion is by

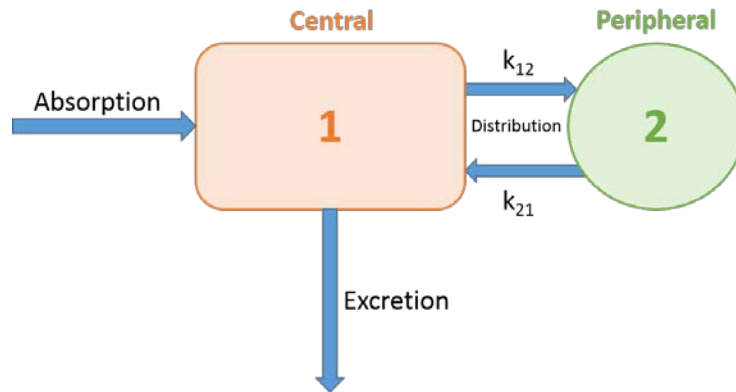
glomerular filtration, with limited diffusion back into circulation. Active tubular secretion is a transporter dependent mode of excretion, and resorption is limited as it too is transporter dependent. PK parameters representing excretion include the half-life and renal clearance.

Pharmacokinetic modelling

When analysing PK data, we can consider the body to have multiple compartments. A single compartment (or non-compartmental) model simplifies the whole body and its organs into a single space.



Two- or multi-compartment models consider a central compartment, which refers to the plasma volume, connected to a peripheral compartment which represents other tissues / organs. The peripheral compartment can be further divided into multiple compartments e.g. fat, muscle, and specific organs. It is assumed that the drug must first enter the central compartment before entry into the peripheral compartment, and in most cases, must return to the central compartment for elimination.



Certain conditions are assumed: the rate of absorption into a specific compartment will have a rate constant (k) and the concentration within a compartment is homogenous. These compartments do not have an anatomical or physical size / shape – they are a theoretical construct for mathematical representation (also discussed in Methods: Glucose Tracer Modelling) (181).

Pharmacokinetic study of metformin intolerance

Chapter 3 of this thesis describes the “Pharmacokinetics of Metformin Intolerance (POMI)” study, which used non-compartmental analysis (NCA) of metformin pharmacokinetics. As our primary requirement was comparison of the degree of drug exposure and its associated PK parameters, NCA is generally the preferred method, as fewer assumptions are required than the model-based methods (182).

Measurement of plasma and urinary metformin concentrations by LC-MS/MS (183) after a single 500mg dose of metformin allowed calculation of a number of pharmacokinetic parameters. The data were arranged in NONMEM format (acronym for non-linear mixed effects modelling, a software package developed for population pharmacokinetics), and analysis performed using the R package NCAPPC (184).

The mathematical equations of the calculations performed for this study are discussed below.

Pharmacokinetic parameters and their calculation

The figure below highlights some of the parameters measured in a PK study.

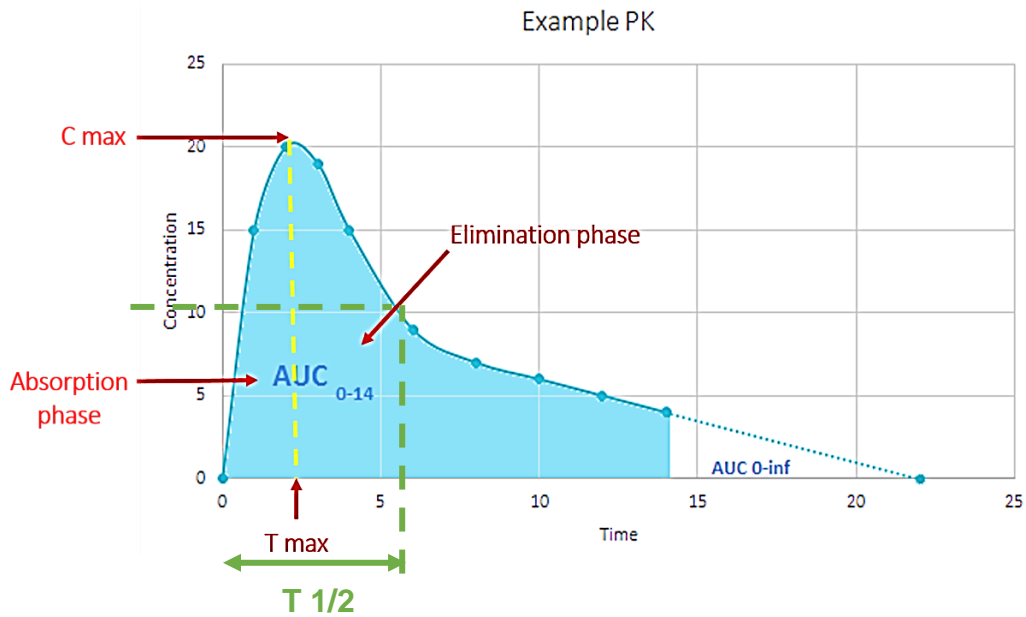


Figure 10 An example of a concentration time curve, with some of the commonly measured PK parameters identified. Solid line represents measured data, dotted line is extrapolation.

Bioavailability (F)

To formally measure the oral bioavailability of metformin, either comparison with IV administration or quantification of the faecal recovery of the drug is necessary. However, estimated fractional drug availability (F, units = fraction or percentage) can be calculated by extrapolating the collected data to calculate area under the concentration time curve from 0 to infinity ($AUC_{0-\infty}$). Assuming that metformin is completely excreted by the kidneys, eventually clearance (CL) would equal renal clearance (CL_R):

$$CL = F \times \text{dose} / AUC_{0-\infty}$$

$$CL_R = Ae_{0-24} / AUC_{0-24}$$

$$F \times \text{dose} / AUC_{0-\infty} = Ae_{0-24} / AUC_{0-24}$$

$$F = (AUC_{0-\infty} / AUC_{0-24}) * (Ae_{0-24} / \text{dose})$$

Where Ae is the cumulative amount of unchanged metformin excreted in the urine.

T_{max}

The time (*T_{max}*, units = time) at which the maximum concentration (*C_{max}*) is achieved can be determined visually from the concentration time curve, as shown in Figure 1.

C_{max}

The maximum concentration of the drug achieved in the systemic circulation (*C_{max}*, units = weight per volume) can be determined from inspection of individual plots of the concentration over time, however this will only give the maximum *measured* concentration.

AUC

The area under the concentration – time curve (*AUC*, units = weight per volume x time) can be calculated from time zero to the last data collection time point, in POMI this was 24 hours. Alternatively the *AUC* from time zero to infinity can be calculated through extrapolation of the collected data, as per Figure 1.

AUC can be calculated using either the trapezoidal method or, as with the metformin *AUC* in the POMI study, the “linear up logarithmic down” method, which gives a more accurate representation of the concentration time curve.

AUC can be reported as total or incremental. Total *AUC* accounts for the full area under the curve, whereas incremental measures only the change from baseline.

Volume of distribution

The volume of distribution (V_d , units = volume) is calculated as the clearance divided by the elimination rate constant (k_e , units = time^{-1}).

$$V_d = CL / k_e$$

$$V_d = (F \times \text{dose} / \text{AUC}_{0-\infty}) / k_e$$

$T_{1/2}$ life

The half-life of a drug is the time required for the quantity to reduce to half to its maximum concentration. This can be calculated using the terminal slope of the log-transformed plasma drug concentration – time curve, using the equation:

$$t_{1/2} = \ln(2) / k_e$$

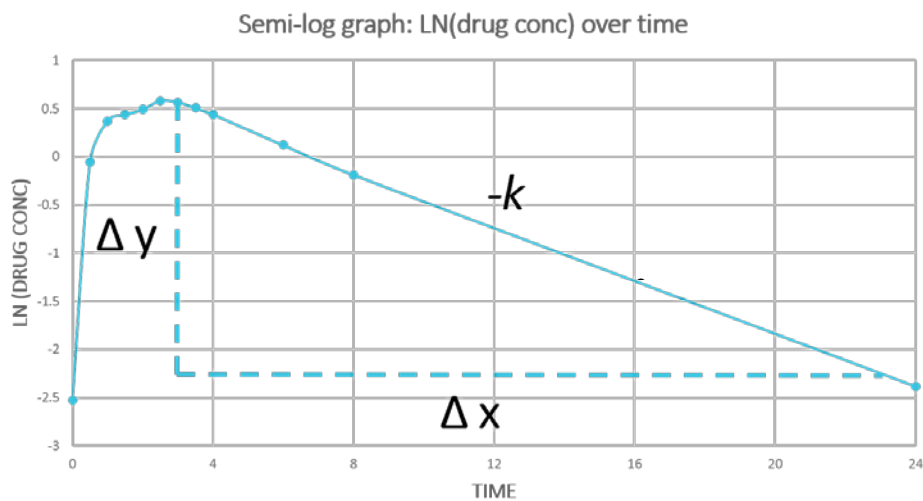


Figure 11 Log-transformed drug concentration is plotted against time. The terminal slope of the curve can be used in the calculation of the $t_{1/2}$ life of the drug.

Clearance

The apparent total clearance from plasma after oral administration (CL/F, units = volume / time) of the drug from plasma is calculated as:

$$CL/F = \text{dose} / AUC_{0-\infty}$$

When using dose in the PK calculations it is important to consider the drug formulation used. For example, in the POMI study, metformin was administered orally as the hydrochloride salt, and therefore, of the 500mg tablet, only 390mg is the pure metformin base. Therefore, in PK calculations, dose should be considered as 390mg.

Methods: Recruit-by-Genotype (RBG) studies

The ImpOCT study, discussed in Chapter 4 of this thesis, uses a recruit by genotype (RBG) study design to assess the impact of genetic variation in a cation transporter on the tolerance of metformin. Here, the rationale, benefits and limitations of the RBG design are discussed.

Genetics and stratified medicine

An individual's genotype is dictated by the gene alleles inherited from their parents, as well as any incident germline mutations they may carry. Their phenotype depends not only on genetic variation, but also on environmental factors and the interaction between genetics and environment.

The fall in genotyping and sequencing costs has driven an increase in genome-wide association studies (GWAS) of large cohorts for genetic characterisation. The subsequent identification of genetic variants and the observation of associated traits has led to a need for prospective studies to prove these observations, to model and validate gene-treatment interactions. By elucidating the mechanism of the gene-treatment interaction and the subsequent impact on treatment efficacy, treatment can be optimised for genetic subgroups – known as stratified medicine.

Traditional randomised control trials (RCTs) are not designed for this purpose and, therefore, often lack power to model such interactions, although in particularly large RCT populations it is still possible.

Recruit-by-Genotype Study Design

Recruit-by-genotype (RbG), also known as recall-by-genotype or genotype-driven recruitment (GDR), is a research strategy that recruits research participants from an existing study population based on genotype, as opposed to traditional study recruitment which focuses on the presence or absence of a medical condition,

clinical outcome or phenotype (185, 186). RbG studies identify potential participants via their genetic data, which has been obtained via a bioinformatics resource, such as a health registry, biobank or previous clinical trial. Participants will have previously consented to their genetic data being stored, with the option for researchers to contact them in future, based on this information. In RbG studies, “cases” and “controls” are identified on the presence or absence of a specific genotype or genetic risk score (GRS). After recruitment, the participants can be exposed to an intervention, much like a traditional RCT, with the two “treatment” arms reflecting genotype.

RbG studies can use single variants or multiple variants for their recruitment approach. Stratification and recruitment using a single genetic variant allows for detailed phenotypic examination and functional characterisation of the genetic variant, if unknown (187). If the direct biological effect of the variant is known, these studies can define the effect size of the variant. However, a single genetic variant can often only explain a small proportion of the variance seen in a trait of interest. On the other hand, a multiple variant approach is adopted to recover some of the lack of power from single variant analyses, which can increase the precision of causal estimate (187). These multiple variant RbG studies often employ a GRS from an independent GWAS, and recall individuals by stratifying their scores. Unlike the single variant recruitment, participants can have differing genotypes.

Statistical power in RBG

Statistical power of RbG studies is based on several factors: minor allele frequency (MAF); anticipated effect size; sampling frame size; and sample size (187, 188). It differs according to whether a single or multiple variant approach is adopted for recruitment. In single variant studies the power is directly related to the MAF and effect size, whereas in multiple variant studies the power depends on the distribution of the genetic risk scores, the number of participants in the tails of the genetic risk score distribution (assuming recruitment will be from the

extremes of the score), and the expected effect size and the gradient of effect seen over the range of the genetic risk score (187).

The statistical power of an RbG study can be further enhanced by group or pair matching participants for age, gender and BMI (187), much as in a traditional RCT.

Online calculators are now available to guide design of RbG studies (187, 188).

Benefits of Recruit-by-Genotype studies

RbG studies have been proven to improve the statistical power, and therefore reduce sample size required to identify a gene x treatment interaction. They are superior for modelling the gene-drug and gene-lifestyle interactions, compared to RCTs of similar size. By recruiting genetically “at risk” participants, there is an improved ability to elicit the treatment response or outcome of interest (188).

	Large effect		Small effect	
MAF	RbG	RCT	RbG	RCT
High Frequency	390	650	700	2500
Moderate Frequency	250	1000	1700	4500

Table 3 Approximate sample size required to achieve 80% power to observe a GRS x metformin interaction for high (MAF = 0.2–0.5) and moderate (MAF = 0.05–0.2) frequency SNPs with both large ($\beta = 0.15–0.30$) and small ($\beta = 0.05–0.15$) effect sizes (188)

The greatest gain in power is seen when comparing the single variant RbG design with conventional recruitment strategies, at the lower end of the MAF range. However, recruitment to an RbG study of sufficient individuals with a single variant of low MAF depends on the availability of a very large bioresource with associated genetic information (187). The size of the genotyped cohort from which participants are recruited is inversely proportional to the MAF under investigation.

By increasing statistical power, and subsequently reducing the study sample size, RbG are more financially and practically viable than equivalently powered RCTs. They are also not subject to reverse causality or confounding factors with respect to the phenotype being studied, resulting in more precise and informative phenotyping (187).

Limitations of Recruit-by-Genotype Studies

RbG studies have clear benefits as listed above, however, this study design is not ubiquitously appropriate. For example, if genotype is strongly correlated with phenotype, a recruit-by-phenotype study is more appropriate and potentially more cost-effective (188).

RbG studies depend on the availability of large scale bioinformatics resources, in the form of health registries, biobanks or large RCTs. These resources should ideally include genotypic data, as well as prescribing and other health data, such as ICD-10 codes, biochemical and anthropometric measures. If the bioinformatics resource being used for recruitment requires genotyping before recruitment can commence, an RbG can become prohibitively expensive (187). However, the cost of extensive genotyping in these sample frames is justified as the resource can then be used by many research teams with multiple objectives (188).

Results obtained through RbG studies are, by design, not representative of the general population, so interpretation should only be applied to the genotype recruited. Extrapolation of results to wider population would be inappropriate. There is also the question of the genetic impact on study participation, retention

and numbers lost to follow-up due to e.g. behaviour or death. If this is unbalanced across genotypes it could impact the trial outcome (187). Similarly, results may be complicated by pleiotropic effects of the genotype in questions, especially in single variant studies. However, this can also be of benefit if the study is designed to investigate and define the range of effects associated with the single variant (187).

In summary, RbG is best considered as a tool in research for replication or confirmation of observational studies, which is only part of the process required to understand the genetic basis of mechanisms of action and causality of outcomes.

Ethics of Recruit-by-Genotype Studies

There are obvious ethical considerations when designing and managing an RbG study (185, 186, 189-196), which have been clearly summarised by Budin-Ljosne et al (185). When participants from an existing study cohort are re-contacted for the purpose of participation in further study, they should be made aware that the reason for their suitability for the RbG study is based upon their genotype (186). This then poses the question of how much information should be made available to these individuals during the recruitment phase of the study, when they are not a participant (192) and have not yet given consent .

Informing the individual that they have a genotype of interest, may lead to unnecessary anxiety or distress – especially if the genotypic result in question is preliminary or has no known clinical sequelae. If the consequence of the genetic variant is known and has clinical significance or is linked to a specific disease, this too can cause stress. Informing the individual of this genotype, without any potential for modification of associated risk, is lacking in benefit to the participant. It may also violate the individual's right not to know (186, 189, 190, 192, 193, 197).

Studies have found that when participants are recruited to RbG studies from a disease register, e.g. cystic fibrosis (CF), individuals with the condition expressed no concerns regarding the genotypic eligibility criteria, whereas “healthy volunteers” recruited by genotype from a biobank, reacted with anxiety due to the perceived or implicated link to the condition under investigation (193).

The ethical implications of RbG studies are inextricably linked to those of a bioinformatics resource. The advent of biobanks – both disease-specific and general – has permitted studies of genotype-phenotype correlation, cohort studies and case-control studies, and are becoming increasingly popular to study gene-health interactions (197). Biobanks must be sufficiently large to support genotype-based study, as discussed above, but also to ensure that the potential participants are not harassed with multiple re-contacts for numerous studies (185).

Indeed, biobanks are a unique research infrastructure, with specific governance requirements (197). The governance structures must balance the rights of the individual with scientific opportunity. They must provide stewardship of data and tissue samples, review the scientific and ethical implications of proposed studies and be adaptive as the scientific community and technology advances. The ethics surrounding a biobank, such as an individual's data protection and anonymity are governed by a committee, which will involve both scientists and community members, to address the ever evolving issues (197).

In summary, RbG studies have clear benefit when investigating gene-treatment interactions, compared to traditional recruitment models. They are, however, not applicable to every research question and the potential benefit must be balanced against the limitations of the study design, cost, and the ethical implications of genetic research.

Methods: Glucose Tracer Modelling

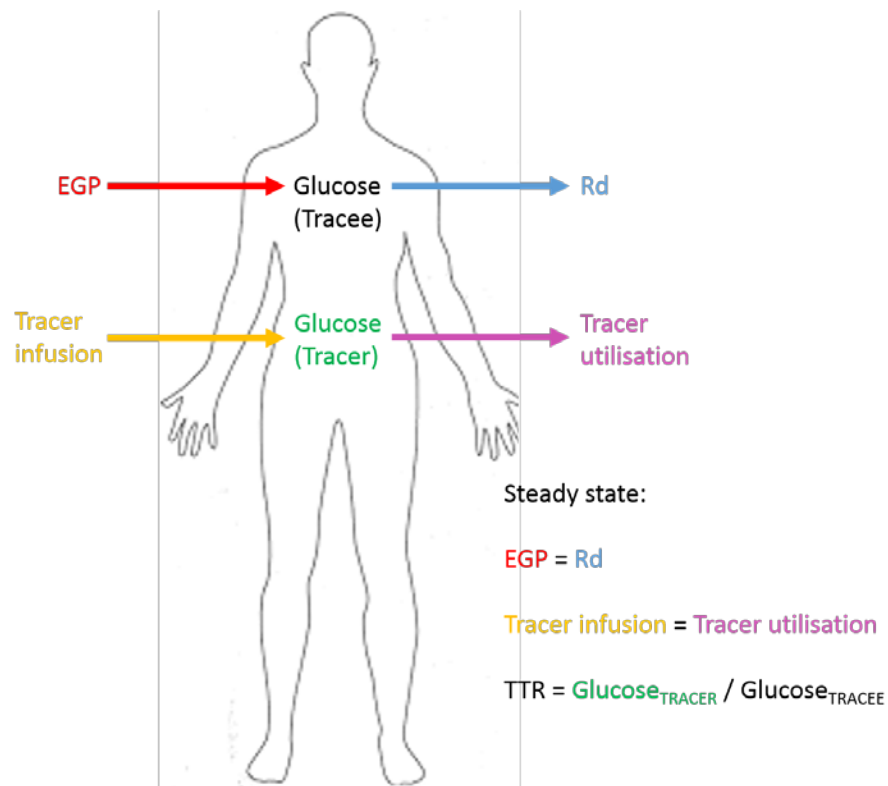
A stable-isotope tracer is a molecule of interest, e.g. glucose, “labelled” with a stable isotope, which results in the labelled molecule having a different molecular mass from the naturally abundant form (198). Metabolic studies can use intravenous infusions and / or ingestion of glucose tracers to determine glucose kinetics, which can be used in the assessment of pharmacological treatments in type 2 diabetes. In such tracer studies, the naturally abundant molecule of interest is known as the **tracee**, and the isotope-labelled molecule is the **tracer**. It is assumed that the tracer will participate in the same metabolic processes and follow the same pathways as the tracee (tracer indistinguishability). The difference in molecular mass of the tracer and tracee can be detected using mass spectrometry (see Methods: Mass Spectrometry), and the tracer to tracee ratio (TTR) can be calculated. The change in the TTR over time allows for calculation of *in vivo* kinetics of the tracee (198).

In Chapter 5 of this thesis, the Response of Individuals with Ataxia Telangiectasia to Metformin and Pioglitazone (RAMP) study used dual tracer mixed meal tests to compare the ability of metformin and pioglitazone to modulate post-prandial glucose homeostasis. During the dual tracer study, following basal samples, a primed (6 mg/kg infused for 1 minute) – continuous (0.06 mg/kg/min for 120 minutes) infusion of [6,6-²H₂] glucose (D2-glucose, Euriso-top, Saint-Aubin, France) was administered over an initial 2 hour period, from -120 to 0 minutes, to reach steady state. Once in steady state, a liquid mixed meal labelled with U13C-glucose (1.7g in 71.9g glucose drink; Cambridge Isotope Laboratories Inc, Andover, MA, USA) was ingested. Over the following 6 hours, a variable infusion of D2-glucose was administered with the rate mimicking the expected endogenous glucose production post-meal, with frequent blood sampling of plasma glucose during the study at time -120, -40, -35, -30, -20, -10, 0, 10, 20, 30, 60, 75, 90, 120, 150, 180, 210, 240, 270, 300, and 360 minutes for measurement of glucose concentration and TTR at every time point. Measurement of the TTR to determine the rate of appearance (Ra) and

disappearance (R_d) of glucose is discussed below. Insulin, c-peptide, glucagon, active and total GLP1, NEFA, adiponectin and leptin were also measured at specific time-points only (see Appendix 5: Tracer Timeline). Indirect calorimetry was performed for periods of 30 minutes at fixed intervals (-60 to -30 minutes in the fasting state as well as 0 to 30, 60 to 90, 120 to 150, 180 to 210 and 240 to 270 minutes after meal ingestion). Urine was collected separately during the basal period and during the meal, total volume was recorded for each period, and samples were stored for glucose measurements.

Steady state

Glucose homeostasis is determined by R_a (endogenous glucose production plus exogenous glucose e.g. ingested / infused glucose), and R_d (utilisation and disposal). In fasted steady state, R_a equals glucose production (EGP), which equals R_d . In steady state during a tracer study, the tracer infusion rate (TIR) equals tracer utilisation (TU).



Therefore, the ratio of tracer infusion rate to glucose production will be constant and equal to the ratio of tracer utilisation to tracee R_d . These are equal to the tracer to tracee ratio (TTR), which is also constant.

$$\text{TTR} = \frac{\text{TIR}}{\text{EGP}} = \frac{\text{TU}}{\text{Rd}}$$

Therefore: $\text{TIR} = \text{TTR} \times \text{Rd}$ or $\text{TTR} \times \text{EGP}$

However, it is important to highlight that the tracer is not massless, and therefore:

$$\text{TTR} = \frac{\text{Tracer}}{(\text{Tracee} + \text{Tracer})}$$

And therefore:

$$\text{TTR} = \frac{\text{TIR}}{(\text{EGP} + \text{TIR})}$$

As total R_a during steady state is equal to EGP plus exogenous glucose i.e. tracer infusion rate:

$$R_{a\text{TOT}} = \frac{\text{TIR} (\text{Tracee} + \text{Tracer})}{\text{Tracer}}$$

$$\text{EGP} = \frac{\text{TIR} (\text{Tracee} + \text{Tracer})}{\text{Tracer}} - \text{TIR}$$

This can also be used to calculate R_d , as $R_a = R_d$ in the fasted steady state.

Non-steady state, single compartment model and Steele's equation

Administration of the liquid mixed meal (Ensure Plus Juice: 71.9g carbohydrate, 0g fat, 20.7g protein, total calories 330 kcal) labelled with U13C-glucose at time 0 stimulates insulin secretion, which suppresses endogenous glucose production and increases glucose utilisation. The degree to which the EGP is suppressed is indicative of hepatic insulin sensitivity, whereas the change in utilisation is indicative of peripheral insulin sensitivity. Unlike the steady state, production \neq utilisation, due to the addition of oral glucose, and because the fluxes of EGP and utilisation change with insulin stimulation. Therefore the steady state equations above no longer apply.

In the non-steady state, the change in the amount (mass) of tracee over time is the difference between its rate of appearance and disappearance, i.e. Ra and Rd.

$$\frac{d(\text{Tracee})_t}{dt} = \text{Ra} - \text{Rd} \quad [1]$$

The change in the amount of tracer over time is equal to the difference in the tracer infusion rate and tracer utilisation:

$$\frac{d(\text{Tracer})_t}{dt} = \text{TIR} - \text{TU}$$

In the single compartment model, $\text{TU} = \text{Rd} \times \text{TTR}_t$, then:

$$\frac{d(\text{Tracer})_t}{dt} = \text{TIR} - \text{Rd} \times \text{TTR}_t$$

$$\text{And} \quad \text{Rd} = \frac{\left(\text{TIR} - \frac{d(\text{Tracer})_t}{dt} \right)}{\text{TTR}_t} \quad [2]$$

In steady state, TTR is equal to tracer / tracee, therefore the change in tracer over time is equal to TTR multiplied by the change in tracee over time. However, in the non-steady state in the single compartment model this becomes:

$$\frac{d(\text{Tracer})_t}{dt} = \frac{d(\text{Tracee} * \text{TTR})}{dt}$$

becomes:
$$\frac{d(\text{Tracer})_t}{dt} = \text{TTR}_t \times \frac{d(\text{Tracee})_t}{dt} + \text{Tracee}_t \times \frac{d(\text{TTR})_t}{dt} \quad [3]$$

Therefore Ra in the non-steady state is:

$$\begin{aligned} \text{Ra} &= \frac{d(\text{Tracee})_t}{dt} + \text{Rd} \\ \text{Ra} &= \frac{d(\text{Tracee})_t}{dt} + \frac{\left(\text{TIR} - \frac{d(\text{Tracer})_t}{dt} \right)}{\text{TTR}_t} \quad [4] \end{aligned}$$

Solving equations (3) and (4) gives:

$$\text{Ra} = \frac{\left(\text{TIR} - \text{Tracee}_t \times \frac{d(\text{TTR})_t}{dt} \right)}{\text{TTR}_t} \quad [5]$$

And:

$$\text{Rd} = \text{Ra} - \frac{d(\text{Tracee})_t}{dt}$$

However, the assumption of instantaneous and complete mixing for the tracer infusion into the entire volume of distribution (V) is incorrect, therefore Steele adapted the above, suggesting that mixing of the tracer between two discrete time points (t1 and t2) occurred in a fraction (p) of the distribution volume only (199, 200).

$$\text{Therefore:} \quad R_a = \frac{\text{TIR} - pV \left(\frac{\sum \text{Tracee}_{t_1+t_2}}{2} \times \frac{\text{TTR}_{t_2-t_1}}{t_{t_2-t_1}} \right)}{\frac{\sum \text{TTR}_{t_1+t_2}}{2}} \quad [6]$$

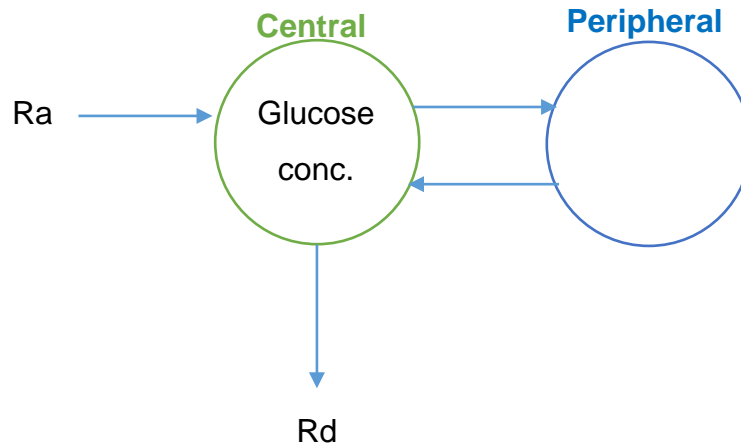
$$R_d = R_a - pV \left(\frac{\text{Tracee}_{t_2-t_1}}{t_{t_2-t_1}} \right) \quad [7]$$

Therefore, from the known infusion rate, glucose concentration and TTR, total R_a and R_d can be calculated. Post-meal, total R_a is the sum of the rate of appearance of oral glucose (R_{aO}) and endogenous glucose production (201, 202). Calculation of the plasma glucose concentration arising from the absorption of ingested glucose is calculated from the ratio of the plasma U13C-glucose concentration to the TTR of U13C-glucose in the ingested glucose (203). EGP is therefore the difference between total and ingested glucose concentrations.

While the Steele equations benefit from their simplicity, they require data smoothing of the infusion rates, and the output (R_a) is sensitive to the smoothing method and data outliers. Importantly, this single compartment model, even when using a fraction of the volume of distribution (pV) does not accurately represent the physiology of glucose kinetics (204).

Two-compartment modelling

The two-compartment model (205, 206) is shown in the diagram below:

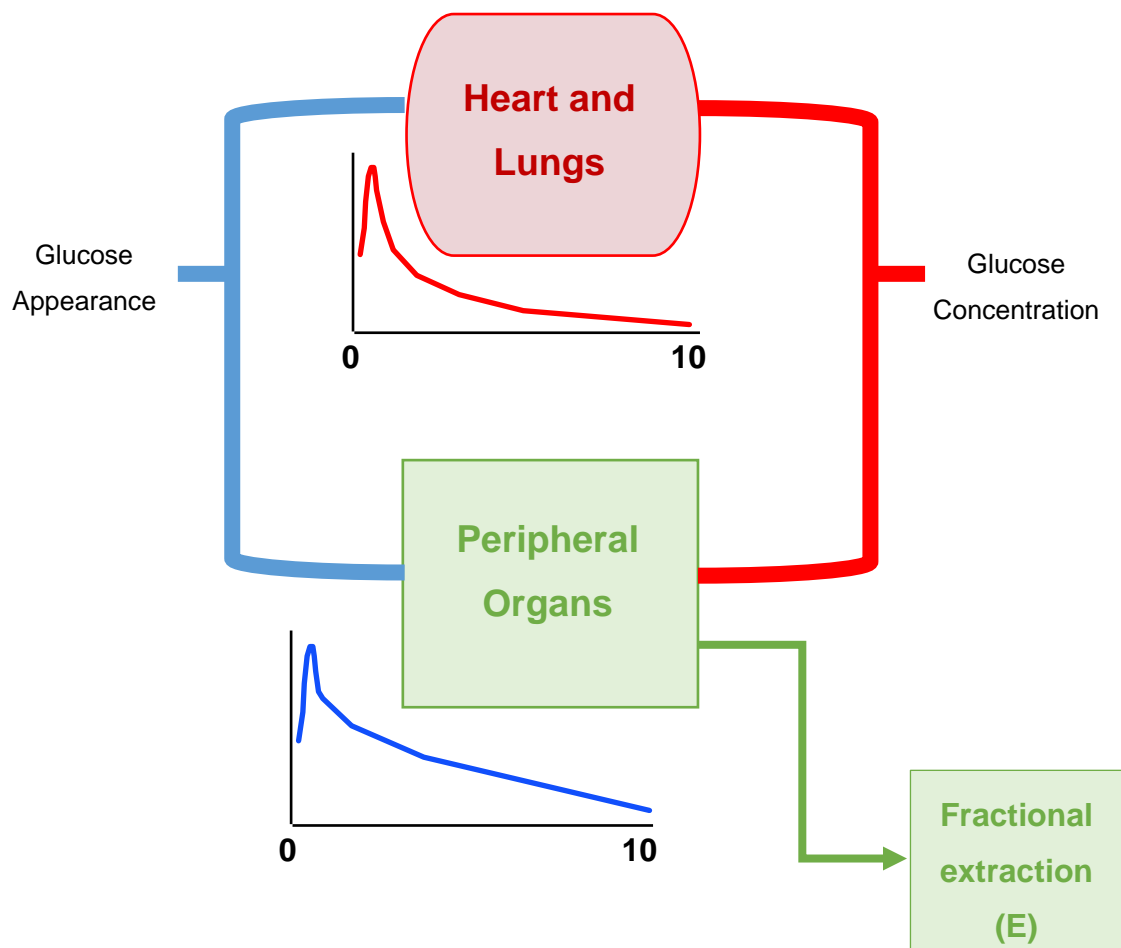


The two-compartment model was designed to reduce the uncertainty of using a proportional approach to the single compartment model. It assumes the central compartment includes the vascular space where we measure the glucose concentration and enrichment, and where the administered infused or ingested glucose appear. It also assumes that the rate at which glucose moves from the central to peripheral compartments remains constant, and that glucose is either: not lost from the peripheral compartment to a third space (207); or is lost, but at the same rate as from the central compartment (205).

While the two-compartment model is a reasonably accurate representation of glucose kinetics, conceptually a circulatory model is a better representation of the system.

Circulatory model

Circulatory models are an extension of organ kinetics used to explain substrate kinetics of the whole body. When compared to the two-compartment, the modified Steele one-compartment model and the standard one-compartment model, the circulatory model of glucose kinetics more accurately predicts non-steady state glucose kinetics after an oral glucose load (208, 209). The model was developed by Mari et al (208-210), and is based upon previous models of organ kinetics, which recognise that when a substrate is administered intravenously, it passes through the heart and lungs, followed by the arterial circulation, through other organs (including brain, liver, kidneys, intestines, muscle – thought of as the peripheral component) before returning to the venous circulation. This can be thought of as two “blocks” – the heart and lungs, and the periphery. At each pass through this circuit, there is fractional extraction at the heart and lungs (negligible) and in the peripheral component.



The line graphs represent the impulse response, or transit time density function, of glucose during a single pass through the circulatory system.

With each pass through the circulatory model, a fraction of the substrate is extracted, therefore clearance is a product of the cardiac output (CO = stroke volume x heart rate) and the fractional extraction.

$$CI = CO \times E$$

In steady state, glucose appearance is equal to clearance and tracee (glucose) concentration is constant. As with the single compartment model, clearance is equal to tracer infusion rate divided by the TTR in steady state. As the tracee concentration is constant, we can see that:

$$CI = CO \times E = \frac{TIR}{\text{Tracer}}$$

CO is calculated using a fixed volume per kg of body weight, corrected for the ratio of glucose in whole blood to glucose in plasma, as glucose is only measured in plasma (209, 211, 212). It is assumed that CO does not vary greatly in the non-steady state, and the fractional extraction of the heart/lung block is unchanged by insulin. However, the fractional extraction in the peripheral block will vary with insulin concentration (211, 212).

The calculations involved in the circulatory model are complex, require the use of the mathematical software Matlab, and are beyond the scope of this thesis. However, they involve the convolution of exponential equations which describe the impulse responses in the two model blocks. The impulse response of the heart block is described by two exponential functions – a rapid upslope starting from zero, followed by a single exponential function describing the downslope returning to zero (212). The impulse response of the periphery is described by four exponential functions – a rapid upslope, and a downslope returning to zero, described by three exponential functions (209). These impulse responses of the

two blocks are converted to linear differential equations and are combined to obtain the differential equations of the circulatory model, which are then solved using Matlab (209, 211, 212). The model equations represent the relationship between the known tracer infusion rate and tracer concentration. Using least squares, the model parameters are adjusted until the model predicted tracer concentration matches the tracer concentration satisfactorily (211). The model can then be used to calculate the exogenous infusion component of the glucose concentration, rate of appearance of oral glucose, glucose clearance and production. The data is output in a form suitable for further statistical analysis.

The circulatory model was used for the analysis of the tracer data obtained in the RAMP study. The modelling was completed using GLUTRAN on Matlab software, analysed by Prof Andrea Mari, at the Institute of Neuroscience, National Research Council, Padova, Italy. I performed the onward statistical analysis of the data using R studio. Results are detailed in Chapter 5, and Appendices 6 and 7.

Methods: Mass Spectrometry

Both the “Pharmacokinetic of Metformin Intolerance (POMI)” and “Response of individuals with Ataxia-telangiectasia to Metformin and Pioglitazone (RAMP)” studies used mass spectrometry for sample analysis.

POMI Study

The POMI study used liquid chromatography tandem mass spectrometry (LC-MS/MS) to measure metformin concentration in the plasma and urine samples. The methods used were described in the “Supplementary Methods” of the journal paper (213), and were written by Dr Niels Jessen, included in Appendix 1. The LC-MS/MS system consisted of an Ultimate 3000 UHPLC system connected to a TSQ Quantiva Triple Quadrupole Mass Spectrometer with heated electrospray ionization (Thermo Scientific, San Jose, CA). The analytical separation was performed using hydrophilic interaction chromatography as previously described by Nielsen et al (183).

RAMP Study

The RAMP study employed dual tracer mixed meal tests to measure glucose kinetics. This involves an infusion of a radiolabelled glucose isotope (D2-glucose), and the ingestion of a second radiolabelled isotope (U13C-glucose), added to a liquid meal. Mass spectrometry was then used to differentiate and measure the ratio of the three glucose isotopes in the blood – D-glucose (unlabelled), D2- and U13C-glucose - according to their molecular weight. The ratio of the fragments can then be used to determine the tracer to tracee ratio (TTR), required for the glucose modelling using the Steel equation or the circulatory model, see Methods: Glucose Tracer Modelling.

Method

Mass spectrometry was performed at the University of Surrey. The process involves three steps:

1. Derivatisation.

Derivatisation is a process which transforms a compound into a product of similar structure, a derivative, with different chemical properties such as reactivity or boiling point. Usually a specific functional group of the compound is targeted by the derivatisation reaction. To prepare glucose samples for gas chromatography, a two-step derivatisation process is used. After deproteinisation of the sample, it is treated with methylhydroxamine hydrochloride to replace the carbonyl group with an oxime group. Next, silylation replaces the hydrogen of the hydroxyl functional groups with trimethylsilyl groups. This results in the formation of methyloxime penta-trimethylsilyl (MOX-TMS) glucose derivative (214, 215).

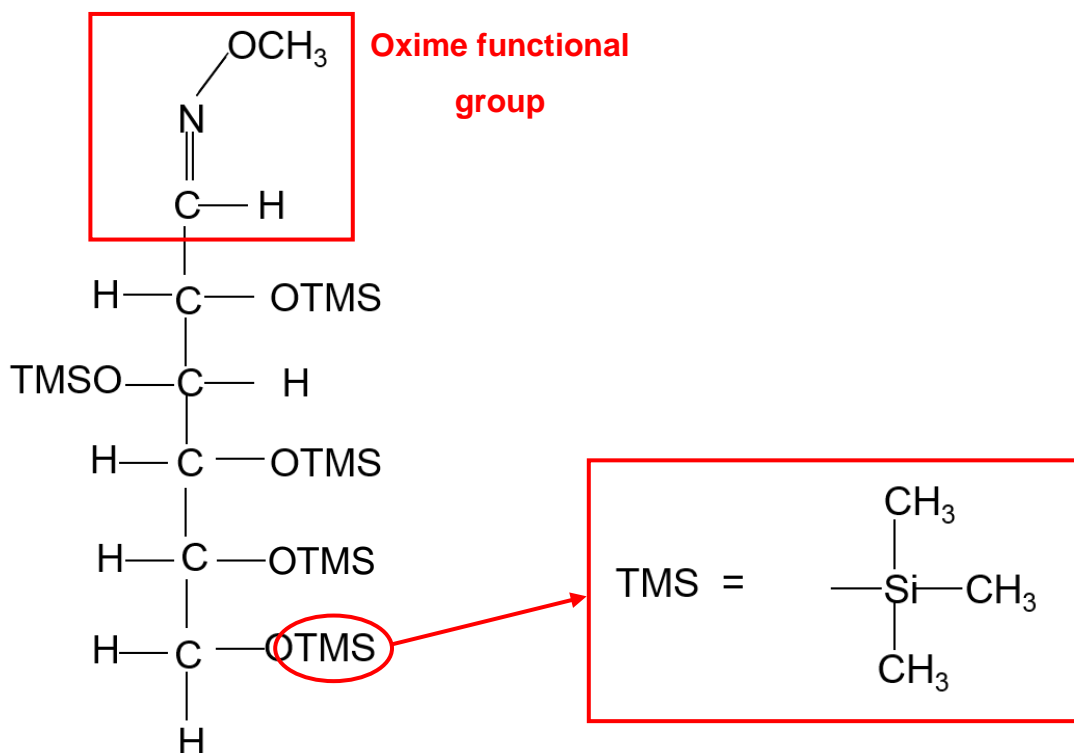


Figure 12 Methyloxime penta-trimethylsilyl (MOX-TMS) glucose

The derivatisation process results in reduced intermolecular H⁺ bonding, and therefore increases volatility, required for gas chromatography. This derivative

also protects the isotope label during fragmentation in the mass spectrometer.

2. Gas chromatography (GC)

The volatile glucose derivative is injected into the GC injection port, and vaporised by heating to 250°C. The gaseous compounds are then separated using the stationary and mobile phases of the capillary column. Carried through the column by the “mobile phase”, an inert gas such as helium, it is the reaction of the gaseous compound with the “stationary phase” – an inert, non-volatile liquid which coats the column – that dictates the retention time and determines when the specific compound will exit the column and enter the ionisation chamber of the mass spectrometer.

The University of Surrey use an Agilent 7890A Gas Chromatographer, with a Restek RX-1 capillary column with cross-bond dimethyl polysiloxane (a silicone) for the stationary phase, and helium as the mobile phase.

3. Mass Spectrometry (MS)

On exiting the GC, the gaseous compound enters the ionisation chamber, where it is ionised and fragmented. In our samples, electron impact ionisation was used (EI), in which the sample is bombarded with high energy (70eV) electron beam, creates positively charged ions, causing the sample to fragment.

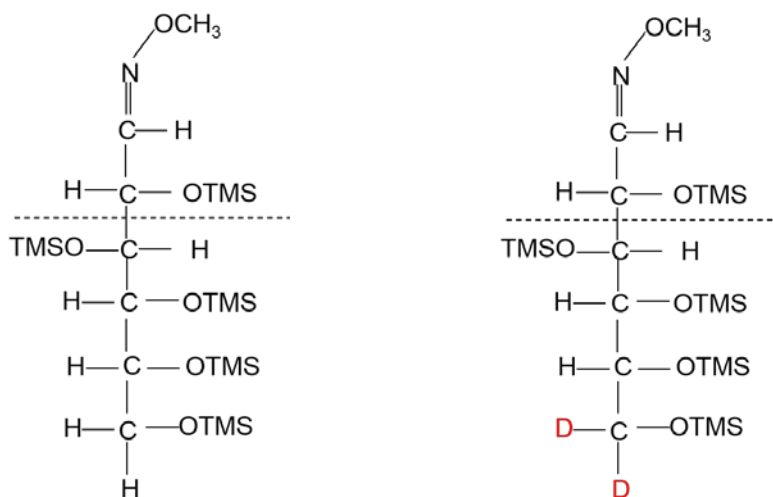


Figure 13 MOX-TMS glucose fragments between C2 and C3. The major fragment of D-glucose (left) has an m/z of 319, whereas D2-glucose (right) has the m/z 321.

The molecular ion m/z (mass to charge ratio) of the MOX-TMS glucose is 569, but when fragmented, the major fragment ion m/z is 319. However, when the derivative of D2-glucose and U13C-glucose fragment, the major fragment ion m/z is 321 and 323 respectively.

Once ionised and fragmented, the sample is separated according to the m/z ratio using a mass filter - a quadrupole. At any time, only ions of a selected m/z can pass through the filter to strike the surface of the detector, producing mass spectra spikes at that particular m/z ratio. The MS measures the abundance of the ion of specific m/z ratio, which can then be used to calculate the tracer to tracee ratio (TTR), for use in glucose kinetics calculations. The TTR is dimensionless, and does not quantify the glucose, but provides information regarding relative abundance.

$$\frac{\text{area of peak at } m/z \text{ 321}}{\text{area of peak at } m/z \text{ 319}} = \frac{\text{tracer}}{\text{tracee}}$$

The University of Surrey adopt a Selected Ion Monitoring (SIM) mode to search for specific ions of known m/z ratio, i.e. 319, 321, 323, using an Agilent 5975 Mass Spectrometry detector.

Glucose Quantification

Alongside mass spectrometry of the glucose sample, the glucose needs to be quantified. The total glucose in the samples was measured at the University of Surrey by enzymatic determination, using the ABX Pentra Glucose PAP CP reagent, and the ABX Diagnostics COBAS Mira Plus.

Methods: Beta cell modelling

Chapter 5 of this thesis reports the results of the “Response of individuals with Ataxia-telangiectasia to Metformin and Pioglitazone (RAMP)” study. This study examines the effects of two commonly used diabetes drugs in a specific patient group, compared to healthy controls. To compare treatment effects, a dual tracer mixed meal test was employed to obtain physiological estimation of glucose kinetics post-meal. Measurement of glucose and C-peptide also allowed for concurrent beta cell modelling to offer a detailed impression of beta cell function and its impact on glucose homeostasis.

Background

Insulin secretion from β -cells is regulated by numerous factors. Stimuli include glucose, amino acids, free fatty acids, and incretin hormones, as well as certain pharmacological agents. Counter-regulatory hormones including glucagon, cortisol and adrenaline, balance the effects of insulin, to prevent hypoglycaemia, through stimulation of glucose production, reduction of glucose uptake, or inhibition of insulin release. The primary mechanism of insulin release is glucose stimulation, with glucose taken up by the β -cell in an insulin-independent manner. Glucose uptake by the β -cell was initially thought to be GLUT2 dependent from murine data (216), but latterly it has been demonstrated that GLUT 1 and, to a lesser extent, GLUT3 expression predominates in human islets and β -cells (217). Within the β -cell, glucose is phosphorylated by glucokinase (218) to glucose-6-phosphate (G6P), which is metabolised via the Krebs cycle to produce ATP. ATP binds to and closes the ATP-dependent potassium channel, resulting in increased intracellular potassium and depolarisation of the cell membrane (219). This opens voltage-gated calcium channels, resulting in an influx of calcium to the cytoplasm, causing migration of vesicles to the membrane, and exocytosis of insulin, which is co-released with C-peptide (219). The process of glucose stimulated insulin release is amplified by other fuels e.g. amino acids, free fatty acids, as well as other hormones e.g. GLP1, and parasympathetic stimulation (220).

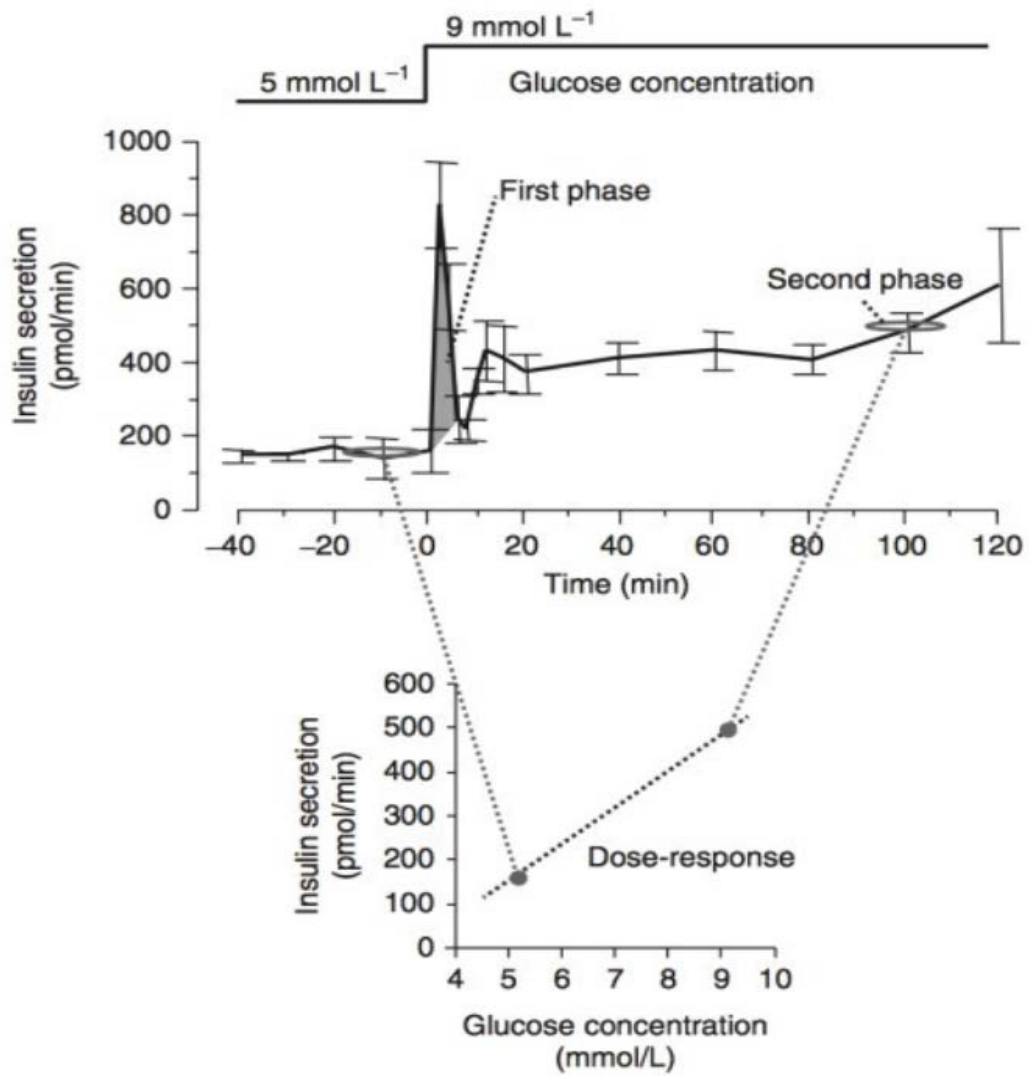


Figure 14 Data from a hyperglycaemic clamp, demonstrating insulin concentration at baseline and elevated glucose concentrations, with a simplified β -cell dose-response curve below. Reproduced with permission from Natali et al (5).

Hyperglycaemic clamp data, as shown above, have demonstrated that the “normal” insulin response is divided into two distinct phases: a rapid first phase lasting up to 10 minutes, and a second sustained phase, which continues until plasma glucose has normalised (221). The insulin concentration can be plotted against glucose concentration to give a rudimentary dose-response curve, the gradient of which is a measure of β -cell glucose sensitivity.

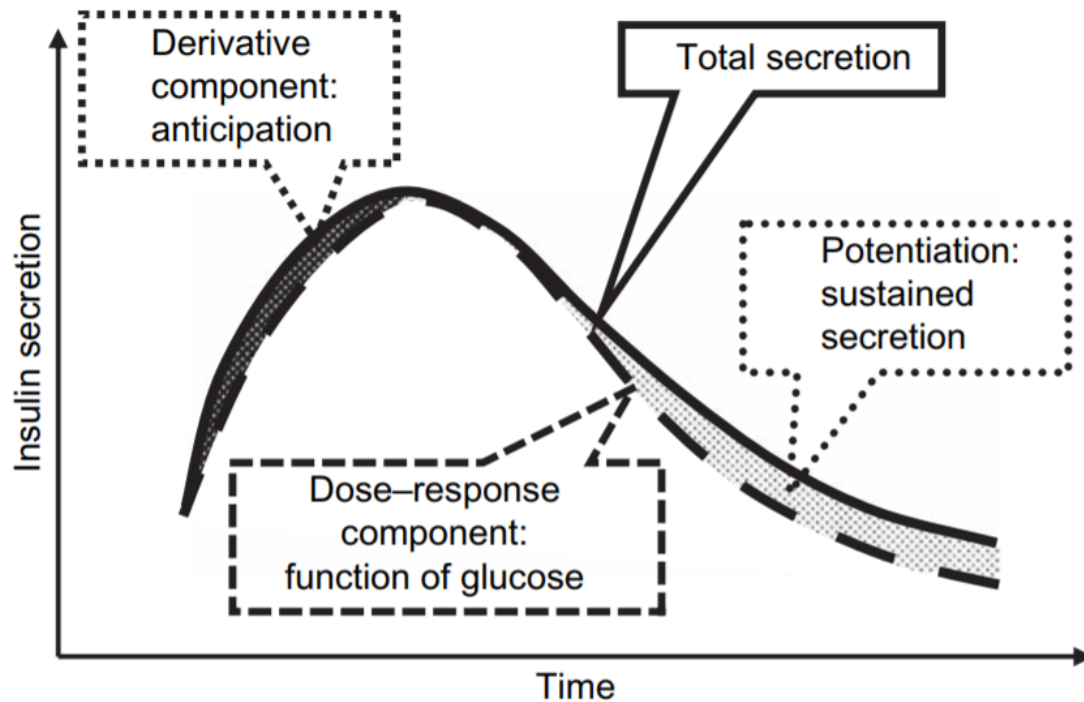


Figure 15 Time course of insulin during OGTT or MMT, demonstrating the dose-response curve, exaggerated response in the early phase, and prolonged response secondary to potentiation. These three components of insulin response are modelled in the beta cell model by Mari et al described below. Figure reproduced with permission from Mari et al (222).

However, while the dose-response component is the most significant component describing insulin secretion, it does not fully explain the insulin secretion seen after a glucose load. As shown in the diagram above, during an OGTT or MMT there is both an early, fast rise in insulin secretion, known as the derivative, early secretion or dynamic component, and sustained elevation of insulin secretion, known as potentiation. Due to these factors, beta cell modelling better estimates the β -cell response to a glucose load.

β -cell modelling

The β -cell model used in the RAMP study is that described by Mari et al (222-224), and consists of three parts – the **glucose model**, the **insulin secretion model** and a **C-peptide model** (224).

Firstly, glucose concentrations are modelled, using what is essentially a single compartment model (see Methods: Glucose Tracer Modelling) to smooth and interpolate the data for use in the beta cell model. The glucose model is described by the differential equation:

$$\frac{dG(t)}{dt} = -kG(t) + R(t)$$

wherein $G(t)$ is glucose concentration, k is a constant (0.012 min^{-1}) and $R(t)$ is a function of time.

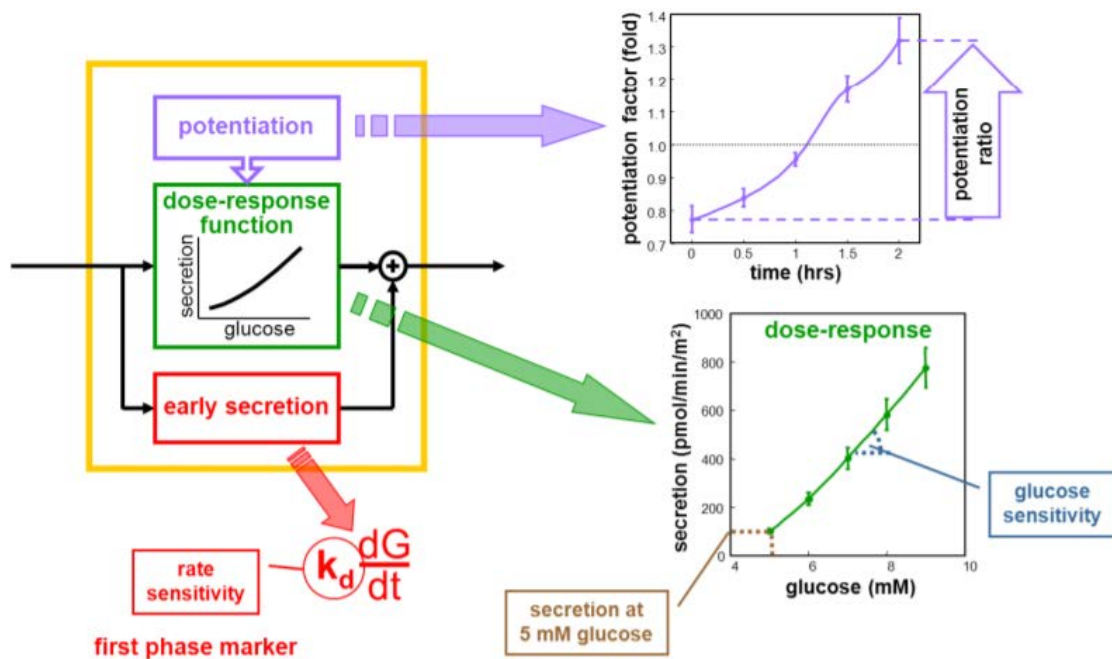


Figure 16 Illustration of the insulin secretion model, and its output. The model consists of three components - early secretion, dose-response, and potentiation. Reproduced with permission from Mari et al (222)

Figure 16 illustrates the components of the insulin secretion model, developed by Mari et al (222, 224). The derivative (early secretion) component is a product of the rate sensitivity (k_d) and the time derivative of glucose concentration, when the glucose concentration is rising (when glucose is falling, the time derivative is negative, and the early secretion component will be zero). The derivative component can be expressed as:

$$\text{Early secretion} = k_d \left(\frac{dG}{dt} \right)^+$$

The time derivative can be thought of as the gradient of the glucose over time curve. As glucose starts to fall, the gradient of the slope becomes negative, and the derivative component will be zero. The exaggerated early insulin response is no longer required, as glucose is falling.

The central and most significant component of the insulin secretion model is the dose-response, which is a function of the glucose concentration, $f(G)$, relating insulin secretion to the glucose concentration (G). This is a complex mathematical expression, detailed in the appendix of (224), and is beyond the scope of this thesis. The dose-response when plotted is a straight line, the gradient of which is the glucose sensitivity, the ability of the β -cell to respond to changes in the glucose concentration. From the dose-response curve, it is possible to predict insulin secretion rate at a known glucose

The final component of the insulin secretion model is potentiation, which modulates the dose-response (222), and is a positive function of time, $P(t)$. It can be expressed as:

$$P(t) = e^{Q(t)}$$

where $Q(t)$ is a function of time. $P(t)$ is greater than 1 when $Q(t)$ is above average, and less than 1 when $Q(t)$ falls below average (224). The average potentiation factor across the meal test will be 1, as the average $Q(t)$ is 0. Plotting the

potentiation factor over time (as shown in the top right of Figure 16) shows that potentiation should increase over the test period. Comparison of the potentiation factor at 2 hours to potentiation at baseline gives the potentiation factor ratio (PFR) which is a measure of the slope of the potentiation factor – time curve. The gradient has been shown to be flattened in obesity, impaired glucose tolerance and type 2 diabetes (222, 225).

In summary, the insulin secretion rate (ISR) can be modelled using:

$$\text{ISR} = P(t) f(G) + k_d [dG/dt]^+$$

where $f(G)$ is the dose–response relating ISR to glucose concentration (G), $P(t)$ is the potentiation factor, k_d is rate sensitivity and $[dG/dt]^+$ equals the time-derivative of glucose concentration when it is positive and zero otherwise.

The final step in the β -cell model is the C-peptide model described by Van Cauter et al (226). This is a two-exponential model, which incorporates the individual's sex, weight, height and age. Similar to the circulatory model discussed in Methods: Glucose Tracer Modelling, C-peptide concentration can be modelled as a convolution production of the impulse response of C-peptide, and its secretion. Therefore, deconvolution of the measured C-peptide concentration can be used to calculate the C-peptide secretion (226). As C-peptide is co-secreted with insulin in an equimolar ratio, the C-peptide deconvolution also calculates insulin secretion. There are advantages to using C-peptide modelling instead of peripheral insulin concentrations. Firstly, insulin undergoes first pass hepatic extraction, where C-peptide does not (226, 227). Secondly, C-peptide also demonstrates constant peripheral clearance, under variable conditions (226, 228), and the clearance kinetics can be described by a one compartment model (226).

Application

Using the models above, insulin secretion, and subsequently other indices of β -cell function, can be modelled using plasma glucose and serum C-peptide concentrations, obtained during an OGTT or MMT – insulin concentrations are not required.

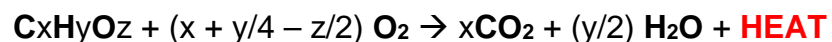
The β -cell model was applied to the MMT data from the RAMP study, with modelling performed by Prof Andrea Mari, at the Institute of Neuroscience, National Research Council, Padova, Italy. The data output was then further analysed using R studio, as described in Chapter 5 of this thesis. Many of the β -cell parameters are discussed in the Appendix 6: RAMP analysis.

Methods: Indirect Calorimetry

The “Response of individuals with Ataxia-telangiectasia to Metformin and Pioglitazone (RAMP)” study uses indirect calorimetry during the dual tracer mixed meal tests, to compare the estimated basal metabolic rate of the participants and to assess for difference in substrate utilisation between groups. These measures were also compared before and after intervention.

Theory

Calorimetry means the measurement of heat. Direct calorimetry used to be the “gold standard” for quantifying human metabolic rate (229, 230). It quantifies temperature fluctuations to measure the heat production of a subject within an enclosed space (229). During all the process of cellular metabolism, some energy is released as heat. As per the first law of thermodynamics, energy is cannot be made or destroyed, so the energy liberated as heat is released into the subject’s environment by heat exchange. The rate of heat production is a measure of cellular metabolism and is directly proportional to energy expenditure and metabolic rate.



Energy-releasing reactions in the body depend on oxygen consumption, and produce carbon dioxide, water and heat. Oxidation is the final common pathway for all substrate metabolism (carbohydrate, fat, protein) (231). The quantification of oxygen consumption or carbon dioxide production can therefore provide an indirect means of measuring cellular metabolism, known as indirect calorimetry.

Indirect calorimetry is now the gold standard, and most widely used method for estimating energy expenditure and substrate utilisation. It is more practical, as it does not require the whole subject to be within a sealed chamber as in direct calorimetry, and can use anything from a hand held device, to face mask, to hood / canopy. Respiratory chambers can also be used, but are less common.

Energy expenditure

Total energy expenditure over a 24 hour period is the sum of the basal metabolic rate, diet-induced thermogenesis and activity-related energy expenditure.

$$\text{TEE} = \text{BMR} + \text{DIT} + \text{AEE}$$

Basal metabolic rate is the amount of energy required to maintain basic cellular function. To measure BMR using indirect calorimetry, several criteria should be met: the individual should be fasted (ideally 12 hours); there should be an absence of gross muscular activity; there should be thermal neutrality; and the individual should be awake. Emotional disturbance or anxiety can affect measurement, as can the female menstrual cycle.

Therefore, the resting metabolic rate (RMR), also known as resting energy expenditure (REE) is often measured as an approximation of the BMR. To measure the RMR, the subject is fasted (8 – 12 hours) and should have abstained from exercise for the preceding 12 hours.

Calculation

Using the abbreviated Weir equation (i.e. excluding nitrogen) (231-233), resting energy expenditure (REE) can be estimated using VO_2 and VCO_2 :

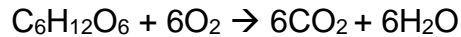
$$\text{REE (kcal/d)} = 1440 (3.94 \text{VO}_2 + 1.11 \text{VCO}_2)$$

Calculation of REE based on respiratory function alone, i.e. with the removal of nitrogen from the Weir equation, can introduce error of approximately 4% in the fasted condition (231). This error decreases as the metabolic rate increases.

Respiratory Quotient

The respiratory quotient (RQ), which is calculated as the ratio of CO_2 produced to O_2 consumed (CO_2 / O_2), indicates which substrate is being metabolised (231, 234).

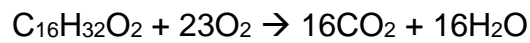
For carbohydrate, e.g. glucose:



Therefore the respiratory quotient of glucose is:

$$6\text{CO}_2 / 6\text{O}_2 = 1.0$$

For lipid, for example, palmitate:



Therefore the respiratory quotient of lipid is:

$$16\text{CO}_2 / 23\text{O}_2 = 0.7$$

This value will vary slightly according to which lipids are being metabolised.

Protein is more complex as the RQ varies slightly according to the amino acids involved, but the RQ for protein is approximately 0.8.

Application

Indirect calorimetry is used in both clinical and research settings. Clinical uses for assessing energy expenditure include: weight management; post-bariatric surgery; energy and nutritional requirement in acute illness such as multi-organ failure; and parenteral nutrition (235, 236).

Indirect calorimetry can be used as a research tool, to estimate BMR in the fasted resting state, or to assess substrate metabolism. If urinary nitrogen is measured, which is difficult to do with accuracy, glucose and lipid oxidation rates can also be calculated (231).

RAMP study

In this thesis, the RAMP study applied indirect calorimetry to the study participants to compare baseline BMR and substrate utilisation between groups, and also to assess how this would change with the study drugs – metformin and pioglitazone.

We used a GEM Nutrition, which is an open circuit indirect calorimeter which uses a ventilation “hood”, and calculates fluxes in O₂ and CO₂ on a minute by minute basis (one minute = one bin).

A previous calorimeter called the Deltatrac II was widely accepted as the gold standard in indirect calorimetry, however this is no longer in production. Other calorimeters are now measured against the Deltatrac II standard. The GEM Nutrition Indirect Calorimeter has been shown to have good day-to-day repeatability, and less variation than other newer models (237).

During the RAMP study, calibration was performed before each use. Gases used for calibration were recommended standard: (BOC) 1 % CO₂ and 20 % O₂. Flow was manually adjusted at the time of calibration to approximately 40 litres/min. Ethanol burning tests were performed on the GEM as a quality check for the calibration.

For indirect calorimetry measurements, participants were supine on a hospital bed, having been resting for the preceding 10 minutes minimum. After calibration, the ventilation hood was worn for 30 minutes at a time, to allow the participant to relax and reach a steady state. This was particularly important for the participants with A-T, to make sure they were comfortable and any intervention related anxiety dissipated before the measurement was taken.

The mean values of EE, VO₂, VCO₂ and RQ, discarded the first 10 bins (minutes) and took the average of the remaining measurements. If there were prolonged fluctuations at the beginning of the measurement, the number of discarded could be adjusted, aiming for a minimum of 15 bins for calculation of the mean values.

Methods: MRI Assessment of Adipose Distribution

As part of the “Response of individuals with Ataxia-telangiectasia to Metformin and Pioglitazone (RAMP)” study, participants underwent an abdominal MRI to assess their adipose volume and distribution to investigate whether people with A-T had a lipodystrophic phenotype, as previously demonstrated in mice (238). MRI was used as an alternative to whole-body DEXA, due to the radio-sensitivity associated with A-T (239).

Magnetic Resonance Imaging (MRI) uses the polar nature of hydrogen ions to measure water and fat quantities in tissues. Under a strong magnetic field, the hydrogen ions are excited, or rotated, and on relaxation emit a radio signal, which is detected by the receiving coil, placed over the anatomy of interest. There is therefore no ionising radiation involved, and repeated measures over time for monitoring can be used.

MRI provides excellent soft-tissue contrast, which allows differentiation of visceral (VAT) and subcutaneous (SAT) adipose tissue compartments. VAT, relative to SAT, is known to correlate more strongly with adverse metabolic risk (240, 241), though more weakly with BMI. The VAT:SAT ratio can be used as a metric of fat distribution (242).

Adipose volume and distribution

Previous MRI studies used “partial abdomen” measures i.e. single or multiple slices at specific anatomical locations e.g. umbilicus or specific vertebrae, to estimate adiposity. A new method was developed in collaboration with Matthew Marzetti and Dr Stephen Gandy from the department of Medical Physics at the University of Dundee, for use in the RAMP study. This method used “whole abdomen” (from diaphragm to pelvic floor) measures, which correlate better with BMI. Participants were scanned on a 3.0T Prisma^{Fit} MRI scanner (Siemens Healthineers, Erlangen, Germany) using multiple coils for a series of axial dual-echo, three point Dixon VIBE (Volume Interpolated Breath-hold Examination)

gradient echo sequence. Segmentation using a signal-intensity threshold cut-off value was applied to derive whole abdomen visceral and subcutaneous adipose tissue volumes. Technical details are described in greater detail in the method validation paper (243).

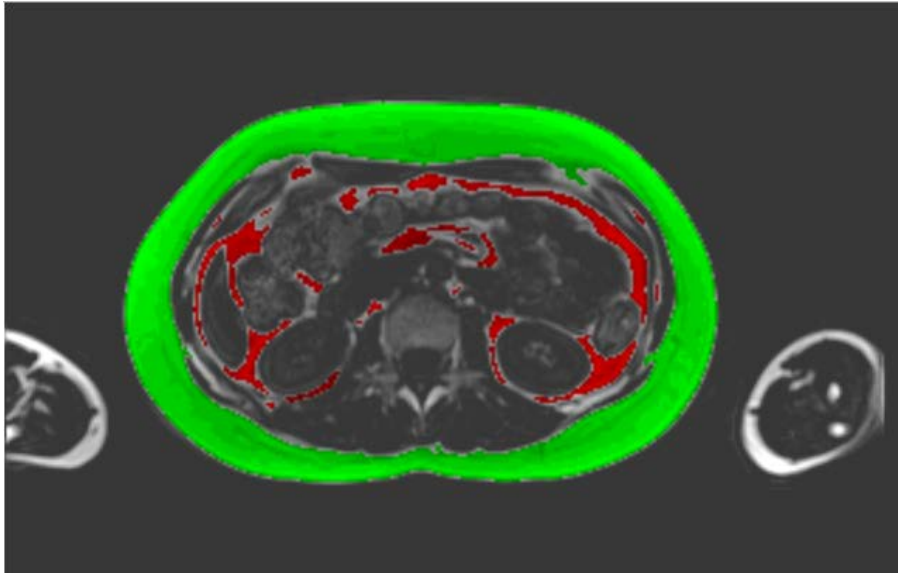


Figure 17 Axial slice at the level of the kidneys, showing visceral adipose tissue (VAT) in red, and subcutaneous adipose tissue (SAT) in green.

Liver fat and iron

During the MRI scan, Liver Lab software was used to measure liver fat and iron content.

Liver fat is measured in two ways – voxel based and image based. Voxel-based requires the user to mark a region of interest on identified liver tissue on the images, prior to spectroscopy being performed (244). Alternatively, fat suppression technique can be used on the whole liver image, where the MR signal is separated into its fat and water components and the difference in signal intensity is used to estimate the fat signal (244).

Liver iron content is measured using relaxation times (245). The higher the iron content of the liver, the higher the relaxation rate ($R2^*$) and shorter the relaxation time ($T2^*$), which can then be directly compared between the study groups.

Methods: Modelling Insulin Sensitivity

The RAMP study, discussed in Chapter 5 of this thesis, uses models of insulin sensitivity to compare the treatment effects of two commonly used diabetes drugs between individuals with A-T and healthy controls.

Insulin sensitivity is highly variable among individuals, and the gold standard approach for assessing insulin sensitivity is the euglycaemic hyperinsulinaemic clamp (EHC) technique. In steady state during the clamp, glucose infusion rate will equal whole body total glucose utilisation, and is therefore a measure of insulin sensitivity (246). However, the EHC is technically challenging to perform well, with frequent blood sampling at five minute intervals and recalculation of glucose infusion rates. Simpler models of insulin sensitivity have therefore been developed, using either fasting measures, or data from oral glucose tolerance tests (OGTT) / mixed meal tests (MMT). Mixed meal tests have the benefit of providing data closer to normal physiology post-meal, and will elicit the effects of incretin hormones (247).

There are numerous indices available. Those which have been employed in the analysis of the RAMP study data are discussed below. Other indices such as QUICKI, Strumvoll, Bergman's minimal model, are not discussed.

Homeostatic model assessment (HOMA)

Homeostatic model assessment (HOMA) can be used to estimate insulin sensitivity and beta cell function from fasting insulin and glucose concentrations (248). It was first developed by Matthews et al in 1985 and has been proven to

be a robust model for both clinical and epidemiological assessment of insulin resistance (249).

HOMA-IR is a measure of whole body insulin resistance, calculated using (250):

$$\text{HOMA-IR} = \text{FPI} \times \text{FPG} / 22.5$$

where FPI is fasting plasma insulin and FPG is fasting plasma glucose. Mean values of steady state insulin and glucose are used where possible, as this improves the coefficient of variation (250). HOMA-IR increases with insulin resistance, with normal insulin sensitivity <1.0, early insulin resistance >1.9, and significant insulin resistance >2.9. The reciprocal of HOMA-IR, calculates a measures of insulin sensitivity:

$$\text{HOMA\%S} = 22.5 / \text{FPI} \times \text{FPG}$$

Beta cell function can also be estimated using:

$$\text{HOMA\%B} = 20 \times \text{FPI} / (\text{FPG} - 3.5)$$

Calculated HOMA%B must be interpreted alongside HOMA-IR, or its reciprocal, HOMA%S, as a measure of beta cell function.

Matsuda Index

The Matsuda Index was first reported by Matsuda and De Fronzo in 1999 (251). It uses both fasting and dynamic measures of insulin and glucose from OGTT data to calculate a whole-body insulin sensitivity index. The Matsuda index has been well validated, and is highly correlated with the rate of whole-body glucose disposal during the euglycaemic clamp (251). It is calculated from insulin and glucose concentrations up to 120 minutes post meal:

$$\text{Matsuda} = 10000 / (\text{FPG} \times \text{FPI} \times \text{MPG} \times \text{MPI})^{1/2}$$

where MPG is mean plasma glucose and MPI is mean plasma insulin. There is an online calculator, or downloadable EXCEL worksheet available. A Matsuda index ≤ 2.5 is in-keeping with whole body insulin resistance (251).

Insulinogenic Index

The insulinogenic index (IGI) can be used as a measure of first phase insulin response to glucose load, using the 0 and 30 minute data from OGTT or MMT. It is calculated as the ratio of the change in insulin to the change in glucose, during the first 30 minutes of the test (252):

$$\text{IGI} = \Delta \text{ insulin}_{0-30} / \Delta \text{ glucose}_{0-30}$$

Although not as extensively validated, it provides an estimation of insulin secretion from a simple test, using a more physiological route of glucose administration than the traditional IVGTT or clamp (249, 252). If the calculated IGI is less than 0.4, there is an insulin secretion defect.

Oral Glucose Insulin Sensitivity (OGIS) index

The oral glucose insulin sensitivity (OGIS) index was developed by Mari et al (253), and is equivalent to the glucose clearance calculated during a clamp. OGIS is calculated using data from a 75g OGTT, namely glucose and insulin concentrations from baseline up to 120 / 180 minutes post-meal. The OGIS incorporates the use of a single-compartment model of glucose kinetics (see Methods: Glucose Tracer Modelling) and the model of insulin action is relatively complex compared to those discussed above. The equation used to define the model are detailed in (253), and there is an online calculator, or downloadable spreadsheet for calculation. Unlike the other indices discussed thus far, OGIS index is corrected for anthropometric data including BMI and BSA. It is closely correlated with the traditional euglycaemic hyperinsulinaemic clamp (253).

Disposition index and oral disposition index

The disposition index (DI) is a constant which can be used as a measure of the beta cells ability to compensate for insulin resistance (254, 255). In an individual with normal beta cell function, the sensitivity – secretory relationship is traditionally described as a rectangular inverse hyperbola, and the product of the two parameters is the disposition index. It was originally defined as the product of the insulin sensitivity index (Si) and acute insulin response (AIR) from the IVGTT, however several studies have since described an oral disposition index (256, 257).

Oral DI can be calculated using indices from the OGTT or beta cell modelling, for example, it is possible to plot the Matsuda Index against the Insulinogenic index, and the product of the two is the oral disposition index (258, 259).

All of the above indices of insulin response are used in the analysis of the RAMP data, detailed in Chapter 5, and Appendix 6: RAMP Analysis.

Pharmacokinetics of metformin intolerance (POMI) study

Contributions:

The following chapter details the “Pharmacokinetics of Metformin Intolerance” (POMI) study.

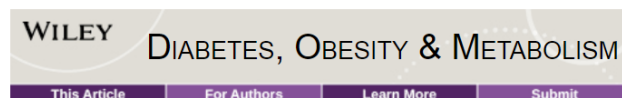
I contributed to the study design along with Dr Paul Connelly and Prof Ewan Pearson, in collaboration with Prof Kim Brøsen and Dr Tor Stage from the University of Southern Denmark.

I recruited all participants, and completed all study visits with assistance from Research Nurses Louise Cabrelli and Heather Loftus.

Sample analysis was performed by Dr James Burns at the Department of Blood Sciences at NHS Tayside, Dundee, Scotland; Dr Flemming Nielsen at the University of Southern Denmark, Odense, Denmark; and Dr Cornelia Prehn and Prof Jerzy Adamski at the Institute of Experimental Genetics, Genome Analysis Center, Munich, Germany.

I analysed the pharmacokinetic data, under the guidance of Dr Tor Stage, and performed further statistical analysis with advice from Dr Mike Lonergan, University of Dundee.

This study has been published:



[Diabetes Obes Metab.](#) 2018 Jul; 20(7): 1593–1601.
Published online 2018 Mar 23. doi: [10.1111/dom.13264](https://doi.org/10.1111/dom.13264)

PMCID: PMC6033038
PMID: [29457876](https://pubmed.ncbi.nlm.nih.gov/29457876/)

Pharmacokinetics of metformin in patients with gastrointestinal intolerance

[Laura J. McCreight](#), MBChB, ¹ [Tore B. Stage](#), PhD, ² [Paul Connelly](#), MBChB, ¹ [Mike Lonergan](#), PhD, ¹
[Flemming Nielsen](#), PhD, ² [Cornelia Prehn](#), PhD, ^{3, 4} [Jerzy Adamski](#), PhD, ^{3, 5, 6} [Kim Brøsen](#), PhD, ² and
[Ewan R. Pearson](#), PhD¹

Introduction

Despite affecting up to 20% of those treated, metformin intolerance is poorly understood (260). Intolerance to metformin is usually characterised by gastrointestinal side-effects (GI SEs) of nausea, abdominal pain, bloating, or diarrhoea. Gradual up-titration of dose following introduction, or slow release preparations can, in some cases, attenuate symptoms of intolerance. However, in 5% of individuals exposed to metformin, the severity of the GI SEs leads to discontinuation of treatment (260). For others, metformin intolerance may result in sub-optimal dosing or poor compliance. These factors: delay optimal glycaemic control in the individual; result in the addition of, or switch to, alternative oral anti-hyperglycaemic agents; and as a result, potentially contribute to increased risk of microvascular complications of diabetes.

Metformin is the first-line pharmaceutical treatment for type 2 diabetes recommended by the ADA-EASD guideline (3). This, and other guidelines (2), recommends metformin based upon prospective (14, 65, 261, 262) and retrospective (64) studies, which demonstrate an improved glycaemic profile with metformin treatment, reduction in cardiovascular mortality (14, 64, 65, 262), no associated hypoglycaemia (261), weight neutrality or weight loss (261). These desirable characteristics, along with its low cost, explain metformin's status as the most extensively prescribed anti-hyperglycaemic agent worldwide. These same characteristics drive the need for ongoing research into the mechanisms underlying intolerance to metformin, aiming to prevent, modulate or treat intolerance. This would not only benefit the individual but could have significant implication for health economy.

Pharmacokinetics of metformin

As discussed in the introduction chapter of this thesis, metformin has a reported oral bioavailability within the range of 55 - 70% (16, 20), with the remainder recovered from the faeces. Metformin is absorbed from the small intestine, and is transporter-dependent (16, 23), therefore genetic variation and efficacy of these

transporters could impact upon: oral bioavailability; maximum drug concentration achieved in the plasma (C_{max}); the time from ingestion to achieving the maximum concentration (T_{max}) and the area under the drug concentration – time curve (AUC).

In the systemic circulation metformin travels unbound to proteins (16), and is easily transported or absorbed into other tissues, including the kidneys, liver, and erythrocytes. This results in large volume of distribution, which contributes to the rate of elimination and plasma half-life of the drug. Again, variation in transporter efficiency could result in variability in PK of and systemic exposure to metformin.

Metformin is not metabolised, and is eliminated via the kidneys, excreted unchanged in the urine (16, 17). Again, this process is transporter dependent and, therefore, exposed to potential variation in efficacy. This could impact upon the renal clearance; plasma half-life of the drug and AUC.

The association between the pharmacokinetics of metformin and metformin intolerance has not previously been studied. Therefore, the Pharmacokinetics of Metformin Intolerance (POMI) study was designed to investigate whether intolerance was associated with variation in the systemic exposure to metformin.

Metformin and the gastrointestinal tract

Metformin has a complex relationship with the gastrointestinal tract (77). It exerts many effects on the intestine as described in the introduction and our review article (77). Multiple hypotheses for the mechanism of GI intolerance to metformin have been proposed, including:

1. Abnormal uptake

Metformin uptake from the gut lumen is transporter-dependent (16, 23). Genetic variation (29, 32, 47, 169) in or inhibition (29, 47) of transporters, such as OCT1, could alter metformin uptake from the intestinal lumen to enterocytes, and subsequently affect efflux of metformin across the basolateral membrane to the

systemic circulation. This would lead to changes in metformin concentration within the GI tract, enterocytes or systemic circulation.

2. Increased lactate production

Previous studies have shown that metformin concentration in enterocytes has been recorded at up to 300 times higher than the systemic concentration (21), and the variation in transporter activity described above could result in even greater differences in some individuals. Metformin is known to increase glucose uptake and anaerobic glucose utilisation in the intestine, resulting in increased lactate production (19, 21, 124, 125, 127). In humans, there is a small but significant increase in systemic lactate when comparing those taking metformin to those who are not (124). We suggest that metformin intolerance may be associated with an increased concentration of metformin in the intestine, or prolonged exposure of the enterocyte to metformin, leading to a greater increase in anaerobic glucose utilisation and lactate production, than in tolerant individuals. The increase in local lactate concentration may contribute to the intolerance to metformin. Intracellular lactate accumulation will lead to a subsequent increase in measurable serum lactate (124).

3. Accumulation of serotonin or histamine

Metformin is known to stimulate the release of serotonin from enterochromaffin cells (148), and is a known substrate for SERT (serotonin transporter) (47, 148, 149). Metformin may inhibit the uptake of serotonin from the intestinal lumen, leading to accumulation of serotonin in the gut. Serotonin activates afferent neurons of the enteric nervous system, and is responsible for peristaltic and secretory reflexes within the intestine, as well as information transmission to the central nervous system (263). Known serotonergic effects on the gut include nausea, vomiting and diarrhoea (264), which are in-keeping with the GI SEs seen in metformin intolerance. Histamine also increases gut motility (265), and

metformin may reduce the enterocytic metabolism of histamine by diamine oxidase (149).

4. Alteration in the bile acid pool

It is recognised that metformin reduces ileal absorption of bile acid (152), leading to an increased concentration of bile acids in the large intestine and potential osmotic diarrhoea. Metformin could potentially alter the conversion of primary bile acids, which are synthesised by the liver, to secondary bile acids. This process depends on dehydroxylation by bacterial 7α -dehydroxylase (266-268), which may be reduced in metformin treatment due to the reduction diversity in the microbiome associated with metformin (159), specifically a reduction in the genera known to produce 7α -dehydroxylase. Bile is usually reabsorbed and returned to the liver, where it can be re-secreted by the liver. It is possible that metformin disrupts this enterohepatic circulation, resulting in an increase in the hormonal and osmotic effects of bile acids in the gut.

The Pharmacokinetics of Metformin Intolerance (POMI) study is an open-label pharmacokinetic study designed to investigate these hypothesised mechanisms for metformin intolerance, by studying how individuals tolerant to metformin differed from those who are intolerant.

Hypothesis

The Pharmacokinetics of Metformin Intolerance (POMI) study was designed to investigate our primary hypothesis that variability in metformin tolerance is associated with systemic metformin concentration, reflecting differences in the pharmacokinetics of metformin.

We also hypothesised that metformin intolerance may be caused by:

1. An increase in systemic lactate compared to tolerant individuals, as a result of metformin-related anaerobic glucose utilisation.
2. A reduction in systemic serotonin, due to metformin-related inhibition of serotonin uptake from the gastrointestinal lumen.
3. An increase in systemic histamine concentration, secondary to a metformin-related reduction in histamine metabolism.
4. A reduction in the systemic bile acid pool, specifically a reduction in secondary bile acids, due to a metformin-related reduction in ileal absorption, and deconjugation of bile acids.

Aims

Our primary objective was therefore to compare the pharmacokinetics (PK) of metformin in individuals identified as tolerant or intolerant of metformin, to assess if intolerance is related to alterations in PK.

Our secondary objectives were to compare plasma lactate; serotonin; histamine and bile acids after metformin dosing, between tolerant and intolerant individuals, to investigate these potential mechanisms of metformin intolerance.

Plasma metformin and serum lactate concentrations were measured, along with targeted metabolomics, in the hours following the administration of a single dose of metformin IR 500mg, to compare the two groups.

Materials and Methods

This study was conducted in the Clinical Research Centre (CRC) at Ninewells Hospital, in Dundee, between June 2015 and April 2016. It was co-sponsored by University of Dundee and NHS Tayside, and ethical approval was given by East of Scotland Research Ethics Committee. The study was conducted in accordance with the Good Clinical Practice guidelines, and the Declaration of Helsinki. The study is registered on the public database ClinicalTrials.gov, identifier NCT03361878. Formal written informed consent was obtained from each individual prior to inclusion.

Recruitment

Individuals were recruited if they had type 2 diabetes (T2D), were white European, and met the criteria for tolerance or intolerance to metformin. Metformin intolerant individuals were defined as those who had previously been treated with a maximum of 1000mg metformin daily for a maximum of 8 weeks, and discontinued treatment due to GI upset (Criterion 1). Alternatively, intolerance was defined as inability to increase metformin dose above 500mg without experiencing GI SEs, despite having an HbA1c >53mmol/mol (Criterion 2). Tolerant individuals were defined as those taking 2000mg metformin daily in divided doses, with no GI SEs. Those taking metformin were asked to discontinue their metformin 72 hours prior to the study. The length of washout period was based on an estimated $t_{1/2}$ for plasma metformin of 5.7 hours (16). Exclusion criteria were: inability to consent; age out with 18 – 90 years of age; eGFR <60 ml/min; pregnancy; history of gastric bypass; evidence of slowed gastric or intestinal motility. None of the patients included were treated with drugs known to affect the pharmacokinetics of metformin in vivo (30): acarbose (269), cephalexine (270), cimetidine (271), dolutegravir (272), pyramethamine (273), ranolazine (274), trimethoprim (275) or tyrosine kinase inhibitors (276).

Ten metformin intolerant individuals were recruited from the DIRECT (175) cohort in Tayside, eight of whom met intolerance Criterion 1. Ten metformin tolerant

individuals were then recruited from the GoDARTS (176) cohort, matching for gender, age, and BMI.

Study design and interventions

Participants attended the CRC at Ninewells Hospital fasted from midnight. At 0900 (time 0) a blood sample was obtained prior to administration of a single dose of oral metformin (IR) 500mg. Further blood samples were taken at 0.5, 1, 1.5, 2, 2.5, 3, 3.5, 4, 6, 8 and 24 hours post-metformin. Urine was collected over the 24 hours following administration of metformin. Participants were given breakfast two hours, and lunch five hours, post-metformin. Plasma metformin and lactate concentrations were measured at all time points, using plasma lactate concentration as a proxy of intestinal lactate production, secondary to metformin concentration within the enterocyte. Plasma lactate was measured using a lactate oxidase method; plasma and urine metformin concentrations were determined using liquid chromatography and tandem mass spectrometry (LC-MS/MS), and the limit of quantification (LOQ) was 0.01 mg/L. Histamine and serotonin, and bile acids were determined using the targeted metabolomic assays Biocrates Absolute/IDQ™ p180 Kit and Biocrates™ Bile Acids Kit, respectively. Full descriptions of analytical methods are provided in the Appendix 1: POMI sample analysis methods.

Outcomes

The primary endpoint was metformin pharmacokinetics as determined by the area under the curve (AUC) of metformin concentration over time. The secondary outcome of the study was to determine whether systemic lactate concentration, a surrogate for metformin concentration in the enterocyte, is associated with metformin intolerance. Additional outcomes included the assessment of serotonin, histamine and bile acids concentrations in acute metformin dosing.

During the study, a Metformin Symptom Severity Score was completed by participants (Appendix 2: MISSS). This questionnaire details the individual's

maximum tolerated dose of metformin, identifies which GI SEs experienced while taking metformin, and scores the severity of the symptoms. This was completed to confirm the phenotype of the cohorts, and gather information as to the nature of the individuals' side effects.

The questionnaire was not used as a diagnostic tool in this study, but as a means of characterising the intestinal intolerance experienced and the perceived severity of this. The “true diagnosis” of intolerance was based upon the inclusion criteria alone.

The MISSS was later adopted in the “Impact of OCT1 genotype and OCT1 inhibiting drugs on an individual's tolerance of metformin (ImpOCT)” study, and is discussed further in Chapter 4 of this thesis.

Statistical methods

Sample size

The study was powered to detect a 30% difference in AUC_{0-24} of the metformin concentration-time curve, with 80% power, and significance of 5%. This value was chosen based on previous studies by Najib et al (277), and required a cohort of ten metformin-intolerant individuals plus ten metformin-tolerant individuals.

Statistical analysis

Pharmacokinetic data were analysed using non-compartmental analysis using the R package NCAPPC (184), in conjunction with the Department of Clinical Pharmacology and Pharmacy, Institute of Public Health, University of Southern Denmark. Pharmacokinetic endpoints are presented as median with interquartile range (IQR, 25th-75th percentiles) and geometric mean ratios with 95% confidence intervals. Pharmacokinetic parameters were calculated as described in Methods: Pharmacokinetics. Statistical significance was determined using unpaired t-test on log-transformed data and accepted at $p < 0.05$.

Creatinine clearance was calculated using the Cockcroft-Gault equation using Ideal Body Weight (IBW), and corrected for Adjusted Body Weight ($ABW = IBW + 0.4 \times (\text{actual body weight} - IBW)$) in those with BMI >25.

All other data were analysed using R studio, and were assessed for normality using Shapiro Wilks method. Those data with a normal distribution are expressed as mean \pm 95% CIs and were compared using unpaired t-test with two tails and unequal variance. Graphic data are plotted as mean \pm SEM. Those data with non-normal distribution were expressed as median with IQR and compared using the non-parametric Mann Whitney U test.

Calculation of incremental area under the curve (iAUC) for lactate, serotonin and bile acids used the linear trapezoidal method.

For the purpose of this study and to minimize multiple testing penalties, we analysed only serotonin and histamine from the Biocrates p180 panel, and accepted values of $p < 0.05$ as statistically significant. For the analysis of the bile acids panel, adjusting for the Bonferroni correction, we accepted a significance level of $p < 0.0024$.

Results

Recruitment

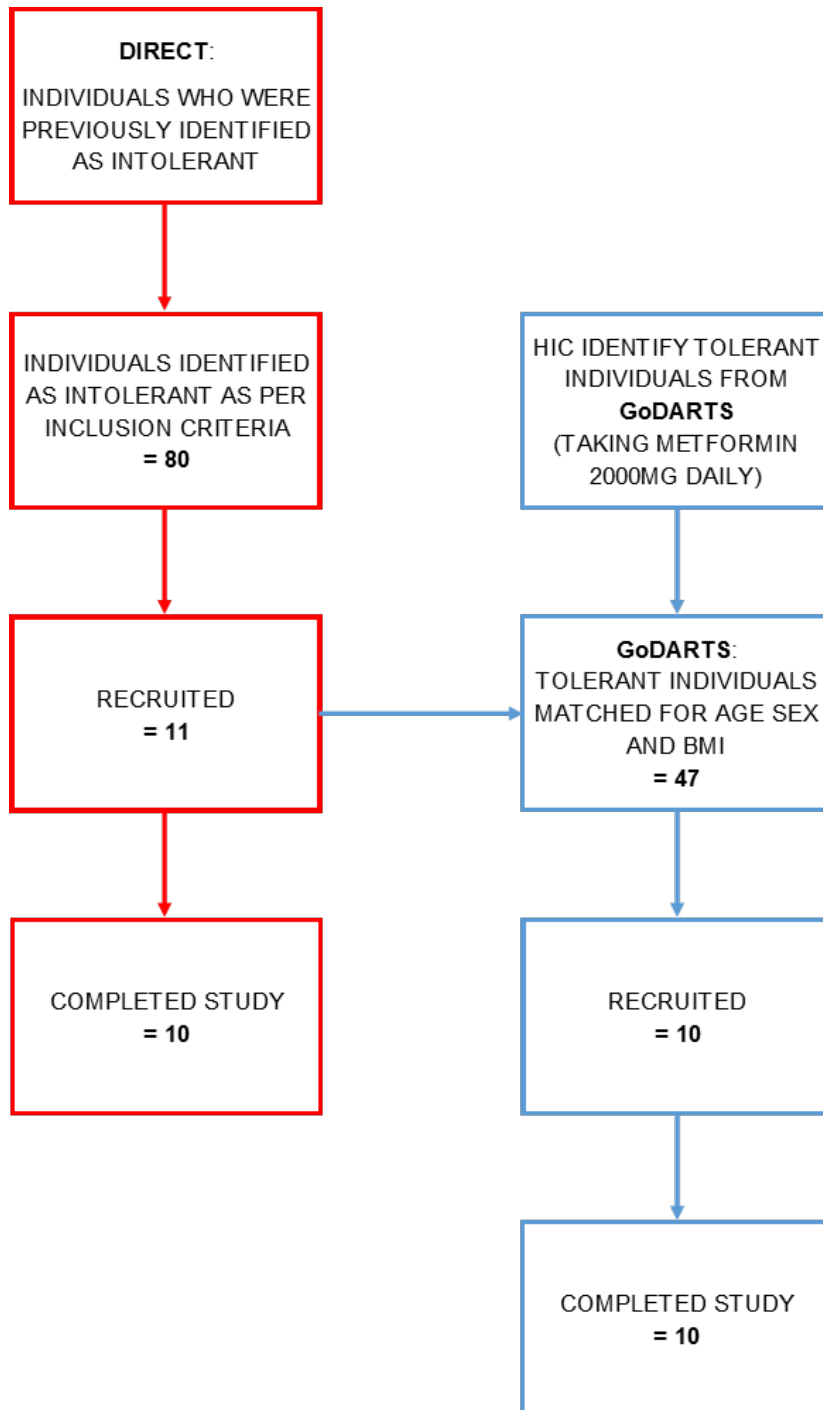


Figure 18 Recruitment flow diagram for the Pharmacokinetics of Metformin Intolerance (POMI) study.

Baseline characteristics

All 20 participants completed the study, with no withdrawals. The baseline characteristics are listed in Table 4. The cohorts were well matched for gender, age and BMI. There was no significant difference in creatinine clearance between the cohorts. HbA1c was different in the two cohorts: 60.0 (55.0 – 68.0) and 72.0 (67.3 – 76.8) mmol/mol in the tolerant and intolerant cohorts respectively, but this should not impact the pharmacokinetics of metformin. This difference is not surprising as the intolerant cohort have discontinued metformin, and their higher HbA1c may represent the difficulty in optimising their medical management. However, both cohorts had additional anti-hyperglycaemic medications prescribed, including SUs, TZDs, DPP4 inhibitors, GLP1 receptor agonists and insulin. Additional medication was administered two hours post-metformin dosing.

Characteristic	Metformin Tolerant	Metformin Intolerant	p
n	10	10	1.000
Female/Male	7/3	7/3	1.000
Age, yrs	67.5 (60.8 – 72.5)	71.0 (65.75 – 80.3)	0.307
Age at diagnosis, yrs	51.5 (51.0 – 58.0)	60.0 (57.3 – 61.8)	0.111
Diabetes duration, yrs	12.0 (9.0 – 15.5)	12.0 (7.5 – 14.8)	0.850
HbA1c, mmol/mol	60.0 (55.0 – 68.0)	72.0 (67.3 – 76.8)	0.012
Weight, kg	90.0 (79.0 – 97.2)	91.2 (79.6 – 104.0)	0.910
BMI	34.6 (26.3 – 38.3)	34.3 (29.5 – 38.5)	0.800
Creatinine Clearance	86.3 (76.6 – 107.3)	78.8 (68.3 – 93.2)	0.353
SU (n)	3	6	0.370
DPP4i (n)	3	1	0.582
GLP1 RA (n)	3	1	0.582
TZD (n)	0	2	0.474
Insulin (n)	4	4	1.000

Table 4 Baseline characteristics of the participants of the POMI study. Data are median (IQR); p value for Mann Whitney U test. For categorical data, p value for Fisher exact test. SU = sulphonylurea; GLP1 RA = GLP1 receptor agonist; DPP4i = dipeptidyl peptidase inhibitor; TZD = thiazolidinedione.

Effect of acute metformin dosing

The Metformin Symptom Severity Score (Appendix 2) was completed by all participants, with a potential score ranging from 0 to 50. The intolerant cohort had a mean severity score of 30.4, much greater than the tolerant cohort's 1.9 ($p < 0.0001$). Of the ten tolerant individuals, eight participants scored 0 for the severity score, with the two individuals who scored 8 and 11 having symptoms of IBS which preceded metformin and were unchanged by metformin treatment. Of the intolerant cohort, 70% of participants had previously experienced nausea with metformin, 50% described abdominal pain or bloating, and 50% suffered from diarrhoea.

During the 24 hour study, 9 of the 10 intolerant individuals experienced GI side effects after 500mg of metformin, while none of the tolerant cohort described any symptoms. Of the intolerant cohort, 50% suffered diarrhoea, 50% experienced nausea, with 30% describing abdominal pain, and 20% complaining of bloating.

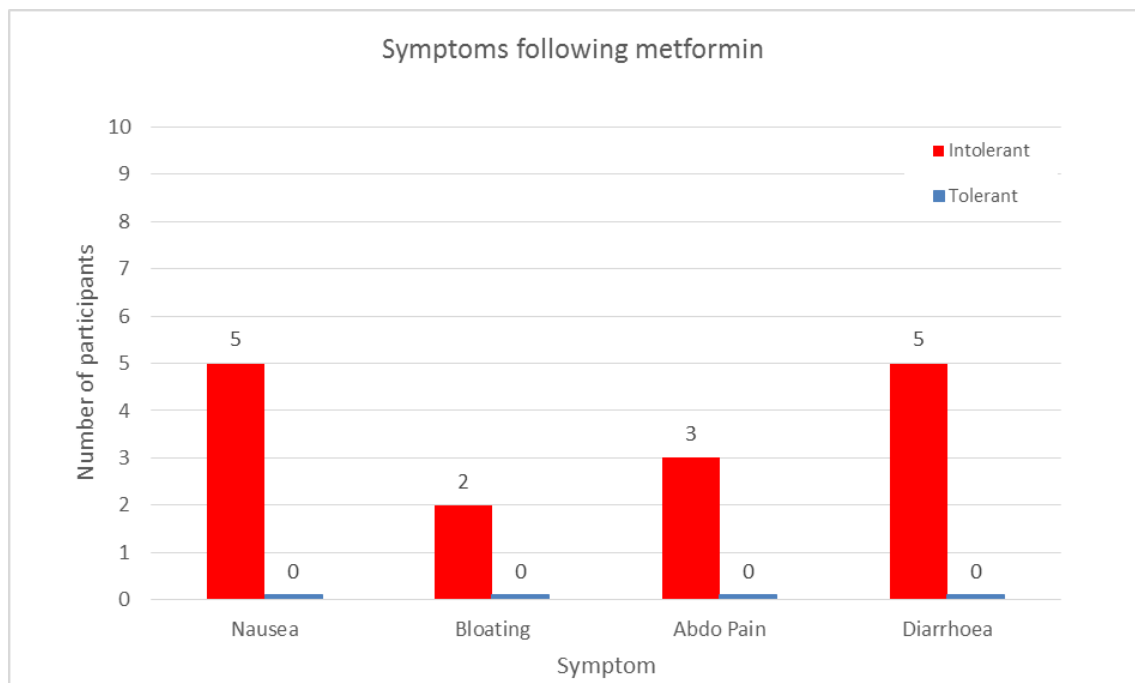


Figure 19 Symptoms of metformin intolerance by phenotype, following a single dose of metformin, 500mg.

Study ID	Symptom			
	Nausea	Bloating	Abdominal Pain	Diarrhoea
MI 01	-	-	Y	Y
MI 02	-	-	-	Y
MI 03	Y	-	-	-
MI 04	Y	Y	-	Y
MI 05	-	-	-	Y
MI 06	-	-	-	-
MI 07	-	Y	Y	-
MI 08	Y	-	Y	Y
MI 09	Y	-	-	-
MI 10	Y	-	-	-
MT 01	-	-	-	-
MT 02	-	-	-	-
MT 03	-	-	-	-
MT 04	-	-	-	-
MT 05	-	-	-	-
MT 06	-	-	-	-
MT 07	-	-	-	-
MT 08	-	-	-	-
MT 09	-	-	-	-
MT 10	-	-	-	-

Table 5 Metformin associated gastrointestinal side-effects after acute dosing

However, as this is an open-label study, it is susceptible to reporting bias in those expecting symptoms of intolerance with metformin, with a potential over-reporting of GI symptoms. It should also be noted that the intolerance seen in the 24 hour study period is acute intolerance. We cannot comment on chronic intolerance, although our inclusion criteria identified individuals with true, chronic intolerance.

Metformin pharmacokinetics in intolerant and tolerant individuals

At time 0 hours (pre-metformin dose) the intolerant group had a plasma metformin concentration, as expected, under the limit of detection. The metformin tolerant group, despite 72 hours of metformin washout, had a detectable metformin concentration, median 0.067 (IQR 0.030 – 0.095) mg/L at baseline. Similarly, at 24 hours, median metformin concentration in the tolerant cohort was higher (0.085, IQR 0.066 – 0.135 mg/L) than the intolerant cohort (0.051, IQR 0.034 –

0.066 mg/L). Although the differences at baseline and at 24 hours post-metformin are significantly different from zero ($p < 0.001$; $p = 0.015$ respectively), the levels are small when compared to the peak metformin concentration after 500mg of metformin. Peak concentration (C_{max}) for both cohorts was reached at 2.5 hours post-dose, with median C_{max} of 2.1 (IQR 1.7 – 2.3) and 2.0 (IQR 1.8 – 2.2) mg/L for tolerant and intolerant cohorts respectively ($p = 0.76$). The plasma metformin concentrations of the groups, over 24 hours post 500mg dose, were not significantly different, with median AUC_{0-24} 16.9 and 13.9 (mg/L)*h in the tolerant and intolerant cohorts respectively ($p = 0.72$), as illustrated in Figure 20.

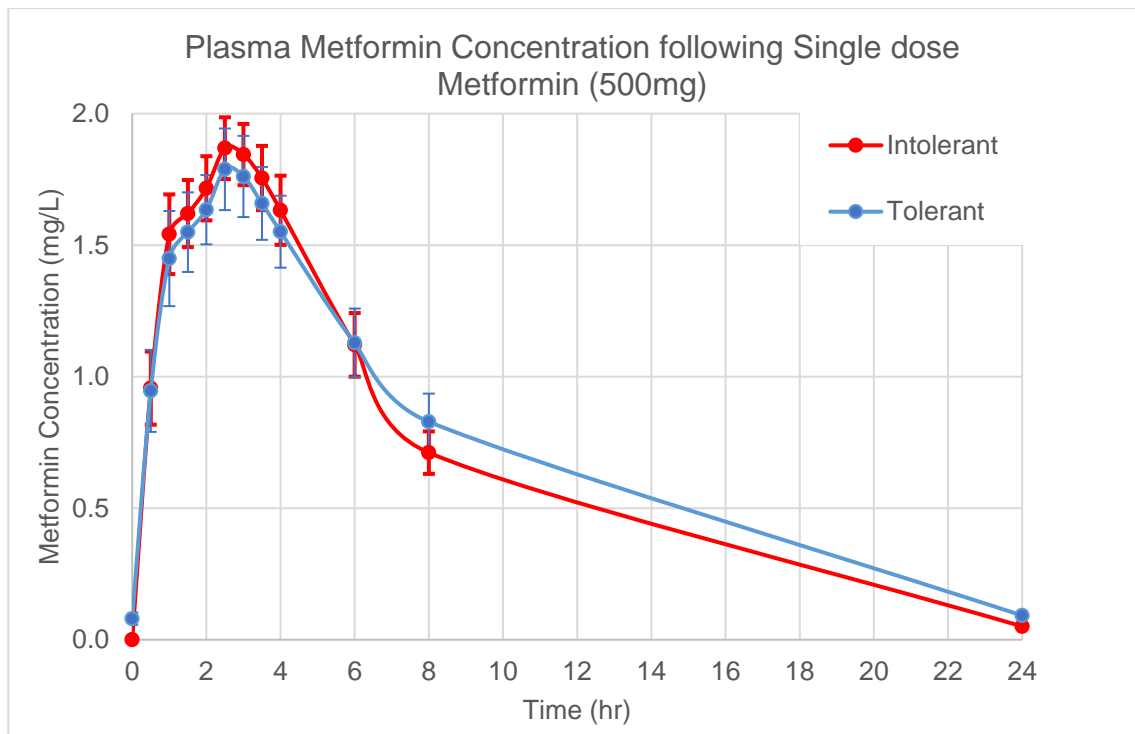


Figure 20 Plasma concentration of metformin over time, following a single dose of 500mg given at time 0 hr. Data points are mean \pm SEM.

The $t_{1/2}$ life of metformin was higher in the tolerant group (4.8 vs 4.1 hours, $p = 0.001$). However, the apparent oral volume of distribution (V/F), apparent total clearance from plasma after oral administration (CL/F), and renal clearance of metformin from the plasma (CL_r) did not differ between the tolerant and intolerant groups (Table 6).

	Intolerant	Tolerant	Geometric Mean Ratio (95% CIs)	<i>p</i>
AUC ((mg/L)*h)	13.9 (12.9 – 16.8)	16.9 (13.9 – 18.6)	0.95 (0.72 - 1.26)	0.72
C_{max} (mg/L)	2.0 (1.8 – 2.2)	2.1 (1.7 – 2.3)	1.04 (0.83 – 1.30)	0.76
T_{1/2} (h)	4.1 (3.8 – 4.3)	4.8 (4.7 – 5.3)	0.82 (0.76 – 0.89)	<0.001
CL/F (L/h)	35.2 (29.4 – 38.1)	28.6 (25.8 – 34.6)	1.07 (0.81 – 1.43)	0.62
V/F (L)	211.4 (164.0 – 225.8)	197.3 (186.0 – 261.3)	0.88 (0.66 – 1.17)	0.36
CL_R (L/h)	17.6 (13.9 – 25.5)	20.5 (14.7 – 25.2)	0.88 (0.56 – 1.41)	0.59
F (%)	71 (62 – 84)	95 (56 – 101)	0.83 (0.53 – 1.27)	0.38

Table 6 Pharmacokinetic parameters after acute metformin dosing. Data are median and IQR; geometric mean ratios with 95% CIs. *P* value for unpaired *t* test.

Serum lactate and metformin intolerance

The lactate concentration increased post-metformin with the median time to peak 3.5h post-dose (Figure 21). Mean peak lactate concentration was 2.4mmol/L for both groups (tolerant 95%CI 2.0 – 2.8 mmol/L, and intolerant 95% CI 1.8–3.0mmol/L). There was no significant difference in the incremental AUC₀₋₂₄ for lactate between the tolerant (6.98 mmol/L*h, 3.03–10.93) and intolerant (4.47 mmol/L*h, -3.12–12.06) groups, *p*=0.55.

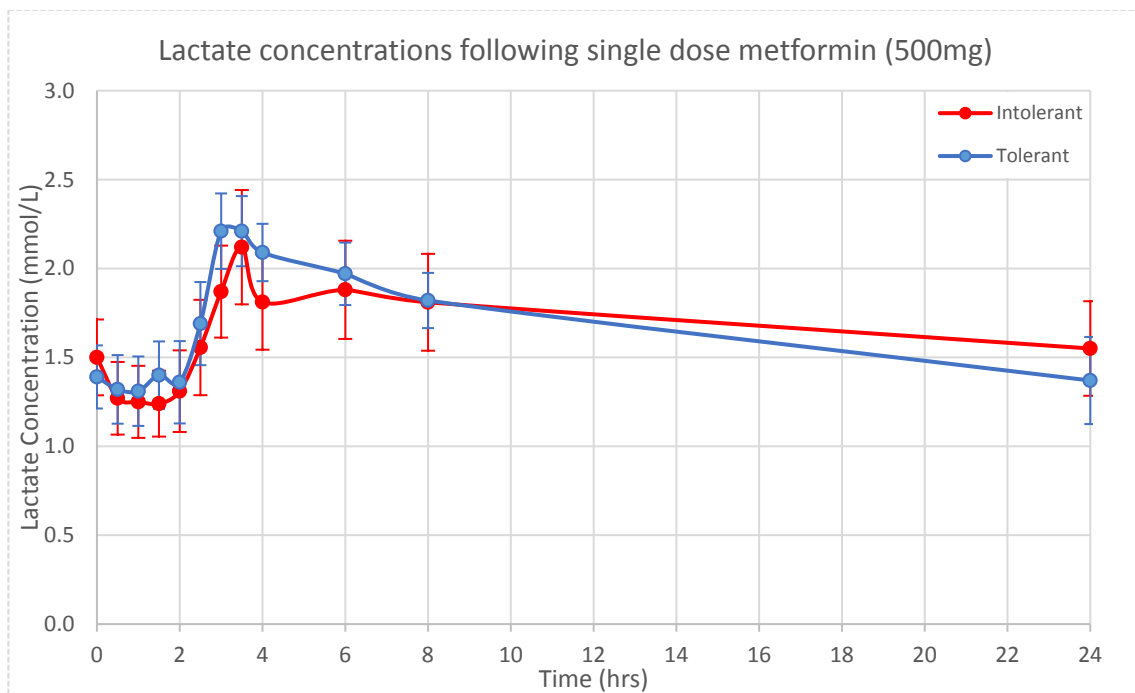


Figure 21 Mean lactate concentration over time, following a single dose of metformin, 500mg at time 0 hr. Data points are mean \pm SEM.

Plasma Serotonin, histamine and bile acid concentrations

The incremental AUC_{0-24} of the serotonin concentration–time curve did not differ between the cohorts ($p = 0.529$), and there was no apparent rise in plasma serotonin following metformin dosing in either group (Figure 22). Histamine levels were below the lower limit of detection in the p180 panel for both cohorts.

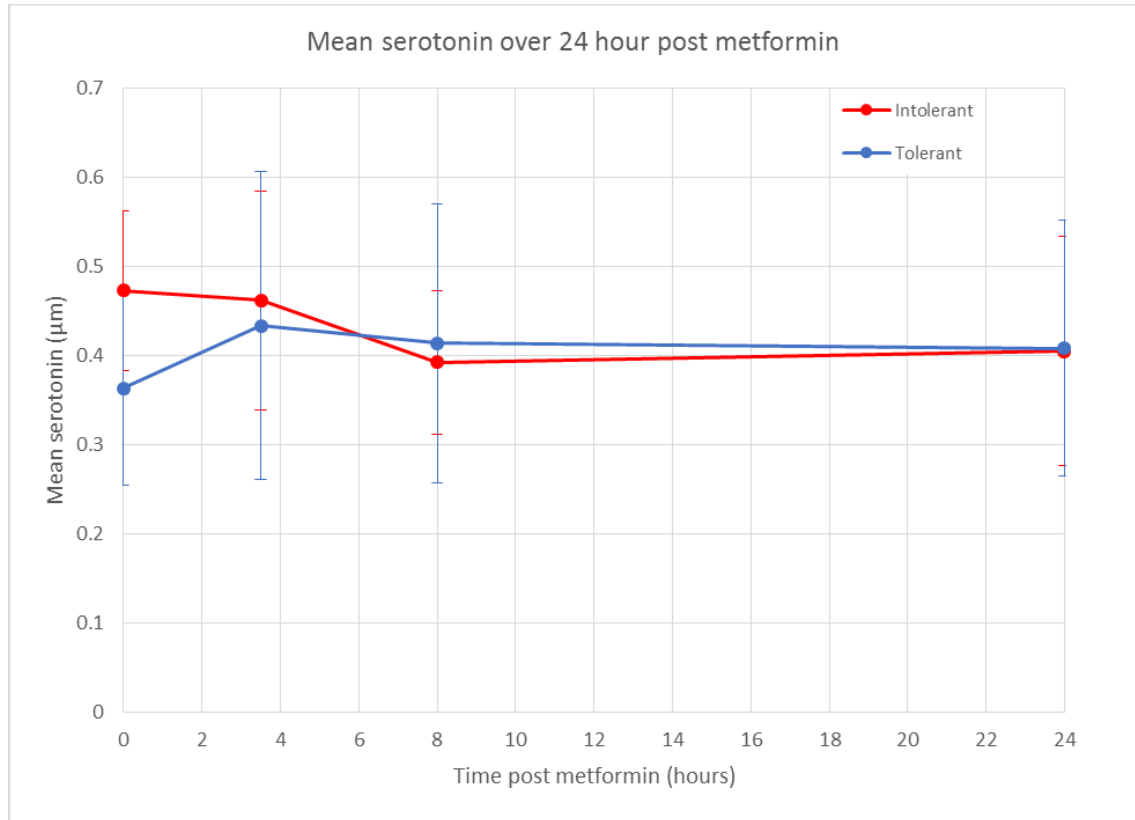


Figure 22 Mean serotonin concentration over time, following a single dose of metformin, 500mg at time 0hr. Data points are mean \pm SEM.

The Biocrates bile acid panel measures the concentration of twenty different bile acids. There was no difference in incremental AUC_{0-24} between the tolerant and intolerant cohorts for each individual bile acid, when corrected for multiple testing. Similarly, when considering the bile acids by class – primary, conjugated primary, secondary and conjugated secondary – no significant difference was identified.

Bile acid (abbreviation)	MI	MT	p
Cholic acid (CA)	-0.73 (-3.3 – 0.71)	0.46 (-0.04 – 2.68)	0.1431
Chenodeoxycholic acid (CDCA)	-0.06 (-3.36 – 5.78)	0.28 (-5.02 – 4.68)	0.8534
Deoxycholic acid (DCA)	1.12 (-3.11 – 4.12)	2.23 (-5.13 – 8.04)	0.5787
Glycocholic acid (GCA)	4.18 (1.38 – 9.99)	1.12 (-0.92 – 4.83)	0.0892
Glycochenodeoxycholic acid (GCDCA)	15.84 (5.63 – 27.04)	9.28 (-5.80 – 25.81)	0.3527
Glycodeoxycholic acid (GDCA)	7.65 (5.55 – 12.53)	3.75 (-9.87 – 15.11)	0.2799
Glycolithocholic acid (GLCA)	0.44 (0.09 – 0.57)	0.15 (-0.39 – 1.21)	0.4813
Glycoursodeoxycholic acid (GUDCA)	0.66 (0.18 – 3.53)	0.14 (-0.86 – 1.99)	0.2799
Lithocholic acid (LCA)	-0.07 (-0.34 – 0.18)	0.01 (-0.30 – 0.20)	0.7054
Muricholic acid, beta (MCA(b))	0.07 (-0.14 – 0.19)	-0.01 (-0.15 – 0.10)	0.4813
Taurocholic acid (TCA)	0.93 (0.23 – 2.13)	-0.01 (-0.19 – 0.61)	0.01854
Taurochenodeoxycholic acid (TCDCA)	2.21 (0.64 – 2.78)	0.46 (-0.45 – 1.61)	0.04326
Taurodeoxycholic acid (TDCA)	0.86 (0.63 – 1.52)	0.04 (-0.52 – 1.25)	0.07526

Taurolithocholic acid (TLCA)	0.07 (0 – 0.20)	0.02 (0 – 0.18)	0.5148
Tauromuricholic acid (a + b) (TMCA(a+b))	0.11 (0.06 – 0.18)	0.00 (-0.11 – 0.06)	0.01469
Tauroursodeoxycholic acid (TUDCA)	0.07 (0.03 – 0.19)	0.02 (-0.04 – 0.09)	0.1211
Ursodeoxycholic acid (UDCA)	0.17 (-0.84 – 0.53)	0.10 (-0.11 – 1.16)	0.9118
Total Primary	-2.05 (-3.83 – 0.75)	0.57 (-4.88 – 6.91)	0.2176
Total Conjugated Primary	0.89 (-3.59 – 4.53)	3.80 (-5.35 – 8.72)	0.2176
Total Secondary	24.19 (10.19 – 43.22)	11.00 (-7.20 – 31.46)	0.4813
Total Conjugated Secondary	11.02 (7.63 – 17.93)	5.19 (-11.09 – 19.50)	0.315

Table 7 Comparison of incremental AUC of bile acids after acute metformin dosing, between tolerant and intolerant cohorts. Data shown as median (IQR), μM^hr. p value for Mann Whitney U test, with Bonferroni correction, significance level = $p < 0.0024$. Three of the twenty measured bile acids were below the LOD, and therefore not analysed.*

Discussion

Metformin intolerance is a common and costly challenge in the management of type 2 diabetes. Despite metformin's status as first line medical treatment for T2DM, its mechanism of action is still debated. Although widely accepted that metformin acts in the liver to reduce gluconeogenesis (72), there is increasing evidence that metformin may exert some of its effect via the gastrointestinal tract (77), and it is unclear which of these potential mechanisms of action may be linked to metformin intolerance. In this study of extreme intolerance, we have shown for the first time that metformin intolerance is unlikely to be mediated by differences in absorption, distribution or elimination of metformin. We also demonstrate that intolerance is not associated with lactate derived from anaerobic glucose metabolism in the gut, altered systemic bile acid or serotonin concentration.

Metformin uptake from the intestine is predominantly via three transporters: OCT1, PMAT and SERT. In observational studies using GoDARTS data, Dujic et al demonstrated increased risk of metformin intolerance in those with reduced function alleles for OCT1 (29), and latterly SERT transporters (47). Studies investigating the effect of OCT1 genotype on the pharmacokinetics of metformin have reported varying results. Shu et al show that, following acute dosing with metformin, the area under the plasma concentration–time curve (AUC) of metformin was significantly greater in those with OCT1 variants compared to those with wild type OCT1 (34). However, steady state pharmacokinetics of metformin appear to be independent of OCT1 genotype (31). Christensen et al identified a number of SNPs in PMAT which were associated with reduced trough steady-state metformin concentrations, significant to $p < 0.05$ level, but this result did not withstand multiple testing (32). The above studies indicate that systemic metformin concentration may differ according to transporter genotype, and genotype has been associated with risk of intolerance, therefore we wanted to see if systemic metformin concentration was associated with intolerance. Our study shows that, despite a well-defined extreme intolerant phenotype, with 90% of the intolerant participants experiencing symptoms of metformin intolerance

after a 500mg dose, neither the C_{max} nor t_{max} (and therefore absorption) of metformin, were significantly different between cohorts (Table 6). The lack of association of metformin PK with severe intolerance suggests that the association reported of OCT1 and SERT variants altering metformin intolerance may reflect an impact of these transporter variants on local rather than systemic metformin concentrations.

We identified a surprising difference in baseline metformin concentration, resulting from detectable metformin in the plasma of the tolerant group after 72 hours washout. The detection of metformin after 72 hours washout may represent an improvement in metformin assay: from gas chromatography, to high-performance liquid chromatography and now liquid chromatography with tandem mass spectrometry. Results from the original pharmacokinetic studies of the 1970s would suggest 72 hours without metformin should result in complete washout (17). The persistence of measurable plasma metformin at 72 hours is likely to be indicative of a two (or more) compartment model, with metformin taken up and released slowly, for example, by erythrocytes. The slow elimination phase of metformin from the erythrocyte compartment has a $t_{1/2}$ of 20 hours (16, 17, 278), compared to a plasma $t_{1/2}$ of 5.7 hours in subjects with normal renal function (16). This is the likely cause of the difference in the calculated plasma $t_{1/2}$ of the two cohorts, as the tolerant cohort had been at steady state while on metformin and likely had higher metformin accumulation in secondary compartments. In contrast, the intolerant group have depleted secondary compartments, which are absorbing some of the excess metformin, and leading to a shorter elimination half-life.

Where transporter dysfunction may lead to reduced efflux and the systemic concentration of metformin, it may also lead to increased enterocytic or intraluminal metformin concentration. Cycling of metformin between lumen and enterocyte, or uptake to enterocyte with reduced efflux, could lead to increased local metformin concentration. The resulting increase in glucose uptake and anaerobic glucose utilisation, leads to a subsequent rise in intracellular lactate

concentration (19, 21, 124, 125, 127). As intracellular lactate rises, it is released into the systemic circulation. Therefore, measuring plasma lactate concentration can be used as a proxy measure of lactate production secondary to intestinal metformin concentration. Serum lactate concentration was not significantly different between tolerant and intolerant cohorts, indicating that enterocyte metformin concentration was similar in both groups. Both groups did see a rise in lactate from 2 hours, peaking around 3.5 hours post-dose, at a mean maximum concentration of 2.4mmol/L, which is above the normal range in clinical practice. Portal venous sampling for lactate concentration may provide a more accurate measure of intestinal lactate production, when compared to peripheral concentrations, but this is extremely challenging to carry out in humans and beyond the scope of this pharmacokinetic study.

The use of metabolomics to measure serotonin and bile acids gave further insight to metformin intolerance. Serotonin was detectable using the Biocrates p180 panel, but metformin dosing did not increase serotonin concentrations. However, this does not rule out a local effect of metformin on serotonin uptake by SERT. Bile acid concentrations varied post-metformin dosing, however we did not identify a difference in systemic concentrations of the individual or grouped bile acid concentrations between tolerant and intolerant cohorts. There was a trend toward a lower total AUC for DCA (deoxycholic acid – a secondary bile acid from the conversion of cholic acid by 7 α -dehydroxylase) in the intolerant group ($p = 0.052$). This is interesting as most bile acids are reabsorbed in the terminal ileum, whereas DCA is absorbed from the colon (152). A reduced plasma concentration may indicate a reduced uptake of DCA, resulting in accumulation in the colon, which could potentially lead to bile acid diarrhoea. Further studies are required to investigate the role of the microbiome, and subsequent changes to bile acid metabolism, in metformin intolerance.

Limitations

We acknowledge this study has a number of limitations. Firstly, the study had a small sample size, but was powered to detect a 30% change in metformin AUC between cohorts. We deemed a priori this would be a clinically important difference when comparing such extremes of intolerance. The similarity in the mean concentrations for the two groups, and overlap of the distributions of individual values, are not consistent with these parameters explaining the mechanism for the marked difference in tolerance seen in these two groups. However, the point estimates for some of the PK parameters and lactate do differ and this difference might achieve statistical significance if the sample size were much larger so it is possible that more subtle differences in metformin PK or the other measures evaluated do contribute to metformin intolerance.

Secondly, we observed incomplete washout of metformin in the tolerant cohort which highlights the need for a longer washout in future studies, but as discussed above, the metformin level at baseline was very low when compared to the peak post-dose concentration and did not impact upon the parameters of metformin absorption.

Thirdly, metformin is known to increase GLP1, and it is possible that this may lead to gastrointestinal symptoms in some cases. However, we were unable to measure GLP1 in our study cohort, due to the concurrent use of DPP4 inhibitors and GLP1 receptor agonists.

We also acknowledge that the administration of metformin two hours prior to food is not in line with clinical practice, and that this may increase the risk of metformin intolerance. In clinical practice, patients are asked to take metformin with or after food, in an attempt to reduce intolerance. However, drug administration in the fasted state is standard practice in pharmacokinetic studies, as this removes confounding factors of digestion and gastrointestinal transit time, which could significantly alter the pharmacokinetics including bioavailability, C_{max}, and T_{max}.

Of note, if intolerance was simply the effect of taking metformin without food, this would likely have been evident in both groups.

Finally, serum lactate concentration increased 2 hours post-metformin dosing, but a potential confounding factor for this rise in lactate is the ingestion of a carbohydrate-rich meal at 2h post-metformin. However, previous studies in healthy volunteers indicate that the lactate concentrations increased transiently to a maximum at 90 minutes post mixed meal, returning to baseline by 180 minutes (279). Participants in the study received a second carbohydrate-rich meal at 5 hours post-metformin dosing, which did not correspond with a further peak in serum lactate. This supports the conclusion that the rise in and peak lactate concentration is associated primarily with metformin dosing, as opposed to ingestion of a carbohydrate-rich meal.

Conclusion

In conclusion, in this pharmacokinetic study of well-defined extreme metformin intolerant and tolerant individuals, we ruled out multiple potential systemic effects of metformin that may have contributed to metformin intolerance. We showed that the difference between tolerant and intolerant cohorts in the absorption, distribution or elimination of metformin, or in systemic lactate, serotonin or bile acid concentrations, were too small to be the mechanism of intolerance.

Impact of OCT1 genotype and OCT1 inhibiting drugs on an individual's metformin tolerance (ImpOCT) study

Contributions:

The following chapter discusses the “Impact of OCT1 genotype and OCT1 inhibiting drugs on an individual's metformin tolerance” (ImpOCT) study.

I wrote the study protocol with Prof Ewan Pearson. Statistical methodology was guided by Prof Peter Donnan. With assistance from Research Nurses Sheena Pritchard, Amanda Anderson and Shirley Fawcett, I recruited study participants and completed all study visits and data collection.

Interim analysis was performed by Prof Peter Donnan, University of Dundee, as an independent statistician.

Final statistical analysis was performed by me, with guidance from Simona Hapca, a statistician from the University of Dundee.

I am the sole author of this chapter.

Introduction

At physiological pH, metformin exists as a hydrophilic cationic species with low lipophilicity, meaning passive diffusion through cell membranes is unlikely (16). Metformin uptake from the intestinal lumen into the enterocyte is, therefore, transporter dependent, predominantly relying on OCT1, PMAT and SERT (23). This transporter-dependent mechanism of uptake is saturable (22) and susceptible to variability in efficacy, due to genetic variation in the transporters, or competitive inhibition by other substrates (280). Theoretically, these factors could impact upon the pharmacokinetics (PK), pharmacodynamics (PD) and tolerability of metformin, by altering bioavailability, absorption and likelihood of drug-drug interactions (DDI) (30, 34, 281, 282).

Metformin intolerance affects up to 25% of those exposed (29), with approximately 5% of those treated with metformin discontinuing therapy due to adverse effects. However, the mechanism and variability of intolerance is poorly understood. Disruption of metformin uptake from the gastrointestinal tract results in an increase in the time the intestinal lumen and enterocytes are exposed to metformin. This may increase local or systemic lactate; alter the bile acid pool; increase intestinal GLP1, serotonin or histamine; or alter the microbiome, all potential mechanisms of metformin intolerance (77).

Transport via OCT1 accounts for approximately 25% of metformin uptake from the gastrointestinal tract (23). OCT1, a polyspecific transporter of the SLC22A family, is implicated in the absorption of numerous commonly prescribed medications (26, 56, 283) – see Appendix 3. This poly-specificity exposes substrates to competitive inhibition, and increases the risk of DDI. Metformin can act as victim or perpetrator in OCT1-related DDI (30), as demonstrated by in vitro, observational and in vivo studies, as shown in Table 8. DDI may affect the pharmacokinetics and pharmacodynamics (PK/PD) of metformin, including tolerability, for the individual.

Drug	Metformin	Effect	Study type	Author
PPI	Victim	Increased metformin intolerance	Human, observational cohort	Dujic et al (29)
Pantoprazole, rabeprazole	Victim	Increased metformin C _{max}	Human, interventional	Kim et al (284)
PPIs: omeprazole, lansoprazole, pantoprazole, rabeprazole	Victim	Reduced uptake of metformin	In vitro	Nies et al (285)
Trospium	Perpetrator	Reduces AUC and C _{max} of trospium	Human, interventional	Oefelein et al (286)
Rifampicin	Victim	Increased AUC and renal clearance of metformin	Human, interventional	Cho et al (287)
Verapamil	Victim	Decreased glucose-lowering effect of metformin	Human, interventional	Cho et al (288)
Berberine	Victim	Increased AUC, decreased clearance of metformin	In vitro	Kwon et al (289)
Clopidogrel	Victim	Decreased liver uptake of metformin	In vitro	Li et al (290)
Quinidine	Victim	Decreased liver uptake of metformin	In vitro	Li et al (290)
Repaglinide	Victim	Decreased liver uptake of metformin	In vitro	Bachmakov et al (291)
Tyrosine kinase inhibitors	Victim	Inhibit metformin uptake	In vitro	Minematsu et al (292)

Table 8 OCT1-related drug-drug interactions involving metformin

Genetic polymorphisms in transporter genes may contribute to variability in drug response (293). Human OCT1 is highly polymorphic (281), with over 85 polymorphisms identified across 52 population groups (294), of which 34 polymorphisms were considered in detail in a recent systematic review (295). Mofo Mato et al demonstrated that the role of OCT1 polymorphisms in therapeutic response to metformin is population specific, with significant difference in the allele frequencies of polymorphisms across different ethnic groups (295), for example, the allele frequency of M420del is 18.5% in Caucasian compared to 5% in African American populations (281).

In study populations of European descent, the most commonly documented OCT1 polymorphisms are M408V (minor allele frequency, MAF = 59.8%), M420del (18.5%), R61C (7.2%), F160L (6.5%), G465R (4%), and G401S (1.1%) (296). Of these, M420del, R61C, G465R and G401S exhibit reduced function in cellular models of OCT1 and its variants, demonstrated as reduced uptake and response to metformin (Figures 23 and 24, reproduced with permission from Shu et al) (281).

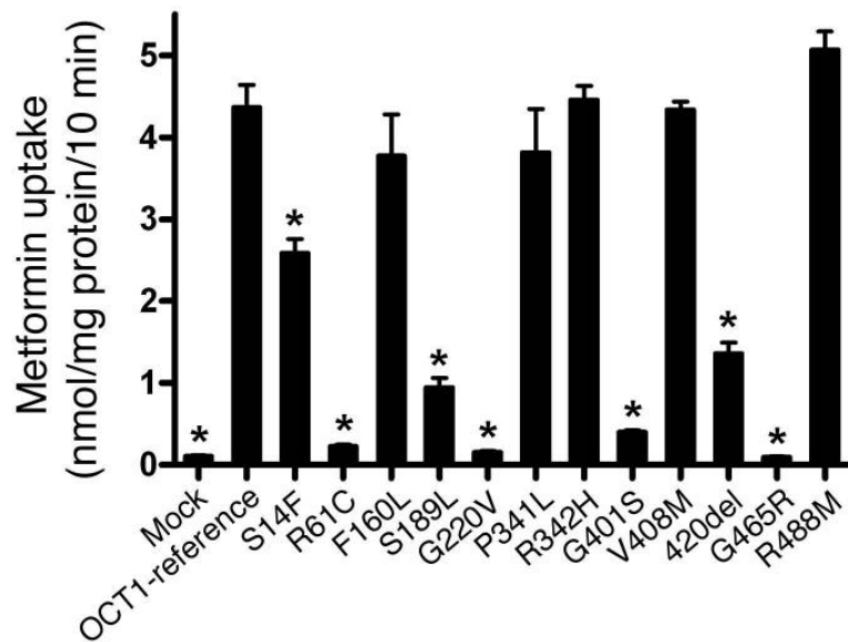


Figure 23 Metformin uptake in stably transfected HEK293 cells expressing OCT1 and its variants. Reproduced with permission from Shu et al.

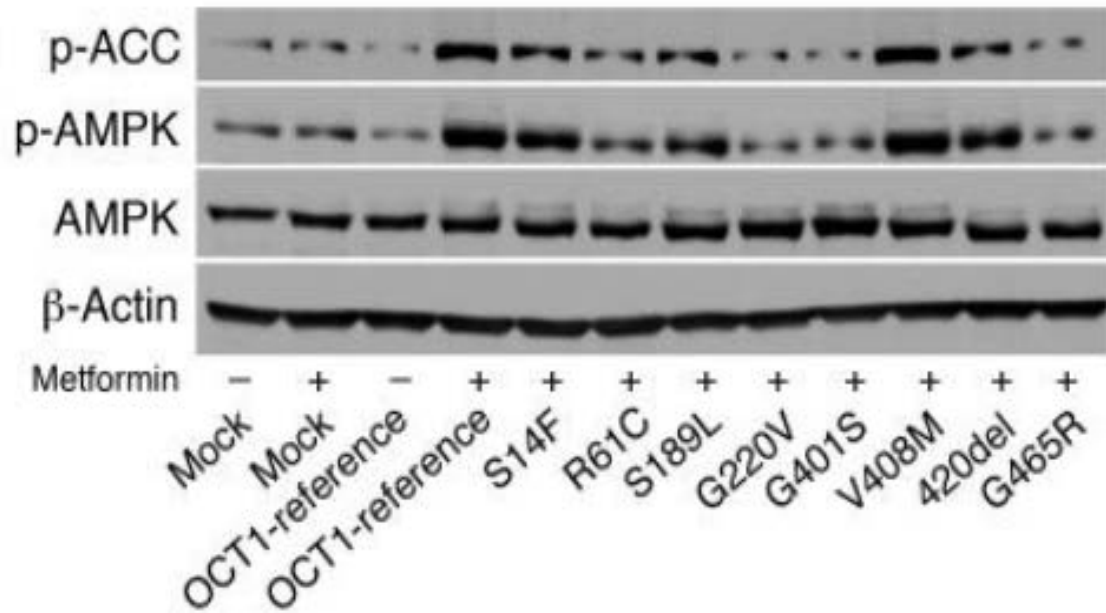


Figure 24 Metformin response in HEK293 cells, transfected with OCT1 and its variants. There is an associated reduction in phosphorylation of AMPK and ACC with all OCT1 variants, except M408V. Reproduced with permission from Shu et al.

Table 9, below, summarises the current evidence for the impact of OCT1 genetic variation on the PK/PD of metformin, focussing on Caucasian populations:

Variant studied	Study Model	PK effect	PD effect	Author	Year
Oct1 knockout mice (-/-) and heterozygote mice	Mouse hepatocyte	Reduced hepatic uptake and accumulation of metformin, according to number of reduced function Oct1 alleles	Reduced AMPK activation, resulting in reduced inhibition of hepatic gluconeogenesis. Fasting plasma glucose reduction lost in Oct1(-/-) mice	Shu et al (281)	2007
OCT1 R61C / M420del / G465R / G401S vs OCT1 wild type	OGTT in healthy Caucasian volunteers, with and without metformin	Not assessed	After metformin treatment, individuals with OCT1 polymorphisms had significantly higher plasma glucose levels and glucose AUC during OGTT, compared to those with OCT1 wild type	Shu et al (281)	2007
OCT1 R61C / M420del / G465R / G401S vs OCT1 wild type	PK study of metformin in healthy Caucasian volunteers, with and without OCT1 variants	Lower volume of distribution; higher AUC; higher Cmax and lower oral clearance of metformin in OCT1 variants	Not assessed	Shu et al (34)	2007

Variant studied	Study Model	PK effect	PD effect	Author	Year
Ten polymorphisms of OCT1, including R61C / M420del / G465R / G401S	PK study of healthy Caucasian male volunteers	Polymorphisms in OCT1 increase renal clearance in a gene-dose dependent manner	Not assessed	Tzvetkov et al (62)	2009
OCT1 R61C / M420del	Observational cohort study of Caucasian patients with T2DM, using GoDARTS data (176)	Not assessed	Loss of function variants did not affect glycaemic response to metformin	Zhou et al (173)	2009
Twelve SNPs (both coding and tagging) of OCT1	Observational cohort study of Caucasian patients with T2DM, using data from the Rotterdam Study	Not assessed	Glycaemic response to metformin reduces with increasing number of minor alleles of rs622342	Becker et al (297)	2009
OCT1 R61C / M420del / G465R / G401S, along with polymorphisms in OCT2 / MATE / PMAT	PK / PD study of metformin transporter polymorphisms in European patients with T2DM	Lower trough metformin concentration at steady-state in M420del heterozygotes. Additive decrease in trough concentration with increasing	Initially reported impact of OCT1 genotype on HbA1c during metformin treatment (32). This signal was lost when data were adjusted for baseline HbA1c (33)	Christensen et al (32)	2011

Variant studied	Study Model	PK effect	PD effect	Author	Year
		number of LOF haplotypes			
OCT1 R61C / M420del / G465R / G401S vs OCT1 wild type	PK study of steady state metformin in healthy European volunteers with 0,1 or 2 variant alleles in OCT1	No difference in steady state AUC of metformin	Not assessed	Christensen et al (31)	2015
OCT1 R61C / M420del / G465R / G401S / C88R vs OCT1 wild type	Observational cohort study of Caucasians patients with T2DM, using GoDARTS data (176)	Not assessed	Increasing risk of metformin intolerance in those: using OCT1 inhibiting drugs; with LOF OCT1 variant; and combination of LOF genotype and inhibiting drugs	Dujic et al (29)	2015
OCT1 M420del / R61C	Prospective observational study of Caucasian patients with newly diagnosed T2DM	Not assessed	Number of reduced function alleles associated with increased risk of metformin intolerance	Dujic et al (298)	2016
Nine candidate polymorphisms in five transporter genes, including	Meta-analysis of pharmacogenomic studies of metformin response in European	Not assessed	No significant impact of polymorphisms on metformin response	Dujic et al (51)	2017

Variant studied	Study Model	PK effect	PD effect	Author	Year
OCT1 R61C / M420del / rs622342	patients with T2DM, using MetGen data (171)				

Table 9 Studies in Caucasian populations, describing impact of OCT1 genetic variation on PK/PD of metformin

As demonstrated in Table 9, the evidence regarding the impact of OCT1 genotype on metformin PK/PD has, thus far, been inconsistent. The somewhat contradictory nature of these results is likely attributable to the variation in study populations, including genetic, physiological and environmental factors. The study designs were also varied, and often observational in nature.

Of particular interest is the gene x drug x drug interaction between OCT1 genotype, OCT1 inhibiting drugs, and metformin, which was observed by Dujic et al in a Scottish Caucasian population (29). Using GoDARTS data (176), they identified an increased risk of metformin intolerance with loss of function variants in OCT1, with the odds ratio of intolerance increasing further with the addition of other OCT1 inhibiting drugs (29). As already discussed, many commonly prescribed medications are substrates of OCT1, including PPIs, codeine, and anti-hypertensives such as doxazosin. This observed association is therefore potentially clinically applicable – if inhibiting drugs could be replaced with alternatives which were independent of OCT1 transportation, clinicians could help increase metformin tolerance and improve efficacy by achieving optimal dosing.

Joint effects of OCT1 genotype and OCT1 interacting drugs on intolerance		
	OR (95% CI)	<i>p</i>
One or no reduced-function allele carriers not treated with OCT1 inhibiting drugs [*]	1.00	
One or no reduced-function allele carriers treated with OCT1 inhibiting drugs [†]	1.62 (1.16-2.26)	0.005
Two reduced-function alleles carriers not treated with OCT1 inhibiting drugs [‡]	2.27 (1.13-4.58)	0.022
Two reduced-function alleles carriers treated with OCT1 inhibiting drugs [§]	4.13 (2.09-8.16)	<0.001

OR, odds ratio for intolerance. Analysis was adjusted for age, sex, and weight.

^{*}93 intolerant and 1030 tolerant patients;
[†]84 intolerant and 516 tolerant patients;
[‡]12 intolerant and 70 tolerant patients;
[§]16 intolerant and 34 tolerant patients.

Table 10 Effect of OCT1 genotype and inhibiting drugs on metformin intolerance. Reproduced with permission from Dujic et al (9).

In the population studied by Dujic et al, proton pump inhibitors were the most commonly prescribed OCT1 inhibiting drug with 17.6% of the study population treated with a PPI (29). The most common OCT1 polymorphism was M420del, with a minor allele frequency of approximately 19.1%. While approximately 40% of the study cohort carried one loss of function allele for OCT1, a further 8.4% carried two loss of function alleles (29). This is a significant proportion, especially when we consider that the incidence of metformin intolerance is often quoted as between 20 and 30%, with approximately 5% discontinuing therapy due to adverse effects. Could this 5% represent the OCT1 RF individuals treated with metformin and a second OCT1 inhibiting drug?

Thus far, interventional studies of OCT1 genotype and metformin have focused on PK / PD. To our knowledge, no interventional studies have considered the effect of OCT1 genotype, or indeed OCT1 dependent drug-drug interactions, on the tolerability of metformin treatment.

This chapter focuses on the Impact of OCT1 genotype and OCT1 inhibiting drugs on an individual's metformin tolerance (ImpOCT) study, which was designed to investigate the impact of OCT1 genotype and use of OCT1 inhibiting drugs, such as PPIs, on metformin intolerance.

Hypothesis and Aims

The study was designed to investigate the observed gene x drug x drug interaction between OCT1, metformin and PPIs, described by Dujic et al (29, 298).

We hypothesised that participants with OCT1 reduced function genotype would have a reduced tolerance of metformin:

- i. compared to those with OCT1 wild type, and
- ii. during treatment with concomitant omeprazole compared to concomitant placebo treatment.

Therefore, the aim of the study was to demonstrate a difference in maximum tolerated dose of metformin between genotypes and when taking concurrent OCT1 inhibiting drug.

Materials and Methods

The ImpOCT study was conducted between the University of Dundee Clinical Research Centre between April 2016 and April 2018. It was co-sponsored by the University of Dundee and NHS Tayside, with ethical approval granted by the East of Scotland Research Ethics Committee. The study was conducted in accordance with the Good Clinical Practice guidelines, and the Declaration of Helsinki.

The study was registered on <http://clinicaltrials.gov> (identifier NCT02586636). Formal written informed consent was obtained from each individual prior to inclusion.

Study design

A recall-by-genotype recruitment model (see Methods: Recruit-by-Genotype (RBG) Studies) was used to populate a randomised, placebo-controlled, double-blind crossover study comparing metformin tolerance during concurrent omeprazole vs placebo use, across OCT1 genotypes.

Study duration was a total of 9 - 10 weeks, consisting of two x four week treatment periods, separated by a washout period of one to two weeks. During each treatment period, metformin was administered as an oral tablet, along with the concurrent treatment (placebo or omeprazole), taken as one capsule twice daily throughout. The concurrent medication was over-encapsulated and labelled by Tayside Pharmaceuticals, as shown in Figure 25 below, to maintain blinding of both researcher and participant.

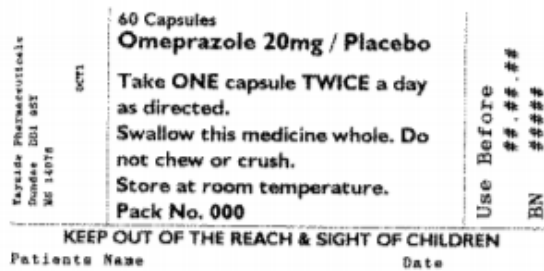


Figure 25 Labelling and over-encapsulation used to maintain blinding of the treatment order for the concurrent medication.

The metformin dose was titrated over each four week treatment period, according to the individual's tolerance, to a maximum of 2000mg daily, in divided doses. Dose titration was on a weekly basis, to establish the individual's maximum tolerated dose i.e. the highest dose at which metformin is agreeable to the participant, without gastrointestinal symptoms of intolerance.

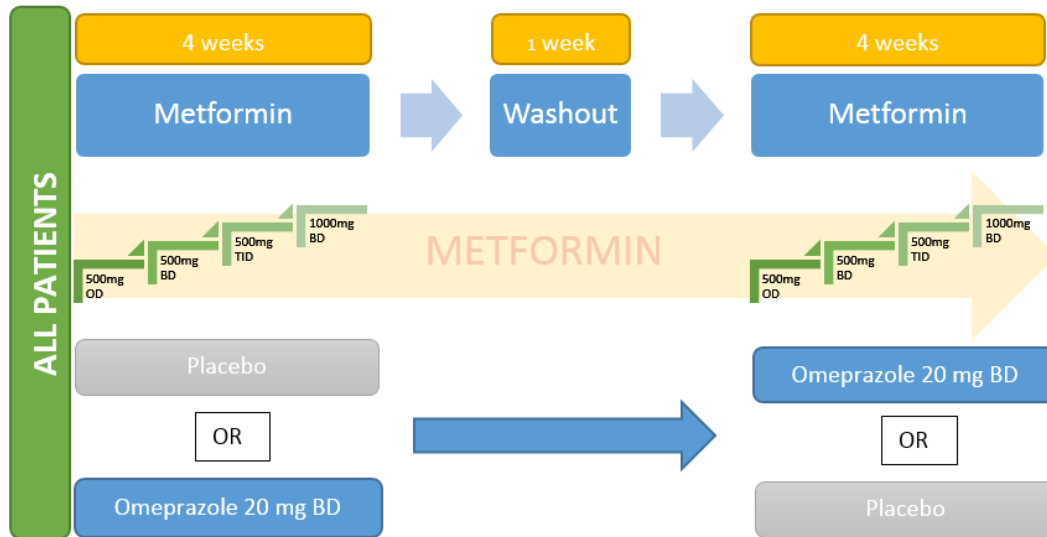


Figure 26 Infographic of the participant journey through the ImpOCT study

Recruitment

Healthy volunteers were recruited, according to their OCT1 genotype, from three Scottish bioresources with genotypic data available - the GoDARTS (176), GoSHARE and GS:SFHS studies (see Methods: Bioinformatics Resources). All participants were White Scottish, non-diabetic individuals with either **two** loss-of-function (LOF) alleles (herein referred to as OCT1 reduced function, RF) or **zero** LOF alleles (OCT1 wild type, WT). We included those with R61C and M420del variants, as these account for the majority (92%) of OCT1 genetic variants in the GoDARTS cohort (29), and also only occur as a haplotype with the wild type allele of each other (29, 298). Other inclusion and exclusion criteria are shown in table 11 below.

Inclusion	Exclusion
Aged 18 - 80	Heterozygous OCT1 genotype i.e. only one loss of function allele
White Scottish	Previous treatment with metformin
OCT1 reduced function or OCT1 wild type	Previous diagnosis of diabetes
Able to complete the symptom severity score and Bristol stool chart independently i.e. no cognitive impairment or visual impairment	Recent involvement (<30 days) in a CTIMP
Normal renal function – eGFR>60	Pregnancy or planning to conceive
	Inability / unwillingness to comply with the protocol
	No known gastrointestinal pathology e.g. inflammatory bowel disease, IBS, coeliac
	Daily treatment with PPI, anti-spasmodic, or anti-motility drugs
	Daily OCT1 inhibiting drugs (unless able to withhold during study period)

Table 11 Inclusion / exclusion criteria for the ImpOCT study

Participants were initially recruited from GoDARTS, before expanding to GoSHARE and, latterly, GS:SFHS. Potential participants were identified by the Health Informatics Centre at the University of Dundee, using the above genotypic

and phenotypic criteria, and were invited to participate via invitation letters (GoDARTS, GoSHARE and GS:SFHS) or telephone calls (GoSHARE).

In our first mail-out via GoDARTS, we subdivided the potential participants into age brackets, and sent an equal number of letters to each genotype, attempting to keep recruitment within the 50-60 year old age bracket, in an attempt to match the cohorts for age. The age bracket was expanded in stages as recruitment continued.

The contact details (excluding genotype) of individuals who responded positively to the invitation letters were made available to the research team via the HIC recruitment tracker, shown below.

The screenshot shows the HIC Recruitment Tracker interface. At the top left is the HIC logo (health informatics centre) and at the top right is the University of Dundee logo. Below the logos is a navigation menu with links: Home, Summary, Patient Search, Information, Reports, Change Password, and Logout. The current project is ImpOCT. The Patient Search section has two dropdown menus: 'View patients with Status: All' and 'View patients with Group: All'. To the right is a search input field labeled 'Search for a patient (name, cohort ID, studyID or CHI):'. Below the search field are three buttons: Search, Clear Search, and Add New Patient. At the bottom, there is a table header with columns: Cohort ID, CHI, Study ID, Group, Patient Name, Contact Advice, Date Consented, Date Contacted, and Recruitment Status. The text 'Showing 15 of 136 Patients Toggle View' is visible above the table.

Figure 27 Screenshot of the HIC recruitment tracker used in the ImpOCT study

Individuals were then contacted by telephone by the research team to discuss the study in more detail and to arrange the screening visit.

As there is overlap between the GoDARTS, GoSHARE and GS:SFHS cohorts, duplicates within the identified potential participants were removed at each

expansion of the recruitment cohort, to prevent repeat invitations and inconvenience for both participants and the research team.

Potential participants from GoSHARE were contacted by telephone or letter by the GoSHARE team to assess interest in the study. The details of those who voiced interest in participating were then passed to HIC, where their details (excluding genotype) could be added to the recruitment tracker for further contact by the research team.

Intervention and sampling schedule

Participants attended the research centre on three occasions – at baseline, at the end of treatment period one and finally at the end of treatment period two. Blood, urine and stool samples were taken at each visit. Baseline HbA1c and U+Es, to exclude undiagnosed diabetes and renal impairment respectively, were processed as part of screening. U+Es were analysed at each subsequent visit to ensure no deterioration in renal function which could be a contraindication to ongoing metformin treatment. The remaining samples were processed and stored at the Clinical Research Centre for future analysis.

	TREATMENT PERIOD ONE W/O TREATMENT PERIOD TWO									
	Baseline	End of week number:								
		1	2	3	4	5	6	7	8	9
Example Metformin dosing:		500 mg OD	500 mg BD	1000 / 500 mg	1000 mg BD	Nil	500 mg OD	500 mg BD	1000 / 500 mg	1000 mg BD
Blinded treatment (omeprazole or placebo)		1 cap BD	1 cap BD	1 cap BD	1 cap BD	Nil	1 cap BD	1 cap BD	1 cap BD	1 cap BD
Medical and drug history	X									
BMI	X				X					X
Bloods	X				X	(X)				X
Urine	X				X					X
Stool	X				X					X
Symptom severity score		X	X	X	X		X	X	X	X
Bristol stool chart		X	X	X	X		X	X	X	X
Con Meds		X	X	X	X		X	X	X	X
Adverse effects		X	X	X	X		X	X	X	X

Table 12 Intervention and sampling schedule for the ImpOCT study

Randomisation

The concurrent medication treatment order (omeprazole / placebo; placebo / omeprazole) was randomised across and within the genotypic groups, using a double randomisation. Therefore, within the two genotypes studied, there was randomisation of treatment order, but with equal numbers allocated to each treatment order within genotype.

Tayside pharmaceuticals performed the double randomisation using www.randomization.com, and held the seed list until data locking.

PACK ID	Treatment 1	Treatment 2	OCT1 Status
1	Placebo	Omeprazole	Combined type 0
2	Omeprazole	Placebo	Combined type 0
3	Omeprazole	Placebo	Combined type 2
4	Placebo	Omeprazole	Combined type 2
5	Omeprazole	Placebo	Combined type 2
6	Placebo	Omeprazole	Combined type 2

Table 13 Excerpt from the randomisation table, produced by Tayside Pharmaceuticals, to dictate concurrent medication treatment order.

Clinical trials pharmacy were blinded to treatment order, and semi-blinded to genotype. They were informed of genotype “A” or “B” to determine the allocation of the appropriate treatment pack to the new participant, according to the pack information given by Tayside Pharmaceuticals. This enabled pharmacy to inform

the research team when interim analysis could be performed (see Statistical Methods).

Participants and research team were blinded to genotype and treatment order throughout the study. Only after data locking was the treatment order and genotype for each individual revealed to the research team.

Symptom severity score and dose titration

Participants were followed-up on a weekly basis by telephone consultation, and monitored for symptoms of metformin intolerance. At the end of the treatment period, the maximum tolerated dose was documented as the highest dose achieved without symptoms of intolerance.

Dose titration followed a predetermined guideline (figure 28, below), to ensure dose titration was objective across participants and members of the research team.

The titration of metformin dose was determined by the participant-perceived tolerance, a calculated symptom severity score (Metformin Intolerance Symptom Severity Score, MISSS), and participant inclination. These dictated whether or not the dose of metformin should be titrated up, down or remain at the current dose.

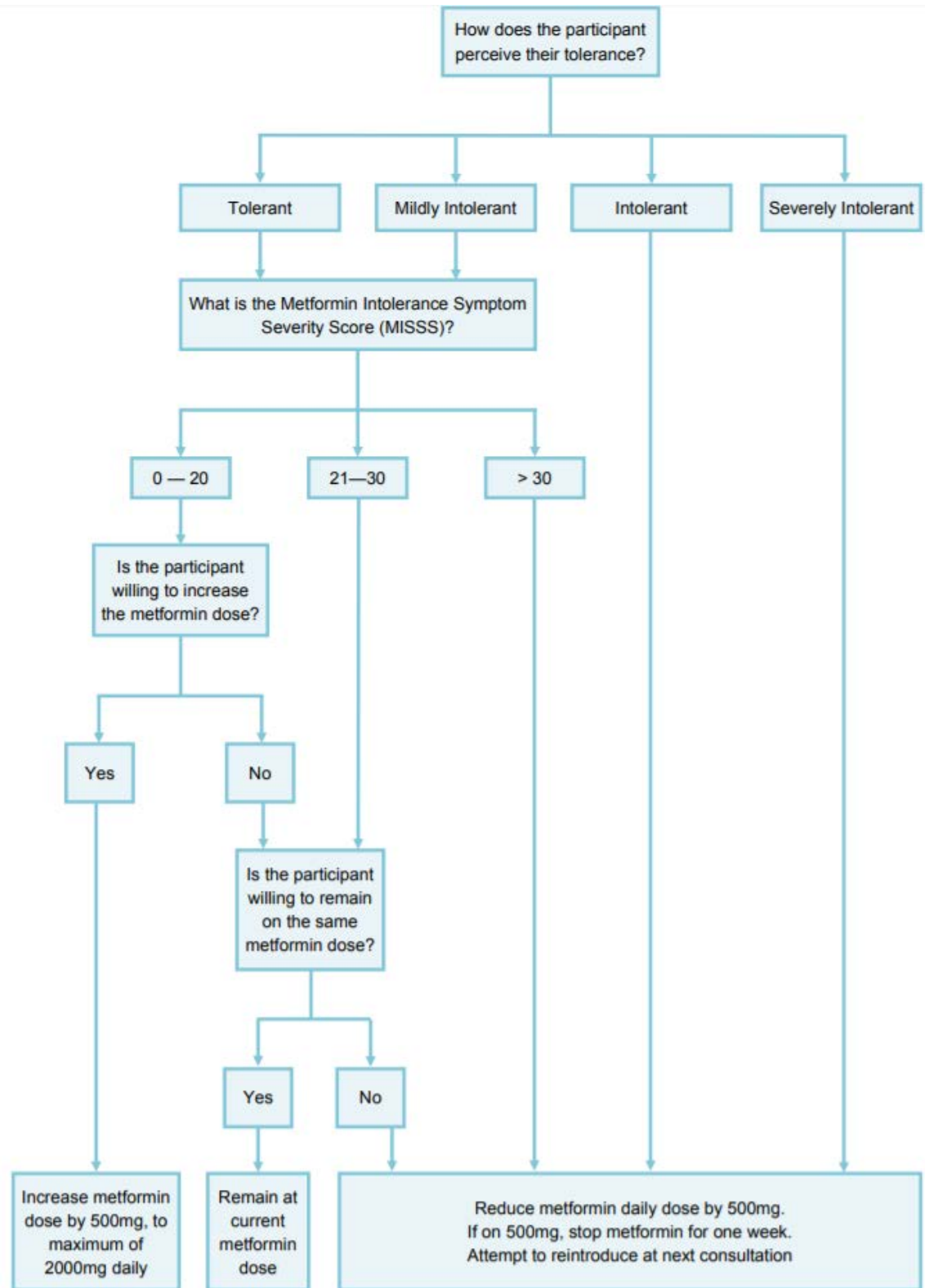


Figure 28 Decision aid for metformin dose titration in the ImpOCT study

The “Metformin Intolerance Symptom Severity Score” (MISSS) was designed for use in this study, but will be applicable to future studies of metformin intolerance. To investigate mechanisms and management of metformin intolerance, we first need to be able to diagnose, assess severity and monitor symptoms of metformin intolerance. However, there are currently no research tools available specifically to assess metformin intolerance. While some questionnaire-based scoring systems, such as the Irritable Bowel Syndrome Severity Scoring System (IBS-SSS) (299) or Severity of Dyspepsia Assessment (SODA) (300), cover some of the symptoms of metformin intolerance, some of their content is inappropriate for use in this setting. Therefore, we have designed a symptom severity score for metformin intolerance, which can be used to define the phenotype of intolerance in research, or to potentially guide clinical management of metformin intolerance.

The Metformin Intolerance Symptom Severity Score (MISSS) (Appendix 2) consists of ten questions. The MISSS incorporates adherence, symptoms of nausea, vomiting, pain, bloating and diarrhoea. In the case of discontinuation of the medication, it considers previously tolerated dosing, or use of modified-release preparations. Finally, it assesses the patient-perceived tolerance, as this will greatly impact upon compliance with treatment. The total maximum score is 50, with the severity score sub-divided as follows: 0-10 = tolerant; 11-20 = mildly intolerant; 21-30 = moderately intolerant; >30 = severely intolerant.

The MISSS was developed based on the well-documented, common GI symptoms of metformin intolerance. We asked participants of the Pharmacokinetics of Metformin Intolerance (POMI) study (213) to complete the score, to confirm their phenotype of “tolerant” or “intolerant” individuals. The study recruited ten white European participants with type 2 diabetes, who were phenotypically intolerant to metformin, with a matched cohort of ten metformin tolerant individuals (matched for age, gender and BMI), and is described in detail in Chapter 3. In the POMI study, we used the MISSS to confirm the participants’ phenotype, to show that the recruitment criteria used to define an individual as phenotypically intolerant had correctly identified those with gastrointestinal

symptoms of metformin intolerance. Figure 29, below, shows the mean MISSS scores for the two study cohorts in POMI, confirming that the recruited participants' phenotype had been correctly identified.

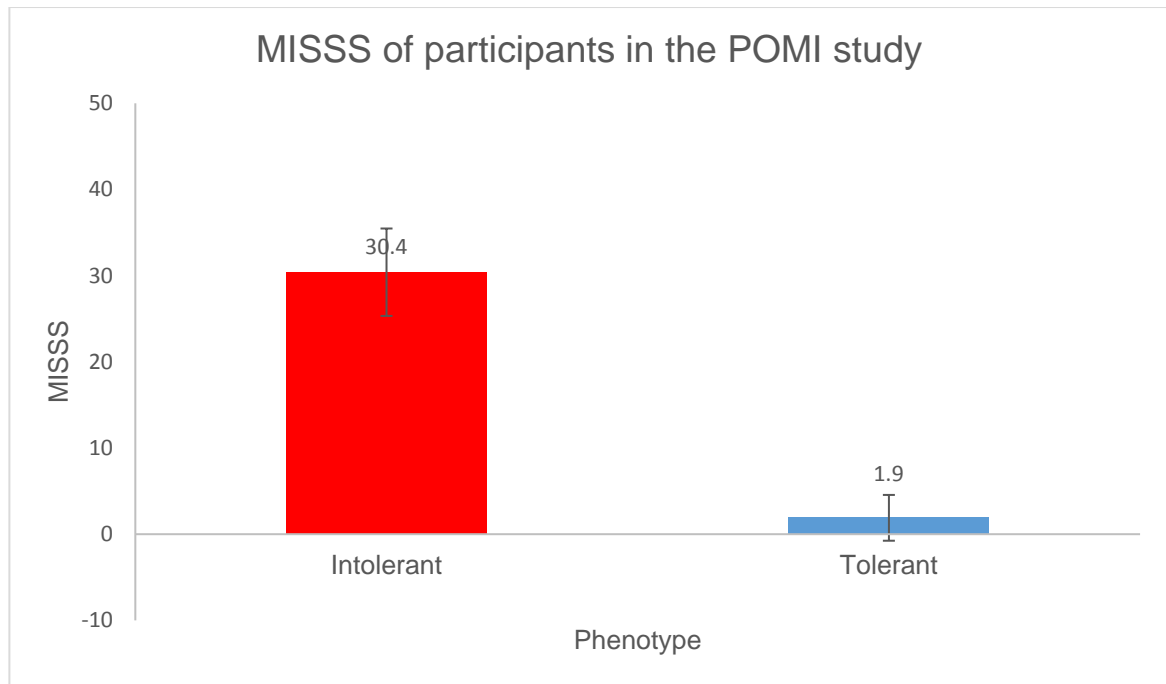


Figure 29 MISSS scores from participants of the POMI study. Data shown as mean with 95% confidence intervals.

The use of the MISSS in the POMI study demonstrates that the score correlated with the metformin intolerance phenotype, and could therefore be used to identify individuals with metformin intolerance. As per Figure 28, the MISSS was used in the ImpOCT study to identify those with intolerance but also to guide titration of metformin dose according to the severity of symptoms.

Statistical methods

Sample size

Accepting a difference of one pill of metformin at maximum tolerated dose as clinically significant, and assuming a SD = 1 with 90% power and 2-sided alpha of 0.05 in the sample size calculation, gives $n = 13$ for a standard crossover. As we have two cohorts A and B, then this would be 13 in each cohort. We chose a

target recruitment of 30 per cohort with interim analysis to allow the study recruitment to be halted if results are already showing significance.

We chose to recruit thirty participants in each cohort as this is a feasible number when considering the availability of genotypic data in, for example, the GoDARTS database, and accounting for the estimated response rate to invitation letters of 10%. We have based our initial estimation of the maximum sample size available on the known rate of reduced function allele incidence. The two most common reduced-function mutation have a combined frequency of approx. 25%, which means, for a person to have two reduced function alleles the likelihood is $0.25 \times 0.25 = 0.0625$ i.e. approximately 6% of the population should have two reduced function OCT1 alleles. On the other hand, the probability of having no reduced function alleles is $0.6 \times 0.6 = 0.36$, i.e. approximately 36% of the population have a normal, or “wild type”, OCT1 genotype.

Interim analysis

This study used the frequentist method of Lan-DeMets which incorporates an alpha spending function to build interim analyses at two recruitment landmarks – 10 v 10, and 20 v 20 and preserve the standard test for significance at the final analysis of $p < 0.05$. Interim analysis was carried out by Professor Peter Donnan, as an independent statistician with treatment allocation blinded. Using the alpha spending function of Lan-DeMets, meant that the initial interim analysis at 10 v 10 would have had to reach significance of $p < 0.0002$ to halt the study, which it did not. Further interim analysis at 20 v 20 needed to reach significance of $p < 0.012$, and again this was not reached. Advice was to complete the study to target recruitment of 30 v 30. Final analysis accepted statistical significance of $p < 0.05$.

Timing of analysis

Analysis of final data commenced after last patient last visit was completed, and data entry was completed and locked. The statistical analysis plan was completed and signed by research team and statistician prior to analysis commencing.

Analysis methods

Analysis was carried out using the statistical software “R Studio”. The data, where applicable, was assessed for normality using Shapiro-Wilks method and inspection of the distribution using QQ plots.

As this is a cross-over study, with correlated data (i.e. the same person assessed on treatment 1 and 2), it is in essence a repeated measures / paired approach for treatment effect. Assessment of genotypic effect is an unpaired fixed effect in the model.

The data were therefore analysed using mixed models, which contain both fixed effects (genotype, treatment, and period) and random (subject) effects. In the mixed model, the “y” outcome variable i.e. the response variable, is the maximum tolerated dose of metformin. This is an ordinal variable, therefore the R package “ordinal” was used for analysis (301). Alternatively, the outcome was transformed into a matrix for use in a generalised binomial model (data shown in Appendix 4: ImpOCT analysis).

In our primary analysis, we considered the independent effects of treatment and genotype, and well as an interaction term of treatment*genotype to assess whether the effect of treatment differs by genotype.

Secondary analyses included age, gender BMI and treatment order in the model, as potential contributing factors for intolerance. Further exploratory analysis was performed using generalised linear models (data in Appendix 4: ImpOCT analysis).

Results

Recruitment flow chart

Participants were initially recruited from GoDARTS, before expanding to GoSHARE and GS:SFHS. From the individuals in the GoDARTS cohort with genotypic information available, Health Informatics Centre (HIC) identified 4514 individuals who met the phenotypic inclusion criteria. Of these, 315 were OCT1 RF, and 2473 were wild type. A total of 543 invitation letters were sent, with 79 individuals responding positively. Of those, 34 were consented and included in the study, with 2 participants withdrawing at the subject's request.

Recruitment expanded to GoSHARE, where HIC identified 6224 individuals who met the phenotypic criteria. Of these, 1118 individuals had genotypic information available, of whom 635 were OCT1 wild type, and 84 were OCT1 RF. After removal of duplicated potential participants from GoDARTS, a total of 145 individuals were approached, with only 8 responding positively. Of these, 3 individuals were consented, with 1 withdrawing at the subject's request.

Recruitment finally expanded to include GS:SFHS, in which 8388 individuals with genotypic data available matched the phenotypic criteria. Of these, 580 individuals were OCT1 RF, and 4552 were wild type. A cohort list was passed to HIC, and 515 invitation letters sent, with 49 positive responses in total. Of these 29 were consented with 2 withdrawing at the subject's request.

Recruitment is summarised in Figure 30, below.

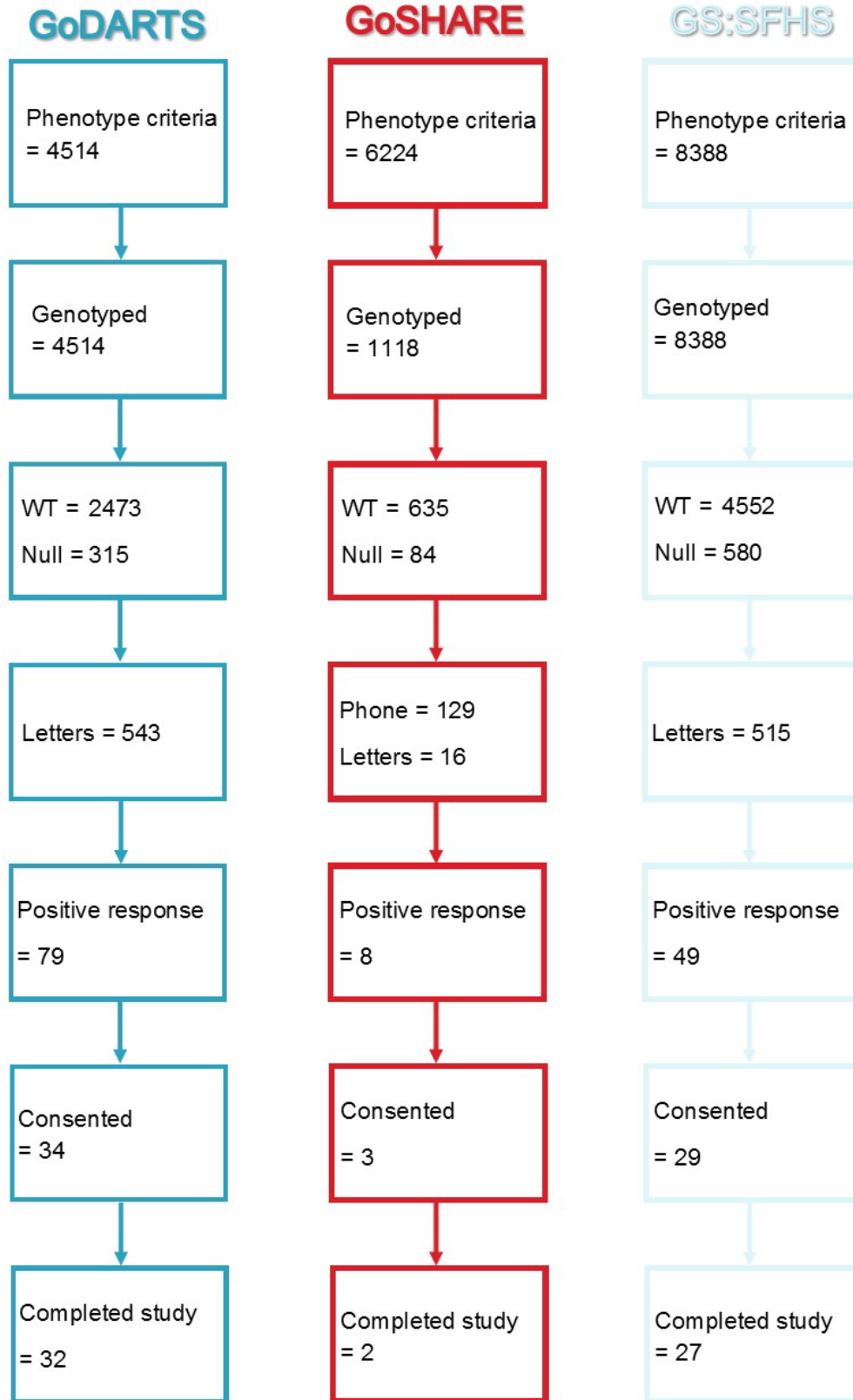


Figure 30 Flow chart of participant recruitment, from three bio-resources

Interim analysis did not reach the specified significance and the independent trial statistician advised recruitment should continue at each stage, to a final number of 30 v 30. Those who withdrew from the study (5 in total) were not included in final analysis, and were replaced with new participants. Unfortunately, our final participant withdrew prior to completing, so recruitment was re-opened at a late stage. Two individuals were recruited in an attempt to ensure that one would complete. In fact, both completed the study, hence a total of 61 participants completed the study. The breakdown of genotype and treatment order is shown in Figure 31:

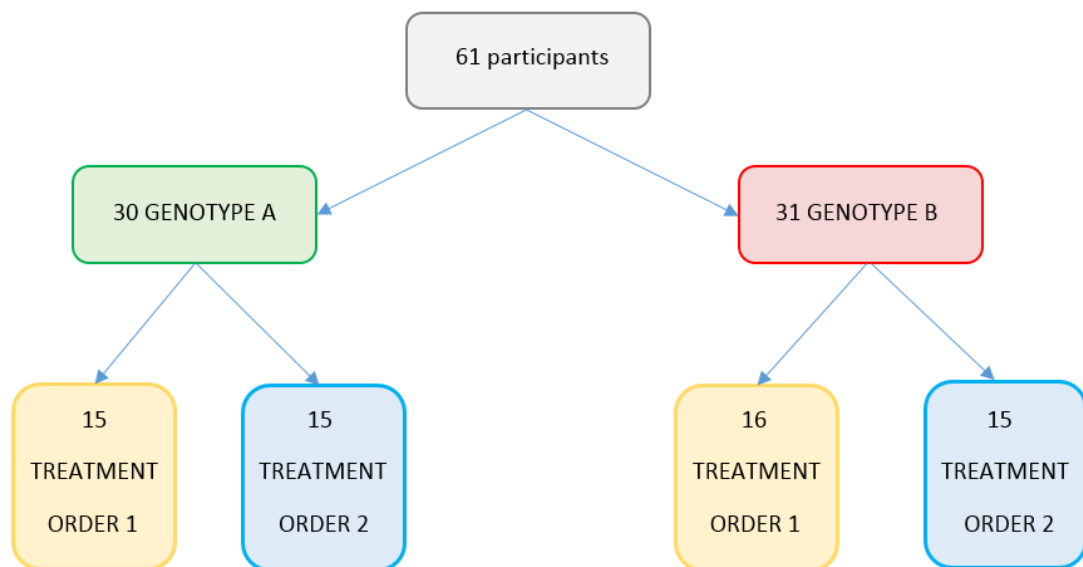


Figure 31 Breakdown of study population according to genotype and treatment order. Genotype A = OCT1 Wild Type; Genotype B = OCT1 Reduced Function; treatment order 1 = omeprazole followed by placebo; treatment order 2 = placebo followed by omeprazole.

Baseline characteristics

The baseline characteristics of the ImpOCT study population are shown in Table 14, below. Of the study population ($n = 61$), 30 were OCT1 wild type, and 31 OCT1 RF. A higher proportion of the wild type group were female (67% vs 45%) but this was not statistically significant ($p = 0.091$). The genotype groups were well matched for age, but there was a significant difference in BMI, with the OCT1 RF group having a higher median BMI (29 vs 26, $p = <0.001$). To our knowledge, there have been no reported associations between obesity and the SNPs included in the ImpOCT study. However, OCT1 polymorphisms are associated with higher total cholesterol and higher LDL levels (302). The difference in BMI highlights one of the difficulties of a double blind, recruit-by-genotype study, as we were not able to match on an individual basis without acquiring insight into participants' genotype.

	Wild Type		OCT -/-		<i>p</i>
n	30		31		
Gender, F (%)	20	(67)	14	(45)	0.091
Age (y)	63	(57-67)	62	(54-66)	0.509
BMI	26.3	(24.1-28.1)	29	(26.5-31.8)	<0.001

Table 14 Baseline characteristics according to genotype. Data are median with IQR, unless otherwise stated. *P* value for Mann Whitney test for continuous data, or chi-square for count data.

Visualisation of the data

The primary outcome, maximum tolerated dose (MTD), was determined as the highest dose the individual could tolerate with participant-perceived tolerance as "Tolerant" or "Mildly Intolerant", along with a MISSS of <20 , and the patient being

willing to remain on the dose (as per dose titration guideline). The MTD was recorded as number of metformin 500mg tablets per day, i.e. 1500mg = 3 tablets. The MTD was then compared during concurrent omeprazole versus placebo.

Wild type:

Figure 32 shows the distribution of metformin tolerability in the OCT1 wild type cohort. The majority (18 out of 30, 60%) were able to tolerate maximum metformin dose (2000mg daily, 4 x 500mg tablets) during both concurrent omeprazole and placebo. Of those who experienced intolerance (12 out of 30, 40%), and did not reach the maximum daily dose of metformin during one or both of the treatment periods, there is a visible trend toward improved tolerance with concurrent omeprazole treatment. Of those experiencing symptoms of intolerance, only 3 out of 12 (25% of within genotype intolerants) had a higher MTD on placebo than omeprazole. The remaining 75% (9 of 12) showed improved tolerance when taking omeprazole.

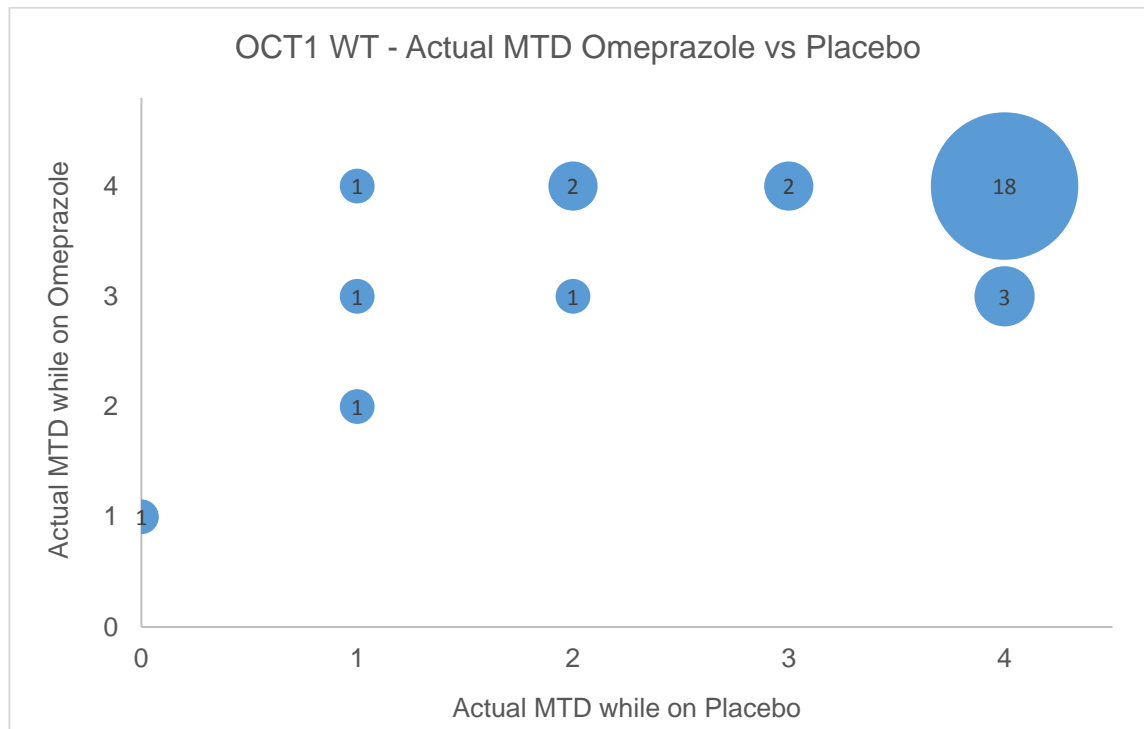


Figure 32 Actual maximum tolerated dose of metformin whilst taking placebo versus omeprazole for the OCT1 wild type group. Bubble size indicates number of individuals.

The trend towards improved tolerance on omeprazole is visually represented in the line graph below (Figure 33). Whilst the majority are able to take the maximum of 2000 mg daily in both treatment periods, the trend of the remaining individuals is towards a lower MTD on placebo.

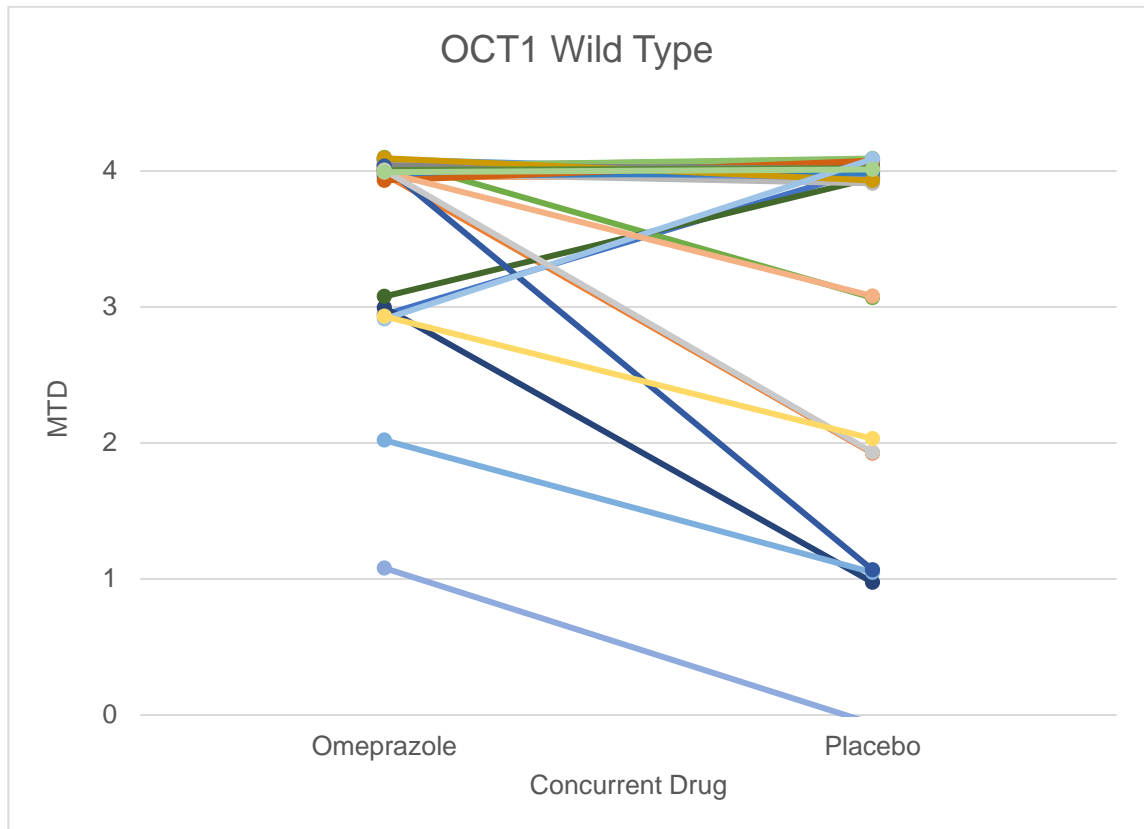


Figure 33 Direction of tolerance of OCT1 wild type individuals. Data have been "jittered" around the data point to reveal overlapping data.

OCT1 RF

Figure 34 shows the distribution of metformin tolerability in the OCT1 reduced function cohort. Again, the majority (20 out of 31, 64.5%) were able to tolerate maximum metformin dose (2000mg daily, 4 x 500mg tablets) during both concurrent omeprazole and placebo. Of those who experienced intolerance (11 out of 31, 35.5%), and did not reach the maximum daily dose of metformin during one or both of the treatment periods, there is no visible trend toward improved tolerance with either concurrent treatment. Of those experiencing symptoms of intolerance, only 4 out of 11 (36.4% of within genotype intolerants) had a higher

MTD on placebo than omeprazole. However, a further 36.4% had a higher MTD on omeprazole than placebo, with the remaining 27.2% (3 of 11) had equivalent MTDs on both concurrent treatments.

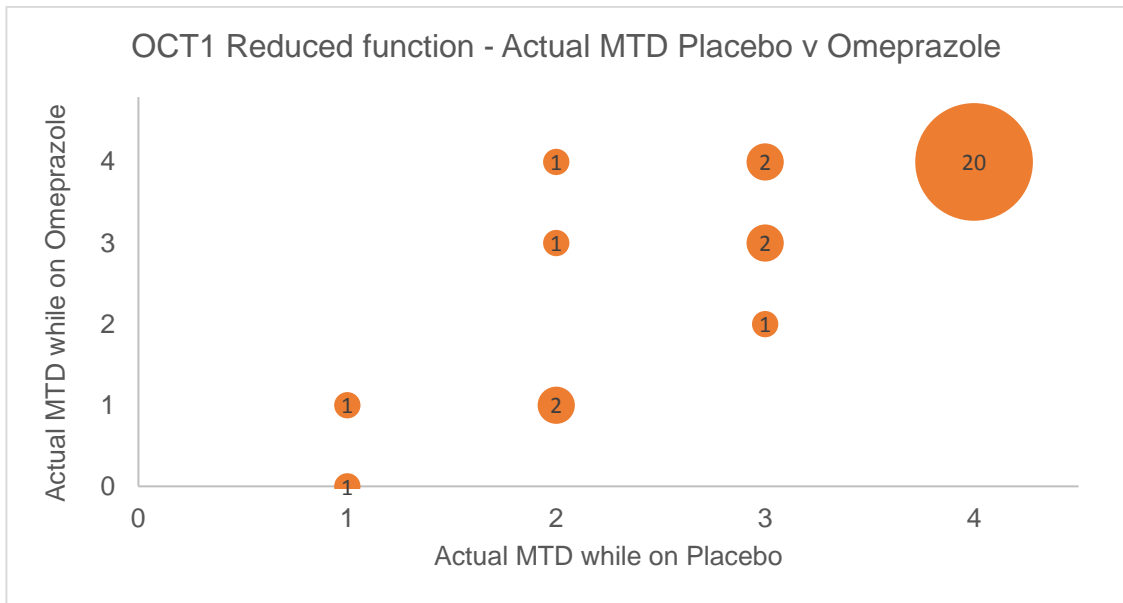


Figure 34 Actual maximum tolerated dose of metformin whilst taking placebo versus omeprazole for the OCT1 RF group. Bubble size indicates number of individuals.

Figure 35, below, confirms visually that there is no obvious trend in MTD across treatments within the OCT1 RF genotype.

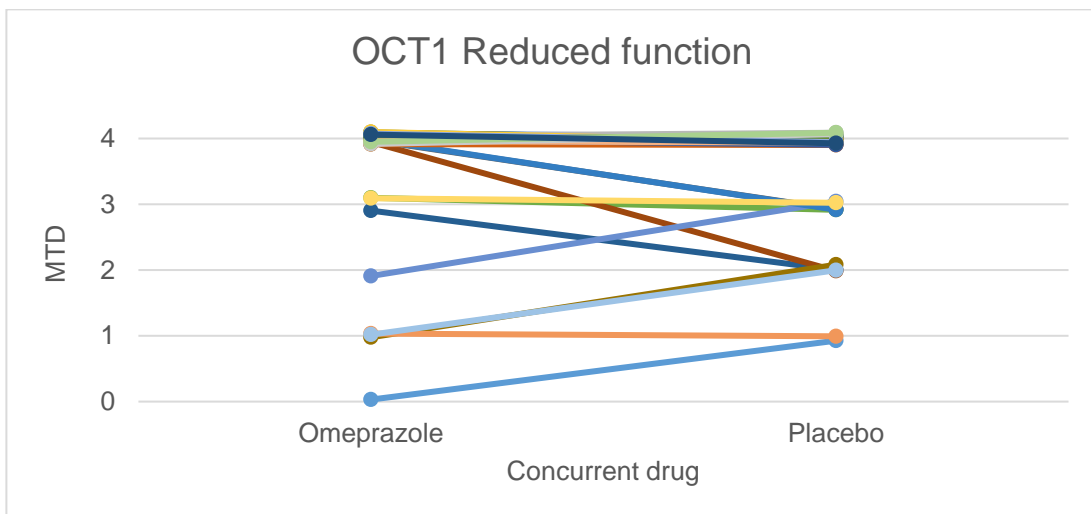


Figure 35 Direction of tolerance of OCT1 RF individuals. Data have been "jittered" around the data point to reveal overlapping data.

Statistical analysis

Testing for normality

The data for age, and BMI were tested for normality using Shapiro Wilks method, and direct visualisation using QQ plots. While BMI is normally distributed across and within genotypes, age is not normally distributed. Therefore, direct comparison of groups as in baseline characteristics above, used non-parametric testing.

Chi-Square Test

The frequency of intolerance across the two genotypes was compared using a Chi-Squared test. The data were reduced to a binomial outcome i.e. success or failure, identifying individual as either tolerant or intolerant. If during **either** treatment period an individual did not reach the maximum tolerated dose of 2000mg daily, they are “intolerant”. The chi-square contingency table is shown below:

	Tolerant	Intolerant	Row total
Wild Type	18	12	30
Reduced function	20	11	31
Column total	38	23	61 (grand total)

The chi-square statistic is 0.1324, with a p value of 0.716 – i.e. no significant difference between genotypes, when considering tolerance as a binomial outcome.

Tolerance during each treatment was considered independently. The contingency table shows the presence or absence of metformin tolerance whilst on concurrent **placebo**:

	Tolerant	Intolerant	Row total
Wild Type	21	9	30
Reduced function	20	11	31
Column total	41	20	61 (grand total)

For the above contingency table, the chi-square statistic is 0.208, with a p value of 0.648, showing no significant difference in genotype tolerance on placebo.

The same test was performed for concurrent treatment with **omeprazole**:

	Tolerant	Intolerant	Row total
Wild Type	23	7	30
Reduced function	23	8	31
Column total	46	15	61 (grand total)

The chi-square statistic is 0.05, with p value of 0.82, therefore there is no significant difference in tolerance between genotypes whilst on concurrent omeprazole.

McNemar Test

The McNemar test was performed for each genotype, to assess for significance in the variation in tolerance within genotype. For R code and outputs please refer to Appendix 4: ImpOCT analysis.

OCT1 wild type:

OCT1 wild type		Omeprazole	
		Tolerant	Intolerant
Placebo	Tolerant	18	3
	Intolerant	5	4

The McNemar test did not identify any significant difference within the OCT wild type tolerance across treatments ($p = 0.723$).

OCT1 reduced function:

OCT1 Reduced function		Omeprazole	
		Tolerant	Intolerant
Placebo	Tolerant	20	0
	Intolerant	3	8

Again, the McNemar test does not identify any significant difference in metformin tolerability within genotype, across treatments ($p = 0.248$).

Both the chi-square and McNemar test are useful, simple statistical tests, however they have numerous limitations. By applying them to the data from the

ImpOCT study, significant information is lost. Using chi-squared loses the detail obtained through the cross-over design, by simplifying into a binary outcome. The McNemar test allows comparison of treatment outcomes within genotype only. To compare the treatment outcomes both within and across genotypes, it is possible to use a Cochran-Mantel-Haenszel (CMH) test.

Cochran-Mantel-Haenszel test

The Cochran-Mantel-Haenszel test allows for the analysis of disease-exposure relationships within subgroups, or strata. In the ImpOCT study, the case / control refers to genotype, and exposure is to the concurrent treatment, with the strata of MTD in each exposure. The contingency table is populated as follows:

		Wild Type					Reduced function				
		Placebo MTD					Placebo MTD				
		0	1	2	3	4	0	1	2	3	4
Omeprazole MTD	0	0	0	0	0	0	0	1	0	0	0
	1	1	0	0	0	0	0	1	2	0	0
	2	0	1	0	0	0	0	0	0	1	0
	3	0	1	1	0	3	0	0	1	2	0
	4	0	1	2	2	18	0	0	1	2	20

The CMH test identifies a **significant difference ($p = 0.003$)** in the frequency of the outcomes across genotype and treatment. For R code / output, please see Appendix 4: ImpOCT analysis.

This can be further investigated with the use of statistical modelling.

Mixed effects model – gene-drug interaction

Cumulative linked mixed models

The data were modelled using the R package “ordinal” which uses cumulative linked mixed models, and accepts ordinal outcomes (301).

The mixed model incorporates fixed (genotype and treatment) and random (subject) effects, with the ordinal outcome of maximum tolerated dose. The model uses Laplace approximation, and provides a means of model selection in the form of AIC, which is an estimator of relative quality of statistical models.

The model of best fit (defined as lowest AIC) identifies both “Treatment” ($p = 0.008$) and the interaction term “Genotype*Treatment” ($p = 0.04$) as significant within the model. The R code and output can be found in the Appendix 4: ImpOCT analysis.

Similar to the CMH test, the model identifies a significant gene x drug interaction. To determine the effect size of this gene x drug interaction, it is necessary to perform sub-analysis of the study data according to genotype, and calculate the odds ratio of metformin tolerance from the model estimates. R code and output detailed in the Appendix 4: ImpOCT analysis.

Odds ratio

	Odds Ratio of Tolerance	95% CI
OCT1 WT, treated with placebo	1.0	-
OCT1 WT, treated with omeprazole	4.02	0.8 – 20.8

Table 15 Odds ratio of tolerance predicted with a cumulative linked mixed model, for OCT1 wild type individuals, using the ordinal package

	Odds Ratio of Tolerance	95% CI
OCT1 RF, treated with placebo	1.0	-
OCT1 RF, treated with omeprazole	1.19	0.2 – 7.1

Table 16 Odds ratio of tolerance predicted with a cumulative linked mixed model, for OCT1 reduced function individuals, using the ordinal package

Odds ratios can be calculated from the exponential of the model estimate for each factor, with 95% confidence intervals of the odds ratio calculated as the exponential of the CIs of the estimate.

Although the sub-analysis does not reach statistical significance, OCT1 wild type individuals an odds ratio of metformin tolerance >4 while taking omeprazole (OR

4.08, 95% CI 0.8 – 20.8) compared to when they were not taking omeprazole. However, in OCT1 RF individuals the addition of omeprazole made no significant difference to the tolerance of metformin. It is this difference between the genotype response to omeprazole which is identified as a gene*drug interaction in the primary model.

Secondary analyses of gender, age, and BMI effects

In addition to genotype and treatment, our secondary analysis included genotype, treatment, age, gender, BMI or treatment order as fixed effects within the mixed model. Using the ordinal package to produce cumulative linked mixed models with each of the above as single fixed effects, only “Treatment” was significant independently.

Of note, BMI has no effect on maximum tolerated dose. Given the significant difference in BMI between the genotype groups, this provides reassurance that the genotype*treatment effect identified by the model is not simply representing the difference in BMI.

Comparing models, the model incorporating the interaction term of genotype*treatment is superior to treatment alone, as per analysis of variance comparison and demonstrated by a lower AIC.

Subsequent models with the addition of age, BMI, gender or treatment order sequentially, to genotype*treatment, did not improve the model goodness of fit.

Following univariate analysis of each term individually, clinically relevant interaction terms were then considered in the model, including interaction of genotype with age / BMI / gender, and interaction of treatment with age / BMI / gender. None of these terms were significant in the model.

Discussion

Hypothesis Review

Metformin uptake from the gastrointestinal tract is transporter dependent, with OCT1 accounting for approximately 25% of metformin transport. This cationic transporter is highly polyspecific and polymorphic, increasing the potential for both genetic variation and competitive inhibition to affect its functionality. Many commonly used drugs are substrates of OCT1, including proton pump inhibitors, certain anti-hypertensives, and analgesia such as codeine and tramadol.

Many studies have been carried out to assess the role of OCT1 in drug-drug interactions between its substrates, and also to assess the impact of genetic variation on PK/PD of its substrates, as summarised in Table 8 and 9. One particular study of note, reported by Dujic et al (29), is the observational cohort study using GODARTS data which identified a gene x drug x drug interaction between OCT1, OCT1 inhibiting drugs, and metformin. The study reported a four-fold increase in the odd ratio of metformin intolerance in individuals with OCT1 RF genotype with concurrent use of OCT1 inhibiting drugs. The biological mechanism and frequency of genetic variation in the transporter, make OCT1 variation a plausible mediator for metformin intolerance.

The ImpOCT study, the first of its kind, is a recruit by genotype, double blind, placebo controlled cross-over interventional study to investigate this observed gene x drug interaction. No previous interventional study of OCT1 genotype has assessed impact on metformin tolerance. The study hypothesis was that individuals with OCT1 reduced function genotype would demonstrate a reduced metformin tolerance, compared to OCT1 wild type individuals, and that this difference in tolerance would be increased by the addition of concurrent treatment with OCT1 inhibiting medication, in the form of the proton pump inhibitor omeprazole. The study was successfully completed, recruiting a total of 61 participants - 30 OCT1 wild type and 31 OCT1 RF individuals. Participants maximum tolerated dose of metformin was then assessed during a randomised

and double-blinded cross-over of concurrent treatment with omeprazole and placebo.

Study Design

The study design is interesting in its own right, and one which has since been adopted by other studies in the research centre at University of Dundee. The use of a double-blind, placebo controlled, cross-over study is a robust study design which increases the power of the study, due to:

- a) The use of paired data, or repeated measures. Each participant acts as their own control, and removes significant confounding factors seen in parallel studies.
- b) Double-blinding removes bias from both the research team and participant.
- c) Placebo-control ensures the effect seen is not the placebo effect, in this case, the drug burden alone which increases intolerance.

The addition of the recruit by genotype model further increases the power of the study, as to perform this study in an unselected population, in the hope of identifying a gene interaction, the sample size would have been significantly larger, with the associated time and financial cost (187, 188). This study design can be easily adapted and re-used for other transporters and their substrates.

Primary analysis: No effect of OCT1 genotype on metformin tolerance

The ImpOCT study did not identify an OCT1 gene effect on metformin intolerance. There was no significant difference in the frequency of tolerance between genotypes ($p = 0.72$). This is in contrast to the results from Dujic et al. observational cohort study, in which OCT1 loss of function variants negatively impacted tolerance.

When considering the mixed model, this study has successfully identified, for the first time in an interventional study, a gene x drug interaction between the OCT1 transporter, concurrent use of omeprazole and metformin tolerance ($p = 0.04$).

Interestingly, the direction of this interaction is opposite to our initial expectation. The hypothesis predicted that OCT1 RF individuals would have a lower tolerance than OCT1 wild type, and that treatment with omeprazole will reduce the tolerance of the OCT1 RF individuals further.

Our results indicate that OCT1 wild type group benefit from an improvement in their metformin tolerance (OR of tolerance 4.02, 95% CIs 0.7 – 20.8) when treated with omeprazole. The improvement in tolerance with the addition of omeprazole may be in keeping with clinical instinct – an individual with symptoms of metformin intolerance such as nausea, may be expected to benefit from a proton pump inhibitor.

However, while the interaction term of genotype * treatment is significant in the model ($p = 0.04$), when the data is subdivided and analysed within genotype to further investigate the interaction, the effect of treatment is no longer significant ($p = 0.1$). This is potentially due to the loss of power associated with the subdivision of the study group, and therefore sample size. However, it may be due to the assumptions of the model, which assumes normal distribution of the ordinal outcome. The outcome of the study, maximum tolerated dose, will not be normally distributed, as the participants' maximum tolerated dose was limited to four tablets of metformin daily. This is because this maximum dose is clinically relevant, and to increase the dose beyond the maximum dose used in a clinical setting would not be ethical. The outcome is therefore left-skewed, resulting in a large variance within the data.

In contrast, the OCT1 reduced function group do not benefit from the addition of PPI, with no significant difference in metformin tolerance with or without omeprazole. The OCT1 reduced function group may therefore be less likely to

continue omeprazole treatment if no clinical improvement was noted, which in observational data, may appear as a reduction in the number of individuals treated with concurrent omeprazole and metformin. It is worth noting that, while omeprazole is an inhibitor of OCT1, it is not a substrate for this transporter (285). Therefore, it is unlikely that the difference in response to omeprazole between genotypes would be explained by reduced uptake of omeprazole.

At first glance, the results of this randomised placebo-controlled trial would appear to be contradictory to those of the observational data reported by Dujic et al (29). However, if considering OCT1 wild type individuals on omeprazole as the reference group, comparison of the less tolerant OCT1 RF individuals treated with omeprazole could be interpreted as a genotype effect when considered in isolation, which would be consistent with the previously reported observational data. However, by comparing across treatment with omeprazole and placebo, our results indicate that rather than a reduction in tolerance for OCT1 RF, there is an improvement in tolerance in the OCT1 wild type group.

Nonetheless, the gene x drug interaction identified by the ImpOCT study is clinically relevant and applicable. It suggests that in patients with metformin intolerance, a trial of concurrent omeprazole may, in up to 36% of cases (i.e. the OCT1 wild type individuals), improve the symptoms of intolerance, which could improve compliance and allow up-titration and optimisation of the metformin dose. In those whose symptoms do not improve with omeprazole, it may be that they are OCT1 RF, and if intolerant, unlikely to benefit from concurrent PPI.

It is anticipated that, in the near future, access to patient's genetic information will be available to guide clinicians at the time of diabetes diagnosis. In this case, patients identified as OCT1 wild type could be offered omeprazole when prescribed metformin and reporting symptoms of intolerance.

Secondary analysis – Gender, Age and BMI.

In addition to the gene x drug interaction, secondary analyses considered the addition of gender, age and BMI into the model, to assess for an improvement in model fit. Using mixed models, none of these terms were significant in the model, neither independently nor in addition to the genotype x treatment interaction term. However, when sub-analysis was performed using generalised linear models, the addition of age improved the fit of the model, without being statistically significant within the model. This data is shown in the Appendix 4: ImpOCT analysis.

Limitations

We acknowledge that the ImpOCT study has a number of limitations. Firstly, we developed a Metformin Intolerance Symptom Severity Score (MISSS) to identify metformin intolerance and guide metformin titration. Although this score is a new research tool, it is grounded in pre-existing clinical knowledge of metformin intolerance and was used in combination with the participant's perceived intolerance and their willingness to increase their metformin dose. This is equivalent to dose titration in clinical practice, when the physician will enquire about the physical symptoms of intolerance but will ultimately be guided by the individual and their willingness to increase the dose. The MISSS had previously been used in the Pharmacokinetics of Metformin Intolerance (POMI) study, where an individual's score was strongly correlated with their metformin tolerance phenotype.

Secondly, the sample size of the study was small. However, the study was powered to identify a difference in the maximum tolerated dose of 500mg of metformin. Recruitment by genotype helped to reduce the sample size required to identify a significant difference. In fact, we recruited a larger study population than indicated from sample size calculation, but incorporated interim analysis to allow for cessation of recruitment if significance was reached in a smaller study population. We are confident, therefore, that there is no significant difference in metformin tolerance between OCT1 genotypes, and that the lack of significant

difference is not due to a lack of power. Although the study failed to identify a genotype effect on tolerance, it has identified a gene * drug interaction, which is clinically relevant and applicable, and is not inconsistent with the observational data reported by Dujic et al (29).

The ImpOCT data were analysed using a mixed model, among other statistical methods. There are numerous types of mixed models, and it is often a challenge to identify the model which is best suited to the data. While no model is perfect, the model used was a regression model for ordinal data, and was chosen based on its ability to handle ordinal outcomes, its inbuilt measures of model “goodness of fit” and the ability to compare models using ANOVA. The resulting model has identified a significant gene * drug interaction. The use of other models, such as generalised linear mixed models and generalised linear models as detailed in Appendix 4, have also shown the gene * drug interaction, which acts as a form of internal replication, and confirms that the interaction is not model dependent.

It is interesting that the results of this randomised placebo controlled study appear to be at odds with the observational data reported by Dujic et al (29). However, this may be because the observational study used a conglomerate of many OCT1 inhibiting drugs to identify an interaction with metformin, where this study used only a single drug – omeprazole. PPIs were associated with an increase in the OR of metformin intolerance (1.94) in the observational data, but this increase was not as marked as, for example, the increase in intolerance associated with citalopram, verapamil, or codeine (Figure 36). These more potent inhibitors of OCT1 may have produced a different result if adopted for the ImpOCT study drug. However, it would not be ethical to treat participants with citalopram or verapamil unless clinically indicated, due to potential side-effects. Codeine may have caused gastrointestinal side-effects independent of metformin, and has the potential to cause opioid dependence. The decision to use a PPI as the study drug was based on: the safety and tolerability profile of the drug class; availability of PPIs over-the-counter; and the frequency with which PPIs are prescribed, as any interaction identified would therefore affect a greater number of patients.

However, it may be that the beneficial effects of PPI on indigestion and gastrointestinal symptoms may dominate those symptoms related to OCT1 inhibition.

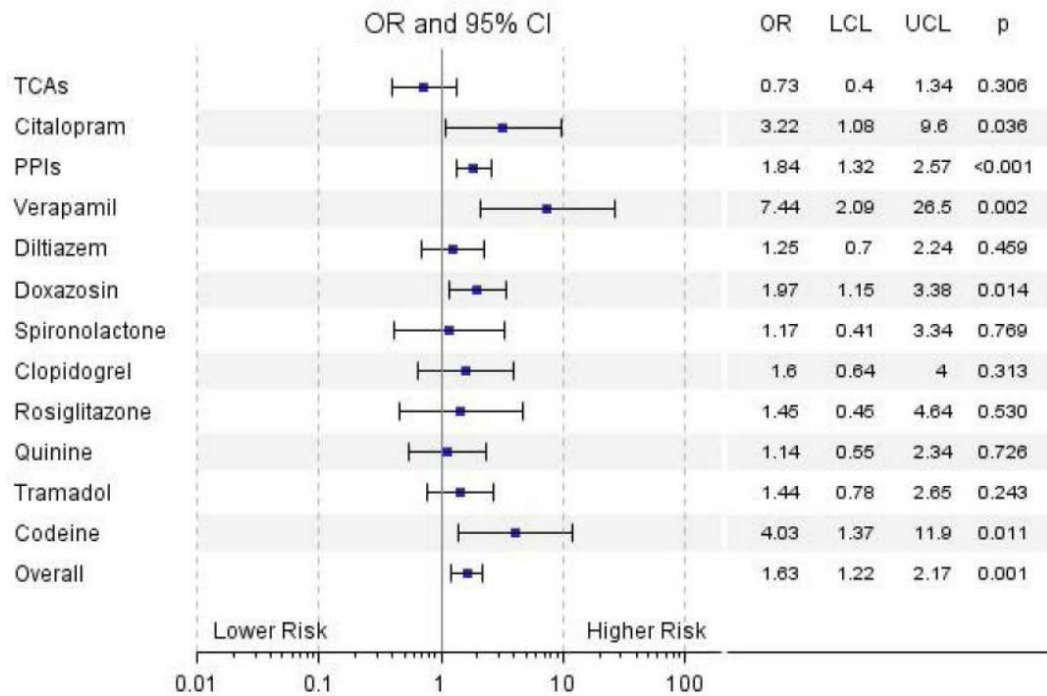


Figure 36 Odds ratios of intolerance from commonly prescribed OCT1 inhibiting drugs, as demonstrated by Dujic et al. Reproduced with permission.

The ImpOCT results do highlight potential limitations of observational cohort studies. Causal associations will always involve correlation, but the identification of a correlation does not necessarily imply causation (303). The use of retrospective pharmacoepidemiological data to assess, for example, intolerance, depends on the use of surrogate endpoints or “proxy” phenotypes based upon prescribing patterns. Therefore, using observational data may lead to misidentification of metformin intolerance. There may also be confounding by indication in the observed increase of metformin intolerance in those prescribed PPIs, as PPIs may be prescribed in response to the symptoms of intolerance.

Conclusion

The ImpOCT study did not identify an OCT1 genotype effect on metformin tolerance per se. However, it has, for the first time in an interventional study, identified a gene * drug interaction between OCT1, omeprazole use, and metformin tolerance. In OCT1 wild type individuals, we identified an improved metformin tolerance when treated with omeprazole. Although this result is not fully consistent with previously reported observational data, this may be due to the methods adopted to identify intolerance in the retrospective data, or confounding by indication of the PPI prescription.

The observed interaction is clinically relevant, applicable and of potential benefit. The results indicate that PPI treatment may be of benefit to a subgroup of those who experience metformin intolerance, by increasing their maximum tolerated dose of metformin. This could lead to improved compliance; allow for optimisation of metformin dosing and known clinical benefits of metformin therapy.

Response of individuals with Ataxia-Telangiectasia to Metformin and Pioglitazone (RAMP) study

Contributions:

The following chapter details the “Response of individuals with Ataxia-Telangiectasia to Metformin and Pioglitazone” (RAMP) study.

I wrote the study protocol with Prof Ewan Pearson, with guidance from previous studies by Prof Margot Umpleby from the University of Surrey.

All participant recruitment, study visits, sample and data collection was completed by me, with the assistance of Research Nurses Louise Cabrelli and Heather Loftus.

In collaboration with Matthew Marzetti and Dr Stephen Gandy from Medical Physics at the University of Dundee, I helped to develop a new method for assessing fat distribution using MRI. The images obtained were analysed using this new method by Matthew Marzetti. I performed statistical analysis on the resulting data.

Glucose kinetics and beta cell modelling was performed by Dr Andrea Mari, from the National Research Council, Padua, Italy. I performed all statistical analysis on the resulting data.

I am the sole author of this chapter.

Introduction

The field of metformin research continues to expand, as new potential clinical applications arise. However, to achieve personalised medicine, there is an ever-growing need for more detailed understanding of the genetics of drug response for metformin. Pharmacogenetics can improve our understanding of the genetics of drug response in a number of ways, as discussed in Chapter 1. Due to the development of biobanks, and the increase in availability and reduction in cost of genotyping, genome-wide association studies (GWAS) are increasingly used to provide genetic insight into drug function. GWAS employ a hypothesis free, unbiased approach, to identify genetic variants associated with a phenotype of interest, and can therefore identify novel drug targets or clarify a drug's mechanism of action (168). Despite metformin's long history of clinical use, the lack of certainty regarding mechanism of action leads to difficulty when investigating the inter-individual variability in glycaemic response to and tolerability of metformin.

GWAS of glycaemic response to metformin

In 2011, Zhou et al applied a genome-wide association approach to investigate glycaemic response to metformin, hoping to gain insight into the mechanism of metformin's action, and to identify genetic variants that may predict efficacy or adverse effects (170). The GWAS was performed on genetic data from 1024 metformin-treated patients of European ancestry, from the GoDARTS cohort. There were 14 SNPs with p-value $<1 \times 10^{-6}$, which were in strong linkage disequilibrium (LD) on chromosome 11q22. The SNP most strongly associated with the phenotype of treatment success (pre-defined as HbA1c of $<7\%$ within 18 months of commencing metformin therapy) was rs11212617, with an odds ratio of 1.35 (95% CI 1.22 – 1.49) for treatment success, and a genome wide significance of $p = 2.9 \times 10^{-9}$. This result has been replicated in an independent set of 1783 GoDARTS participants, in 1113 UKPDS participants, and in a meta-analysis of these, including an additional 1365 individuals from three cohorts

(DCS; Rotterdam Study; CARDS Trial) (304). The functionality of this ATM SNP is not yet known. The SNP of interest falls within a large block of LD which includes a number of genes, of which the Ataxia-Telangiectasia Mutated (*ATM*) gene was identified as a possible candidate for metformin response.

This chapter describes the “Response of individuals with Ataxia-Telangiectasia to Metformin and Pioglitazone (RAMP)” study, which was designed to further investigate the potential link between the *ATM* gene and glycaemic response to metformin.

ATM gene and encoded protein kinase

ATM is located on human chromosome 11q22-q23 (305) and is made up of 66 exons (four non-coding and 62 coding) spanning 150 kb. The *ATM* gene encodes ATM, a serine / threonine protein kinase belonging to the phosphatidylinositol 3 kinase-like kinase (PIKK) family. ATM is involved in the coordination of cellular responses to DNA damage, specifically double-strand DNA breaks (DSBs). ATM interacts with MRN complex at the site of the DNA break, and initiates DNA end resection in preparation for repair via the homologous recombination pathway (306). ATM is therefore predominantly found in the nucleus, with a small proportion of the protein in the cytoplasm. Along with DNA damage repair, ATM is involved in cellular pathways of oxidative stress and metabolism including insulin signalling (306).

The hypothesis that *ATM* is the candidate gene associated with metformin response was based upon the following evidence linking the *ATM* gene with metabolism:

1. ATM deficiency and diabetes

Homozygous loss of function mutations in the *ATM* gene result in the rare neurodegenerative condition Ataxia-Telangiectasia (A-T, discussed in detail below), which is associated with insulin resistance, diabetes and fatty liver disease. This association between the loss of function of *ATM* and insulin

resistance in humans supports *ATM* as a potential candidate gene of those identified by the GWAS of metformin response.

2. ATM and AMPK

The ATM protein kinase is involved in the activation of AMPK (306-308). As discussed in the introduction of this thesis, AMPK activation is an established pathway of metformin's mechanism of action. ATM is activated by reactive oxygen species (ROS) in cell cytoplasm, to regulate protein synthesis, cell survival and autophagy. Activation of ATM by ROS, leads to phosphorylation and activation of LKB1, which subsequently activates AMPK (306). The mechanism of metformin activation of AMPK by inhibition of complex 1 of the respiratory chain, is also thought to be LKB1-dependent (309, 310).

However, IGF-1 stimulates phosphorylation of tyrosine residues in the ATM molecule, which results in phosphorylation of AMPK-alpha subunit via in an LKB1-independent manner (311). This ATM-dependent, LKB1-independent pathway of AMPK phosphorylation has been implicated in the mechanism of action of the diabetes drug AICAR (307).

Of note, ATM is involved in the regulation of mitochondrial function. There is abnormal structural organisation and intrinsic dysfunction of mitochondria in A-T cells, which demonstrate reduced mitochondrial respiratory activity, resulting in continuous oxidative stress (312), a known contributor to the development of diabetes.

3. ATM and insulin signalling

A-T is associated with insulin resistance and glucose intolerance. This may be due to the interaction of ATM with various components of the insulin signalling pathway, from translational activity to cellular glucose uptake.

Insulin and IGF-1 stimulate protein synthesis via ATM-dependent phosphorylation of eIF-4E-binding protein 1 (4E-BP1), which releases eIF-4E – a translation

initiation factor (313). ATM-deficiency could therefore reduce translational activity, resulting in poor growth, metabolic abnormalities and insulin resistance.

p53 is a tumour suppressor, which is also involved in the regulation of transcriptional activity and the expression of genes involved in metabolism, mitochondrial respiration, glucose transport, adipocyte function and glucose homeostasis (314). ATM phosphorylates p53 at a site that regulates transcriptional activity, and mice with germ line mutation of this specific phosphorylation site have increased metabolic stress, impaired glucose tolerance and insulin resistance (314).

In a mouse model of A-T, *in vitro* studies have shown that macrophages and hepatocytes have decreased insulin receptor substrate (IRS) expression, specifically mRNA and protein levels of IRS-2 (315). ATM also regulates the transcriptional activity of cAMP response element binding protein (CREB), which induces IRS-2. Inactivation of IRS-2 leads to insulin resistance, impaired insulin secretion, and reduced beta cell survival (316, 317). In ATM-deficient mice there is also increased phosphorylation of IRS-1 by Jun N-terminal kinase (JNK), which disrupts insulin signalling (315), and contributes to insulin resistance.

Reduced IRS-2 expression or activation results in a reduction in phosphatidylinositol-3-kinase (PI3k) activity – one of the most important pathways of insulin signalling – and subsequently decreased AKT phosphorylation, which impedes insulin signalling (315, 318). AKT kinase (also known as protein kinase B) promotes cell proliferation and survival in response to insulin stimulation, and is required for insulin-induced translocation of glucose transporter 4 (GLUT4) to the plasma membrane. GLUT4 is the primary transporter of glucose into cells, allowing glucose to move down the concentration gradient into the cell cytoplasm, where it is quickly phosphorylated to glucose-6-phosphate, thereby maintaining the glucose gradient. In mouse muscle cells transfected with kinase dead ATM, there is inhibition of GLUT4 translocation to the cell surface in response to insulin

(319), resulting in a reduction in glucose uptake. Disruption of GLUT4 is known to cause insulin resistance and glucose intolerance (320).

4. ATM-deficient mice and insulin sensitivity

In ATM +/- mice, hyperinsulinaemic euglycaemic clamp data demonstrate reduced insulin-associated suppression of endogenous glucose production, in-keeping with hepatic insulin resistance (315). Similarly, oral glucose tolerance testing (OGTT) and insulin tolerance testing (ITT) of high-fat diet fed ATM +/+, ATM +/- and ATM -/- mice confirmed that the lack of ATM is associated with glucose intolerance and insulin resistance. These ATM-deficient mice developed a metabolic syndrome phenotype, with elevated blood pressure, increased adiposity (specifically intra-abdominal fat) with decreased adiponectin levels compared to the ATM +/+ mice, despite no significant difference in weight or metabolic rate (measured by indirect calorimetry) (315). However, fasting cholesterol, triglycerides and non-esterified fatty acids (NEFAs) did not differ significantly between genotypes (315).

In contrast, another study of ATM-deficient mice reported normal fasting insulin sensitivity from clamp data, but impaired insulin secretion and an age-related decrease in insulin and C-peptide levels, resulting in hyperglycaemia in older animals (316). The OGTT data from this study highlighted a delay in glucose-stimulated insulin secretion in the ATM-deficient mice (316). The authors hypothesised that repeated delay in insulin secretion in response to glucose load would result in recurrent episodes of transient hyperglycaemia, which could aggravate β -cell dysfunction, with progression to β -cell failure and reduced insulin secretion in the older animals (316).

Ataxia-Telangiectasia

Ataxia-telangiectasia (A-T) is a rare, autosomal recessive condition caused by homozygous loss of function mutations in the *ATM* gene (239), affecting between 1 in 40,000 to 100,000 people worldwide (321), increasing in areas of

consanguinity. Over 400 distinct genetic mutations have been described in the *ATM* gene (322), 85% of which are null mutations resulting in truncation of the protein and total absence of ATM kinase activity. Missense and splice mutations result in reduced kinase activity (323). It is estimated that 1 in 100 people are carriers of an ATM mutation in Western populations (324). In A-T, most patients are compound heterozygotes, inheriting a distinct mutation from each parent (322). Parents of individuals with A-T (obligate heterozygotes), although generally healthy, have increased risk of certain cancers (breast and gastrointestinal) and ischaemic heart disease (325).

Often referred to as ATM Syndrome (323), A-T is a complex DNA damage response (DDR) syndrome, with significant variation in the age of onset, constellation and severity of features (239). The severity of an individual's phenotype is thought to correlate with their genotype and degree of residual ATM kinase activity (326, 327). The different presentations are broadly categorised according to severity, typically "classic" (no residual kinase activity) and "variant" (residual kinase activity).

A-T is characterised by: progressive cerebellar ataxia often requiring wheelchair assistance by adolescence; telangiectasia (classically ocular); oculomotor apraxia; immunodeficiency associated with recurrent respiratory infections; progeria; sensitivity to ionising radiation; predisposition to cancer, typically lymphoma or leukaemia; poor growth; gonadal atrophy; and delayed puberty.

A-T is also associated with insulin resistance, diabetes and fatty liver disease, which highlighted *ATM* as a gene of interest when considering the GWAS of metformin response.

Ataxia-telangiectasia and insulin resistance

A case series of 8 individuals with ataxia-telangiectasia reported in 1970, described an "unusual" form of diabetes in 5 of the patients (328). The authors describe hyperglycaemia without ketosis or glycosuria, with markedly increased

insulin levels in response to administered glucose, and stunted glucose response to both endogenous and exogenous insulin, in-keeping with insulin resistance (328). Interestingly, the authors also comment on hepatic dysfunction of unknown aetiology in all 5 individuals - likely fatty liver disease. It has been suggested that the insulin resistance seen in A-T is associated with reduced affinity of the insulin receptor for insulin, caused by inhibitors of insulin binding (328, 329). However, as detailed above, ATM is now known to interact with the insulin signalling pathways in numerous ways.

To confirm the case reports of insulin resistance in A-T, a collaborative study between Papworth hospital and the University of Dundee compared OGTT data from 10 non-diabetic individuals with A-T and 10 healthy controls (330). The two groups were well matched for age, gender and BMI. The fasting glucose and fasting insulin concentrations were comparable in the two groups, however after glucose load the individuals with A-T had higher, prolonged glucose excursions despite increased insulin levels (330). This, along with the calculated Matsuda Index (a measure of insulin sensitivity), confirmed that the non-diabetic individuals with A-T were more insulin resistant than the control cohort.

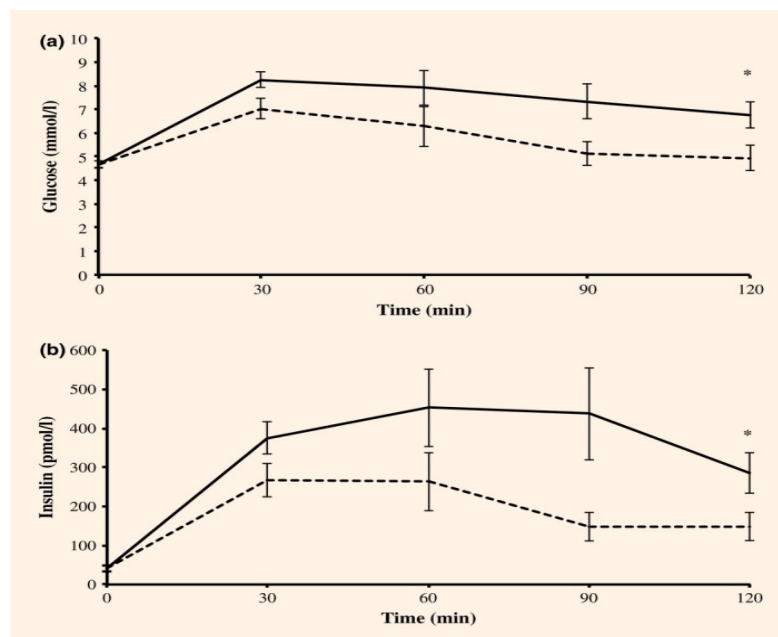


Figure 37 OGTT data from A-T (solid line) and healthy controls (dashed line). Reproduced with permission from Connelly et al (330).

ATM deficiency and response to metformin

Further investigation into the link between the *ATM* gene and metformin response followed. Unpublished data from the McCrimmon lab at the University of Dundee, demonstrate that *ATM* (+/-) mice were markedly hyperglycaemic compared to wild type mice. However, euglycaemia was restored by metformin treatment, as shown in Figure 38.

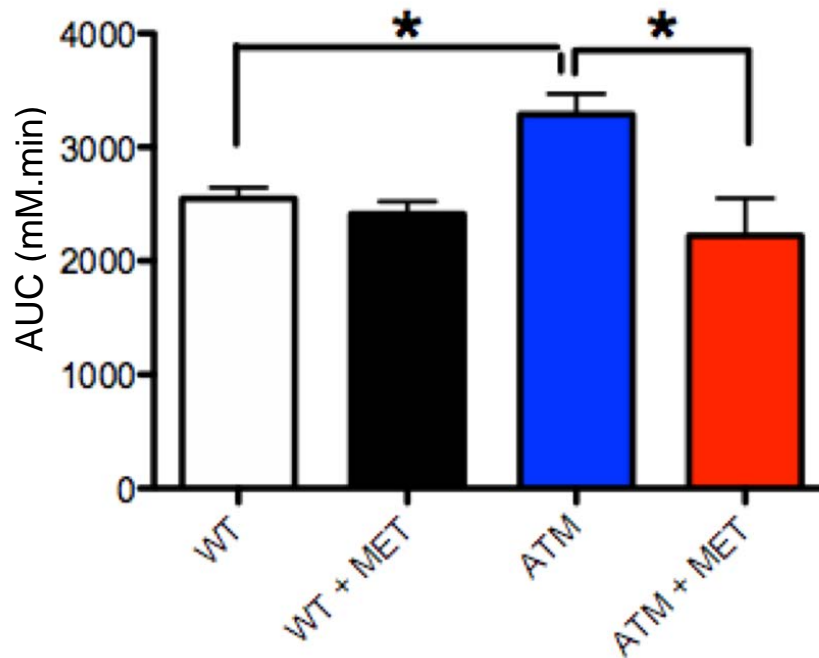


Figure 38 Area under the glucose concentration time curve from glucose tolerance testing in wild type (WT) and *ATM* heterozygote (*ATM*) mice, with and without metformin (MET). Reproduced with permission, from Gallagher et al, unpublished data.

This observed improvement in glycaemia in the *ATM* +/- mice could support the hypothesis that the *ATM* gene is linked to metformin response.

ATM and adipocyte function

As well as insulin resistance, Takagi et al noted that *ATM* -/- mice exhibited abnormal adipose distribution, with decreased intrascapular and subcutaneous, but increased visceral adipose tissue (238). This could be compared to the human metabolic syndrome, in which there is increased accumulation of visceral fat

associated with insulin resistance. Alternatively, this phenotype may be more similar to lipoatrophic diabetes, in which abnormal development of adipose tissue leads to impaired secretion of adipokines – a family of hormones secreted by adipose tissue, including adiponectin and leptin. The *ATM*^{-/-} mice had reduced adiponectin levels, which is in-keeping with insulin resistance (331, 332). Interestingly, low levels of leptin are reported in the *ATM* knockout mice, which, as in congenital leptin deficiency, could cause hyperphagia, insulin resistance and hyperlipidaemia (333).

In vitro studies using mouse embryonic fibroblasts (MEFs) to investigate the observed abnormal adipocyte distribution and function in *ATM* knockout mice, demonstrate failure of adipocyte differentiation, due to a loss of ATM-dependent transcriptional activation of C/EBP α and PPAR γ expression (238). However, adipocyte differentiation was restored in *ATM*^{-/-} MEFs when treated with the PPAR γ agonist rosiglitazone, as demonstrated by an increase in C/EBP α on western blot, and increased lipid visible on Oil Red O staining. Treatment with pioglitazone improved glucose tolerance and increased serum adiponectin concentration in the *ATM*^{-/-} mice, indicative of a restoration of adipocyte function (238).

While metformin improved glucose tolerance and insulin sensitivity in this mouse model of ATM-deficiency, it did not impact upon the adiponectin levels, suggesting that metformin improved the glycaemic response through an adipocyte-independent pathway (238).

Pioglitazone

Pioglitazone belongs to the thiazolidinedione (TZD) drug class, also known as glitazones, which are a family of anti-hyperglycaemia drugs designed to treat type 2 diabetes. First reported by Takeda Pharmaceuticals in 1980, ciglitazone was the first compound of the class. In studies of mouse models of insulin resistance, ciglitazone lowered blood glucose without an increase in insulin secretion. In fact,

the insulin concentration in these hyperinsulinaemic animals was decreased, indicating an improvement in insulin sensitivity (334).

Since then, multiple compounds have been developed in the glitazone class, but only three have reached clinical use since the 1990s – pioglitazone (335, 336), rosiglitazone (336, 337) and lobeglitazone (338). Pioglitazone is the only drug of this class available in the UK, since rosiglitazone was banned from use in 2010 due to associated increased risk of coronary heart disease, and consequentially, death (339).

Pioglitazone is a peroxisome proliferator-activated receptor gamma (PPAR γ) agonist. PPARs are nuclear receptors, which act as transcription factors for over 100 genes, playing an important role in carbohydrate and lipid metabolism. Pioglitazone is currently licensed for use in type 2 diabetes as an anti-hyperglycaemia drug, used alone; in combination with metformin, a sulphonylurea or both; as well as alongside insulin (340). It is available as a combination with metformin. More recently, pioglitazone has been suggested for the pharmacological management of non-alcoholic steatohepatitis (NASH) (341, 342), as pioglitazone is associated with a reduction in inflammation, steatosis and necrosis (341).

Incidence of heart failure increases when pioglitazone is used in combination with insulin, especially in patients with history of risk factors such as myocardial infarction. The MHRA advise that pioglitazone use is therefore contraindicated in individuals with a history of heart failure, and should be discontinued if there is evidence of deterioration in the cardiac status (340). If response is inadequate at 3-6 months, treatment should be discontinued (340). Of interest, and not included in the BNF, is the modestly increased risk of any pneumonia or lower respiratory tract infection associated with long-term use of TZDs (343).

Response of individuals with Ataxia-telangiectasia to Metformin and Pioglitazone (RAMP) study

The RAMP study was designed to investigate the link between the *ATM* gene and metformin response, by studying individuals with A-T compared to healthy controls. However, due to the reported improvement in adipocyte function and insulin resistance associated with thiazolidinedione treatment in *ATM* knockout mice, it was decided that the RAMP study should include pioglitazone as a comparator drug alongside metformin, to assess response to these commonly prescribed diabetes drugs in humans with A-T, and how their response compares to healthy controls.

The RAMP study therefore recruited individuals with A-T and healthy controls for an open label crossover study, in which participants were initially treated with metformin, followed by pioglitazone.

Hypothesis and Aims

The study hypotheses were:

1. Individuals with A-T are insulin resistant compared to healthy controls.
2. Individuals with A-T have evidence of adipocyte dysfunction and abnormal distribution of adipose tissue, as in *ATM*-knockout mice.
3. Individuals with A-T have an exaggerated response to metformin compared to the general population, based upon the GWAS data described (170), as well as mouse data, and anecdotal evidence of metformin treatment in patients with diabetes and A-T.
4. Pioglitazone treatment improves the insulin resistance associated with A-T, based upon the mouse model of A-T discussed above (238).

The objectives of the RAMP study were therefore:

- a. Further characterise the insulin resistance seen in Ataxia-telangiectasia.
- b. Assess adipocyte function and adipose distribution in A-T and controls through measurement of adipokines and MR imaging of fat distribution.
- c. Compare the change from baseline in insulin sensitivity during metformin treatment between the A-T and control groups.
- d. Compare the change from baseline in insulin sensitivity during pioglitazone treatment between the A-T and control groups.
- e. Compare the change in insulin sensitivity during metformin and pioglitazone treatment in A-T individuals, to identify the superior treatment for the insulin resistance of A-T.

Materials and Methods:

Ethics and funding

The Response of individuals with Ataxia-Telangiectasia to Metformin and Pioglitazone (RAMP) study was conducted at the Clinical Research Centre at Ninewells Hospital, Dundee, between September 2016 and August 2017. It was co-sponsored by the University of Dundee and NHS Tayside, with ethical approval granted by the East of Scotland Research Ethics Committee. The study was conducted in accordance with the Good Clinical Practice guidelines, and the Declaration of Helsinki.

The study was registered on <http://clinicaltrials.gov> (identifier NCT02733679). Formal written informed consent was obtained from each individual prior to inclusion.

Study design

This non-randomised, non-blinded, open label crossover study compared how A-T patients and 'healthy' controls responded to two commonly used diabetes drugs – metformin and pioglitazone.

The total time in study was approximately 17 weeks, with two eight week treatment periods, separated by a minimum of one week washout period. Treatment or washout periods could be extended where necessary to accommodate flights and hotel availability, due to the national recruitment required for the study.

During treatment period one, participants were treated with metformin, titrated to 1000mg twice daily over the first four weeks, remaining on maximum dose for the remainder of the treatment period. During treatment period two, participants were treated with pioglitazone, titrated to 30mg once daily over the first two weeks, continuing on 30mg daily for the remainder of the treatment period. Each participant had three study visits to the Clinical Research Centre in Ninewells

Hospital, Dundee – visit 1 for screening, consent and baseline investigations, visit 2 after metformin treatment, and visit 3 after pioglitazone treatment.

Each visit lasted for 1.5 days – one “half” day for baseline bloods (including U+Es, LFT, leptin and adiponectin) and preparation for the tracer study, followed by a full day visit for a dual tracer mixed meal test with indirect calorimetry (see below). During the baseline visit, the half day visit also included MR imaging, and fat biopsy. Throughout the study, individuals were contacted weekly by telephone to ensure they were tolerating their medication without any side effects, and to advise on dose titration.

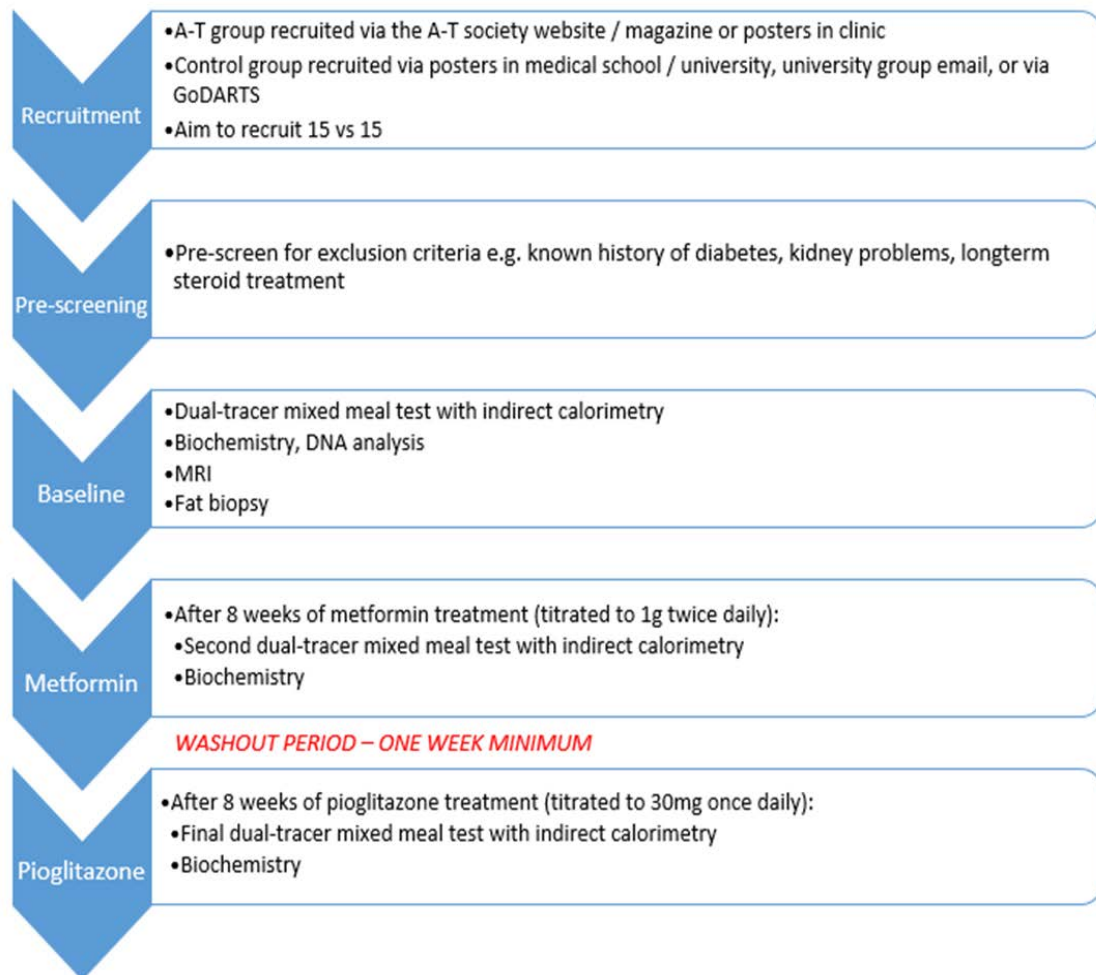


Figure 39 Flow diagram of the participant journey through the RAMP study

Recruitment

Participants were recruited from across the UK, using various media.

A-T is a rare condition, therefore recruitment for the A-T participants was on a UK-wide basis. The A-T group were either recruited from the national A-T clinic in Papworth Hospital, Cambridge or via the A-T Society - a charity involved in raising the awareness of A-T, supporting research into A-T, and providing care and support for individuals and families living with A-T.

Posters and information leaflets were displayed at the national clinic. Clinicians were asked to identify patients who fit the inclusion criteria for recruitment and provide them with information regarding the study, if they were interested in taking part.

The A-T society published information regarding the study on their website and in their magazine. They provided the opportunity to speak to members of the charity at their annual “Family Day”, primarily to inform their members of the planned study, to garner interest and receive feedback on feasibility of the study design. Latterly, the charity directly approached their members who fit the inclusion criteria, sending invitation letters, and prompting families to contact the research team if interested.

Control participants were recruited from the Tayside area, or via the “Bring a Buddy” scheme. In Tayside, posters were displayed around Ninewells Hospital and Medical School, and group emails were sent to the medical students from the University of Dundee, to advertise the study. Permission was granted for recruitment of controls from the Genetics of Diabetes Audit and Research Tayside Study (GoDARTS) cohort, however this was never used.

One unique recruitment strategy employed by the RAMP study was the “Bring a Buddy” scheme. This enabled participants with A-T to identify their own “control”, who would then accompany them to Dundee and participate in the study. The

suggested “Buddy” could not be a relative, nor have A-T, but ideally was the same age and gender. We asked that the Buddy was similar in size to the A-T participant, in an attempt to control for BMI.

The “Bring a Buddy” scheme was intended to make the participant with A-T more comfortable, having a friend to go through the experience with, and to have moral support during travel and on study visits. We hoped that this would increase the likelihood of each individual’s compliance and completion of the study. The “Buddy” could also act as a carer for the participant with A-T, as these individuals were mostly wheelchair users and required assistance with eating, personal care and transfers.

Inclusion and exclusion criteria

The criteria for inclusion / exclusion are detailed in Table 17, below.

Initially we planned to recruit only those with “classic” A-T, however due to the small number of individuals with classic A-T who fit the remaining inclusion criteria, the decision was made to widen the inclusion criteria to include “variant” A-T.

Whilst the most closely matched control group would have been a group of ataxic wheelchair users, as these are most similar to patients with A-T, recruitment of this patient group would be difficult and the study demands would be excessive for this group, without affording any potential benefit. Therefore a healthy control group, matched for age and sex, was chosen. This cohort was more likely to manage the demands of the study. This control group has the added advantage that the data obtained in this study can be used as control for planned future studies on metformin action.

BMI matching was broadly attempted, but rather than matching 1:1 with the cases, controls with a “normal / healthy” BMI – i.e. BMI 20-25 – were recruited.

This allowed for recruitment of both cohorts in parallel as it was deemed unlikely that the AT patients would be out-with this BMI range.

Inclusion Criteria		Exclusion Criteria
A-T	Control	
Age 18 – 60	Age 18 – 60	HbA1c \geq 48mmol/mol
Diagnosis of Ataxia Telangiectasia - classic or mild variant (as opposed to related conditions e.g. AOA1)	Sex-matched to cases, where possible	Active malignancy
White European descent	White European descent	History of heart failure
Non-diabetic	Non-diabetic	Long-term oral steroid treatment
Normal renal function, eGFR > 60 ml / min / 1.73m ²)	Normal renal function, eGFR > 60 ml / min / 1.73m ²)	Recent (<30 days since completion) or current participation in another clinical trial or interventional study
	BMI 20 - 25	Pregnancy

Table 17 Inclusion and exclusion criteria for participant recruitment for the RAMP study.

Intervention and sampling schedule

The participants had three visits during the 17 week study. Each visit lasted for a maximum of 1.5 days. The intervention schedule for each visit is detailed in Table 18, below.

Visit	Time in study	Total duration	Investigation	Duration
1	Baseline, Wk 0	1.5 days	Anthropometry	5 minutes
			Vital signs	5 minutes
			Tracer study	8 hours
			MRI	45 minutes
			Bloods	5 minutes
			Fat biopsy	15 minutes
2	Week 8, steady state metformin	1.25 days	Anthropometry	5 minutes
			Vital signs	5 minutes
			Tracer study	8 hours
			Bloods	5 minutes
3	Week 17, steady state pioglitazone	1.25 days	Anthropometry	5 minutes
			Vital signs	5 minutes
			Tracer study	8 hours
			Bloods	5 minutes

Table 18 Intervention and sampling schedule for the RAMP study

Tracer studies of glucose metabolism

The main investigation at each study visit was a dual tracer mixed meal test (MMT), which is described in greater detail in Methods: Glucose Tracer Modelling. In brief, participants received a standardised meal the evening before the MTT. They were fasted from midnight, able to drink only clear fluids from midnight onwards. They attended the CRC at 0800, and had two cannulae inserted, one for a continuous infusion of D2-glucose, the other for blood sampling. The D2-glucose was a primed-continuous infusion for the first two hours to reach steady state, at which time (time 0) a mixed meal labelled with U13C glucose was given, along with a 1g dose of liquid paracetamol. From time 0 onwards, the D2 glucose infusion rate was varied to mimic the expected endogenous glucose production rate, for a further 6 hours.

Blood samples were taken at 21 time points over the 8 hour period. Samples were analysed for glucose at every time-point, using mass spectrometry (see Methods: Mass Spectrometry) to differentiate endogenous from labelled glucose. Insulin, C-peptide, glucagon, active and total GLP1, NEFAs, and paracetamol level (used as a measure of gastric emptying) were also measured, at 16 / 16 / 6 / 6 / 12 / 7 time points respectively.

During the MTT, urine was collected pre- and post-meal. Volume of urine collected was documented and samples were taken for urinary glucose detection and quantification.

Throughout the 8 hour study, the participants wore an indirect calorimetry hood at 6 time points for 30 minutes each, for measurement of their metabolic rate, as per Methods: Indirect Calorimetry. The timing and frequency of the blood sampling and indirect calorimetry can be seen in more detail in the Appendix 5: Tracer timeline and task list.

From the mass spectrometry data from glucose samples collected during the MMT, tracer modelling allows calculation of: the rate of appearance of glucose

from the meal; endogenous glucose production and glucose clearance. Beta cell modelling using C-peptide and glucose data allows calculation of glucose sensitivity, insulin secretion rates and rate sensitivity (see Methods: Beta Cell Modelling).

Outcomes

To characterise the insulin resistance in A-T, baseline measures of insulin, glucose and calculated HOMA-IR will be compared to healthy controls. Other parameters including baseline adipocyte function and adipose distribution will help to further define the phenotype of insulin resistance in this condition.

The primary outcome is change from baseline in insulin sensitivity during metformin treatment. Indices of insulin sensitivity and the change in EGP will be compared across groups.

Secondary outcomes include: the change from baseline in insulin sensitivity during metformin using other parameters including glucose clearance and HOMA-IR; the change from baseline in insulin sensitivity (EGP, HOMA-IR, clearance) during pioglitazone treatment; comparison of treatment effects within each group; and assessment of treatment effect on adipocyte function comparing change in adipokines concentration.

MRI studies of fat distribution

During the baseline visit, all participants who met the standard safety criteria for MRI underwent MR imaging of their abdomen, for assessment of their adiposity. In collaboration with Matthew Marzetti and Dr Stephen Gandy from Medical Physics, we developed a new method of calculating visceral to subcutaneous adipose tissue (VAT:SAT) ratio (see Methods: MRI for VAT:SAT ratio), which has since been published in the British Journal of Radiology (243).

Assessment of liver fat and iron content was undertaken using the software “Liver Lab”. These parameters were measured at baseline only, and compared across

the two groups. During the scan, an operator would identify two regions of interest (ROI) within the liver, being careful to avoid obvious blood vessels. Liver Lab could then calculate a percentage fat fraction of these two regions using T1 and T2 times. Finally, liver iron deposition was estimated using the R2* - a higher R2* equates to a shorter T2*, implying greater iron deposition (344).

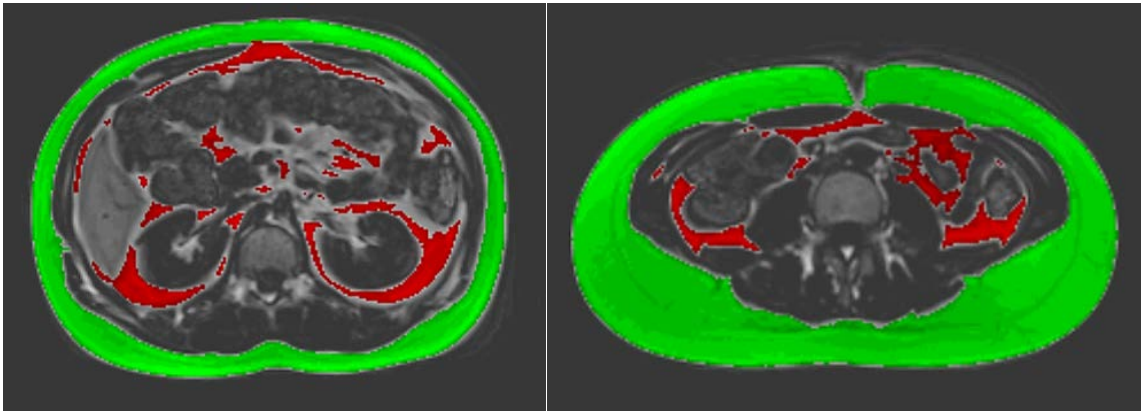


Figure 40 Images obtained from MRI for adipose distribution and VAT:SAT calculation. Subcutaneous fat is coloured green, and visceral fat is red. Image on left is a male with A-T, while the image on the right is a female control.

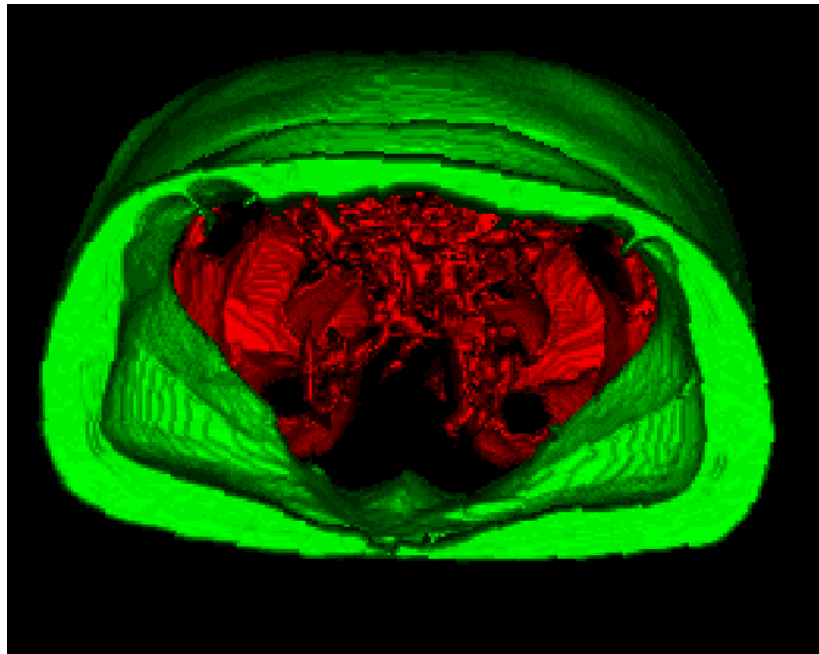


Figure 41 A composite 3D image obtained from MRI. Participant is a male with A-T.

Statistical methods

Sample size

Our sample size calculation was based on the expected change in endogenous glucose production in metformin treatment ($\Delta\text{EGP}_{\text{MET}}$). Hundal et al report the baseline and post-metformin EGP in T2DM and at baseline in healthy controls (345). We estimated that the EGP would change minimally in the healthy control (estimated range 0.05 – 0.1 $\text{mmol}\cdot\text{m}^{-2}\cdot\text{min}^{-1}$), but that the change in EGP in the A-T group would be greater than that seen in T2DM (>0.17 ; estimated range 0.18 – 0.22 $\text{mmol}\cdot\text{m}^{-2}\cdot\text{min}^{-1}$), to support the GWAS result linking *ATM* to improved glycaemic response to metformin.

Assuming equal variance with $\text{SD} = 0.1$, power of 80%, two-sided alpha of 0.05, and a sampling ratio of 1, the sample size required for the $\Delta\text{EGP}_{\text{MET}}$ ranges for the two groups are shown in Figure 42 below.

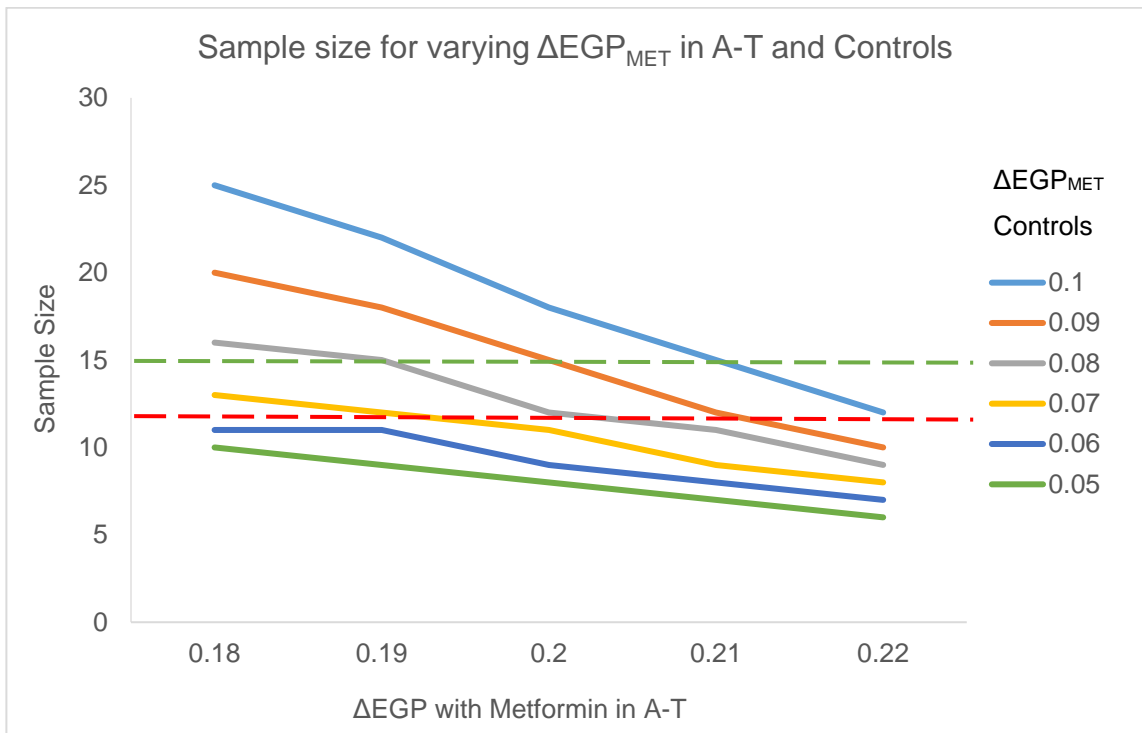


Figure 42 Sample size calculations for varying $\Delta\text{EGP}_{\text{MET}}$ with $\text{SD} = 0.1$, power 80% and two-sided alpha of 0.05.

The red and green dashed lines represent sample size of 12 and 15 in each group, respectively. The recruitment target was initially 15 per group, to allow for withdrawal, to a minimum of 12 per group.

However, it became clear that recruiting 15 individuals with A-T would prove difficult, due to the recruitment criteria and prevalence of A-T in the UK. The sample size was therefore recalculated based upon a sampling ratio of 2, equal variance with $SD = 0.1$, power of 80% and two sided alpha 0.05. Assuming average ΔEGP_{MET} in the A-T of 0.2 and controls 0.07 respectively, the required sample size was 7 and 14 participants respectively. We aimed to recruit 8 and 15, replacing any participants who withdrew.

Statistical analysis

Statistical analyses were performed using R studio. Data were tested for normality using Shapiro-Wilks or inspection of the data using QQ plots, or distribution of the residuals, where appropriate.

Normal data are presented as mean +/- SEM, and compared within group using the paired t test, and across groups using the non-paired t test. Non-normal data are presented as median with IQR and compared using Mann-Whitney U test. Categorical data were compared using Fisher's exact test.

Area under the concentration time curve, when calculated, used the trapezoidal method. The meal mean value was calculated as the AUC over time, to get the mean value for the duration of the MMT.

Linear and mixed effects models were used for additional analyses. The data were modelled using the R package "stats" in R studio, which can model both linear and generalised linear models. For mixed effects models, the R package "nlme" was used for analysis.

To compare insulin sensitivity of the two groups at baseline, linear regression models were used to assess which covariates were significant in predicting the

outcome of the model (insulin sensitivity). The covariates which best explain the variance of the outcome, as per adjusted R^2 , are included in the model. This can be employed to confirm if genotype (A-T or control) is significant in determining insulin sensitivity.

To compare the change from baseline during treatment between the groups, a mixed effects model is required to identify a genotype (A-T vs Control) by treatment interaction. As the data is paired, with each individual having baseline and post-treatment measures, the effect of the individual is included in the model as a random effect. The fixed effects within the model are the genotype * treatment interaction terms, and the outcome is a measure of insulin sensitivity.

To assess which drug is best for the treatment of insulin resistance and diabetes in A-T, it is necessary to compare data from the A-T group across the three visits, using a mixed model. The model allows comparison of the change in insulin sensitivity from baseline with each treatment, while accounting for the random effect of the individual.

Results:

Recruitment

The recruitment flow chart below summarises the participant recruitment for the RAMP study.

Initially it was thought that the majority of our A-T group would be recruited via the National Centre for A-T, in Papworth Hospital, Cambridge. However, after a visit to the unit, it became clear that individuals with A-T visit the “clinic” once per year, involving a 48 hour stay in hospital, which included numerous investigations and consultations with a broad multi-disciplinary healthcare team. Inclination to participate in clinical research would understandably be at its lowest whilst undergoing multiple investigations and enduring repeated blood samples.

Instead, all of our recruited participants were identified via the A-T Society. Through their database, it was clear that our original target of 15 individuals with A-T was going to be difficult. In their UK database, there were approximately 60 individuals who fit the inclusion criteria for the A-T group. Considering the extent of disability in A-T, and the intensive nature and distance of travel required for the study, it became clear that recruitment of 15 individuals might not be achievable. Our sample size calculation was therefore repeated (see statistical analysis – sample size) with an increase in the sampling ratio, to allow for a smaller case cohort by increasing the control cohort, to achieve the same power.

The flow diagram below illustrates participant recruitment from the available sources for the RAMP study.

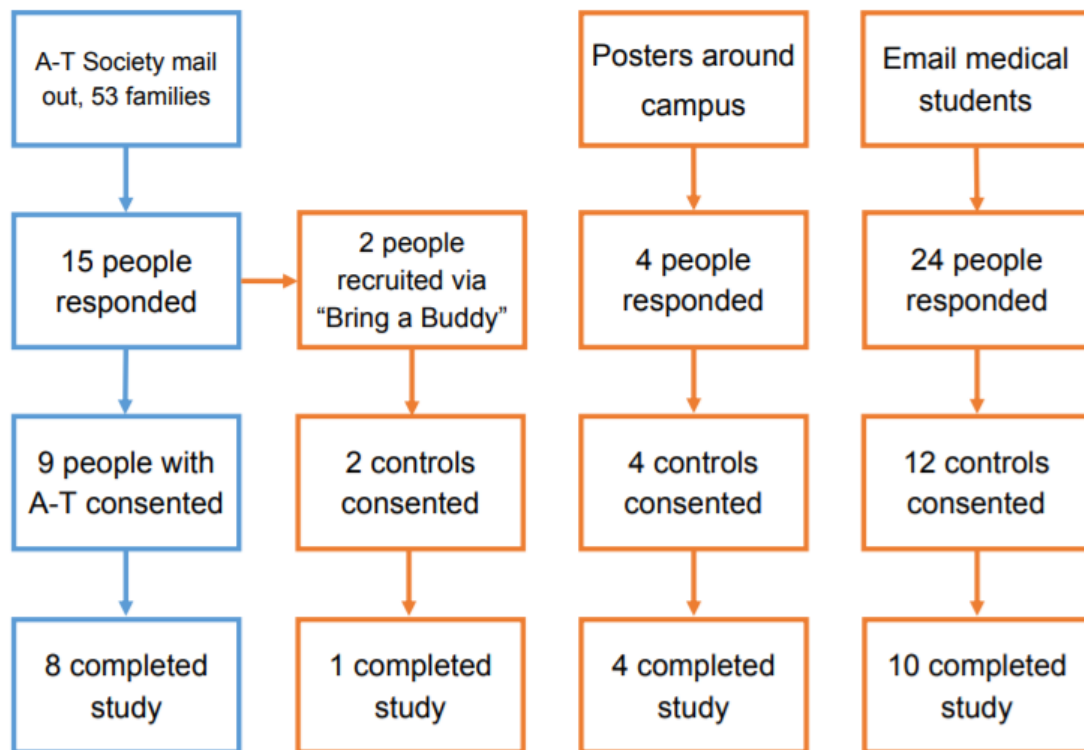


Figure 43 Recruitment flow diagram for the RAMP study

Of the nine people with A-T recruited, one participant withdrew due to personal reasons and difficulty in the logistics of attending the study visits. Of the control group, 3 participants withdrew, two of whom vomited during the tracer study and the decision was made to discontinue the study. The final participant experienced symptoms of metformin intolerance and did not wish to continue in the study.

None of the data from individuals who withdrew has been included in the final analysis.

Baseline characteristics

The two groups were well matched for age, BMI, and baseline HbA1c, as shown in Table 19, below. Although not significant, it is worth noting that the two groups were different, for example, the A-T group were 62.5% female, while the control group were 40% female ($p = 0.24$).

As discussed, we anticipated that the chosen control group would not be ideal controls for the cases, as the majority of the individuals with Ataxia-Telangiectasia were wheelchair users, with a subsequent reduction in muscle mass. However, the groups were well matched for BMI, despite this potential difference in lean mass.

The A-T group included both classic and variant A-T, with four of each subtype recruited. Due to the small cohort, the A-T results were analysed as one group, with sub-analysis performed in some instances. However, the study was not powered to detect differences between the A-T sub-groups and this subgroup analysis should be viewed as exploratory only.

	AT	CONTROL	<i>p</i>
n	8	15	
GENDER, F (%)	5 (62.5)	6 (40.0)	0.24
AGE	23 (20.8 - 27.3)	22 (20 - 23.5)	0.49
BMI	23.2 (18.9 - 27.1)	23.3 (22.1 - 26.7)	0.43
HbA1C	35 (30.8 - 38.0)	34 (30 - 36)	0.68

Table 19 Baseline characteristics of RAMP participants. Data are median (IQR), unless otherwise stated. P values for Mann Whitney test for continuous data, Chi-squared for categorical data.

There was no significant difference in the absorption of paracetamol between the groups at baseline, when comparing median AUC of paracetamol over time (A-T 989 [IQR 762 – 1444], vs control 1041 [IQR 499 – 1269] mg/l.min, $p = 0.75$). The rate of appearance of oral glucose (RaO) did not differ between groups at any visit, therefore it can be assumed that gastric emptying was comparable between groups.

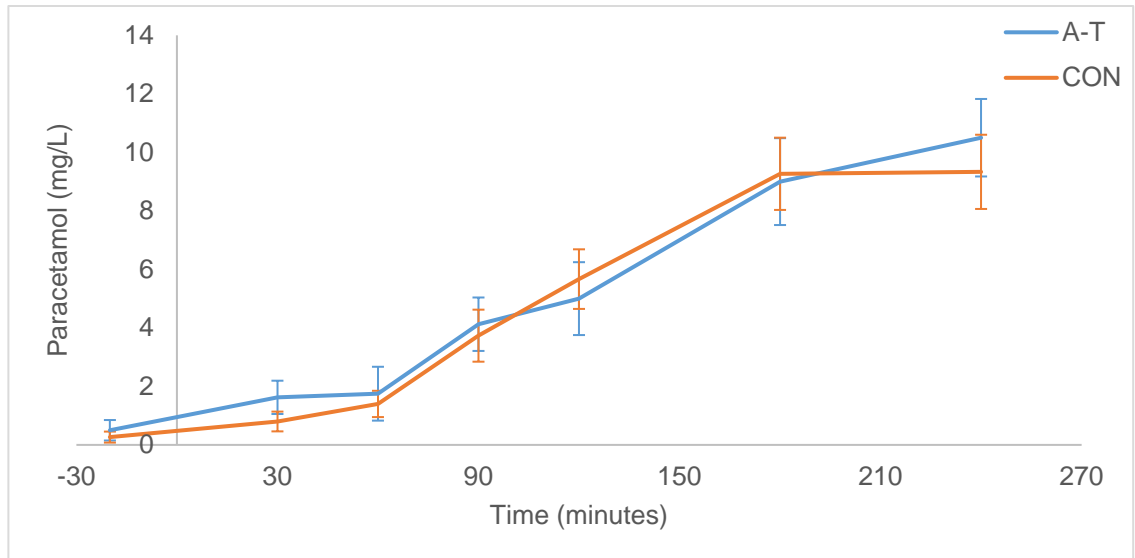


Figure 44 Paracetamol concentration over time. Data are mean (SEM).

The results have been analysed and are reported in the following sections:

1. Defining the phenotype – based on the comparison of the baseline data for the two groups.
2. Response to metformin – based on the comparison of metformin parameters to baseline, subdivided into fasting and MMT, and compared across groups.
3. Response to pioglitazone – as for metformin.
4. Comparison of treatment effects – based on the comparison of the change from baseline for each treatment within the A-T group.
5. Adipose distribution and function – based on the baseline MRI data, along with adipokine and NEFA data across treatments.

Each section will draw on comparison of the raw data, simple models e.g. HOMA, tracer modelling and beta cell modelling, where appropriate. Additional results are shown in Appendix 6: RAMP analysis, and results are summarised in table form in Appendix 7: Summary table RAMP results.

Individuals with A-T are insulin resistant

Fasting profile at baseline

The A-T group were insulin resistant compared to controls, as expected. Median fasting glucose at baseline (A-T 4.8 [IQR 4.4 – 5.1], vs control 4.6 [IQR 4.5 – 4.7] mmol/l, $p = 0.68$) was comparable between groups, however, median fasting insulin was significantly higher in the A-T group (A-T 61.1 [IQR 26.1 – 134.6] vs control 15.1 [IQR 7.8 – 24.9] pmol/l, $p = 0.002$). Median fasting glucose clearance and endogenous glucose production were not different between the groups at baseline. Fasting insulin secretion rate (ISR) was higher in the A-T group (A-T 96 [IQR 54 – 111] vs control 48 [IQR 38 – 64] pmol/min/m², $p = 0.04$). In the context of comparable fasting glucose, glucose clearance and endogenous glucose production, the increased rate of insulin secretion represents resistance to the action of insulin.

The A-T group have a higher median HOMA-IR than controls (A-T 2.19 [IQR 0.96 – 4.14] vs control 0.51 [IQR 0.27 – 0.89], $p = 0.002$). The wide interquartile range in the A-T group reflects the heterogeneity within the group. However, when subdivided into “classic” and “variant” A-T, both subgroups have higher HOMA-IR than controls (classic 4.4 [IQR 3.0 – 6.7]; variant 1.4 [IQR 1.0 – 2.0] and control 0.5 [IQR 0.3 – 0.9], $p = 0.009$ and $p = 0.036$ respectively), and the A-T subgroups are not significantly different ($p = 0.34$).

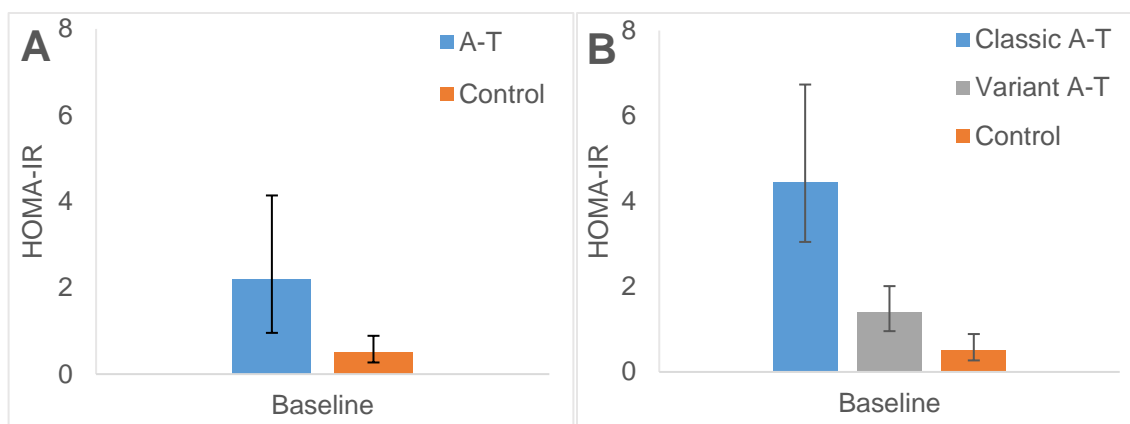


Figure 45 HOMA-IR at baseline (A), with A-T subdivided into classic and variant (B). Data are median (IQR).

Meal Test (MMT)

Despite comparable fasting glucose levels, meal mean (AUC divided by time) glucose was higher in the A-T group (A-T 6.3 [IQR 6.1 – 6.7] vs control 5.2 [IQR 5.0 – 5.6] mmol/l, $p < 0.001$). The A-T group also had higher mean insulin concentration (A-T 393 [IQR 275 - 2103] vs control 147 [IQR 95 - 227] pmol/l, $p = 0.005$) and mean insulin secretion rate during the MMT (A-T 878.8 [IQR 63.6 – 125.3] vs control 47.0 [IQR 40.4 – 56.3] nmol/m², $p = 0.003$).

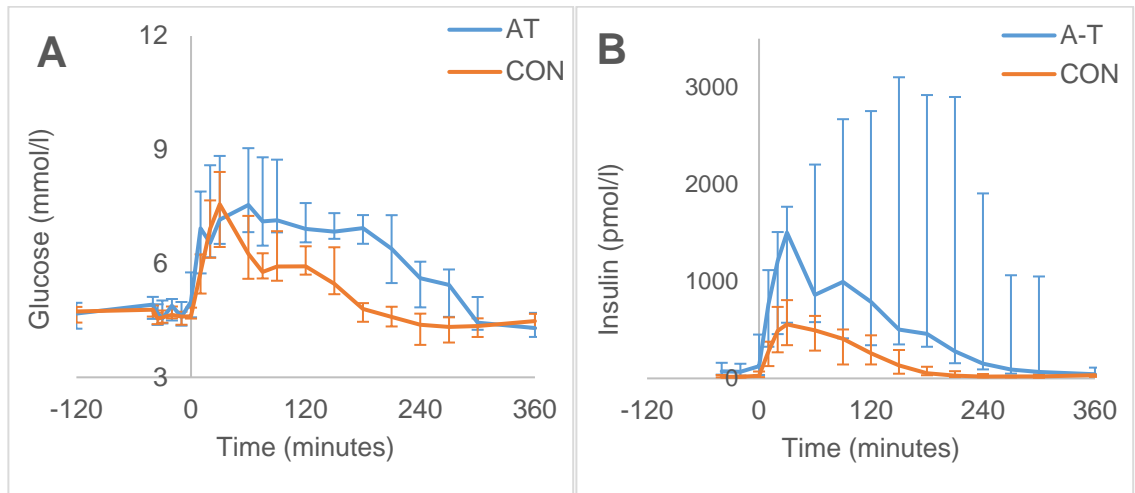


Figure 46 Plasma glucose (A) and plasma insulin (B) concentration during baseline MMT. Data are median (IQR).

The mean glucose clearance during the MMT appears higher in the control group at baseline (see figure 49), though not statistically significant (A-T 2.8 [IQR 2.7 – 3.2] vs control 3.3 [IQR 3.1 – 3.5] ml/min/kg, $p = 0.13$). This is despite higher mean insulin concentration and secretion rate in the A-T group, indicating peripheral insulin resistance in the A-T group.

Conversely, mean endogenous glucose production during the meal was lower in the A-T group than controls (A-T 3.7 [IQR 3.3 – 4.4] vs control 5.2 [IQR 4.8 – 6.5] $\mu\text{mol}/\text{min}/\text{kg}$, $p = 0.004$), with a greater, though not significant, suppression from fasting EGP (see figure 49). This could indicate that the A-T group have preserved hepatic insulin sensitivity, however, this was in the context of markedly elevated insulin concentrations throughout the MMT.

The median Matsuda index (251), was lower in the A-T group at baseline (A-T 2.7 [IQR 1.2 – 5.9] vs control 8.8 [IQR 6.2 – 17.7], p 0.002), in-keeping with whole body insulin resistance in the glucose-stimulated state, in this patient group. Similarly, the A-T group have a lower oral glucose insulin sensitivity (OGIS) index (A-T 322 [IQR 198 - 374] vs controls 444 [IQR 404 - 474], p <0.001), similar to that seen in obese individuals or those with IGT (253). However, the median insulinogenic index (IGI) was not different between groups (A-T 4.3 [IQR 2.0 – 7.2] vs control 1.5 [IQR 1.3 – 2.6], p 0.09), and secretion appeared normal (i.e. >0.4) in both groups.

The Matsuda index can be plotted against the ISR to demonstrate beta cell function and the product of the two values gives the oral disposition index (256, 257). The resulting plot (Figure 47) has an inverse non-linear distribution, similar to that seen in the traditional rectangular hyperbola of the disposition index (346). This indicates that at lower insulin sensitivity, the beta cell is appropriately upregulated to secrete more insulin. Glucose sensitivity (A-T 87.6 [IQR 68.3 – 101.1] vs control 91.4 [IQR 62.3 – 101.1] pmol/min/m²/mmol, p = 1.0) – calculated as the slope of the dose response curve – is also comparable between the two groups. Therefore, the beta cell function of the two groups appears comparable.

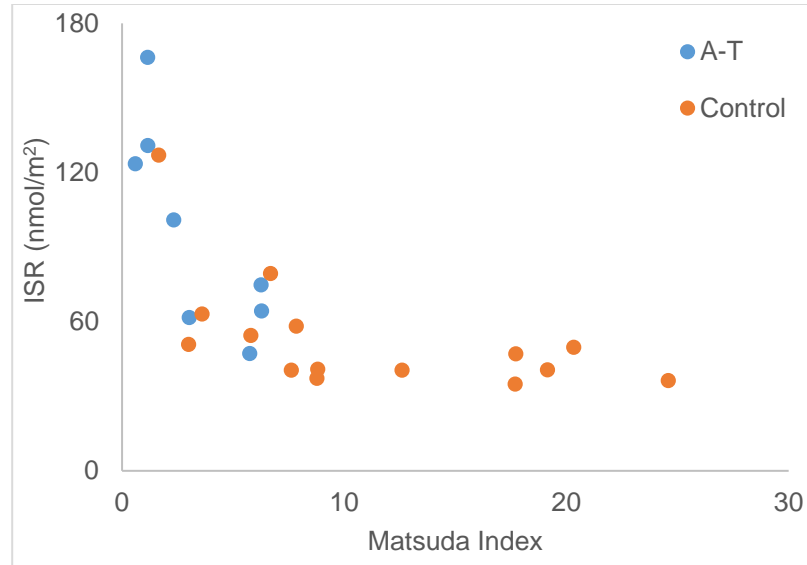


Figure 47 ISR plotted against Matsuda index, showing the typical hyperbolic relationship of the disposition index.

There was no significant difference between the genotype groups in fasting or mean glucagon, active GLP1, total GLP1, resting energy expenditure (REE) or respiratory quotient (RQ) at baseline.

Linear regression model

Linear regression models can be used to assess which covariates are significantly associated with insulin sensitivity. With OGIS as the response variable, individual variables of clinical interest and relevance were modelled independently, before combining the significant terms (genotype, mean glucagon during MMT, and adiponectin) in a full model, along with age, sex and BMI. The full model was then simplified to the model of best fit, as per adjusted R^2 .

The final model identifies genotype ($p < 0.001$), mean glucagon ($p < 0.001$) and age ($p = 0.048$) as significant terms, which contribute to the model of best fit (adjusted R^2 0.66, $p = 2.49 \times 10^{-5}$). Controlling for BMI improves the model fit marginally (to adj. R^2 0.69), however, BMI is not significant within the model ($p = 0.12$).

Of note, visceral adipose tissue and liver fat fraction were significant independently when modelling OGIS, however, due to missing MRI data in some participants, it was not included in the full model.

Summary

From the baseline data we have demonstrated that the A-T group are insulin resistant compared to healthy controls, likely caused by peripheral insulin resistance. The insulin resistance is evident at fasting and in the glucose-stimulated state, as demonstrated by elevated HOMA-IR and Matsuda indices respectively.

Response to metformin

Fasting profile on metformin

Metformin treatment reduced median fasting insulin concentration in the A-T group only (baseline 61.1 [IQR 26.1 – 134.6] to metformin 38.0 [IQR 26.0 – 111.6] pmol/l, $p = 0.04$), in the context of unchanged fasting glucose concentration in either group. There remained a difference in fasting insulin between the groups (A-T 38.0 [IQR 26.0 – 111.6] vs control 16.3 [IQR 11.1 – 25.2] pmol/l, $p = 0.02$). Fasting ISR post-metformin did not change from baseline in either group, and therefore, fasting ISR remained higher in the A-T group compared to controls (A-T 73.5 [IQR 56.7 – 121.0] vs control 52.4 [IQR 41.6 – 58.4] pmol/min/m², $p = 0.05$).

HOMA-IR remains higher in the A-T group after metformin treatment (A-T 1.4 [IQR 0.9 – 3.6] vs control 0.5 [IQR 0.4 – 0.9], $p = 0.01$), without significant change from baseline in either group.

Mixed meal test (MMT) post-metformin

Meal mean glucose and insulin were not different from baseline in either group after metformin treatment, with the between-group difference in mean glucose (A-T 6.6 [IQR 6.4 – 7.2] vs control 5.5 [IQR 5.3 – 5.7] mmol/l, $p < 0.001$), mean insulin (A-T 491 [IQR 254 – 1780] vs control 184 [IQR 125 – 220] pmol/l, $p = 0.01$) and mean insulin secretion rates (A-T 101 [IQR 67 - 142] vs control 52 [IQR 45 - 62] nmol/m², $p = 0.007$) remaining significant.

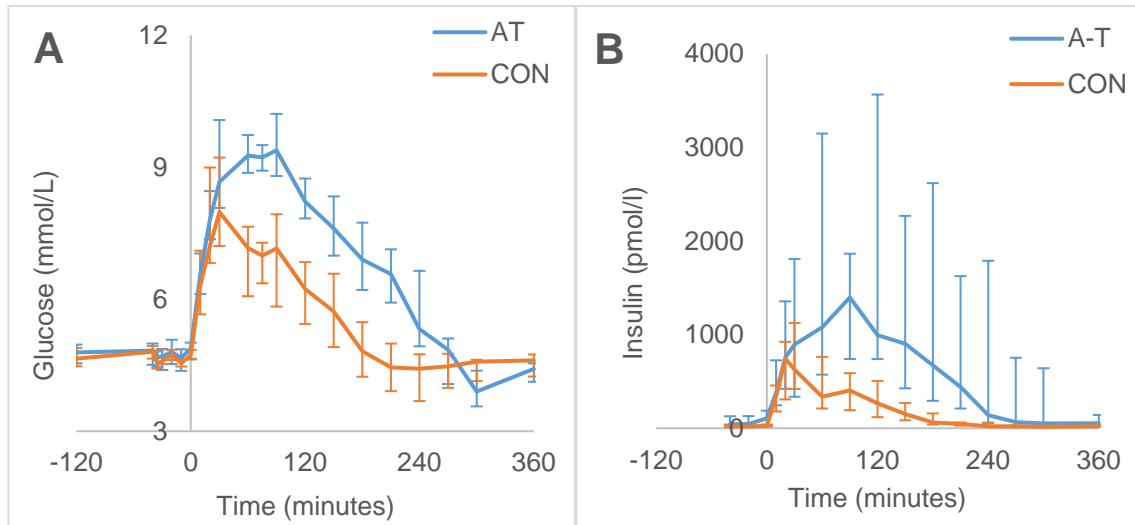


Figure 48 Meal mean (AUC / time) glucose (A) and insulin (B) post-metformin. Data are median (IQR).

There was no metformin-related change in beta cell function, with no change in glucose sensitivity ($p = 0.87$) nor in ISR for specified glucose ($p = 0.21$). The median Matsuda index for the A-T group did not change from baseline, remaining lower than controls despite metformin treatment (A-T 3.2 [IQR 1.3 – 4.6] vs control 7.9 [IQR 4.5 – 13.3], $p = 0.008$). Similarly, there was no change from baseline in the OGIS index in either group, with the A-T group remaining less insulin sensitive than controls (A-T 308 [IQR 161 - 346] vs control 437 [IQR 396 - 458], $p = 0.009$).

The Insulinogenic index was lower following metformin in the A-T group only (metformin 1.54 [IQR 0.73 – 3.71] vs baseline 4.35 [IQR 1.99 – 7.20], $p = 0.016$), with a similar insulin response to the control group (A-T 1.54 [IQR 0.73 – 3.71] vs control 1.53 [IQR 1.16 – 2.20], $p = 0.92$).

Differences in glucose kinetics following metformin

Despite unchanged fasting glucose concentration (and a reduction in fasting insulin in the A-T group), metformin treatment was associated with an increase in fasting glucose clearance from baseline in both groups (A-T: baseline 2.3 [IQR 2.2 – 2.8] vs metformin 2.6 [IQR 2.3 – 3.1] ml/min/kg, $p = 0.04$; control: baseline 2.7 [IQR 2.3 – 2.8] vs metformin 3.0 [IQR 2.7 – 3.4] ml/min/kg, $p < 0.001$).

Interestingly, metformin treatment resulted in a *rise* in the endogenous glucose production at fasting in the control group only (baseline 10.9 [IQR 10.1 – 12.4] to metformin 13.8 [11.7 – 15.0] $\mu\text{mol}/\text{min}/\text{kg}$, $p < 0.001$); this effect was not significant in the A-T patients.

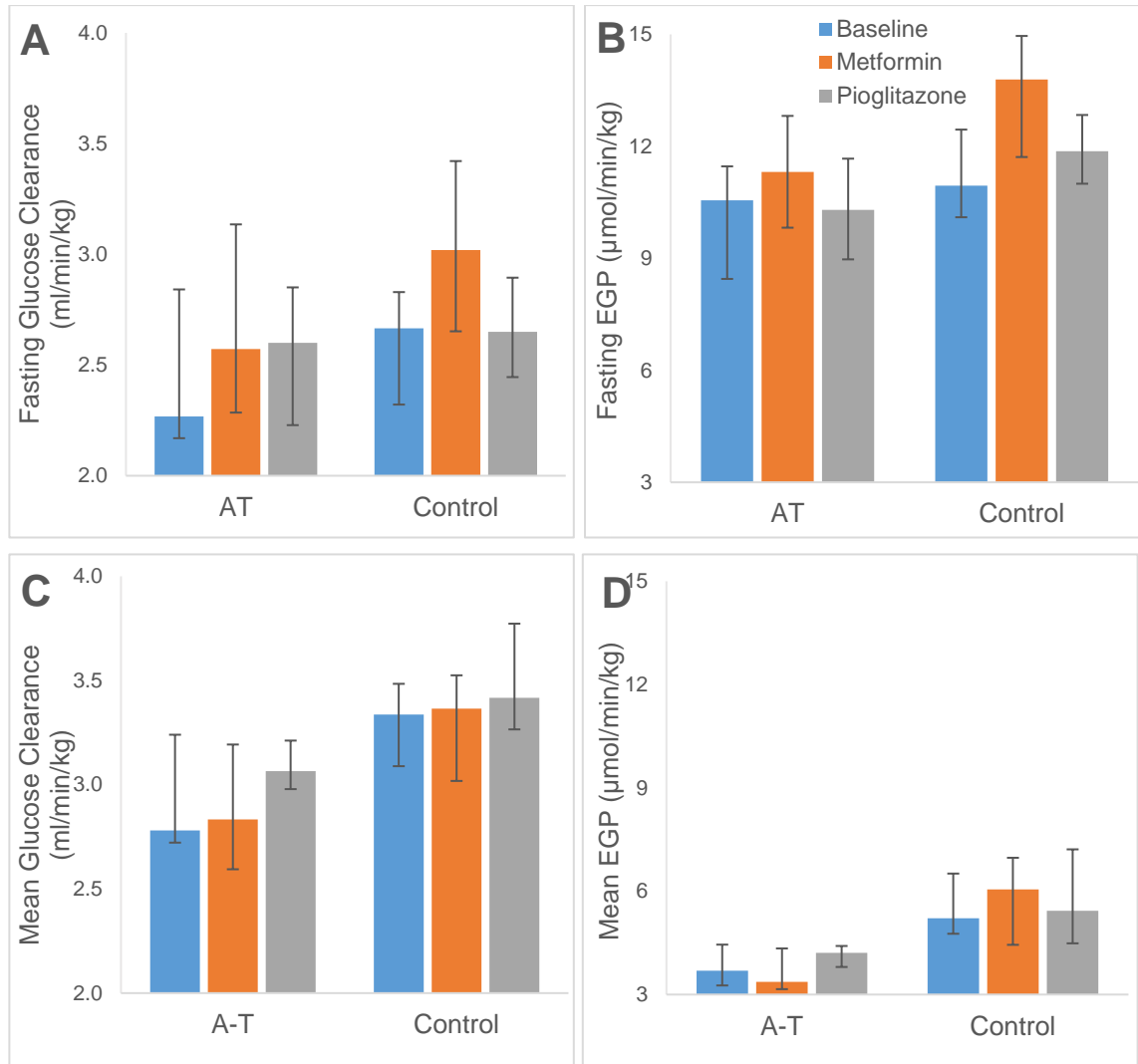


Figure 49 **Fasting** glucose clearance (A) and endogenous glucose production (EGP) (B) and **meal mean** glucose clearance (C) and EGP (D) at all visits for both genotypes. Data are median (IQR).

Within the genotype groups, the mean glucose clearance was not significantly different following metformin compared to baseline. However, comparing the two groups following metformin treatment, the control group had a higher mean

glucose clearance than the A-T group (control 3.4 [IQR 3.0 – 3.5] vs A-T 2.8 [IQR 2.6 – 3.2] ml/min/kg, $p = 0.04$).

Similarly, following metformin treatment there was no change from baseline in the mean glucose production within group, therefore glucose production remained higher in the control group (control 6.1 [IQR 4.4 – 7.0] vs A-T 3.4 [IQR 3.2 – 4.3] $\mu\text{mol}/\text{min}/\text{kg}$, $p = 0.02$), as at baseline.

Other effects of metformin

In the **control group only**, metformin treatment was associated with a significant increase from baseline in:

- **Fasting active GLP1** (baseline 0.4 [IQR 0.3 – 1.3] to metformin 1.6 [IQR 0.8 – 3.3] pg/ml, $p = 0.02$)
- **Mean active GLP1** (baseline 2.7 [IQR 1.8 – 4.3] to metformin 3.7 [IQR 2.5 – 6.8] pg/ml, $p = 0.048$)
- **Fasting total GLP1** (baseline 5.5 [IQR 4.0 – 11.9] to metformin 8.4 [IQR 7.7 – 12.7] pg/ml, $p = 0.03$)
- **Mean total GLP1** (baseline 11.1 [IQR 6.7 – 13.5] to metformin 13.7 [IQR 7.8 – 36.5], $p = 0.03$)
- **Meal mean glucagon** (baseline 54.5 [IQR 35.8 – 71.0] to metformin 58.4 [IQR 42.3 – 78.4], $p = 0.007$).

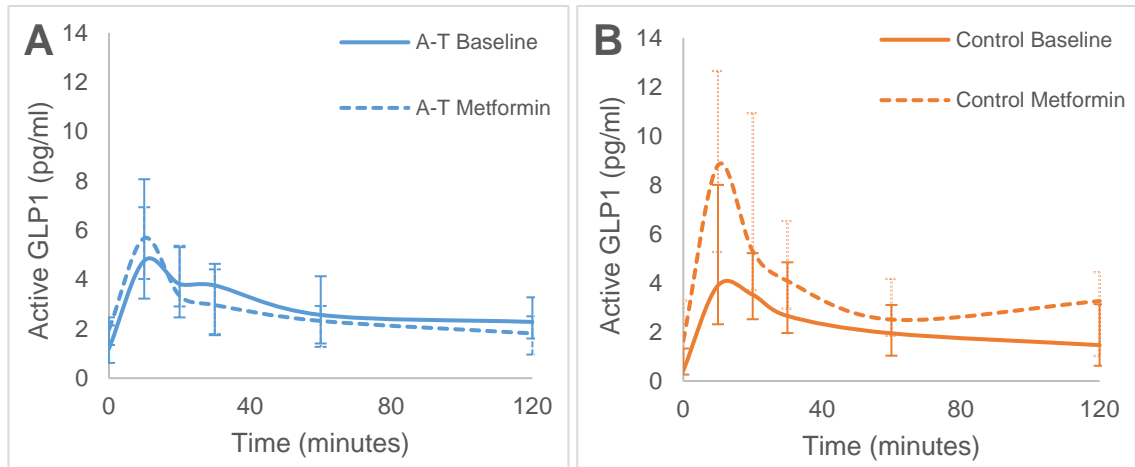


Figure 50 Active GLP1 over the MMT at baseline and post-metformin in the A-T (A) and control (B) group

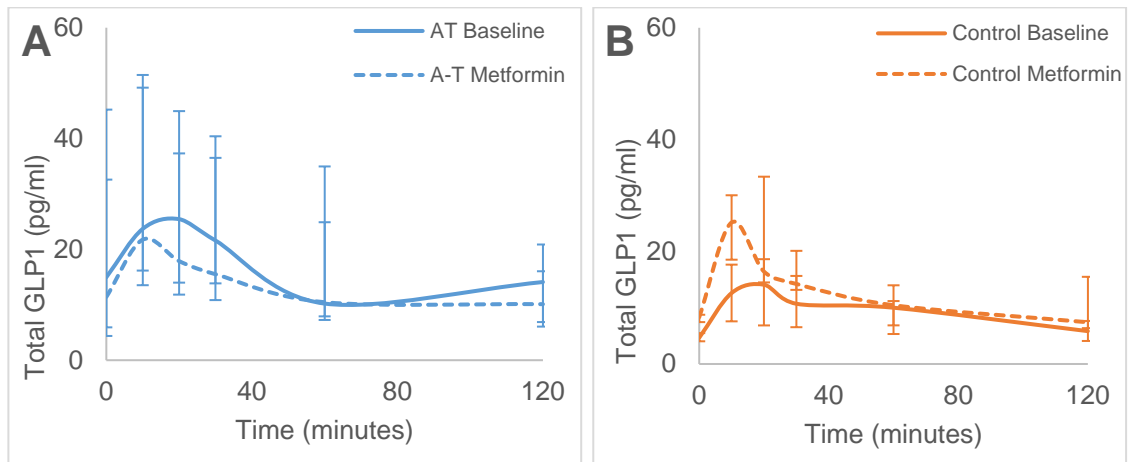


Figure 51 Total GLP1 over the MMT at baseline and post-metformin, in the A-T (A) and control (B) groups. Data are median (IQR).

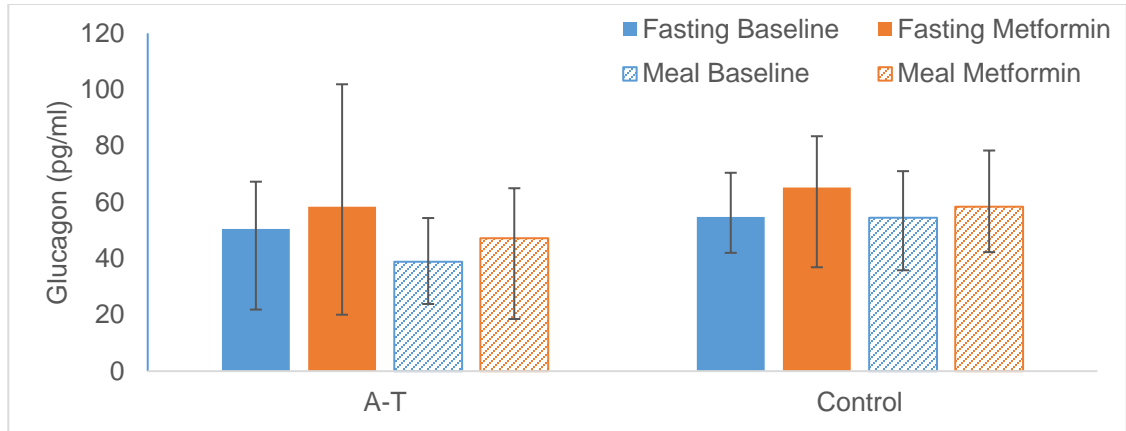


Figure 52 **Fasting** and **meal mean** glucagon at baseline and post-metformin for both genotypes. Data are median (IQR).

However, metformin treatment did not significantly affect GLP1 or glucagon within the A-T group. Direct comparison of the two groups following metformin did not identify a significant difference in GLP1 or glucagon.

BMI was reduced post-metformin in the control group (23.3 [IQR 22.1 – 26.7] to 23.2 [IQR 21.2 – 26.0] kg/m², $p = 0.02$), but was unchanged in the A-T group.

There is a loss of potentiation in the A-T group (see Appendix 6: RAMP analysis) compared to the control group, indicating a reduced incretin effect (347), as seen in obesity and type 2 diabetes. This is in-keeping with the lack of increment in GLP1 following metformin treatment in the A-T group. This may represent blunted response to metformin, as one would expect an increase in GLP1 with metformin, as seen in the control group.

Mixed effects model

To compare the change from baseline during metformin treatment between the groups, mixed effects modelling was used.

In a mixed effects model using OGIS as the outcome variable to assess for a gene x metformin interaction affecting insulin sensitivity, there was no significant

interaction identified between genotype and metformin. Treatment was not significant, however genotype was significant independently ($p = 0.001$).

lme (OGIS ~ Genotype * Treatment), AIC = 494

Model term	<i>P</i> value
Genotype	0.001
Treatment	0.8
Genotype * Treatment	0.9

Controlling for age, sex and BMI improves the fit of the model:

lme (OGIS ~ Genotype * Treatment + Age + Sex + BMI), AIC = 477

Model term	<i>P</i> value
Genotype	<0.001
Treatment	0.58
Genotype * Treatment	0.98
Age	0.02
Sex	0.86
BMI	0.10

Age is not significant independently, but is significant when added to the genotype * treatment interaction term as shown above. This is in-keeping with the modelling at baseline.

Secondary analysis was performed to include other terms which were significant independently in linear mixed models of OGIS. Mean active GLP1 was the only term besides genotype which was independently significant. Therefore, mean active GLP1 was added to the model above to achieve the model of best fit:

lme (OGIS ~ Genotype * Treatment + Mean a.GLP1 + Age + Sex + BMI),

AIC = 464

Model term	P value
Genotype	<0.001
Treatment	0.12
Genotype * Treatment	0.35
Age	0.01
Sex	0.95
BMI	0.07
Mean a.GLP1	0.008

The lack of a significant gene * drug interaction means that individuals with A-T do not have an exaggerated response to metformin, when considering insulin sensitivity. However, given that metformin has many potential mechanisms and

may not work solely (if at all) by improving insulin sensitivity, we modelled other parameters in which there was a significant difference between groups using non-parametric testing. This included BMI, fasting and mean active and total GLP1; mean glucagon; EGP and glucose clearance. None of these models identified a gene*metformin interaction (for full models and output see Appendix 6: RAMP analysis).

Response to pioglitazone

Fasting profile on pioglitazone

Pioglitazone treatment markedly reduced fasting insulin concentration in the A-T group only (baseline 61.1 [IQR 26.1 – 134.6] to 28.0 [IQR 20.9 – 110.1] pmol/l, $p = 0.008$). Similarly, the fasting ISR was reduced (though not significantly) from baseline in the A-T group (baseline 96.0 [IQR 53.8 – 110.6] vs pioglitazone 63.7 [IQR 59.7 – 90.5] pmol/min/m², $p = 0.20$), such that the fasting ISR following pioglitazone treatment was no longer significantly different between groups (A-T 63.7 [IQR 59.7 – 90.5] vs control 55.7 [IQR 47.0 – 74.7] pmol/min/m², $p = 0.27$).

There was no change from baseline in fasting glucose concentration, clearance or production in either group following pioglitazone treatment.

In-keeping with the reduction in insulin concentrations, there was a reduction in HOMA-IR from baseline in the A-T group (baseline 2.19 [IQR 0.96 – 4.14] to pioglitazone 0.97 [IQR 0.76 – 3.54], $p = 0.023$). However, despite this reduction, the HOMA-IR of the A-T group following pioglitazone treatment remained higher than that of the control group (0.97 [IQR 0.76 – 3.54] vs 0.61 [IQR 0.53 – 0.80], $p = 0.016$). The HOMA-IR of the control group remained unchanged (baseline 0.51 [IQR 0.27 – 0.89] to pioglitazone 0.61 [IQR 0.53 – 0.80], $p = 0.76$).

Mixed meal test (MMT) post-pioglitazone

In the A-T group, pioglitazone reduced the meal mean glucose (baseline 6.4 [IQR 6.1 – 6.7] to pioglitazone 5.9 [IQR 5.7 – 6.2] mmol/l, $p = 0.02$), in the context of a lower meal mean insulin concentration (baseline 393 [IQR 275 – 2103] to pioglitazone 252 [IQR 195 – 823], $p = 0.02$) and lower mean ISR during the MMT (baseline 87.8 [IQR 63.6 – 125.3] vs pioglitazone 78.3 [IQR 49.7 – 111.9] nmol/m², $p = 0.008$), indicating an improvement in insulin sensitivity. Despite lower meal mean glucose in the A-T group, there was no difference in glucose clearance ($p = 0.20$) or production ($p = 0.31$) during the MMT (Figure 49).

There was no change in the control group meal mean glucose or insulin concentrations.

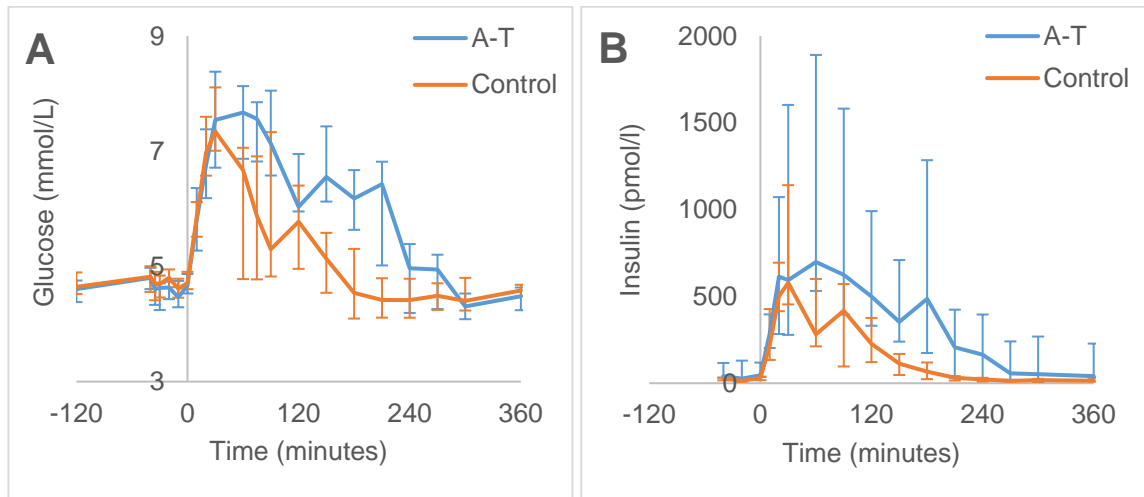


Figure 53 Glucose (A) and insulin (B) over the duration of the MMT post-pioglitazone. Data are median (IQR).

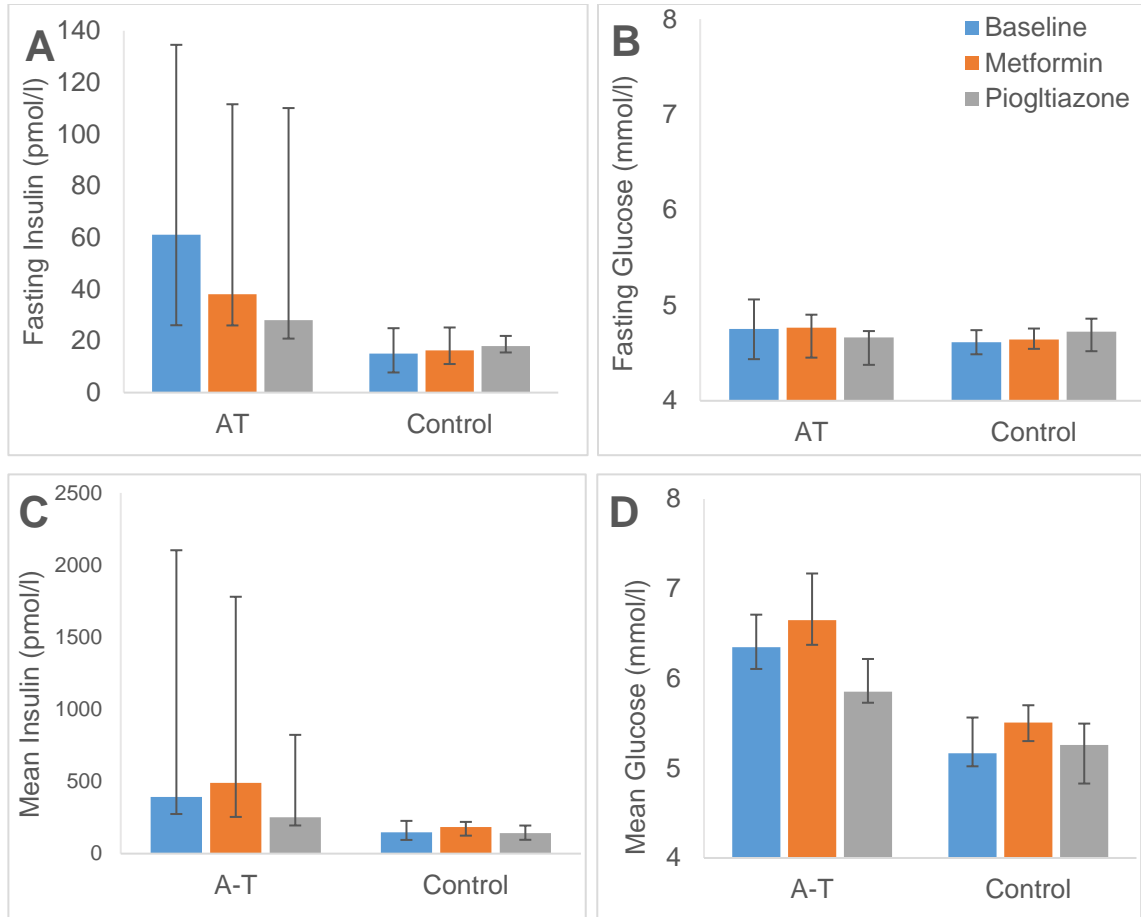


Figure 54 **Fasting insulin (A) and glucose (B) and meal mean insulin (C) and glucose (D) at all visits, both genotypes. Data are median (IQR).**

Following pioglitazone treatment, the median Matsuda index of the A-T group increased (baseline 2.7 [IQR 1.2 – 5.9] to pioglitazone 5.3 [IQR 1.6 – 7.1], $p = 0.0078$), and was no longer significantly different from the control group (A-T 5.3 [IQR 1.6 – 7.1] vs control 8.2 [IQR 6.1 – 13.3], $p = 0.06$).

Similarly the OGIS index increased in the A-T group with pioglitazone treatment (baseline 322 [IQR 198 – 374] to pioglitazone 364 [IQR 322 – 426], $p = 0.008$), while the control group remain unchanged (baseline 444 [IQR 404 – 474] to pioglitazone 453 [IQR 408 – 467], $p = 0.8$). However, the two groups remain significantly different post-pioglitazone (A-T 364 [IQR 322 – 426] vs control 453 [IQR 408 – 467], $p = 0.03$), indicating that the OGIS may be a more sensitive index for comparison of treatment effects.

As the OGIS and Matsuda indices increased, in-keeping with an improvement in insulin sensitivity, so too the IGI decreased in the A-T group (baseline 4.35 [IQR 1.99 – 7.20] to pioglitazone 1.88 [IQR 1.28 – 3.88], $p = 0.078$), although not reaching significance. The IGI was not different between groups post-pioglitazone (A-T 1.88 [IQR 1.28 – 3.88] vs control 2.22 [IQR 1.37 – 2.79], $p = 0.92$).

Other effects of pioglitazone

Pioglitazone had no significant effect on fasting or mean glucagon, active or total GLP1 in either group, therefore, as at baseline, the two groups had comparable glucagon and GLP1 following pioglitazone treatment.

Interestingly, the median fasting respiratory quotient was increased by pioglitazone treatment in the A-T group only (0.9 [IQR 0.8 – 1.0] to 1.1 [IQR 1.0 – 1.2], $p = 0.04$), indicating a move from fatty acid to carbohydrate oxidation. REE of the A-T group was also reduced following pioglitazone (1377 [IQR 1275 – 1450] to 1169 [IQR 1046 - 1288] kcal/day, $p = 0.03$), in the context of unchanged BMI.

Mixed effects model

To compare the change from baseline during pioglitazone treatment between the groups, mixed effects modelling was used, as performed for the metformin data, to identify a genotype * pioglitazone interaction.

In a linear mixed effects model of OGIS, there is an interaction between A-T and pioglitazone ($p = 0.001$). Pioglitazone treatment was not significant independently ($p = 0.72$) as it did not affect OGIS in controls. However, genotype was significant independently ($p < 0.001$), as OGIS was lower in the A-T group at baseline.

Model 1: lme (OGIS ~ Genotype * Treatment), AIC = 479

Model term	<i>P</i> value
Genotype	<0.001
Treatment	0.7
Genotype * Treatment	0.001

Controlling for age, sex and BMI improves the fit of the model:

Model 2: lme (OGIS ~ Genotype * Treatment + Age + Sex + BMI), AIC = 459

Model term	<i>P</i> value
Genotype	<0.001
Treatment	0.77
Genotype * Treatment	0.001
Age	0.05
Sex	0.22
BMI	0.25

Secondary analysis was performed to include other terms which were significant independently in simple linear mixed models of OGIS, specifically mean active GLP1, leptin, and basal and mean glucagon.

Model 3: lme (OGIS ~ Genotype * Treatment + Age + Sex + BMI+ mean a.GLP1 + Leptin + basal Glucagon + mean Glucagon),

AIC = 466

Model term	<i>P</i> value
Genotype	<0.001
Treatment	0.99
Genotype * Treatment	<0.001
Age	0.04
Sex	0.75
BMI	0.07
Mean a.GLP1	0.14
Leptin	0.20
Basal Glucagon	0.19
Mean Glucagon	0.89

The model above was then simplified to achieve model of best fit:

Model 4: lme (OGIS ~ Genotype * Treatment + Age + BMI + mean a. GLP1 + basal Glucagon), AIC = 459

Model term	P value
Genotype	<0.001
Treatment	0.87
Genotype * Treatment	0.001
Age	0.03
BMI	0.07
Mean a.GLP1	0.08
Basal Glucagon	0.009

However, despite equal AIC, ANOVA of model 2 and model 4 indicates that model 2 is superior and is the model of best fit.

Metformin versus pioglitazone

To assess which drug is best for the treatment of insulin resistance and diabetes in A-T, it is necessary to compare data for the A-T group across the three visits, using a linear mixed model. The model allows comparison of the change in insulin sensitivity from baseline with each treatment, while accounting for the random effect of the individual.

Therefore, OGIS was modelled in a subset of the data, looking at the A-T group only, with treatment as a fixed effect and the effect of the individual as a random effect in the model.

Model AT: lme (OGIS ~ Treatment) in A-T only, AIC = 249

Model term	<i>P</i> value
Metformin	0.73
Pioglitazone	0.002

In A-T, there is no effect of metformin on OGIS ($p = 0.73$), but pioglitazone was highly significant (0.002), indicating that pioglitazone would be the treatment of choice to improve insulin sensitivity in A-T.

Adipocytes in A-T

Adipokines

Baseline

The baseline adiponectin concentration was lower in the A-T group (A-T 2528 [IQR 2008 – 4887] vs control 6262 [IQR 4051 – 89940] ng/ml, $p = 0.03$), despite comparable visceral adipose volume (A-T 1.82 [IQR 0.97 – 2.5] vs control 1.47 [IQR 0.87 – 1.9] litres, $p = 0.5$). Low adiponectin in the A-T group is in-keeping with the mouse model of A-T (238). Hyposecretion of adiponectin has been linked to obesity, diabetes, hyperlipidaemia, hypertension and atherosclerosis, and can be primary (caused by genetic disorders) or secondary (due to visceral fat accumulation) (331). Adiponectin is thought to promote insulin sensitivity via activation of AMPK, so reduction in adiponectin could lead to reduced insulin sensitivity.

However, unlike the mouse model, leptin concentrations were markedly increased in the A-T group (A-T 24013 [IQR 14591 - 30836] vs control 4867 [IQR 2501 - 12717] pg/nl, $p 0.004$) in the absence of obesity, likely representing leptin resistance.

Post-metformin

Adiponectin levels increased in the A-T group after metformin treatment (baseline 2528 [IQR 2008 – 4887] to metformin 3306 [IQR 2309 – 5390] ng/ml, $p = 0.15$). Though this observed increase was not statistically significant, the median adiponectin levels in the two groups were no longer statistically different post-metformin (A-T 3306 [IQR 2309 – 5390] vs control 5975 [IQR 3382 – 7966] ng/ml, $p = 0.12$).

On the other hand, leptin concentration remained higher in the A-T group than controls (A-T 17812 [IQR 6578 – 19918] vs control 5457 [IQR 1614 – 8170] pg/nl, $p 0.01$), despite a trend towards improvement with metformin treatment (baseline

24013 [IQR 14591 – 30836] to metformin 17812 [IQR 6578 – 19918] pg/ml, $p = 0.08$).

Post-pioglitazone

Adiponectin was markedly increased by pioglitazone treatment in both groups without change in BMI (A-T baseline 2528 [IQR 2008 – 4887] to pioglitazone 12461 [IQR 4451 – 15843] ng/ml, $p = 0.008$; and controls baseline 6262 [IQR 4051 – 89940] to pioglitazone 15123 [IQR 9594 – 19384] ng/ml, $p = 0.001$).

Leptin remained higher in the A-T group post-pioglitazone compared to controls (A-T 14812 [IQR 9362 – 22789] vs control 5323 [IQR 1648 – 7921] pg/ml, $p = 0.01$). Although the leptin concentration appeared lower following pioglitazone treatment compared to baseline in the A-T group, this was not statistically significant (baseline 24013 [IQR 14591 - 30836] to pioglitazone 14811 [IQR 9362 – 22789] pg/ml, $p = 0.15$).

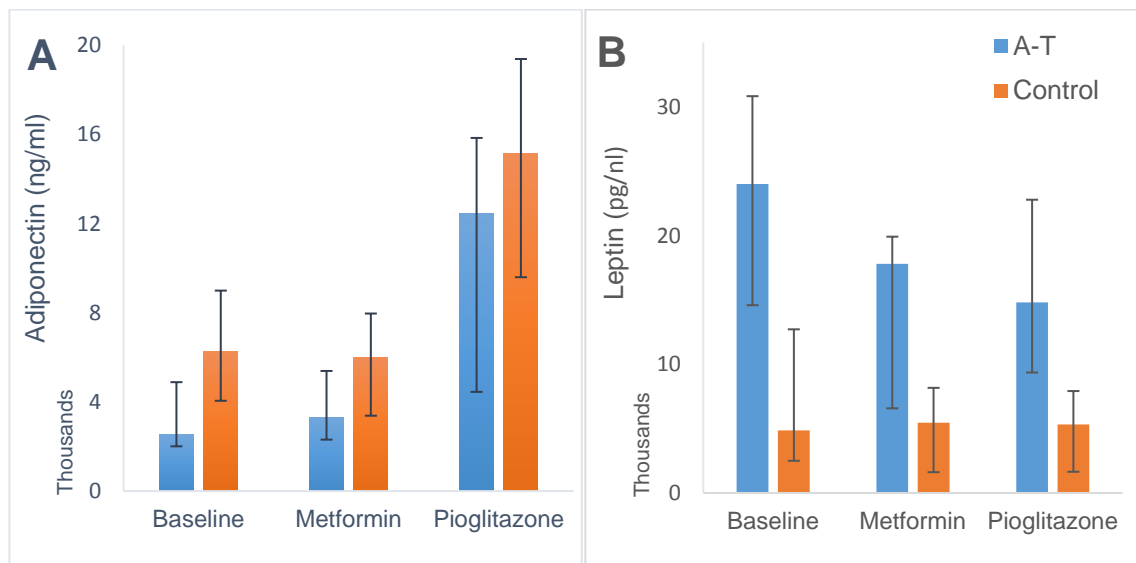


Figure 55 Serum adiponectin (A) and leptin (B) concentrations at baseline, post-metformin and post-pioglitazone in A-T and Control groups. Data are median (IQR).

NEFA in A-T

Elevated fasting NEFA concentration at baseline (A-T 0.72 [IQR 0.65 - 0.88] vs control 0.53 [IQR 0.45 – 0.68] mmol/l, $p = 0.03$), serves as further evidence of insulin resistance in the A-T group. This is despite comparable volume of visceral fat (as detailed below), which is known to be an important source of NEFA due to its lipolytic activity (348). The higher concentration of NEFA may be due to the reduced adiponectin concentration, with subsequent reduction in insulin sensitivity, and an increase in lipolysis (349).

Basal NEFA remained higher in the A-T group than controls during metformin therapy (A-T 0.74 [IQR 0.62 – 0.81] vs control 0.56 [IQR 0.51 – 0.60] mmol/l, $p = 0.03$), with no significant treatment effect within either group.

However, pioglitazone treatment resulted in decreased fasting and mean plasma NEFA from baseline in both groups (A-T fasting: baseline 0.72 [IQR 0.65 - 0.88] to pioglitazone 0.54 [IQR 0.43 – 0.60] mmol/l, $p = 0.008$; Control fasting: baseline 0.53 [IQR 0.45 – 0.68] to pioglitazone 0.46 [IQR 0.36 – 0.56] mmol/l, $p = 0.02$; A-T mean: baseline 0.25 [IQR 0.22 – 0.28] to pioglitazone 0.18 [IQR 0.14 – 0.20], $p = 0.016$; Control mean: baseline 0.21 [IQR 0.19 – 0.26] to pioglitazone 0.16 [IQR 0.14 – 0.20], $p = 0.007$). There was no longer any difference between the groups indicating an improvement in insulin sensitivity in the A-T group.

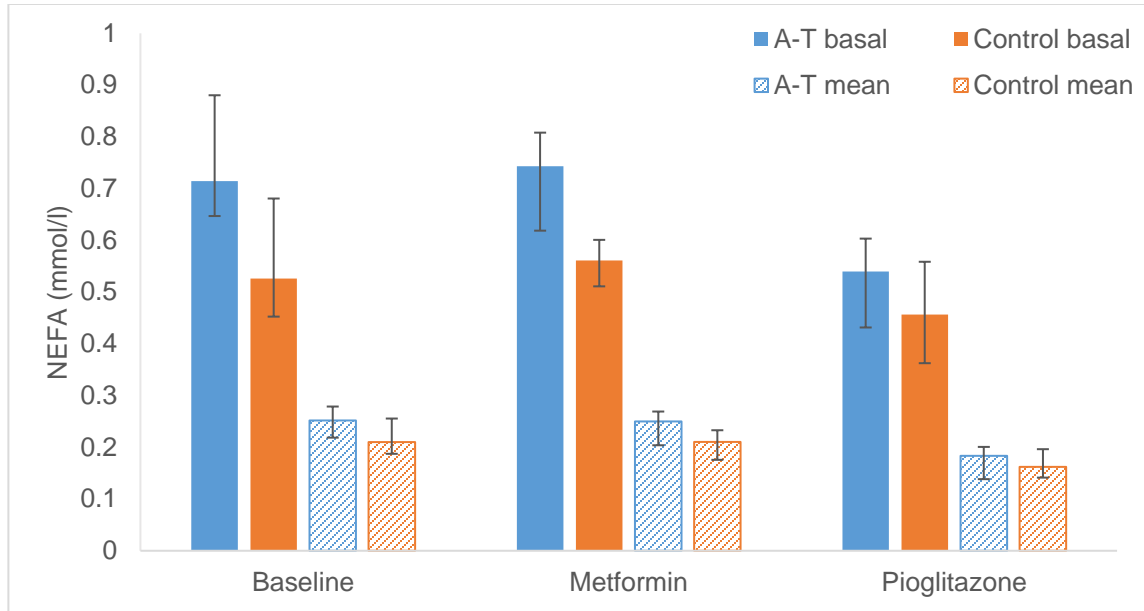


Figure 56 Basal and meal mean (AUC / time) plasma NEFA at each visit. Median (IQR).

Adipose distribution

The table below show the MRI data for the two groups:

	A-T	Control	p value
VAT (L)	1.8 (0.97 – 2.5)	1.5 (0.87 – 1.9)	0.54
SAT (L)	6.3 (4.4 – 8.9)	4.9 (3.0 – 6.4)	0.20
VAT:SAT	0.22 (0.20 – 0.38)	0.31 (0.25 – 0.39)	0.49
Total (L)	8.8 (5.7 – 11.0)	6.7 (4.0 – 8.0)	0.17
Liver fat fraction (%)	3.3 (1.6 – 10.5)	1.4 (1.0 – 1.8)	0.09
Liver Iron R2*	42.4 (39.0 - 59.3)	36.1 (33.8 – 39.9)	0.19

Table 20 MRI assessment of adipose volume and distribution. VAT = visceral adipose tissue; SAT = subcutaneous adipose tissue; VAT:SAT = visceral to subcutaneous adipose tissue ratio. Data are median (IQR).

While there was no difference identified between the two groups based on the MRI data shown, this is likely due to lack of power. Not all of the RAMP study participants were able to undergo MRI, and this resulted in 7 individuals with A-T

and 14 healthy controls being successfully scanned. The study was also not powered based upon the MRI outcomes.

Although the numbers are small, and it is therefore difficult to draw meaningful conclusion, it is interesting that the estimations of liver fat indicate a trend towards increased liver fat in the A-T group, which would be in-keeping with their insulin resistant phenotype. Of note, the individuals with classic A-T had increased liver fat compared to healthy controls (17.8% vs 1.4%, p 0.01), which is in-keeping with insulin resistance and the propensity for fatty liver disease in these individuals.

However, the VAT:SAT ratio was not different in the two groups ($p = 0.49$), and there is no evidence of a lipodystrophic phenotype as described in the ATM deficient mouse model.

Discussion

Research into metformin's mechanism of action is ongoing, over 60 years after its introduction to clinical use. The application of GWAS to the question of variability in metformin response identified a locus on chromosome 11 associated with glycaemic response to metformin. We hypothesised that the *ATM* gene was the likely causal gene at this locus, due to documented associations between *ATM* and the insulin signalling pathway; AMPK activation; and the insulin resistant phenotype seen in ATM-deficient mice and humans with A-T. Preliminary mouse data appeared to support the hypothesis that ATM was linked to metformin response, as metformin treatment of *ATM* +/- mice reverted glycaemia to normal levels of the wild type littermates. However, data from another mouse model of A-T identified a potential lipodystrophic phenotype in *ATM*-knockout mice, with abnormal adipose differentiation and reduced adipokine production, both of which responded well to treatment with TZDs, with concurrent improvement in glycaemia.

The "Response of individuals with Ataxia-telangiectasia to Metformin and Pioglitazone (RAMP)" study was designed to investigate the link between ATM

and metformin response, with the TZD pioglitazone as a comparator drug, due to the impressive data regarding response to TZDs in the mouse model of A-T. To our knowledge, the RAMP study is the first physiology study of its kind in this patient group, using dual tracer mixed meal tests and other investigations including MRI, to compare glucose kinetics, beta cell function and metabolic phenotype of individuals with A-T and healthy controls, presenting a unique opportunity to define the metabolic phenotype in this rare condition.

We confirmed that A-T is associated with peripheral insulin resistance, compared to healthy controls. Although unable to validate the pharmacogenetics result linking ATM to enhanced metformin response, we have demonstrated that A-T may be associated with a blunted response to metformin. In contrast, pioglitazone markedly improved insulin sensitivity and adipocyte function in the A-T group.

Metabolic phenotype in A-T

As expected, our data confirm that individuals with A-T are insulin resistant. Despite comparable age, BMI, and adipose volume and distribution, the A-T group had elevated fasting and meal mean insulin during the MMT at baseline. This reflects higher insulin secretion rates, secondary to insulin resistance. Despite normal fasting glucose and elevated mean insulin concentrations, the A-T group had greater excursion in mean glucose post-meal. This differs slightly from previously reported OGTT data, where both fasting glucose and insulin concentrations were comparable to healthy controls (330).

Elevated HOMA-IR, low OGIS and Matsuda indices in the A-T group confirm the presence of insulin resistance. The insulin resistance appears to be predominantly peripheral, with apparently normal beta cell function. The insulinogenic index is within normal range and the glucose sensitivity is comparable to healthy controls, therefore the beta cells are equally sensitive to glucose flux.

Interestingly, when the potentiation factor is plotted against time up to 120 minutes, the gradient of the curve is lower in the A-T group, which is in-keeping with a reduced incretin response (347), despite comparable GLP1 levels during the baseline visit. Reduced potentiation has previously been reported in impaired glucose tolerance and diabetes (222).

A-T is not associated with improved insulin sensitivity in response to metformin

From the RAMP data, we have been unable to identify an enhanced metformin effect on insulin sensitivity in the A-T group, compared with the controls.

The A-T group did have lower fasting insulin concentration following metformin, with an elevated fasting glucose clearance, with a (albeit non-significant) reduction in their fasting ISR. This suggests an improvement in *peripheral* insulin sensitivity, although this did not continue after glucose load, with their mean glucose, insulin and insulin secretion rate remaining higher than the control group and unchanged from baseline. Calculated indices of insulin sensitivity did not show any improvement with metformin in either group. Alternatively, metformin may increase glucose clearance via an insulin-independent pathway, which would then appear to improve peripheral insulin sensitivity.

A linear mixed effects model used to assess the impact of genotype and treatment on insulin sensitivity, did not identify a gene x metformin interaction between A-T and metformin.

However, metformin has many potential mechanisms of action, and may not work solely (if at all) by improving insulin sensitivity. When considering other mechanisms, there may be indication to suggest that the A-T group have a blunted response to metformin, compared to controls. The control group had a significant reduction in BMI post-metformin, where the A-T group did not. The control group had an increase in active and total GLP1 from baseline – a well-documented response to metformin (130, 140, 143) – but this not evident in the

A-T group. Similarly, there was an increase in mean glucagon post-metformin in the control group, which was not seen in A-T. However, secondary analyses using mixed effect models with GLP1, glucagon, glucose clearance or production as the outcome variable did not identify a gene x metformin interaction. Therefore, we have been unable to clinically validate the results of the GWAS, and it is unlikely that A-T is associated with altered response to metformin, either enhanced or blunted.

This may be because the GWAS data identified a SNP at a locus which included a number of genes, of those *ATM* was thought to be the causal gene. However, it is possible that one of the other genes from the locus identified is responsible for the GWAS signal.

Alternatively, as the minor allele frequency of the SNP identified by the GWAS is 44%, it is possible that we recruited individuals with wild type alleles of this SNP. However, through recruitment of individuals with A-T who typically have two different mutations in each allele of their *ATM* gene, often associated with truncation of the protein, we hoped to demonstrate a larger effect size than that expected from the SNP alone. However, without performing a recruit-by-genotype study, it is impossible to predict if the study population carry the SNP of interest.

It may be that, in order to fully expose a blunted response, the A-T group would need to be compared to insulin resistant individuals without A-T. This “control” group may have a greater physiological response to metformin than the normoglycaemic insulin sensitive controls used in RAMP, which would unmask the reduced response in A-T, by comparison.

Response to metformin in controls

The RAMP data has provided some interesting insight into metformin action. As discussed above, both groups had increased fasting glucose clearance after metformin treatment, which has been previously reported in clamp data (350, 351). This could reflect an improvement in peripheral insulin sensitivity, resulting

in increased glucose utilisation. Alternatively, the increase in clearance could represent increased glucose uptake by the intestine, which has recently been postulated as a “glucose sink” (352, 353).

The control group have a metformin-related counter-regulatory increase in their mean glucagon, perhaps to prevent hypoglycaemia in the context of increased glucose clearance in these normoglycaemic individuals. In-keeping with this, they have an increase in their fasting glucose production, which could be due to glucagon-induced glycogenolysis or gluconeogenesis. This has been described previously in healthy subjects, with a metformin-related increase in glucose clearance associated with a rise in glucagon, lactate and cortisol (354), and a subsequent increase in glucose production from gluconeogenesis and glycogenolysis.

This metformin-associated increase in EGP appears to defy conventional wisdom that metformin’s mechanism of action lies mainly in the reduction of hepatic gluconeogenesis. However, these pathways of metformin response are not necessarily mutually exclusive. In the context of hyperglycaemia, such as in individuals with type 2 diabetes, the metformin-associated increase in glucose clearance may not be sufficient to induce hypoglycaemia or stimulate counter-regulatory mechanisms, such as glucagon. In this setting, the hepatic effects of metformin to reduce gluconeogenesis are permissible. However, in the healthy individual with normoglycaemia, increased glucose clearance may risk hypoglycaemia, thereby stimulating glucagon secretion. The inhibitory effect of metformin on hepatic gluconeogenesis would be outweighed by the stimulatory effects of glucagon on glycogenolysis and gluconeogenesis.

In contrast to the healthy controls, the individuals with A-T, who have greater mean glucose post-meal than the control subjects, did not have elevated glucagon, nor elevated glucose production, indicating that the increase in glucose clearance did not stimulate a counter-regulatory response.

Pioglitazone improves insulin sensitivity in A-T

The data from the RAMP study supports the mouse data that TZDs improve glycaemia and insulin resistance in A-T. Despite no change in fasting glucose concentration, and a reduction in their mean glucose during the meal, the A-T had reduced fasting and mean insulin concentrations, reflecting a reduction in mean insulin secretion rate. There was no change in glucose production or clearance during pioglitazone treatment, despite the reduced insulin secretion rate, in-keeping with greater response to circulating insulin, due to reduced peripheral insulin resistance.

Calculated indices of insulin sensitivity (OGIS and Matsuda) are increased by pioglitazone treatment in the A-T group, and HOMA-IR is reduced, reflecting the improved insulin sensitivity the treatment confers.

Beta cell modelling did not reveal statistically significant changes in beta cell glucose sensitivity, although this was numerically greater than at baseline. The lack of significance may be due to the wide interquartile range and heterogeneity within the A-T group. Similarly the rate sensitivity was lower post-pioglitazone, but this did not reach significance. It is likely, therefore, that pioglitazone improves in beta cell sensitivity to glucose, as well as increasing peripheral insulin sensitivity.

The pioglitazone-associated increase in insulin sensitivity may be partly explained by an increase in adiponectin secretion, which is known to promote insulin sensitivity. Both groups had a large increment in adiponectin levels post-pioglitazone compared to baseline, with associated decrement in NEFA, both at baseline and during the meal. The reduced NEFA concentration is in-keeping with an improvement in insulin sensitivity, and subsequent reduction in lipolysis. In the A-T group, pioglitazone also reduced circulating leptin, as would be expected in improved insulin sensitivity. This did not reach significance, again likely due to the heterogeneity of the A-T cohort.

Pioglitazone in the management of diabetes in A-T

Within the A-T group, when the treatment effects of pioglitazone are directly compared to the effects of metformin, it is clear that pioglitazone is a superior treatment for the insulin resistance seen in this condition. In a mixed effects model, treatment with pioglitazone ($p = 0.0018$), but not metformin ($p = 0.73$), was significant in predicting insulin sensitivity.

Currently, if an individual with A-T was diagnosed with diabetes, the first-line oral agent prescribed, as per ADA-EASD guidance (3), would be metformin. Our data clearly shows that in this patient group, metformin treatment would not be as effective as treatment with pioglitazone. We suggest, therefore, that a more patient-centred approach when treating diabetes in these individuals would be early consideration of pioglitazone, either as monotherapy or in conjunction with metformin.

Pioglitazone has been implicated in the management of NAFLD (341, 342, 355), which could strengthen the argument for its use in A-T. Two of the four individuals with classic A-T had deranged liver function, with elevated ALT. These same individuals had evidence of fatty liver on MRI, and had a reduction in ALT with pioglitazone treatment. Obviously, this is not statistically significant, and it is impossible to draw conclusion from such small numbers, but does highlight an area for future research.

As with any medical therapy, potential benefits need to be weighed against risk. Pioglitazone is associated with a moderate increased risk of pneumonia. In this immunocompromised patient group with a pre-disposition to recurrent infection, this potential adverse effect clearly needs to be discussed and balanced against the potential benefits. Early review of treatment response is recommended after 3 – 6 months, with discontinuation if no perceived benefit.

Adipocyte dysfunction in A-T

In contrast to the mouse data reported by Takagi et al, individuals with A-T did not have a lipodystrophic phenotype. MRI data comparing visceral and subcutaneous adipose deposition, confirmed no difference in adipose volume or distribution in A-T compared to controls. However, there was a trend towards increased liver fat and iron deposition. As the RAMP study sample size was not calculated based on MRI parameters, it is likely that the study was simply not powered to detect the potential difference in liver fat content. However, it is recognised that A-T is associated with fatty liver, so this trend would not be unexpected.

There is, however, evidence of adipocyte dysfunction in the A-T group. Insulin resistance is associated with low adiponectin levels, as seen in the mouse model of ATM deficiency, and now in humans with A-T. While reduction in adiponectin may be secondary to insulin resistance (356), it could also represent disruption of insulin-stimulated adiponectin secretion. Insulin stimulates secretion of adiponectin by activation of the PI3K pathway (357). ATM deficiency is associated with reduced PI3K activity (315, 318), therefore it may be possible that stimulation of adiponectin secretion from adipocytes of individuals with A-T is reduced due to this negative impact on insulin signalling. The resulting reduction in adiponectin could contribute to insulin resistance and increased insulin concentrations.

Pioglitazone is a PPAR γ selective agonist, and PPAR γ is a key transcriptional factor in adipokine gene expression (358), which has been shown to increase adiponectin levels, even in normal glucose tolerance, in the absence of insulin resistance (359, 360). This was evident in our data, as adiponectin was dramatically increased post-pioglitazone in both groups.

Unlike the mouse model of ATM deficiency, leptin was markedly elevated in the A-T group, in the absence of obesity. This is likely secondary to the elevated insulin concentrations in A-T, with subsequent increase in leptin secretion. Of note, insulin stimulates leptin secretion via a PI3K independent pathway (361), or

in the chronic setting, through glucose metabolism associated upregulation of transcription of leptin mRNA (362). Therefore, it could be possible that ATM dysfunction would negatively impact upon adiponectin secretion via the PI3k pathway, without reducing leptin secretion.

Elevated NEFA concentrations at baseline and after metformin in the A-T group are secondary to increased lipolysis as a result of insulin resistance. The reduction in insulin resistance post-pioglitazone results in a reduction in lipolysis, and subsequently, NEFA concentration.

Limitations

The RAMP study was a physiology study of glucose kinetics, beta cell function and adipocyte function in a rare condition associated with diabetes. The study provided a unique opportunity to study the insulin resistance in A-T, and has provided interesting insight into the appropriate management of this condition. However, we recognise a number of limitations within the study design and subsequent results.

Firstly, the study was non-blinded, with both researchers and participants fully aware of the study drug and dosing. This exposes a study to potential bias, especially if measuring subjective end points. However, in the RAMP study, the end points were biochemical parameters and were therefore less prone to bias or interpretation than, for example, symptom severity scoring.

Secondly, the treatment order was not randomised and did not include placebo control. This was deliberate. It was recognised that the effects of pioglitazone treatment on insulin sensitivity, liver fat, and adipocyte function, may be longer lasting than the effects of metformin. It was therefore decided that metformin treatment should precede pioglitazone treatment. The treatment periods were separated by a one week washout, which is sufficient for metformin (16, 213). The treatment periods were also eight weeks in duration, so it is unlikely that any carried over effect of metformin would have been evident 9 weeks after

discontinuation. Placebo control was not included, as each individual had a baseline visit, which acted as the intra-individual control for each treatment, rather than increasing tablet burden or time in study to include a placebo treatment period.

Thirdly, the RAMP study was a small study, with only eight individuals with A-T recruited. However, the study was appropriately powered to identify a change in insulin sensitivity with metformin. Due to the low frequency of the condition, the stipulated inclusion and exclusion criteria, the time commitment and travel required to attend the research centre in Dundee, as well as the comorbidities and vulnerable nature of this patient group, the potential study population was severely limited, with only approximately 60 individuals in the UK fitting the basic criteria.

As a consequence of anticipated difficulty in recruitment, we opted to include both classic and variant A-T in the A-T group. There is increased in-group variability, and at times, the clear impression of two separate metabolic phenotypes. However, both subgroups were insulin resistant. It is difficult to comment on the differences between the subgroups, as the study is not powered to do so, however, the impression stands that residual ATM kinase activity confers a less severe metabolic phenotype.

While it appears that pioglitazone was more effective in the treatment of insulin resistance in the A-T group, we recognise that overweight females are known to respond better to pioglitazone than other demographic subsets. As the A-T group were predominantly female (62.5%) and matching was not exact (control group females 40%), it is possible that this difference contributed to the improved pioglitazone response seen in the A-T group. However, the A-T group were not overweight, and although predominantly female, when controlling for age, sex and BMI in the mixed model, sex was not a significant variable.

Lastly, and potentially the biggest limitation to this study and its interpretation, was the chosen control group. To assess for *ATM*-associated improvement in response to metformin, the ideal control group would have been a group of wheelchair users with evidence of insulin resistance, which would obviously have posed a significant challenge for recruitment. However, for the purpose of defining the metabolic phenotype in A-T, comparison to healthy controls was useful, and for comparison of treatment effects of metformin and pioglitazone, the A-T individuals acted as their own control. As discussed, it would be useful to compare the A-T group to those with a similar level of insulin resistance, such as individuals with pre-diabetes, to compare metformin response and potentially unmask a blunted response in the A-T group.

Conclusion

The “Response of individuals with Ataxia-telangiectasia to Metformin and Pioglitazone (RAMP)” study is the first study of its kind in A-T, and to our knowledge, the most detailed assessment of the metabolic phenotype associated with this rare condition. We have confirmed that individuals with A-T are peripherally insulin resistant, and have a marked improvement in insulin sensitivity with pioglitazone treatment.

However, we were unable to validate the results of the GWAS study previously reported by our research group. Contrary to our hypothesis, there was no evidence in the RAMP data to suggest that A-T is associated with an enhanced response to metformin as assessed by OGIS. Similarly, no gene*drug interaction was identified to explain variance in other parameters which differed between groups, such as BMI or GLP1. It may be that a recruit-by-genotype study design is required, where individuals with the identified genome-wide significant SNP are recruited to assess response to metformin. Alternatively, the GWAS signal may be associated with another gene from the identified locus.

We have confirmed that there is abnormal adipokine secretion in A-T, and identified a potential increase in liver fat and iron deposition, although this requires further investigation.

The RAMP study has not only improved our understanding of the metabolic dysfunction in A-T, but it has also provided guidance for the management of diabetes in A-T.

Conclusions

Metformin is the most commonly used oral medication for type 2 diabetes, with an impressive safety and benefit profile. It continues to garner new interest from other fields in medicine, especially oncology. As such, research into metformin is ever increasing. Part of metformin's intrigue lies in the fact that it precedes modern drug discovery and testing protocols, and its mechanism of action remains relatively elusive – or at least debatable. More recently, in addition to the widely accepted cellular mechanisms of action such as metformin's effect on AMPK or gluconeogenesis, the gastrointestinal tract has been highlighted as a site of particular interest in both efficacy and tolerability.

Metformin has considerable variability in its efficacy and tolerability, and the challenge of predicting this variability is inextricably linked to understanding the site and mechanisms of action of the drug. This thesis has employed pharmacokinetics, pharmacogenetics and physiology studies to add to this field of metformin research.

What have we learned?

Pharmacokinetics of Metformin Intolerance

Chapter 3 of this thesis details the “Pharmacokinetics of Metformin Intolerance” (POMI) study, employed a pharmacokinetics study to compare individuals who were tolerant to those who were intolerant of metformin. The study data presented demonstrates that the PK of metformin does not differ significantly in the two phenotypes, nor does the systemic lactate, serotonin, or bile acid pool, suggesting that these are not the underlying mechanism of metformin intolerance.

It is possible that intolerance may be multifactorial, however, and that these individual effects of metformin, when accumulated, could cause intolerance. However, our data clearly show that intolerance is not driven by one of these factors independently. In fact, the results from this recruit-by-phenotype study

suggest that metformin intolerance is likely to be mediated by local factors within the lumen or enterocyte.

Areas for further investigation

Firstly, it would be interesting to further investigate the link between metformin transporter genotype, pharmacokinetics and tolerance of metformin, as genotype was not considered in the POMI study. To do so, a large recruit-by-genotype study would be necessary, to compare two genotypes of a known transporter e.g. OCT1, along with pharmacokinetic data, in tolerant and intolerant individuals.

Secondly, as the results from this recruit-by-phenotype study suggest that metformin intolerance is likely to be mediated by local factors, there is a need to undertake more mechanistic studies that investigate the local (luminal) environment, especially the microbiome, in intolerant vs tolerant individuals.

Thirdly, while the systemic lactate did not differ post-metformin between the phenotypic groups, it is possible that the gastrointestinal symptoms of intolerance are driven by an increase in local lactate concentrations. Portal venous sampling for lactate concentration would provide a more accurate measure of intestinal lactate production, rather than using peripheral concentrations as a proxy measure. However, obtaining portal venous samples for research purposes would prove extremely challenging in humans, both physically and ethically.

Lastly, we did not measure GLP1 levels in this study of metformin intolerance. A further study to compare the change in GLP1 concentrations post-metformin in tolerant and intolerant individuals, would be of interest.

Impact of OCT1 genotype and OCT1 inhibiting drugs on an individual's metformin tolerance

Chapter 4 of this thesis reports the findings from the “Impact of OCT1 genotype and OCT1 inhibiting drugs on an individual's metformin tolerance” study. This study employed a recruit-by-genotype design to investigate observed

associations between metformin intolerance and OCT1 genotype and inhibition. While our data did not validate the observation that loss of function in OCT1 negatively impacts on metformin intolerance, we did identify a gene*drug interaction between OCT1, metformin and omeprazole, which may explain the observed data. Individuals with wild type OCT1 have an improved tolerance of metformin when concurrently treated with omeprazole. Conversely, those with reduced function variants in OCT1 do not benefit from the addition of omeprazole. Therefore, this study, for the first time, has identified a clinically relevant and applicable gene*drug interaction between OCT1, metformin and omeprazole.

[Areas for further investigation](#)

The identified gene*drug interaction has clinical application and potential benefit. However, there is still significant research required to fully characterise and understand metformin intolerance. Using the stool, serum and urine samples collected opportunistically during the ImpOCT study, there is the potential to gain further insight into the mechanism of metformin intolerance.

Firstly, using the stool samples collected at baseline and after each treatment period, we can study the microbiome to assess for alterations in the variety and abundance of species present before and after metformin. Furthermore, we can compare the change in species seen in individuals who were tolerant to that seen in intolerance, to assess if the microbiome may contribute to metformin intolerance.

Secondly, serum and urine samples taken before and after metformin could be used to assess the PK of metformin with and without concurrent use of an OCT1 inhibiting drug. This may, however, prove difficult to interpret, and would involve complex modelling due to the variability in metformin dosing across the study population, as well as the timing of samples from metformin dose. The PK analysis may therefore be best applied to the tolerant individuals, all of whom achieved the maximum tolerated dose of 2000mg daily.

Lastly, the study design developed for the ImpOCT study is easily applicable to other drug transporters, their genetic variants and substrates. For example, the study design could be adopted for the investigation of the impact of genetic variation in the serotonin transporter (SERT) on metformin tolerance.

Response of individuals with Ataxia-Telangiectasia to Metformin and Pioglitazone

Chapter 5 of this thesis describes the “Response of individuals with Ataxia-Telangiectasia to Metformin and Pioglitazone” (RAMP) study, which used dual tracer mixed meal tests to study the physiological effects of metformin and pioglitazone in individuals with A-T vs healthy controls. This study provided a wealth of data on the metabolic phenotype of this rare genetic condition, and provided a useful comparison of potential treatments for the diabetes associated with A-T.

While this study did not validate the results of the GWAS which implicated ATM in metformin response, it has shown that A-T may be associated with a blunted response to metformin, though this may only become evident when compared to individuals with a similar metabolic phenotype or equivalent level of insulin resistance, rather than healthy controls. The study data also suggest that in the treatment of insulin resistance and diabetes in this patient group, pioglitazone may be a more effective treatment than metformin – a deviation from the current management guidelines for type 2 diabetes.

The RAMP study also demonstrated some interesting glucose kinetics in healthy controls post-metformin, including an *increase* in EGP and glucose clearance. This lends support to the theory that metformin increases glucose clearance as a mechanism of glycaemic control, with the gastrointestinal tract acting as a potential site of clearance.

Areas for further investigation

The RAMP study has identified a number of areas for further research. As mentioned, comparison of metformin response in the A-T group to individuals with pre-diabetes may be more informative.

Secondly, we are in the process of developing a protocol for a study of the adipose biopsies taken from all participants at baseline. Based on the adipokine data from RAMP, we believe that adipose tissue plays an active role in the metabolic phenotype seen in A-T. By performing lipidomic and proteomic analysis of the adipose tissue obtained at the baseline visit, we hope to further define the lipid and protein complement of adipose tissue in A-T, which could give insight into insulin signalling in adipose and pathogenesis of insulin resistance in A-T. The information learned could ultimately help identify treatment targets or guide management of insulin resistance and diabetes in A-T.

Ideally, cell culture could also be performed using the stromal vascular fraction of the adipose tissue, permitting drug response experimentation to assess insulin and pioglitazone response. This will be dependent upon the quantity of tissue available post-lipidomic analysis.

Thirdly, a wider study of pioglitazone treatment in A-T would be the next logical step to assess for clinical benefit. It would be interesting to obtain MR imaging before and after pioglitazone treatment to assess for a reduction in liver fat fraction. Alternatively, it would be ideal to be able to apply Liver Lab software to existing MRI images from A-T patients, to investigate the trend towards increased iron deposition in the liver, which may be associated with a chronic pro-inflammatory state. This would likely prove technically difficult, as specific imaging sequences and breath holds were required to obtain images for Liver Lab analysis.

Lastly, the Sanger institute in Cambridge have successfully developed iPSCs from A-T patients. As part of a collaboration with the Centre for Regenerative

Medicine at the University of Edinburgh, our intention is to study how these iPSCs respond to insulin, as well as deriving hepatocytes for drug response experiments using insulin, metformin and pioglitazone.

Conclusion

This thesis has contributed new and varied data to the field of metformin research, which is both clinically relevant and applicable. Importantly, it has highlighted areas for additional research and has challenged our interpretation of previous studies.

Appendix 1: POMI sample analysis methods

Determination of metformin concentrations in plasma and urine samples.

The concentration of metformin in plasma and urine samples were determined at the Department of Clinical Pharmacology and Pharmacy, Institute of Public Health, University of Southern Denmark, by use of liquid chromatography and tandem mass spectrometry (LC-MS/MS). The LC-MS/MS system consisted of an Ultimate 3000 UHPLC system connected to a TSQ Quantiva Triple Quadrupole Mass Spectrometer with heated electrospray ionization (Thermo Scientific, San Jose, CA). Data acquisition was performed in single reaction monitoring (SRM) mode. Metformin was quantitated by positive ionisation at the transition from (m/z) 130.4 – 71.1, and with (m/z) 130.4 – 60.1 as a qualifier trace. Metformin-d6 (internal standard) was monitored from (m/z) 136.4 – 77.1. The analytical separation was performed using hydrophilic interaction chromatography as described by Nielsen et al (183).

The sample preparation of the plasma samples consisted of a single protein precipitation step. To a 100 µL plasma sample, 10 µL 25 µg/mL metformin-d6 (internal standard), 20 µL 0.53M ammonium acetate and 390 µL acetonitrile were added. The sample was vortex mixed for 30 sec and centrifuged at 3.000g for 15 minutes. The urine samples were diluted (1:50) before use, but were otherwise treated as the plasma samples. A volume of 10 µL of the supernatant was injected onto the LC-MS/MS system. Calibration curves, as well as quality control samples, were prepared and included in each batch of analysis. The intra- and interday variability was < 8%. The limit of detection (LOD) for the method was 1 ng/mL and limit of quantification (LOQ) was 10 ng/mL.

Determination of histamine, serotonin and bile acid concentrations

EDTA plasma samples from time points 0, 3.5, 8 and 24 hours post-metformin were used for targeted metabolomics measurements, which were done in the

Metabolomics Platform of the Genome Analysis Center, Helmholtz Zentrum München). Histamine and serotonin were quantified using the Biocrates Absolute/DQ™ p180 Kit and bile acids using the Biocrates™ Bile Acids Kit (BIOCRATES Life Sciences AG, Innsbruck, Austria).

The measurements of plasma samples with the Absolute/DQ™ p180 Kit and FIA- and LC-ESI-MS/MS (flow injection analysis-/liquid chromatography-electrospray ionisation-tandem mass spectrometry) have been described in full detail by Zukunft et al (363). Out of 10 µL sample, 188 metabolites can be quantified simultaneously. The assay includes free carnitine, 39 acylcarnitines, 21 amino acids, 21 biogenic amines, hexoses, 90 glycerophospholipids, and 15 sphingolipids.

Using the Biocrates™ Bile Acids Kit and LC-ESI-MS/MS, 20 bile acids can be quantified out of 10 µL plasma. The assay includes cholic acid, chenodeoxycholic acid, deoxycholic acid, glycocholic acid, glycochenodeoxycholic acid, glycodeoxycholic acid, glycolithocholic acid, glyoursodeoxycholic acid, hyodeoxycholic acid, lithocholic acid, alpha-muricholic acid, beta-muricholic acid, omega-muricholic acid, taurocholic acid, taurochenodeoxycholic acid, taurodeoxycholic acid, tauroolithocholic acid, tauromuricholic acid (sum of alpha and beta), taoursodeoxycholic acid, ursodeoxycholic acid. Compound identification and quantification were based on scheduled multiple reaction monitoring measurements (sMRM). We provide the description on how sample preparation and mass spectrometric measurements were performed in the laboratory (364). In short, 10 µL of internal standard solution in methanol were pipetted onto the filter inserts of a 96 well sandwich plate. After drying the filters for 5 min at RT in a nitrogen stream, 10 µL of blank, calibration standards, quality control samples and plasma samples were pipetted into the distinct respective wells and the filters were dried again for 5 min. For extraction of metabolites and internal standards, 100 µL of methanol were added and the plate was shaken for 20 min at 650 rpm. The metabolite extracts were eluted to the lower deep well plate by a centrifugation step (5 min at 500 x g at RT). The upper filter plate was

removed, the extracts were diluted with 60 μ L ultrapure water, and the plate was shaken for 5 min at 450 rpm and placed into the cooled auto sampler (10 °C) for LC-MS/MS measurements. The LC-separation was performed using 10 mM ammonium acetate in a mixture of ultrapure water/formic acid v/v 99.85/0.15 as mobile phase A and 10 mM ammonium acetate in a mixture of methanol/acetonitrile/ultrapure water/formic acid v/v/v/v 30/65/4.85/0.15 as mobile phase B. Bile acids were separated on the UHPLC column for Biocrates™ Bile Acids Kit (Product No. 91220052120868) combined with the precolumn SecurityGuard ULTRA Cartridge C18/XB-C18 (for 2.1 mm ID column, Phenomenex Cat. No. AJ0-8782). All solvents that have been used for sample preparation and measurement were of HPLC grade.

Both Biocrates methods has been proven to be in conformance with the EMEA-Guideline "Guideline on bioanalytical method validation" (July 21st 2011) (365) which implies proof of reproducibility within a given error range. Sample preparation and FIA- and LC-MS/MS measurements were performed as described by the manufacturer in the manuals UM-P180 and UM-BA. Analytical specifications for LOD (limit of detection), LLOQ and ULOQ (lower and upper limit of quantification), specificity, linearity, precision, accuracy, reproducibility, and stability were described in Biocrates manuals AS-P180 and AS-BA. The LODs were set to three times the values of the zero samples (PBS). The LLOQ and ULOQ were determined experimentally by Biocrates. Samples were handled using a Hamilton Microlab STAR™ robot (Hamilton Bonaduz AG, Bonaduz, Switzerland) and a Ultravap nitrogen evaporator (Porvair Sciences, Leatherhead, U.K.), beside standard laboratory equipment. Mass spectrometric analyses were done on an API 4000 triple quadrupole system (Sciex Deutschland GmbH, Darmstadt, Germany) equipped with a 1200 Series HPLC (Agilent Technologies Deutschland GmbH, Böblingen, Germany) and a HTC PAL auto sampler (CTC Analytics, Zwingen, Switzerland) controlled by the software Analyst 1.6.2. Data evaluation for quantification of metabolite concentrations and quality assessment was performed with the software MultiQuant 3.0.1 (Sciex) and the Met/IDQ™

software package, which is an integral part of the Absolute/IDQ™ and Biocrates™ Bile Acids Kits. Metabolite concentrations were calculated using internal standards and reported in μM .

Determination of plasma lactate concentrations

Fluoride oxalate samples were analysed for plasma lactate using a lactate oxidase method on a Siemens ADVIA 2400 Chemistry System (analysed by Biochemical Medicine, Department of Blood Sciences, NHS Tayside).

Appendix 2 : Questionnaire to Assess Character and Severity of Metformin Intolerance

1. Are you still taking metformin?
 - Yes (if still taking skip to question 6) 0
 - No 5

If you are **no longer taking** metformin:

2. Was the metformin stopped due to side-effects?
 - Yes (go to question 3) 5
 - No (go to question 6) 0

3. What dose were you taking at the time of discontinuing metformin?
 - 500mg once daily (1 tablet once daily) 4
 - 1000mg once daily (2 tablets once daily) 3
 - 500mg twice daily (1 tablet twice daily) 2
 - 2000mg once daily (four tablets once daily) 1
 - 1000mg twice daily (two tablets twice daily) 0

4. Had you previously been on a lower dose of metformin, which you tolerated without significant side-effects?
 - Yes 0
 - No 1

a) If yes, what was the maximum dose you tolerated?

_____ 2

(if 500 mg OD)

5. Have you been trialled on a modified release preparation of metformin (e.g. Glucophage SR)?
 - Yes 2
 - No 0

In the last week of taking metformin, have you experienced?

6. Nausea?

- Yes 1
- No 0
- a) If yes, how many times?
 - More than once a day 4
 - Once a day 3
 - Occasionally 2
 - Only once 1
- b) How would you score its severity from 1 - 5 (where 1 is mild, not causing distress or affecting your daily routine, and 5 is very severe, causing marked distress and / or disrupting your daily activities)? _____ / 5

7. Abdominal bloating / pain?

- Yes 1
- No 0
- a) If yes, how often?
 - More than once a day 4
 - Once a day 3
 - Occasionally 2
 - Only once 1
- b) How would you score its severity from 1 - 5 (where 1 is mild, not causing distress or affecting your daily routine, and 5 is very severe, causing marked distress and / or disrupting your daily activities) ? _____ / 5

8. Diarrhoea?

- Yes 1
- No 0
- a) If yes, how often?
 - More than once a day 4
 - Once a day 3
 - Occasionally 2
 - Only once 1
- b) How would you score its severity from 1 - 5 (where 1 is mild, not causing distress or affecting your daily routine, and 5 is very severe, causing marked distress and / or disrupting your daily activities) ? _____ / 5

9. Have you experienced any of the side-effects you have described above PRIOR to starting metformin?
- Yes -5
 - No 0
- a) If yes, whilst taking metformin have the symptoms:
- Improved -1
 - Worsened 1
 - Stayed the same 0

TOLERANCE:

10. Would you describe yourself as:

- a) Tolerant of metformin treatment 0
- b) Mildly intolerant of metformin treatment 1
- c) Intolerant of metformin treatment 2
- d) Severely intolerant of metformin treatment. 3

Thank you for taking the time to complete this questionnaire.

For Clinical Staff Use:

TOTAL SCORE: ____ / 50

Score:

0 – 10 = tolerant (T)

11-20 = mild intolerance (MI)

21-30 = intolerant (I)

31-50 = severely intolerant (SI)

Severity Score (__/50)	Score based tolerance (T / MI / I / SI)	Patient perceived tolerance (T / MI / I / SI)	Correlation (Y / N)

Appendix 3: OCT1 inhibiting drugs

Commonly prescribed drugs known to be substrates for OCT1
PPIs (omeprazole, lansoprazole)
TCAAs (amitriptyline)
Citalopram
Calcium-channel blockers (verapamil, diltiazem)
Alpha-adrenoceptor blockers (doxazosin, prazosin)
Spirolactone
Clopidogrel
Repaglinide
Rosiglitazone
Quinine
Antiarrhythmic drugs (quinidine, disopyramide, propafenone)
Tramadol

Codeine
Morphine
Ketoconazole
5-HT ₃ receptor antagonists (tropisetron, ondansetron)
Antipsychotic agents
Tyrosine kinase inhibitors

Appendix 4: ImpOCT Analysis

McNemar Test R code and Output:

OCT1 wild type:

```
wildtype <-
  matrix(c(18,3,5,4),
        nrow=2,
        dimnames=list("Omeprazole" = c("Tolerant","Intolerant"),
                      "Placebo" = c("Tolerant","Intolerant")))

mcnemar.test(wildtype)
```

```
      McNemar's Chi-squared test with continuity correction

data:  wildtype
McNemar's chi-squared = 0.125, df = 1, p-value = 0.7237
```

OCT1 Null:

```
OCT1Null <-
  matrix(c(20,0,3,8),
        nrow=2,
        dimnames=list("Omeprazole" = c("Tolerant","Intolerant"),
                      "Placebo" = c("Tolerant","Intolerant")))

mcnemar.test(OCT1Null)
```

```
      McNemar's Chi-squared test with continuity correction

data:  OCT1Null
McNemar's chi-squared = 1.3333, df = 1, p-value = 0.2482
```

Cochran-Mantel-Haenszel test

Due to the large number of “zero” cells, the addition of a delta value to all cells is required for analysis. In the following R code, delta = 0.25:

```
MTD_GENEXDRUGdelta.25 <-
  (array(c(0.25,1.25,0.25,0.25,0.25,
           0.25,0.25,1.25,1.25,1.25,
           0.25,0.25,0.25,1.25,2.25,
           0.25,0.25,0.25,0.25,2.25,
           0.25,0.25,0.25,3.25,18.25,
           0.25,0.25,0.25,0.25,0.25,
           1.25,1.25,0.25,0.25,0.25,
           0.25,2.25,0.25,1.25,1.25,
           0.25,0.25,1.25,2.25,2.25,
           0.25,0.25,0.25,0.25,20.25),
         dim=c(5,5,2),
         dimnames= list(Omeprazole = c("Omp 0","Omp 1","Omp 2","Omp 3","Omp 4"),
                        Placebo = c("Pbo 0","Pbo 1","Pbo 2","Pbo 3","Pbo 4"),
                        Genotype = c("wild Type", "Null"))))

mantelhaen.test(MTD_GENEXDRUGdelta.25)
```

Cochran-Mantel-Haenszel test

```
data: MTD_GENEXDRUGdelta.25
Cochran-Mantel-Haenszel M2 = 36.0848, df = 16, p-value = 0.002816
```

Cumulative linked mixed models

Code:

```
ordinalmodel <- c1mm2(as.factor(MTD) ~ Genotype*as.factor(Treatment),
                    random = ID,
                    data=impoct, Hess=TRUE,
                    link="logistic")
summary(ordinalmodel)
```

Output:

```
Cumulative Link Mixed Model fitted with the Laplace approximation
Call:
c1mm2(location = as.factor(MTD) ~ Genotype * as.factor(Treatment),
      random = ID, data = impoct, Hess = TRUE, link = "logistic")

Random effects:
      Var Std.Dev
ID 85.32734 9.23728

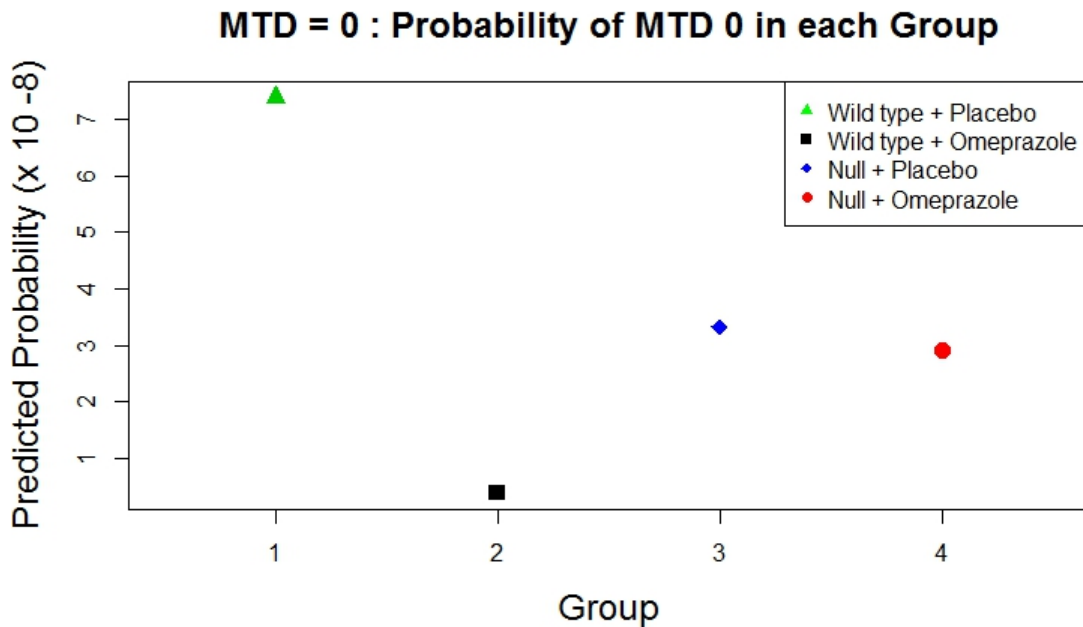
Location coefficients:
              Estimate Std. Error z value Pr(>|z|)
GenotypeB      -2.0554   1.8721   -1.0979 0.2722425
as.factor(Treatment)2 -2.9857   1.1293   -2.6440 0.0081936
GenotypeB:as.factor(Treatment)2  2.8527   1.3953    2.0445 0.0409010

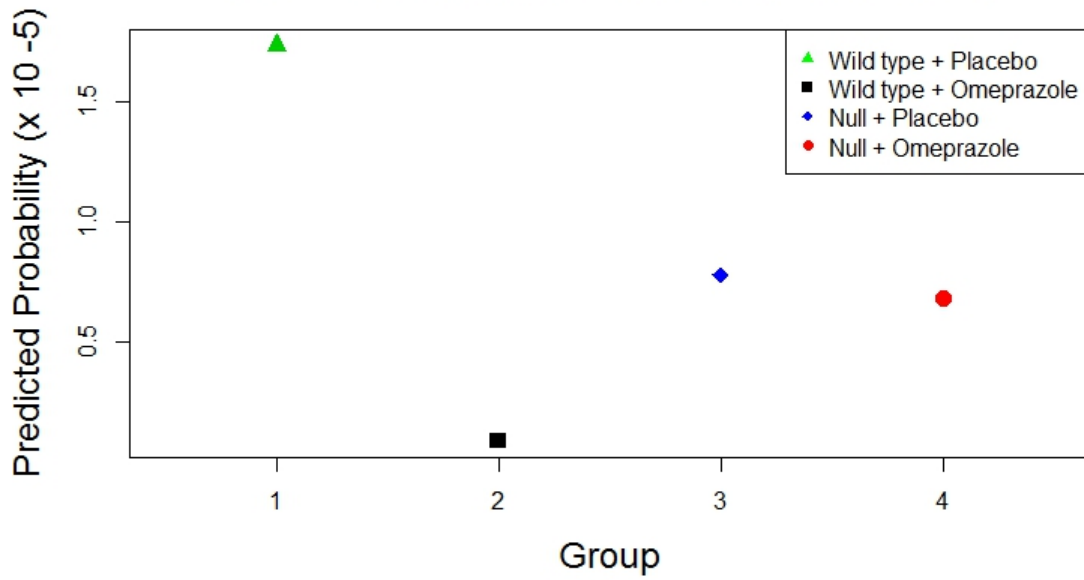
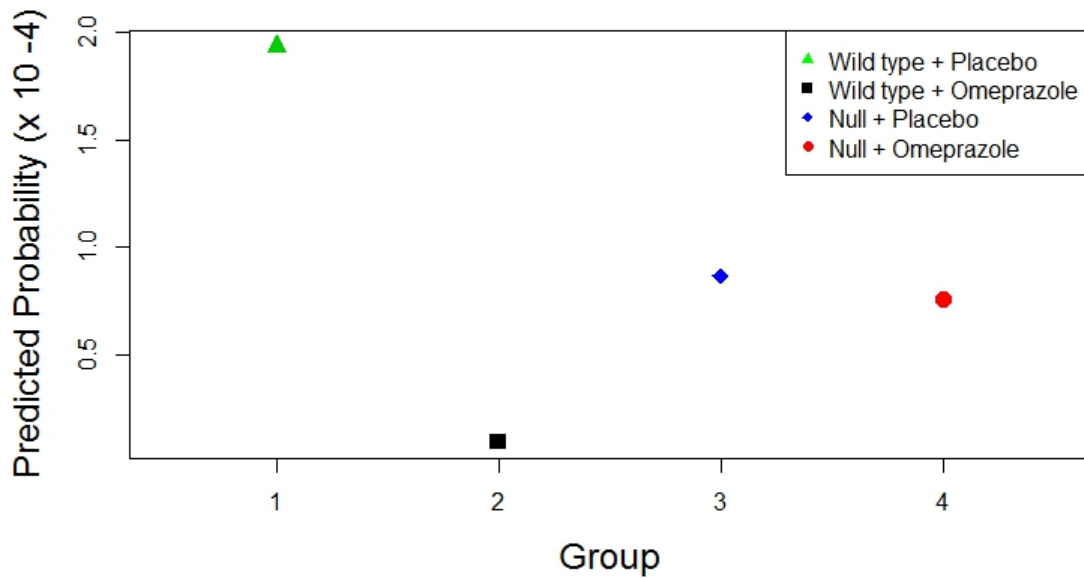
No scale coefficients

Threshold coefficients:
      Estimate Std. Error z value
0|1 -19.4060   4.0837   -4.7521
1|2 -13.9427   2.8224   -4.9400
2|3 -11.4516   2.4520   -4.6702
3|4  -8.8662   2.1030   -4.2159

log-likelihood: -97.89157
AIC: 211.7831
Condition number of Hessian: 2158.399
```


Figure 57, below, shows the predicted probability of each maximum tolerated dose, from 0 to 4 tablets daily, across groups. Individuals who are OCT1 wild type taking concurrent omeprazole have a lower probability of a MTD of 0, 1, 2 or 3 tablets per day, compared to other groups. However, they have a higher probability of achieving the MTD of 4 tablets per day. In contrast, while taking placebo, the OCT1 wild type individuals have a higher probability of reaching a lower tolerated dose, i.e. 0, 1, 2, or 3 tablets daily, compared to other groups, and a lower probability of achieving the maximum tolerated dose of 4 tablets daily. Note the difference in the vertical scale across plots.



MTD = 1 : Probability of MTD 1 in each Group**MTD = 2 : Probability of MTD 2 in each Group**

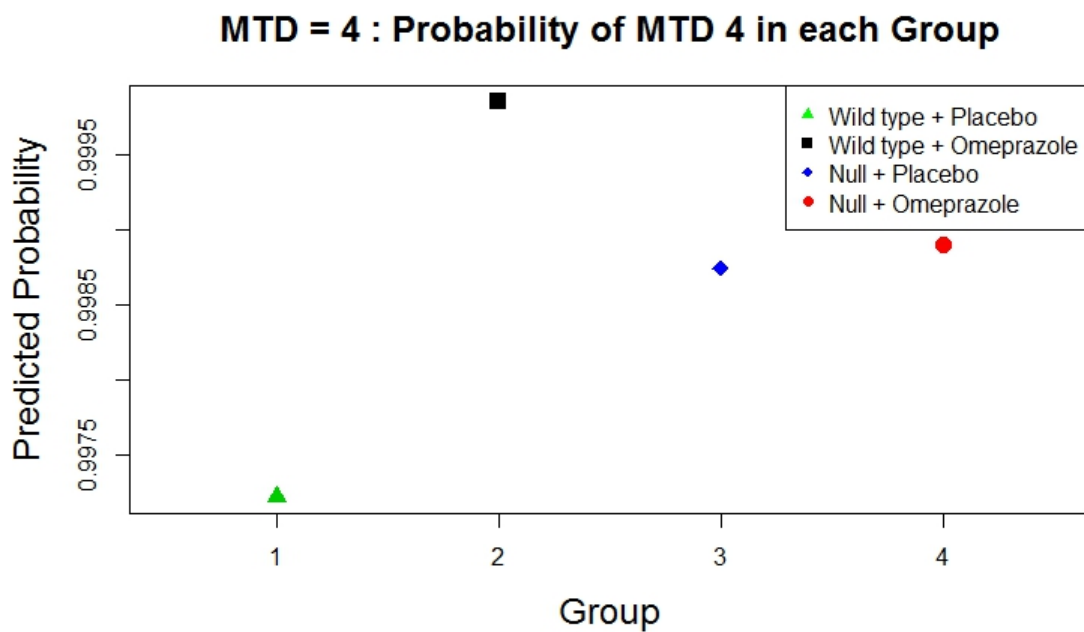
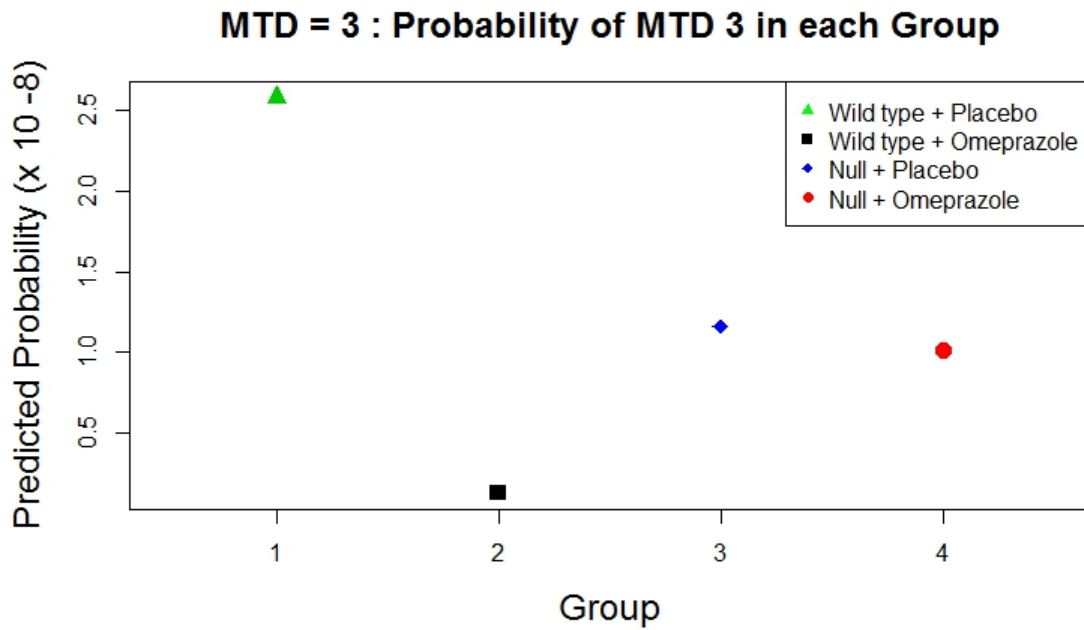


Figure 57 Predicted probability of each maximum tolerated dose, according to group.

Group 1 = Wild type + Placebo; Group 2 = Wild type + Omeprazole; Group 3 = Null + Placebo;
Group 4 = Null + Omeprazole.

This can be compared in a single plot of the predicted probabilities of each dose, for all groups.

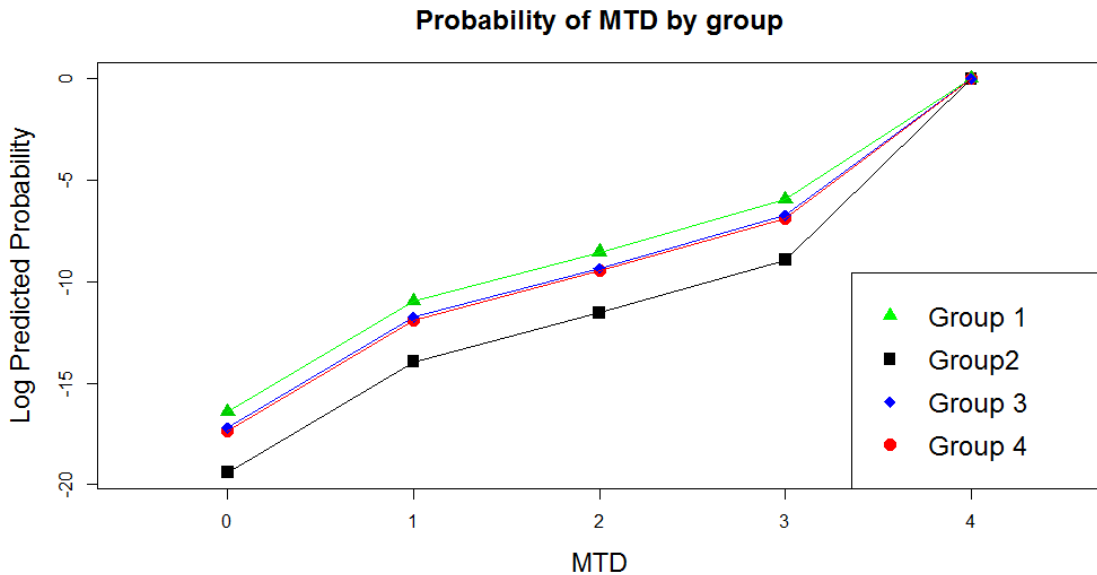


Figure 58 Predicted probabilities of each MTD across groups.

Figure 57 shows that individuals with OCT1 wild type, when treated with placebo, have a higher probability of achieving lower tolerated doses. The OCT1 wild type group, when treated with omeprazole, have a reduced probability of lower tolerated doses. However, when examining the probability of achieving the maximum tolerated dose of 4 tablets per day, the probability is greatest in wild type individuals treated with omeprazole.

Generalised Linear Mixed Models

Using a mixed model to incorporate both fixed and random effects, it is possible to predict the probability of the MTD of metformin based on genotype and treatment. With maximum tolerated dose as the outcome, genotype and treatment effects as fixed, and the individual as a random effect, and we can use a mixed model to predict probability of achieving maximum dose of metformin.

The model below, which uses the “MASS” package in R, adopts penalised quasi-likelihood (see Methods: Mixed Models) to model response, and can be used to predict probabilities on the scale of the response variable.

Code:

```
SAPmodel <- glmmPQL(cbind(MTD,X4.MTD)~Genotype*as.factor(Treatment),
                    random=~1|ID,
                    family=binomial,
                    data = impoct)
summary(SAPmodel)
```

Note the glmmPQL model does not handle ordinal outcomes, and therefore our outcome of MTD (0, 1, 2, 3, 4 tablets per day) is transformed into a matrix:

(Number of tablets tolerated; Maximum number minus number actually tolerated)

i.e. (MTD, 4 – MTD)

This is one of the reasons why we opted to use the ordinal package for primary analysis - to prevent the need for transformation of the response variable.

Output:

```

Linear mixed-effects model fit by maximum likelihood
Data: impoct
AIC BIC logLik
NA NA NA

Random effects:
Formula: ~1 | ID
(Intercept) Residual
StdDev: 2.27145 0.6146762

Variance function:
Structure: fixed weights
Formula: ~invwt
Fixed effects: cbind(MTD, X4.MTD) ~ Genotype * as.factor(Treatment)
Value Std.Error DF t-value p-value
(Intercept) 3.843923 0.5489072 59 7.002866 0.0000
GenotypeB -0.792048 0.7532136 59 -1.051558 0.2973
as.factor(Treatment)2 -1.353121 0.3325296 59 -4.069175 0.0001
GenotypeB:as.factor(Treatment)2 1.243054 0.4434208 59 2.803328 0.0068
Correlation:
(Intr) GntypB a.(T)2
GenotypeB -0.729
as.factor(Treatment)2 -0.427 0.311
GenotypeB:as.factor(Treatment)2 0.320 -0.366 -0.750

Standardized Within-Group Residuals:
Min Q1 Med Q3 Max
-2.8479151 0.2371208 0.3561338 0.4665371 1.7462745

Number of Observations: 122
Number of Groups: 61

```

As shown, both “Treatment” and the interaction term “Genotype*Treatment” are significant within the simplified model.

The glmmPQL model has been used for validation of our result, rather than for primary analysis, as the model requires transformation of the ordinal outcome as mentioned above, but also does not offer a measure of model fit, e.g. AIC or p value. The package does not allow comparison of models using anova, and therefore, we could not assess for model superiority.

The simplified model was used to predict probability of the outcome, and the output is plotted below:

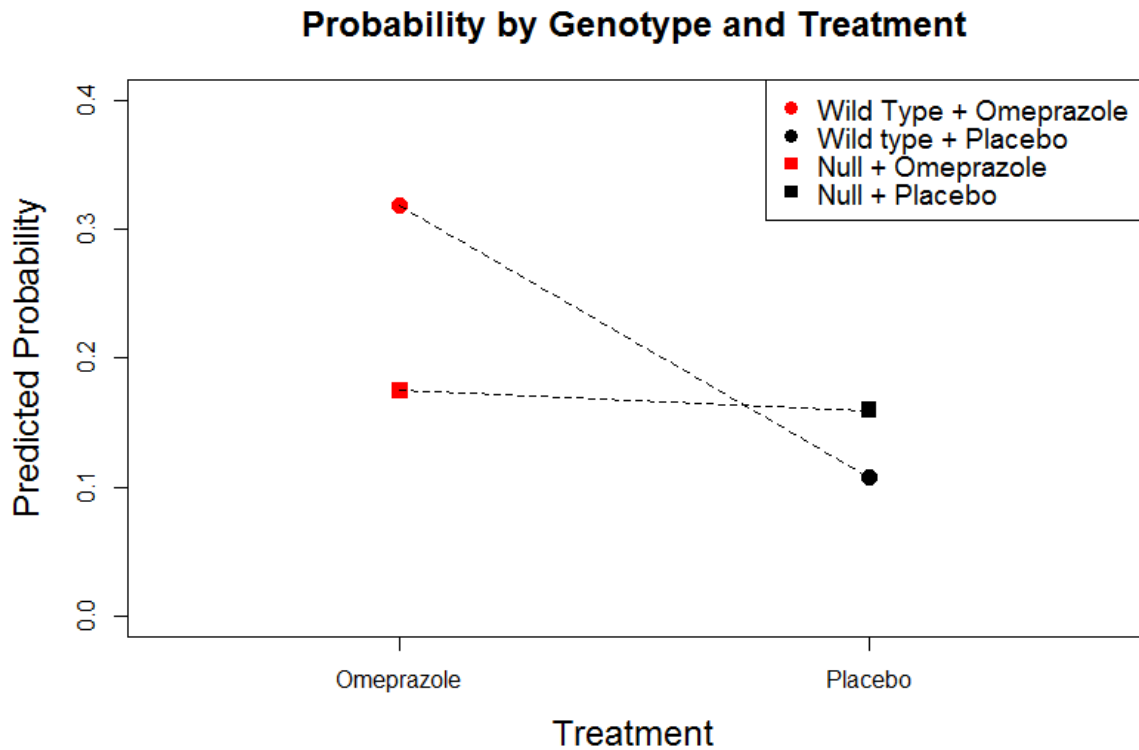


Figure 59 Mixed model (glmmPQL) predicted probability of MTD with genotype and treatment

Similar to the CMH test and the ordinal model, the model demonstrates a significant gene x drug interaction, with OCT1 Wild Type having a significantly higher predicted MTD of metformin during concurrent omeprazole use, compared to OCT1 null, or concurrent placebo use. The effect size of this gene x drug interaction is demonstrated using the odds ratio of metformin tolerance, calculated from the mixed model above.

Odds Ratio

	Odds Ratio of Tolerance	95% CI
OCT1 WT, treated with placebo	1.0	-
OCT1 null, treated with placebo	1.57	(0.38 – 6.44)
OCT1 WT, treated with omeprazole	3.87	(2.02 – 7.43)
OCT1 null, treated with omeprazole	1.75	(0.43 – 7.22)

Table 21 Odds ratio of metformin tolerance as calculated from the generalised linear mixed model, using penalised quasi-likelihood

Odds ratios can be calculated from the exponential of the model estimate for each factor, with 95% confidence intervals of the odds ratio calculated as the exponential of the CIs of the estimate.

As shown in the table above OCT1 wild type individuals are nearly four times more likely to tolerate metformin while taking omeprazole. However, in OCT1 null individuals the addition of omeprazole only increased the OR of tolerance by 0.1.

This result is in-keeping with our primary analysis, that OCT1 wild type have an improved metformin tolerance on omeprazole treatment.

Generalised linear models

An alternative method for analysing a cross-over study, is to adopt a generalised linear model, to assess the intra-individual response to the exposure. In this method, the model is tested within the individual, removing the random effect of the individual.

This gives a model with the MTD on omeprazole as the dependent variable, and genotype and MTD on placebo (MTDP) as fixed effects. In this model, the outcome has to be transformed into a matrix, rather than an ordinal variable. The model and plotted predicted outcome is shown below. This generalised linear model once again demonstrates a significant gene * drug interaction, with omeprazole treatment improving tolerance in the OCT1 wild type group.

`lm1 <- glm (cbind (MTDO, X4.MTDo) ~ Genotype * MTDP, family=binomial).`

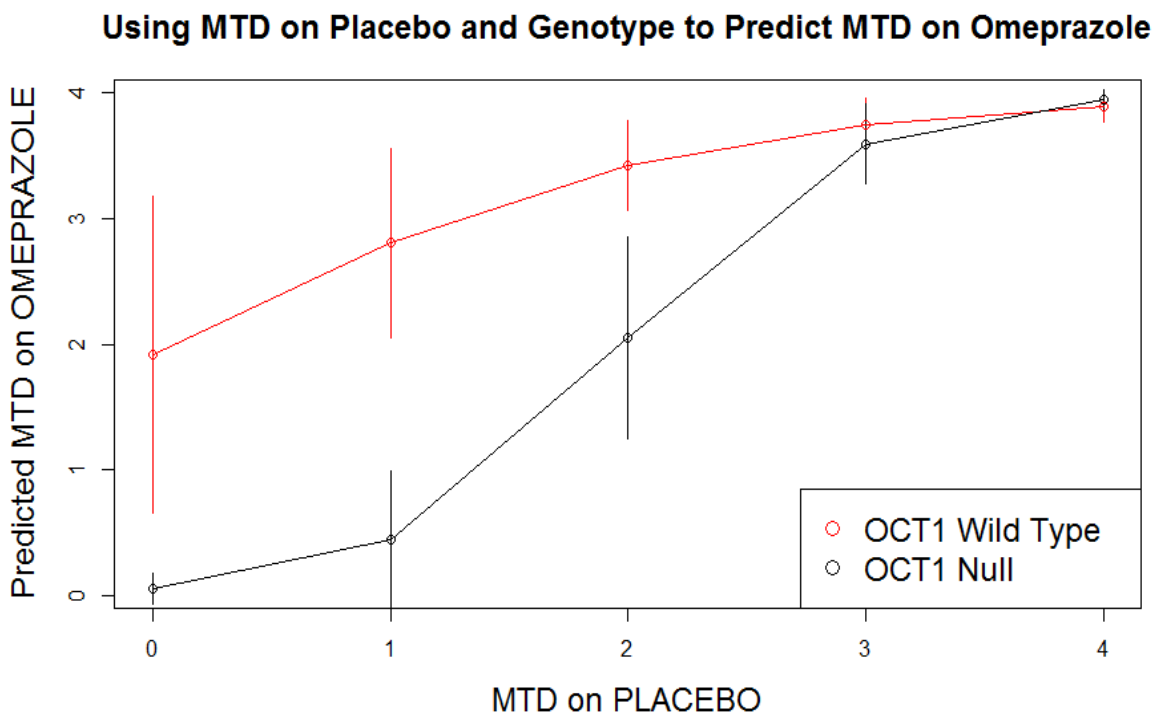


Figure 60 Predicted MTD on Omeprazole, from Genotype and MTD on placebo

When we consider terms individually in the linear model, such as age, BMI, gender, MTDP and concurrent treatment order (referred to as sequence), BMI and MTDP are significant. Interaction terms genotype*sequence, and genotype*MTDP are both significant independently. When all of the above significant variables are added to the model, the resulting simplified model is:

```
lm2 <- glm (cbind (MTDO,X4.MTDO) ~ Genotype*as.factor (Sequence) +
            Genotype* MTDP,
            family=binomial)
```

Using AIC as an estimate of relative quality of the model, the addition of age as an independent variable, improves both model lm1 and lm2, although age is not a significant term within either model.

The linear model of best fit was identified as:

```
lm3 <- glm (cbind (MTDO, X4.MTDo) ~ Genotype * as.factor(Sequence) +
            Genotype * MTDP +
            Age * Genotype,
            family = binomial)
```

Model lm3 was used to predict the MTD on Omeprazole, according to an individual's genotype, age, MTD on placebo, and sequence of concurrent treatment. The model was used to predict outcomes for age 40, 50, 60 and 70 years. Figures 61 – 64 show the model predictions. Sequence 1 refers to omeprazole treatment followed by placebo, sequence 2 is placebo followed by omeprazole.

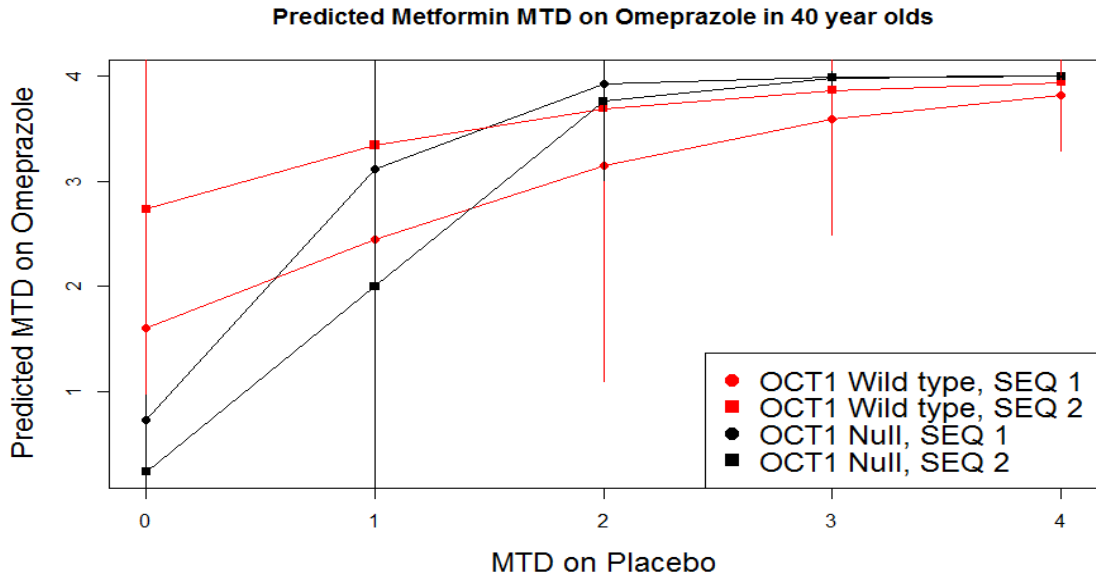


Figure 61 Predicted MTD on Omeprazole in 40 year olds, modelled using *lm3*

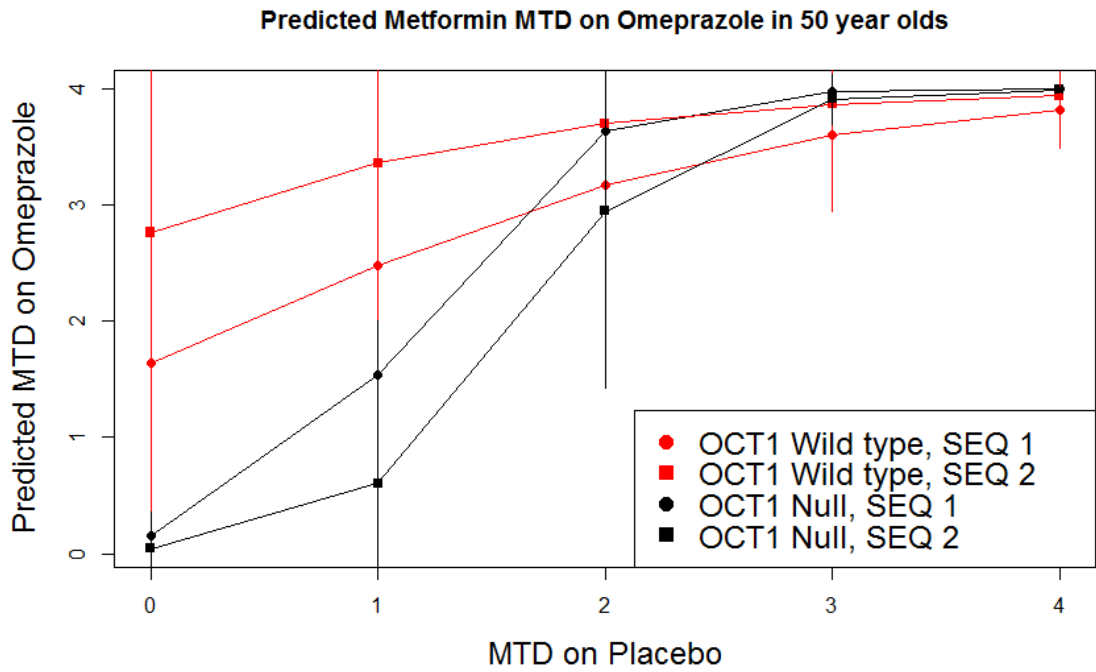


Figure 62 Predicted MTD on Omeprazole in 50 year olds, modelled using *lm3*

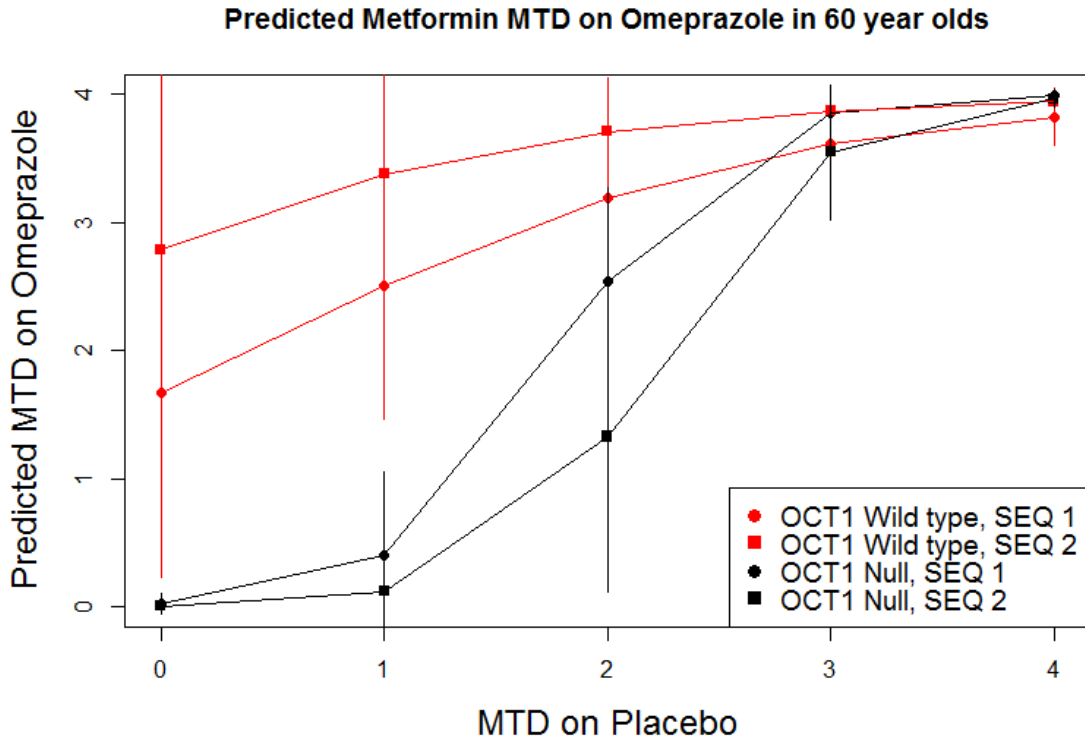


Figure 63 Predicted MTD on Omeprazole in 60 year olds, modelled using Im3

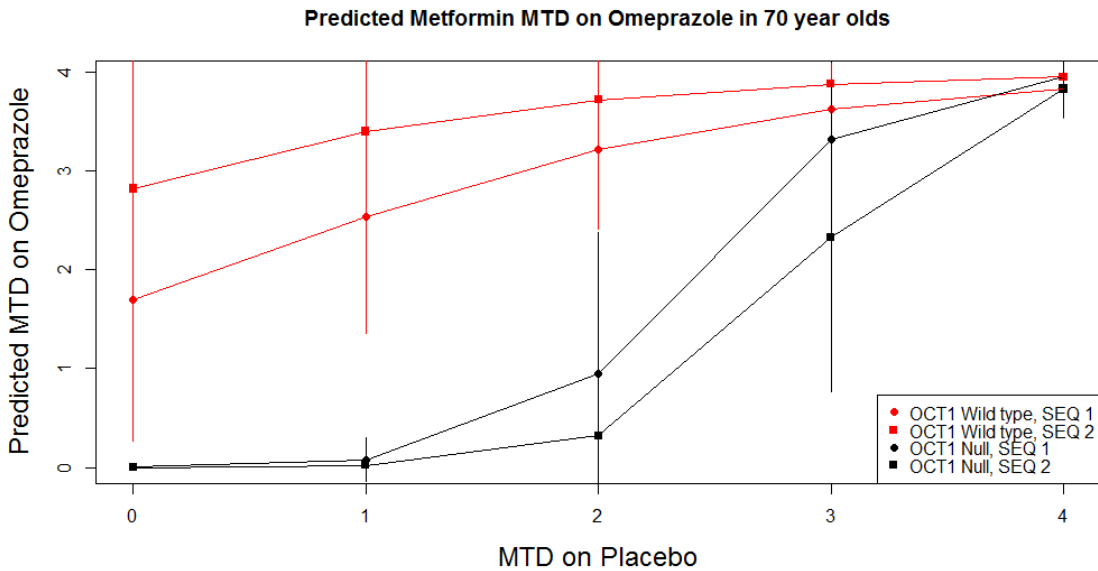


Figure 64 Predicted MTD on Omeprazole in 70 year olds, modelled using Im3

Figures 61 - 64 clearly demonstrate a reducing metformin tolerance with advancing age in the OCT1 Null group. In contrast, metformin tolerance in the OCT1 wild type group is not affected by age.

The difference in tolerance between the treatment sequence groups, although significant in the model, does not appear significant in the plots, as the trajectory of the genotype plots is similar across sequence, and the standard error of the sequence is consistently overlapping within genotype. Interestingly, the direction in which sequence appears to impact on tolerance is divergent in the genotype groups.

Discussion

Sub- analyses – the Impact of Age

The sub-analyses of the data using generalised linear models to consider how the maximum tolerated dose achieved on placebo affects that achieved on omeprazole, once again confirmed the gene x drug interaction seen in the mixed models. The model of best fit also included age and treatment sequence as interaction terms with genotype (although this model had only marginally lower AIC than the model without sequence included).

Prediction of the MTD on omeprazole using this model of best fit clearly demonstrated an age effect on tolerance in the OCT1 null group. This is in-keeping with previous data from GoDARTS which found that individuals intolerant of metformin were older than the tolerant cohort (29). In 40 and 50 year olds, there is no significant difference in tolerance between the genotype groups. However, as age advances into the 6th and 7th decades, the OCT1 null group's MTDO reduces.

The contribution of treatment sequence to the model is potentially a psychological effect of time in study or the effect of experiencing symptoms within the first treatment period on the individual's interpretation or reporting of symptoms. Interestingly, the two sequences had opposing effects on the two genotypes.

While the outcomes of the linear models are intriguing and shed additional light on the potential mechanism of metformin intolerance, the models are not as well suited to the data, as the random effect of the individual is lost. Therefore these are viewed as sub-analyses only.

Appendix 5 Tracer Timeline

Time (mins)	Time from beginning	Target time	Actual time	Target D2 Glucose Infusion rate (mg/kg/min)	Actual D2 Glucose Infusion Rate (mg/kg/min)	Bloods?	Blood bottles	Indirect calorimetry?	Urine collection	Signature	comment
-120	0			6		Y	G		Pre-meal urine collection into 24 hour collection bottle.		
-119	1			0.06		-					
-110	10			0.06		-					
-65	55			0.06		-		Calibrate			
-60	1h			0.06		-		Start run			
-40	1h20			0.06		Y	G, Y, P				
-35	1h25			0.06		Y	G				

-30	1h30			0.06		Y	G				
-20	1h40			0.06		Y	G, Y (5ml),				
-10	1h50			0.06		Y	G				
-5	1h55			0.06		-		Calibrate	Empty bladder		
At time 0 give the liquid meal with U13-C Glucose added. When finished the drink, give 1g liquid paracetamol.											
0	2h			0.042		Y	G, Y, C, P	Start run	Post meal urine collection into second 24 hour urine		
10	2h10			0.036		Y	G, Y, C, P				
15	2h15			0.036		-					
20	2h20			0.030		Y	G, Y, C, P				
30	2h30			0.021		Y	G, Y (5ml),				

45	2h45			0.021		-			collection bottle		
55	2h55			0.021		-		Calibrate			
60	3h			0.021		Y	G, Y (5ml),	Start run			
75	3h15			0.021		Y	G				
90	3h30			0.021		Y	G, Y(5ml),				
115	3h55			0.021		-		Calibrate			
120	4h			0.024		Y	G, Y(5ml),	Start run			
150	4h30			0.024		Y	G, Y, P				
175	4h55			0.024		-		Calibrate			
180	5h			0.027		Y	G, Y(5ml),				

210	5h30			0.027		Y	G, Y	Start run			
235	5h55			0.027		-		Calibrate			
240	6h			0.030		Y	G, Y(5ml),	Start run			
270	6h30			0.030		Y	G, Y				
280	6h40			0.033		-					
300	7h			0.039		Y	G, Y				
360	8h			stop		Y	G, Y				

End of tracer study checklist:

- Remove cannulae
- Give emergency contact details
- Give medication: Metformin (Visit 1)
- Pioglitazone (Visit 2)
- Collect XS meds: Metformin (visit 2)
- Pioglitazone (visit 3)
- Arrange weekly telephone call
- Arrange date(s) for next visit(s)

CRC number for 9am – 5pm. NHS helpline out of hours.

Time	Urine Volume
-120 to 0 mins (pre-meal)	
0 to 360 (post-meal)	

Appendix 6: RAMP analysis

Individuals with A-T are insulin resistant

HOMA

Comparing insulin sensitivity (HOMA-%S) and beta cell function (HOMA%B), the resulting plot has an inverse non-linear distribution, similar to that seen in the traditional rectangular hyperbola of the disposition index (346). This indicates that at lower insulin sensitivity, the beta cell is appropriately upregulated to secrete more insulin. Therefore, at least in the fasted state, the beta cell function of the two groups appears comparable, as both have normal fasting glucose.

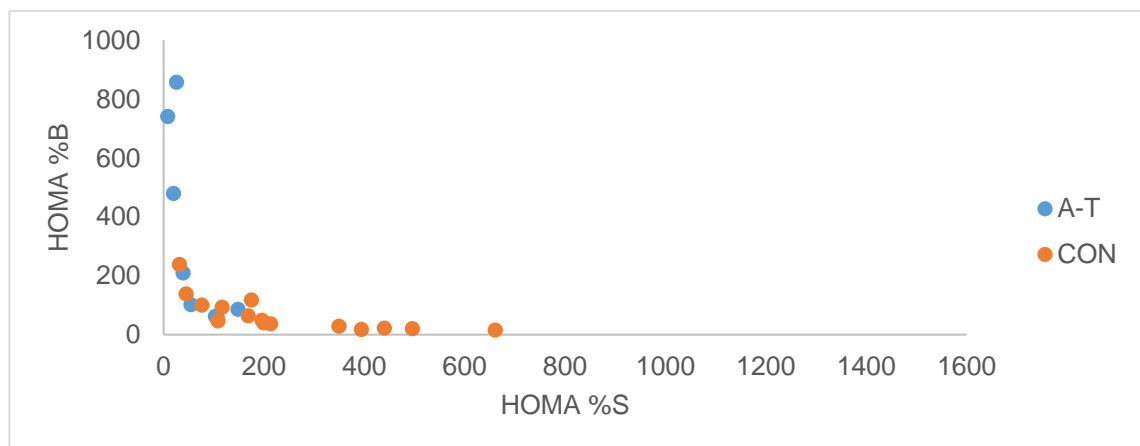


Figure 65 Comparison of calculated insulin sensitivity (HOMA%S) and beta cell function (HOMA%B) at baseline.

However, HOMA measurements are correlated indices, as both are proportional to fasting insulin and glucose. They are, therefore, interdependent and not ideal for assessing beta cell function (346). For a more accurate assessment, OGTT data or beta cell modelling, using C-peptide deconvolution (226) to calculate insulin secretion, is required.

Beta cell modelling

The dose-response curve for the two groups at baseline was remarkably similar, indicating equivalent beta cell function in the two groups. Glucose sensitivity (87.6 vs 91.4, $p = 1.0$) - calculated as the slope of the dose response curve - and the insulin secretion rate at known glucose (4.7mmol/l) (A-T 83.4 vs 61.5, $p = 0.51$), were, therefore, also comparable between the two groups

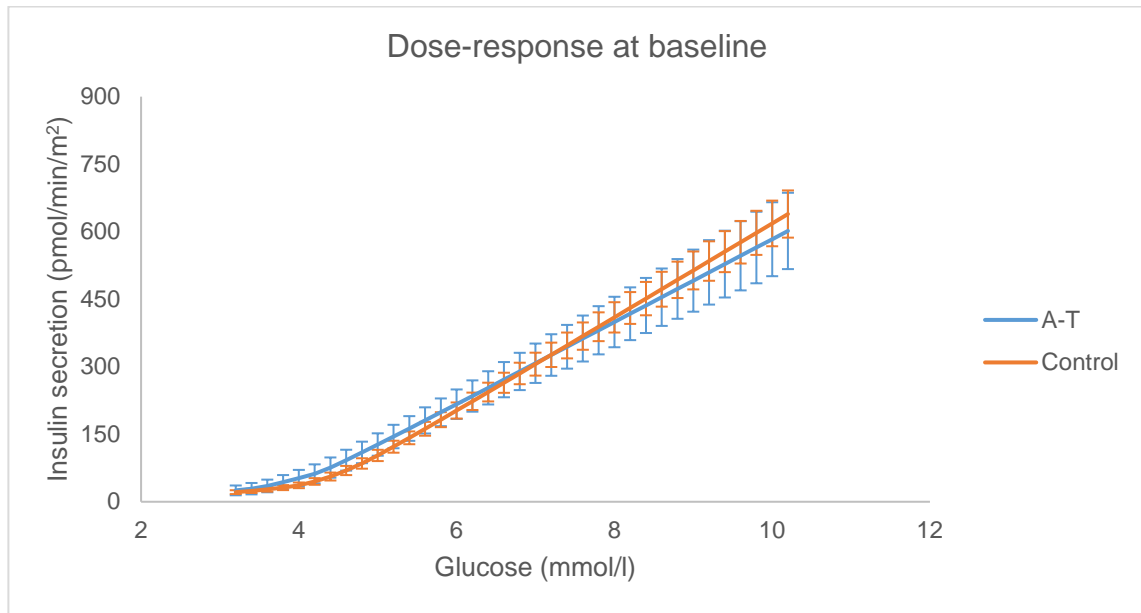


Figure 66 Dose-response curve at baseline. Data are mean (SEM).

Rate sensitivity, a marker of first phase insulin response, although numerically greater in the A-T group, was not statistically different from the controls (970.6 vs 789.0, $p = 0.36$). Elevation of the rate sensitivity would be in-keeping with the picture of insulin resistance.

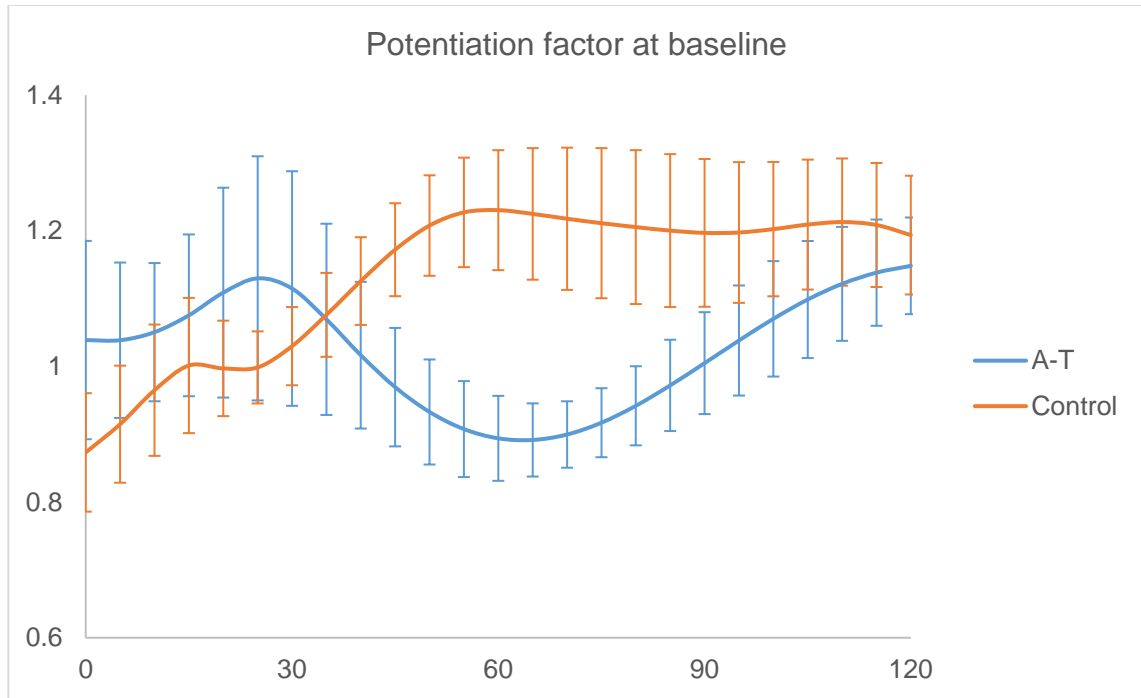


Figure 67 Potentiation factor over the first 120 minutes of the MMT. The lesser gradient of the A-T slope is in-keeping with impaired glucose tolerance. Data are mean (SEM).

The potentiation factor during the first 120 minutes of the MMT is shown in the figure above. The flatter profile of the potentiation factor is similar to that seen in impaired glucose tolerance and diabetes (222).

Disposition index and Beta Cell Function

The disposition index (DI) is a constant which can be used as a measure of the beta cells ability to compensate for insulin resistance (254, 255). In an individual with normal beta cell function, the sensitivity – secretory relationship is traditionally described as a rectangular inverse hyperbola, and the product of the two parameters is the disposition index. It was originally defined as the product of the insulin sensitivity index (Si) and acute insulin response (AIR) from the IVGTT, however several studies have since described an oral disposition index (256, 257). Oral DI can be calculated using indices from the OGTT or beta cell modelling, for example, it is possible to plot the Matsuda Index against the

Insulinogenic index, and the product of the two is the oral disposition index (258, 259).

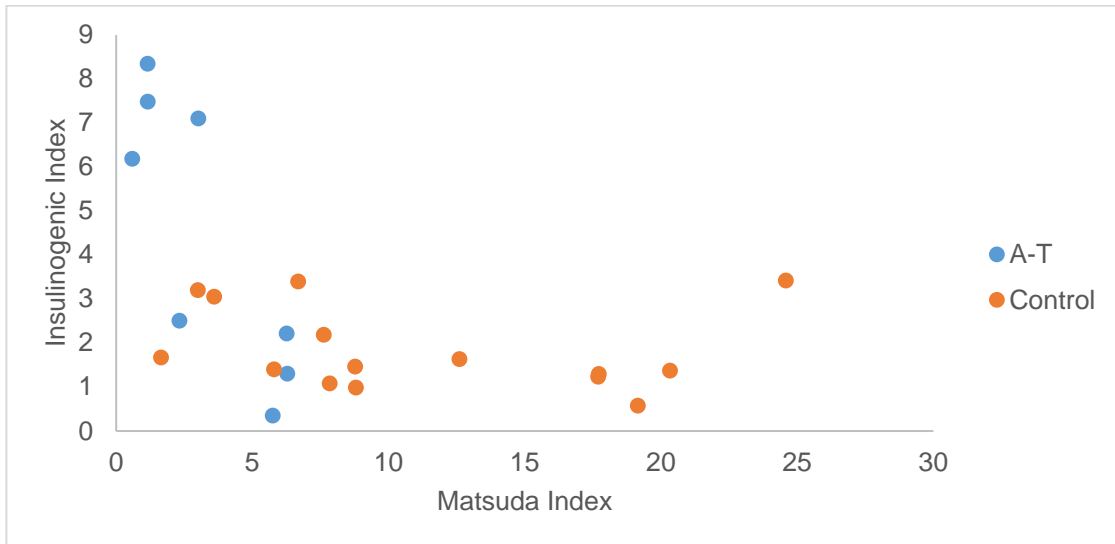


Figure 68 Insulinogenic index (IGI) plotted against the Matsuda insulin sensitivity index results in the rectangular inverse hyperbola associated with the disposition index. As beta cell function reduces the hyperbola moves closer to the origin.

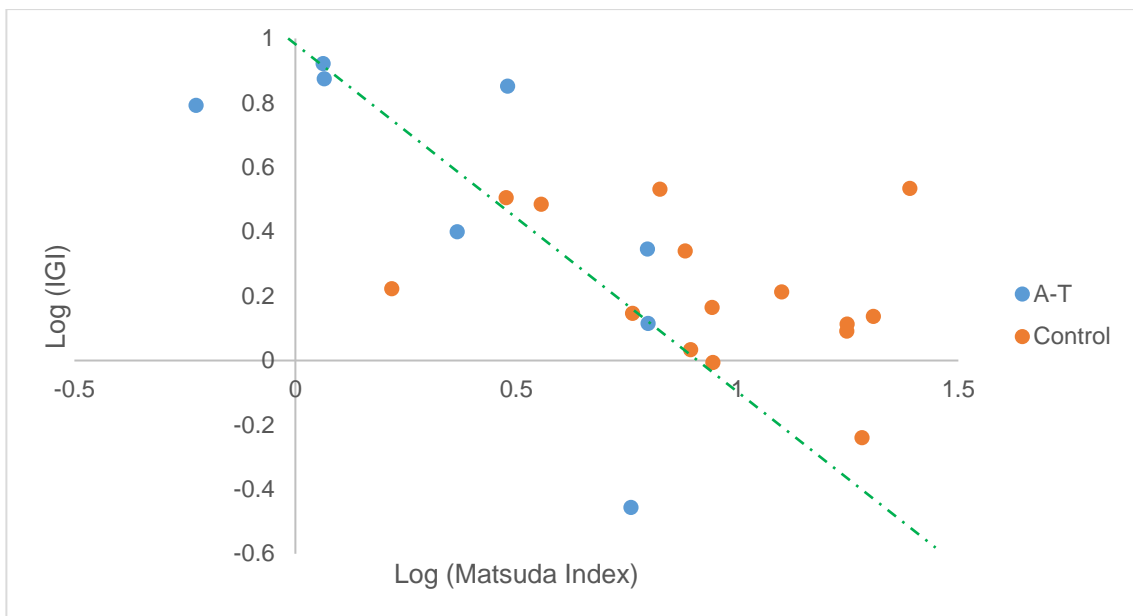


Figure 69 Proof of hyperbolic relationship between IGI and Matsuda index. When log values of the indices are plotted, there should be a negative linear relationship, with slope = -1.

Alternatively, the Matsuda index can be plotted against the ISR. This is more robust as the ISR is calculated from C-peptide deconvolution and therefore the two measures are more independent, though not entirely so, as using the same OGTT data. Therefore this comparison was included in the main results chapter.

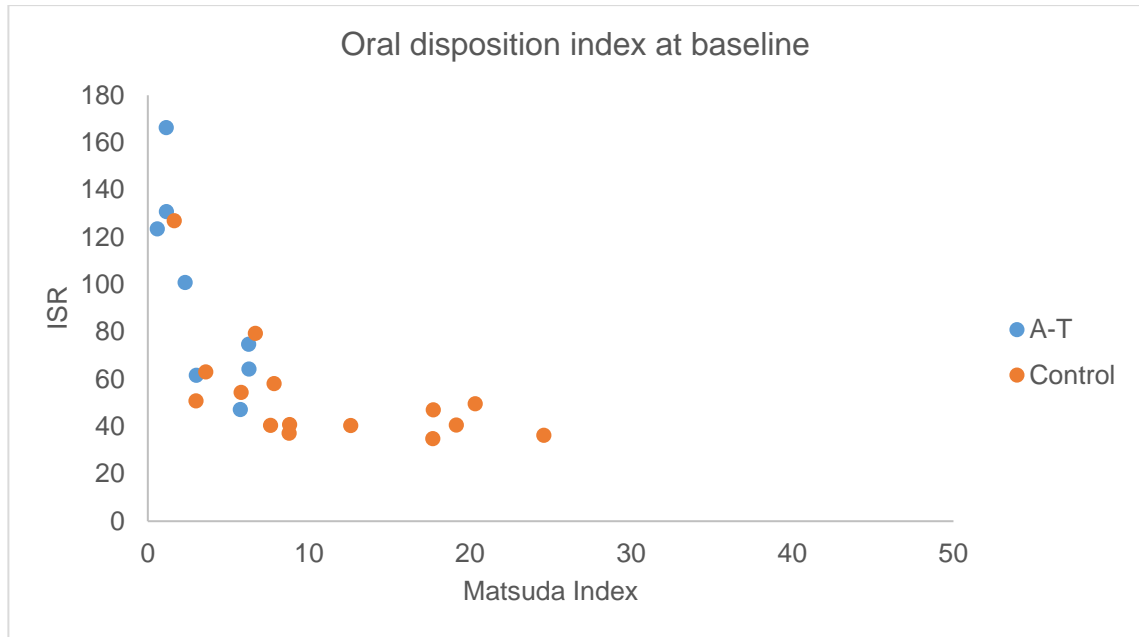


Figure 70 ISR plotted against Matsuda index, showing the typical hyperbolic relationship.

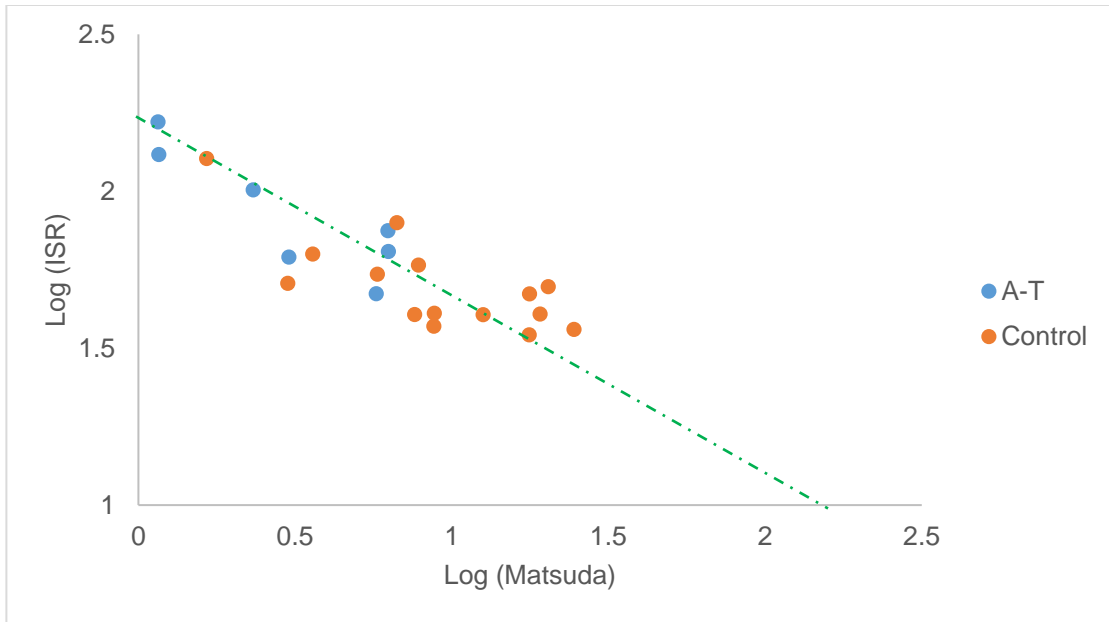


Figure 71 Log ISR plotted against log Matsuda has a slope of -1.

Response to metformin

HOMA-IR

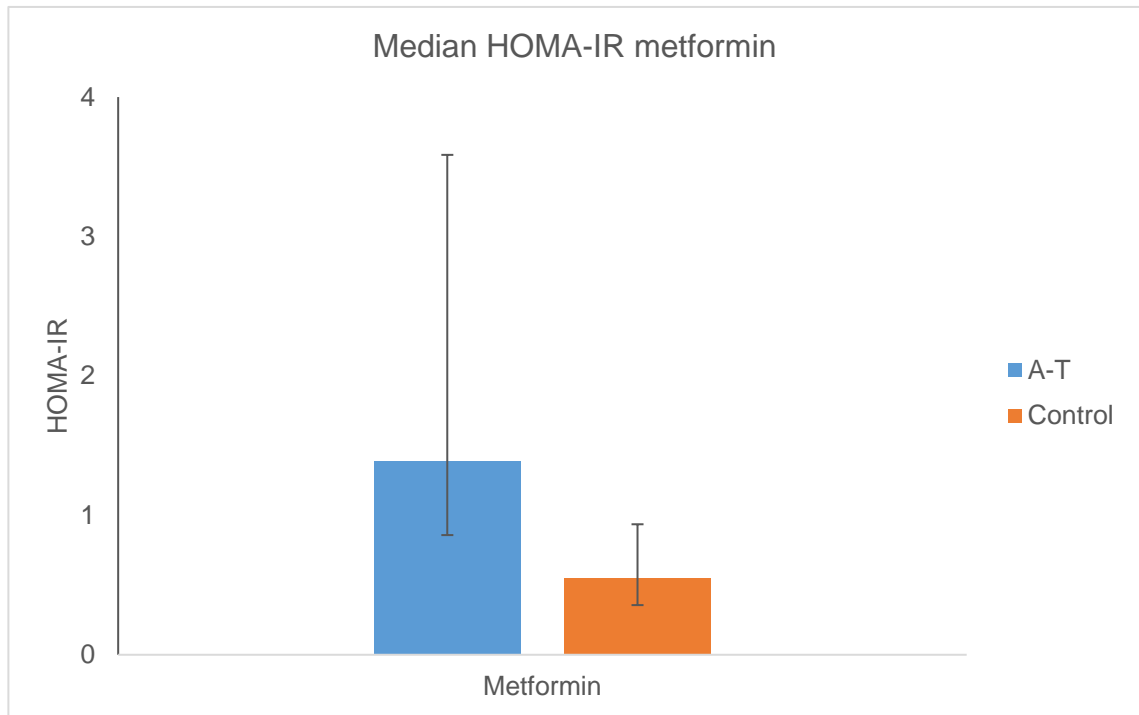


Figure 72 HOMA-IR after metformin treatment. Data are median (IQR).

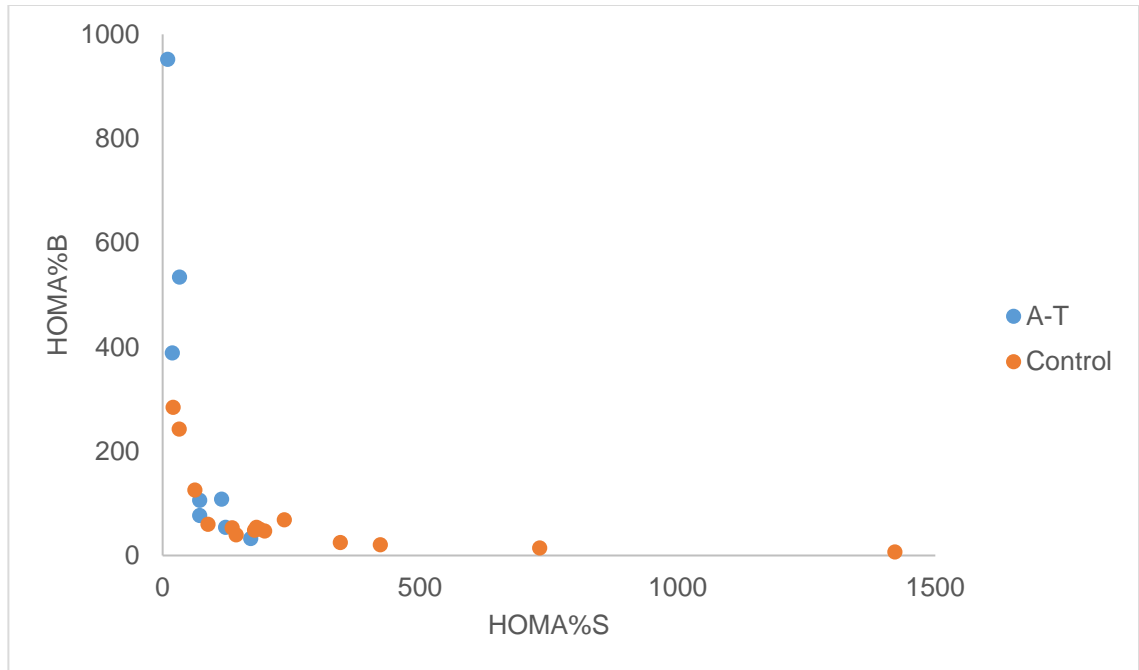


Figure 73 HOMA%B compared to HOMA%S post-metformin.

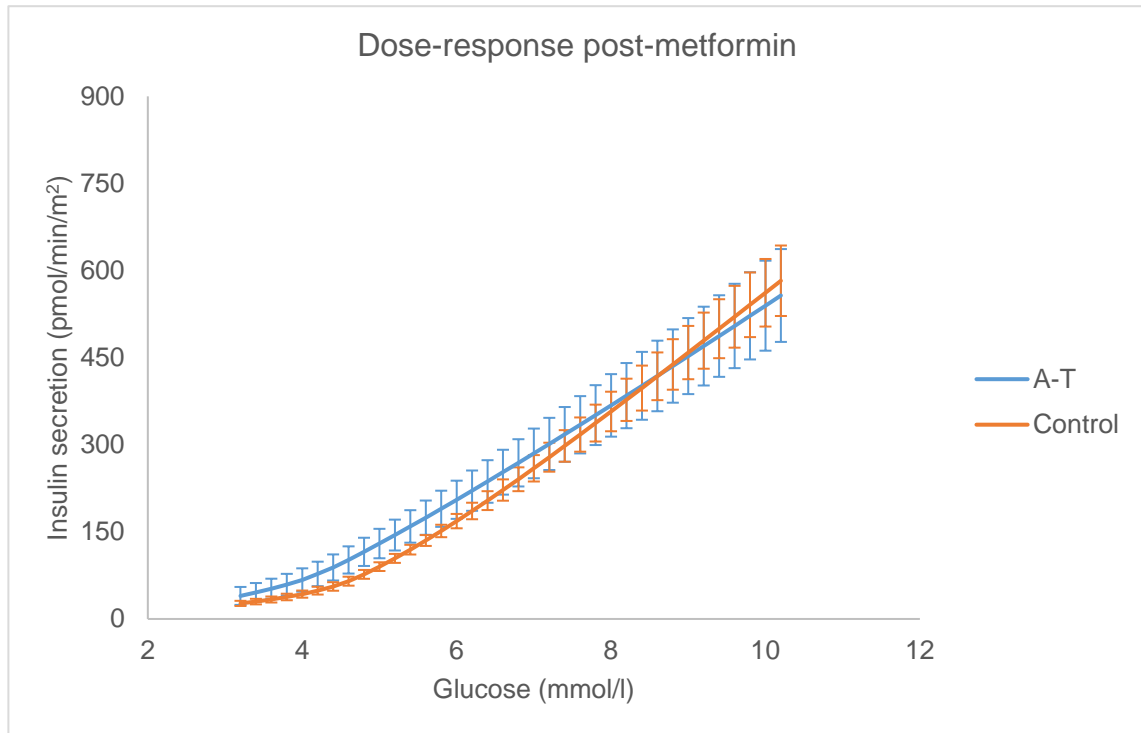
Beta cell modelling

Figure 74 Dose-response curve of insulin secretion according to glucose concentrations post-metformin. Data are mean (SEM).

The dose-response curve shown above remained similar between groups, and unchanged from baseline. There is therefore no change in glucose sensitivity ($p = 0.87$) nor in ISR for specified glucose ($p = 0.21$). Rate sensitivity was unchanged from baseline, with no difference between groups.

The potentiation factor profile was flatter in the A-T group, as shown in the figure below. As for baseline, this could represent impaired glucose tolerance. However, in A-T, there is obvious loss of the initial potentiation, which is evident in the control group. This may indicate a reduced incretin effect (347), especially as there was no increment in GLP1 in the A-T group, as would be expected with metformin.

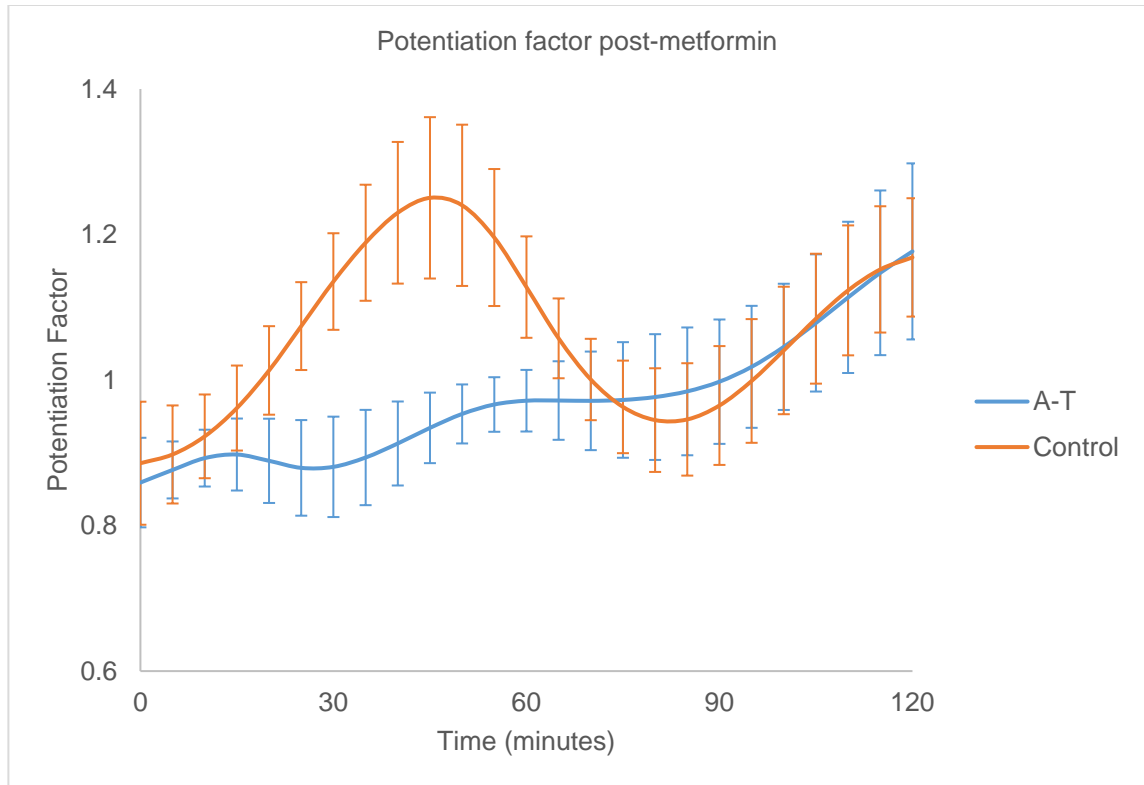


Figure 75 Potentiation factor post-metformin up to 120 minutes post-meal. Again, A-T group have a flatter profile, and loss of the initial potentiation post-meal. Data are mean (SEM).

Insulin sensitivity and secretion indices

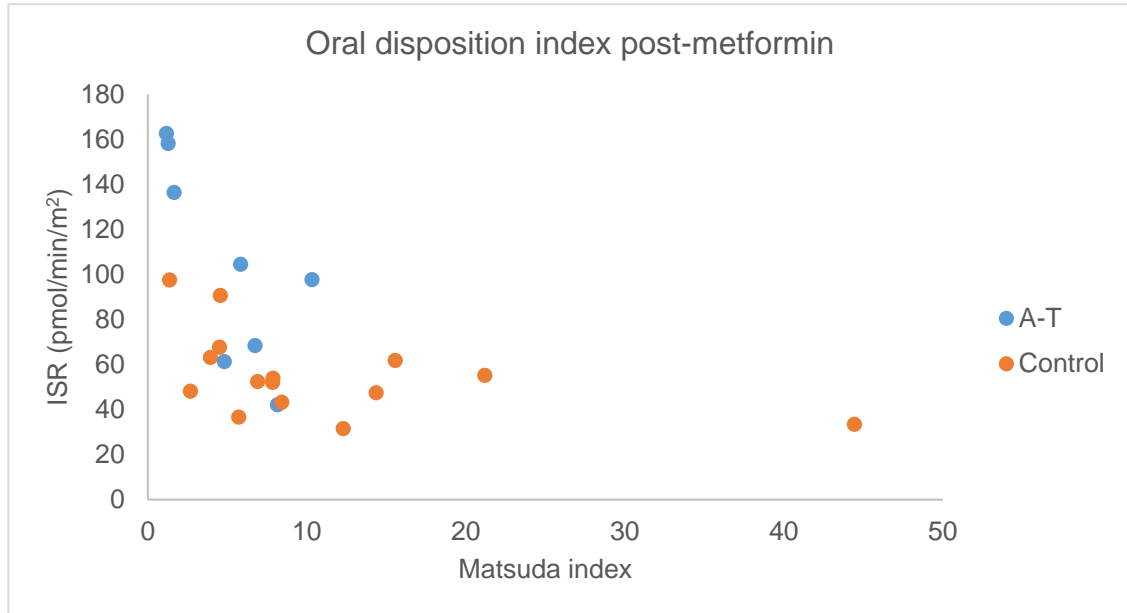


Figure 76 Comparison of the Matsuda index and ISR as an oral disposition index.

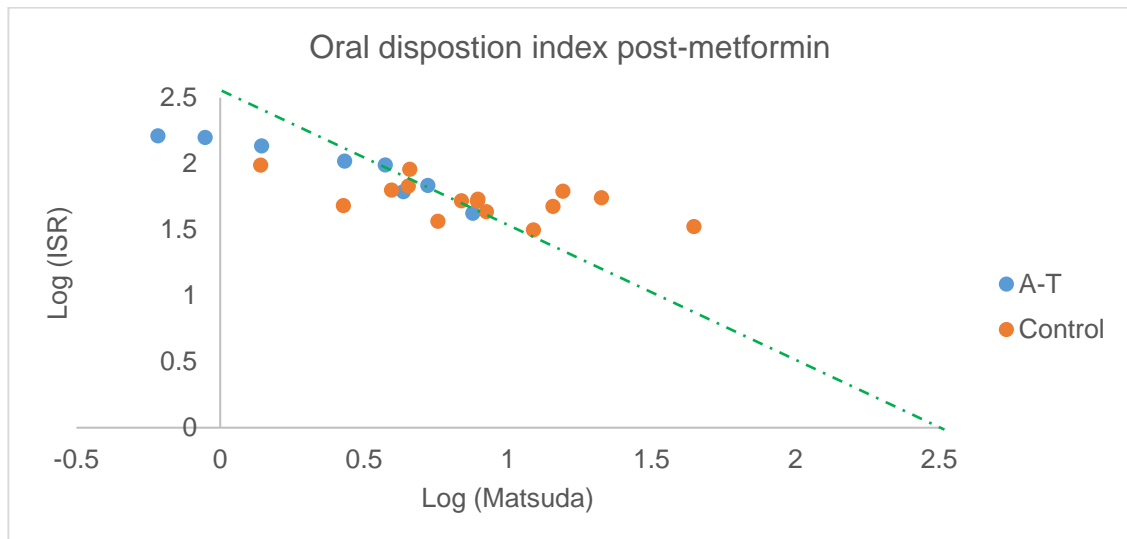


Figure 77 Oral disposition – $\log(\text{Matsuda})$ against $\log(\text{ISR})$ with the slope of -1.

Response to pioglitazone

HOMA

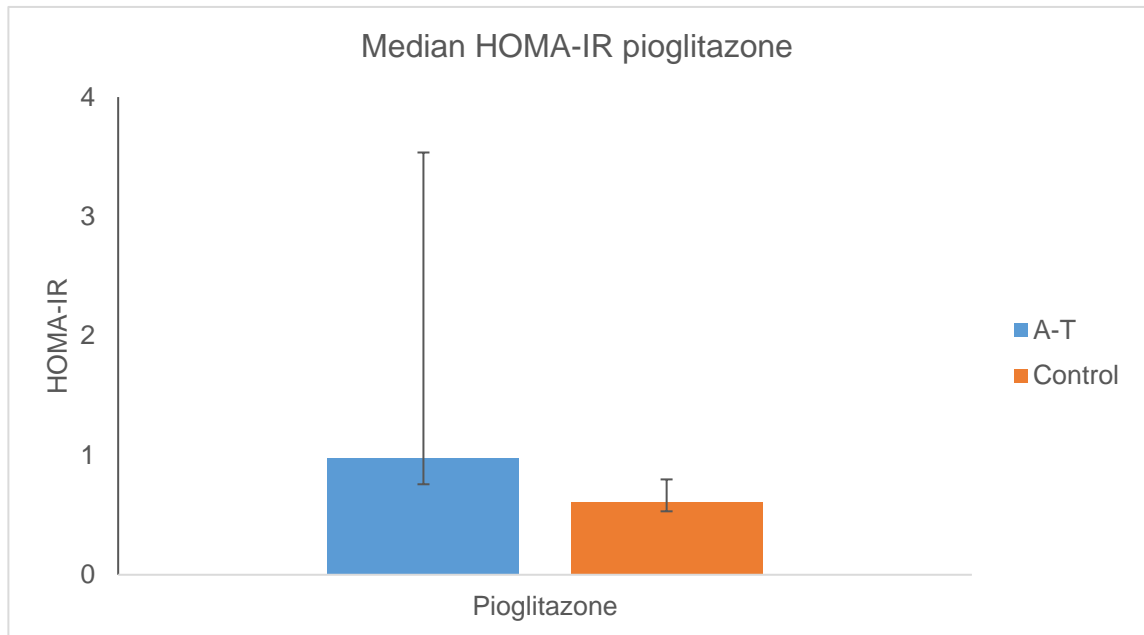


Figure 78 HOMA-IR after pioglitazone treatment. Data are median (IQR).

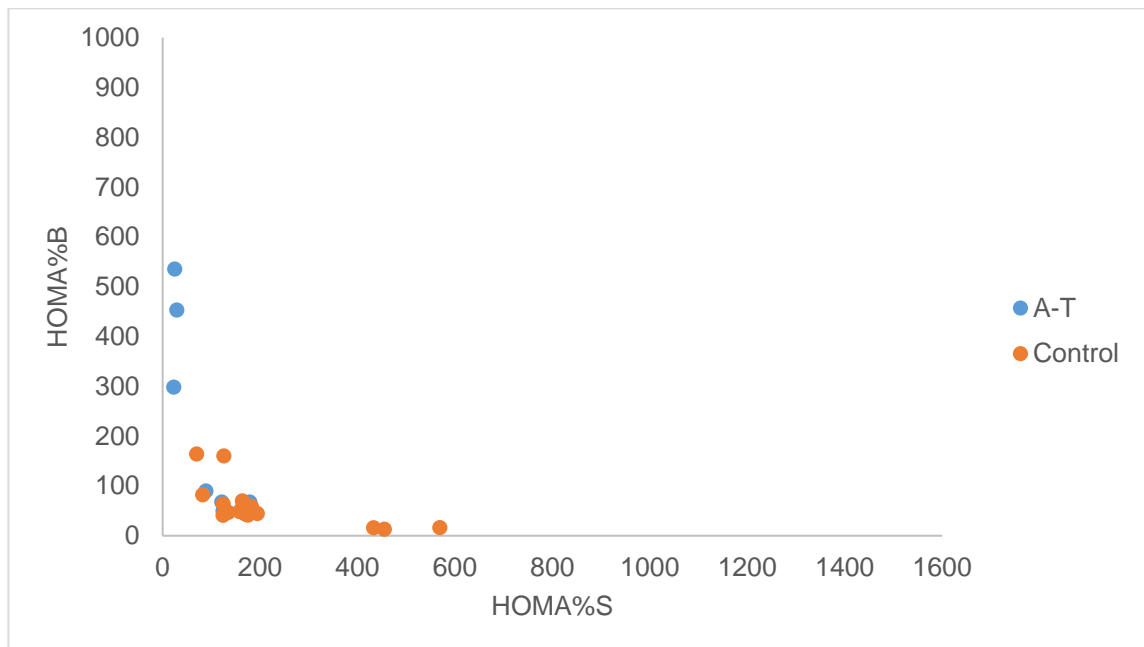


Figure 79 HOMA%B compared to HOMA%S while taking pioglitazone. The axes scales have been kept constant for each study visit, to demonstrate the left shift of the hyperbola.

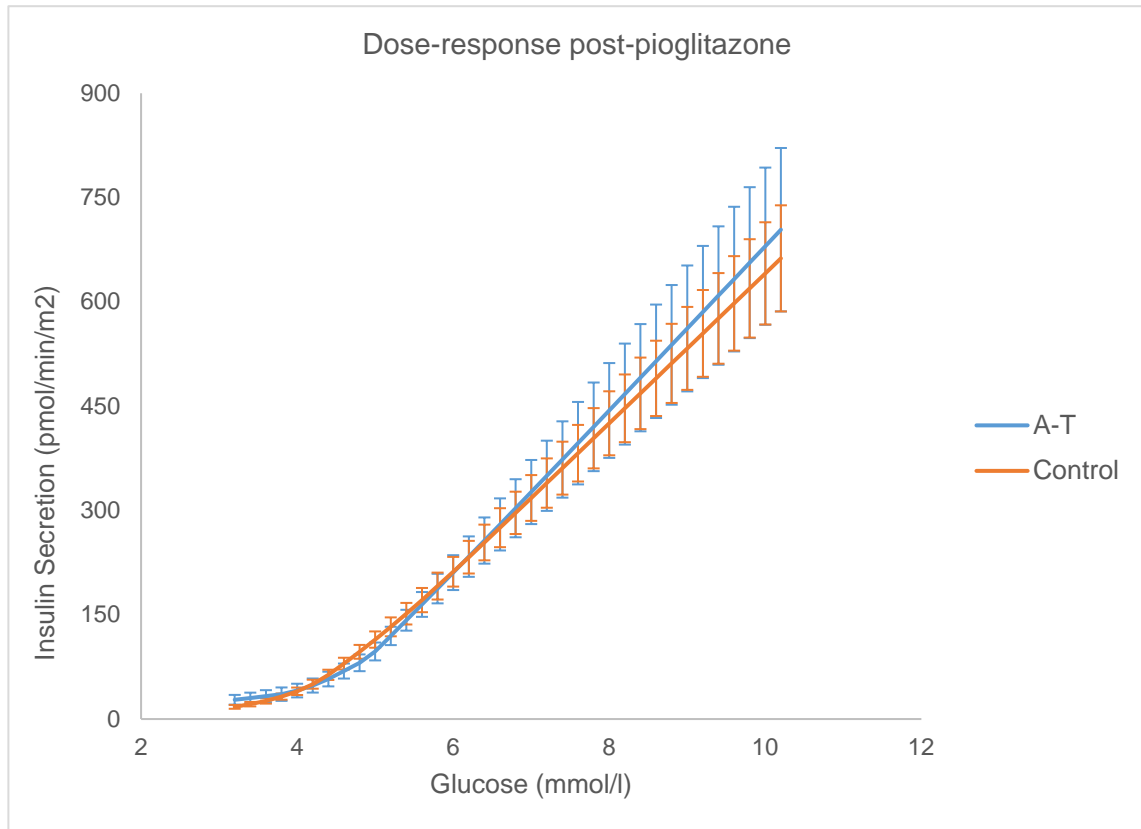
Beta cell modelling

Figure 80 Dose-response curve following pioglitazone treatment. Data are mean (SEM).

There was a reduction in the mean ISR over the duration of the MMT in the A-T group. Although not significant, both ISR at reference glucose (83.4 to 66.5, $p = 0.3$) and rate sensitivity (970 to 645, $p = 0.6$) were lower compared to baseline in the A-T group, and glucose sensitivity increased (87.6 to 97.2). This is evident from the perceived increased gradient in the dose-response curve shown above.

The control group did not demonstrate any change from baseline in insulin or glucose concentration, nor in fasting or mean ISR. However their ISR at reference glucose was increased (61.5 to 78.0, $p = 0.03$), which would be in-keeping with the increased gradient of the dose-response curve.

Despite the improvement in glucose tolerance and insulin resistance, the profile of potentiation in the A-T group remains flatter than the controls.

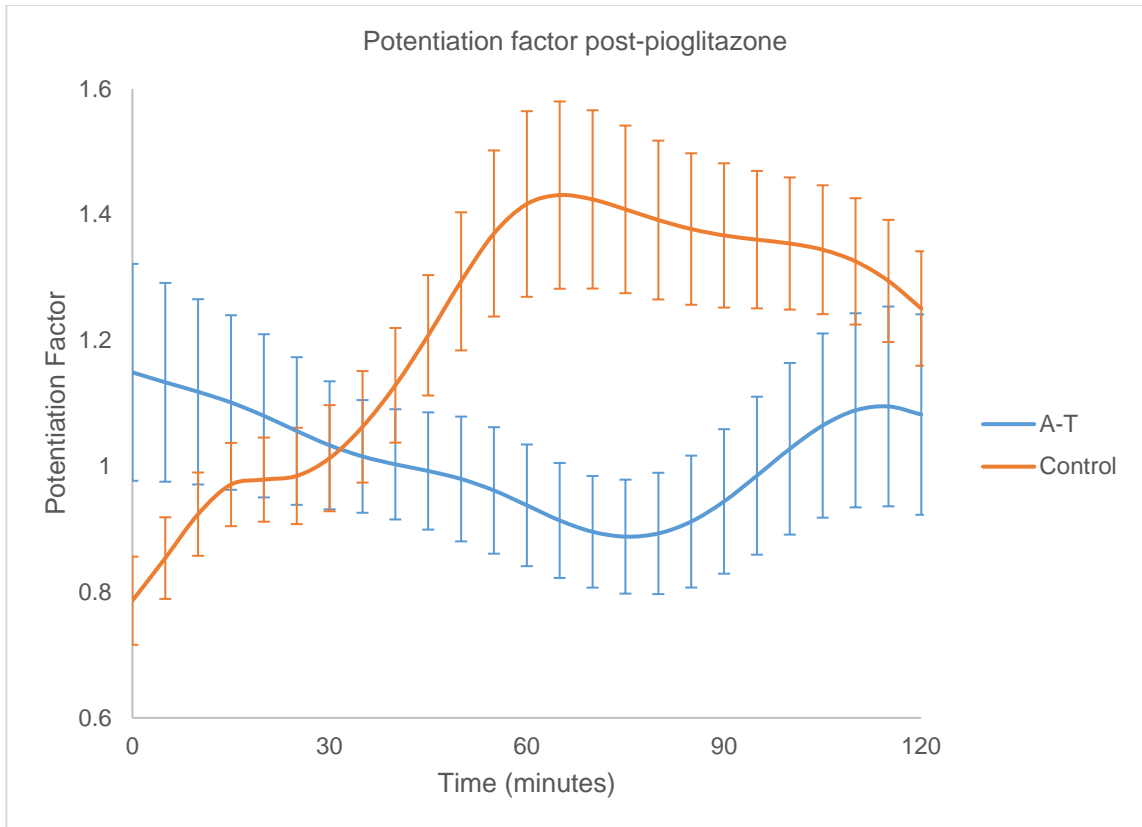


Figure 81 Potentiation factor post-pioglitazone. Flatter profile persists despite improved glucose tolerance in the A-T group, lending support to the theory that there is a reduced incretin effect in these individuals. Data are mean (SEM).

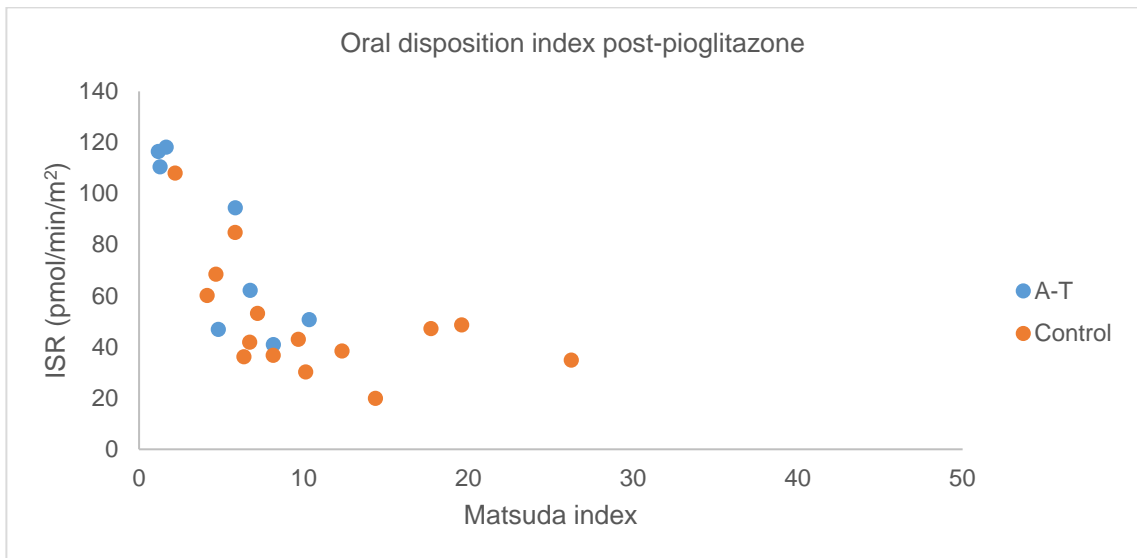


Figure 82 Comparison of Matsuda index and ISR as an oral disposition index.

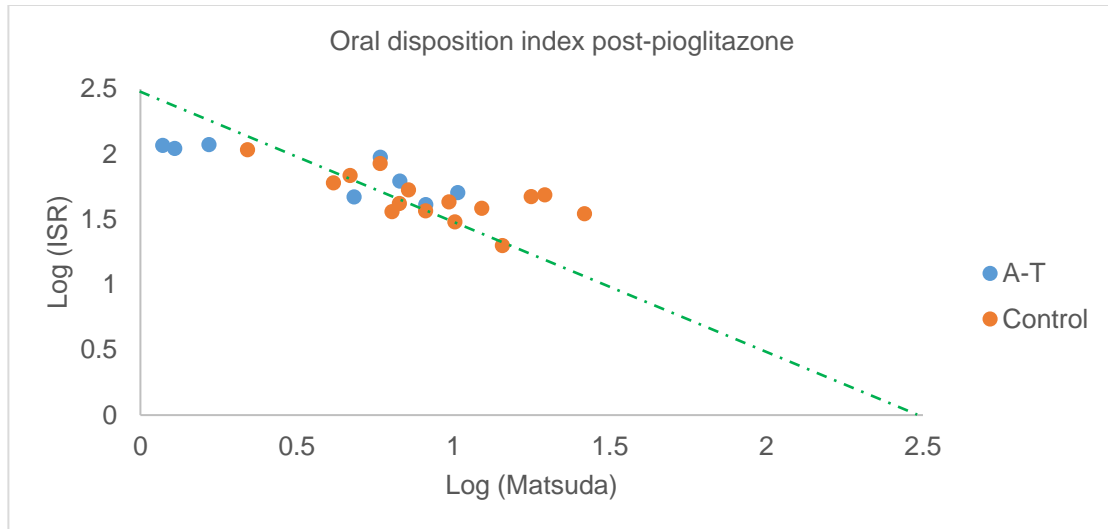


Figure 83 Oral DI: $\log(\text{Matsuda})$ plotted against $\log(\text{ISR})$. The green dashed line represents a gradient of -1, inkeeping with the inverse hyperbolic relationship between sensitivity and secretion.

Metformin mixed effects models

The following mixed effects models were used to analyse a subset of the RAMP data, including only baseline and metformin results, to assess for a gene*drug interaction explaining the variance of each of the following outcomes:

BMI

```
modelbmi <- lme (BMI ~ Genotype * Treatment)
```

Model term	P value
Genotype	0.57
Treatment	0.04
Genotype*Treatment	0.53

This confirms that metformin does effect BMI. However, there is not a gene*drug interaction between ATM and metformin, to explain the variance in BMI. Even when controlling for age and gender, there is no gene*drug interaction identified.

Fasting active GLP1

`modelglp <- lme (Basal Active GLP1 ~ Genotype * Treatment)`

Model term	P value
Genotype	0.13
Treatment	0.03
Genotype*Treatment	0.17

Once again, this model confirms that metformin has a significant effect on fasting active GLP1, but no gene*drug interaction is identified. Controlling for age, sex and BMI had little effect on the model.

Mean active GLP1

`modelaglp <- lme (Mean Active GLP1 ~ Genotype * Treatment)`

Model term	P value
Genotype	0.39
Treatment	0.09
Genotype*Treatment	0.11

There were no significant terms in the model of mean active GLP1, with no improvement by controlling for age, sex and BMI.

Fasting total GLP1

```
modeltglp <- lme (Basal Total GLP1 ~ Genotype * Treatment)
```

Model term	P value
Genotype	0.78
Treatment	0.08
Genotype*Treatment	0.65

There were no significant terms when modelling fasting total GLP1, again with no change when controlling for age, sex and BMI.

Mean total GLP1

```
modelmtglp <- lme (Mean Total GLP1 ~ Genotype * Treatment)
```

Model term	P value
Genotype	0.87
Treatment	0.06
Genotype*Treatment	0.20

It is likely that metformin does explain some of the variance in mean total GLP1, though strictly has not reached significance. This was not improved by the addition of age, sex, and BMI to the model.

Mean glucagon

```
modelgcg <- lme (Mean Glucagon ~ Genotype * Treatment)
```

Model term	P value
Genotype	0.91
Treatment	0.05
Genotype*Treatment	0.53

Metformin treatment does affect mean glucagon concentration, though there is no gene*drug interaction. Controlling for age, sex and BMI does not improve the model.

Fasting EGP

```
modelfgp <- lme (Fasting EGP ~ Genotype * Treatment)
```

Model term	P value
Genotype	0.57
Treatment	0.005
Genotype*Treatment	0.20

Metformin increases fasting EGP, but this is a drug effect, not a gene*drug interaction. When controlling for age, sex and BMI, both BMI ($p = 0.007$) and Treatment are significant in the model.

Mean EGP

```
modelmgp <- lme (Mean EGP ~ Genotype * Treatment)
```

Model term	P value
Genotype	0.02
Treatment	0.18
Genotype*Treatment	0.41

Interestingly, there is a genotype effect on mean EGP, with the A-T group having a lower mean EGP. The model does not show the metformin effect on EGP nor a gene*drug interaction. When controlling for age, sex and BMI, both sex ($p = 0.02$) and BMI ($p = 0.02$) are significant, along with genotype ($p = 0.01$).

Fasting Clearance

```
modelfcl <- lme (Fasting Clearance ~ Genotype * Treatment)
```

Model term	P value
Genotype	0.02
Treatment	0.003
Genotype*Treatment	0.20

Metformin increases fasting glucose clearance, although there was no gene*drug interaction identified. Controlling for age, sex and BMI, BMI was significant ($p = 0.03$), alongside metformin ($p = 0.006$).

Mean Clearance

```
modelmcl <- lme (Mean Clearance ~ Genotype * Treatment)
```

Model term	P value
Genotype	0.06
Treatment	0.42
Genotype*Treatment	0.99

There were no significant terms within the model of mean glucose clearance, though the A-T genotype was trending towards a reduction in mean glucose clearance. When controlling for age, sex and BMI, genotype becomes significant ($p = 0.01$), and so is BMI ($p = 0.003$).

In summary, no gene*drug interaction was found when considering the effect of A-T genotype and metformin treatment, on BMI, GLP1, glucagon, EGP, or clearance.

Appendix 7: Summary table RAMP results		A-T			Control		
		Baseline	Metformin	Pioglitazone	Baseline	Metformin	Pioglitazone
Insulin conc. (pmol/l)	Fasting	61.1 (26.1 – 134.6)	38.0 (26.0 – 111.6)	28.0 (20.9 – 110.1)	15.1 (7.8 – 24.9)	16.3 (11.1 – 25.2)	18.0 (15.5 – 21.9)
	Mean	393.0 (274.6 – 2102.7)	490.8 (254.4 – 1780.4)	252.4 (195.2 – 823.2)	147.2 (94.9 – 227.0)	184.4 (124.7 – 219.9)	142.2 (95.8 – 194.7)
Glucose conc. (mmol/l)	Fasting	4.8 (4.4 – 5.1)	4.8 (4.5 – 4.9)	4.7 (4.4 – 4.7)	4.6 (4.5 – 4.7)	4.6 (4.5 – 4.8)	4.7 (4.5 – 4.9)

	Mean	6.3 (6.1 – 6.7)	6.6 (6.4 – 7.2)	5.9 (5.7 – 6.2)	5.2 (5.0 – 5.6)	5.5 (5.3 – 5.7)	5.3 (4.8 – 5.5)
Glucagon (pg/ml)	Fasting	50.5 (21.8 – 67.3)	58.4 (20.0 – 101.9)	54.7 (20.5 – 90.2)	54.8 (42.0 – 70.5)	65.2 (36.9 – 83.4)	57.4 (42.1 – 73.9)
	Mean	38.8 (23.9 – 54.4)	47.2 (18.4 – 65.0)	38.0 (20.1 – 65.6)	54.5 (35.8 – 71.0)	58.4 (42.3 – 78.4)	53.6 (38.6 – 74.1)
Active GLP1 (pg/ml)	Fasting	1.2 (0.6 – 2.5)	2.0 (1.3 – 2.1)	0.8 (0.2 – 2.4)	0.4 (0.3 – 1.3)	1.6 (0.8 – 3.3)	0.5 (0.2 – 0.9)

	Mean	3.4 (2.6 – 4.7)	3.0 (1.6 – 3.6)	2.9 (1.7 – 4.6)	2.7 (1.8 – 4.3)	3.7 (2.5 – 6.8)	2.4 (1.6 – 3.3)
Total GLP1 (pg/ml)	Fasting	15.0 (4.4 – 32.6)	11.4 (5.9 – 45.2)	13.8 (7.0 – 31.5)	5.5 (4.0 – 11.9)	8.4 (7.7 – 12.7)	6.6 (3.7 – 13.7)
	Mean	18.4 (10.7 – 26.9)	12.7 (8.9 – 35.4)	18.0 (13.0 – 25.4)	11.1 (6.7 – 13.5)	13.7 (7.8 – 36.5)	12.5 (7.1 – 26.2)
Leptin (pg/ml)		24013 (14591 – 30836)	17812 (6578 – 19918)	14812 (9362 – 22789)	4867 (2501 – 12717)	5457 (1614 – 8170)	5323 (1648 – 7921)

Adiponectin (ng/ml)		2528 (2008 – 4887)	3306 (2309 – 5390)	12461 (4451 – 15843)	6262 (4051 – 89940)	5975 (3382 – 7966)	15123 (9594 – 19384)
NEFA (mmol/l)	Fasting	0.72 (0.65 – 0.88)	0.74 (0.62 – 0.81)	0.54 (0.43 – 0.60)	0.53 (0.45 – 0.68)	0.56 (0.51 – 0.60)	0.46 (0.36 – 0.56)
	Mean	0.25 (0.22 – 0.28)	0.25 (0.20 – 0.27)	0.18 (0.14 – 0.20)	0.21 (0.19 – 0.26)	0.21 (0.18 – 0.23)	0.16 (0.14 – 0.20)
RaO		58.4 (55.1 – 62.4)	59.1 (53.4 – 61.5)	58.6 (54.9 – 62.6)	59.2 (56.7 – 61.5)	59.4 (54.2 – 62.0)	60.6 (54.9 – 61.5)

Glucose Clearance (ml/min/kg)	Fasting	2.3 (2.2 – 2.8)	2.6 (2.3 – 3.1)	2.6 (2.2 – 2.9)	2.7 (2.3 – 2.8)	3.0 (2.7 – 3.4)	2.6 (2.4 – 2.9)
	Mean	2.8 (2.7 – 3.2)	2.8 (2.6 – 3.2)	3.1 (3.0 – 3.2)	3.3 (3.1 – 3.5)	3.4 (3.0 – 3.5)	3.4 (3.3 – 3.8)
Glucose Production (μ mol/min/kg)	Fasting	10.6 (8.4 – 11.5)	11.3 (9.8 – 12.8)	10.3 (9.0 – 11.7)	10.9 (10.1 – 12.4)	13.8 (11.7 – 15.0)	11.9 (11.0 – 12.8)
	Mean	3.7 (3.3 – 4.4)	3.4 (3.2 – 4.3)	4.2 (3.8 – 4.4)	5.2 (4.8 – 6.5)	6.1 (4.4 – 7.0)	5.4 (4.5 – 7.2)

EE (kcal / day)	Fasting	1377 (1275 – 1450)	1167 (1088 - 1201)	1169 (1046 - 1288)	1603 (1341 – 1823)	1523 (1309 – 1732)	1468 (1358 - 1629)
	Mean	1531 (1382 - 1580)	1429 (1253 - 1681)	1387 (1260 - 1525)	1745 (1494 - 1941)	1752 (1539 - 1926)	1728 (1508 - 1799)
RQ	Fasting	0.91 (0.84 – 0.99)	0.95 (0.91 – 1.07)	1.10 (1.02 – 1.18)	0.96 (0.86 – 1.01)	0.90 (0.84 – 0.98)	0.93 (0.83 – 1.09)
	Mean	0.87 (0.85 – 0.92)	0.89 (0.87 – 0.94)	0.97 (0.92 – 0.99)	0.89 (0.87 – 0.91)	0.88 (0.86 – 0.90)	0.87 (0.86 – 0.95)
Glucose Sensitivity (pmol/min/m ² /mmol)		87.6 (68.3 – 101.1)	76.7 (64.4 – 92.8)	97.2 (68.7 – 123.2)	91.4 (62.3 – 101.1)	73.4 (62.1 – 92.1)	79.2 (59.7 – 129.8)

Rate Sensitivity (pmol/m ² /mmol)		970.6 (575.0 – 1425.7)	650.3 (438.3 – 982.6)	644.6 (343.3 – 1195.9)	789.0 (303.8 – 964.0)	481.5 (254.9 – 697.8)	479.3 (330.4 – 768.2)
Potentiation Factor Ratio (PFR) (100-120) :(0 – 20) mins		1.04 (0.84 – 1.21)	1.26 (1.15 – 1.42)	1.11 (0.78 – 1.55)	1.21 (0.82 – 2.12)	1.11 (0.98 – 1.62)	1.28 (1.05 – 1.97)
ISR at known glucose (4.7mmol/l) (pmol/min/m ²)		83.4 (51.5 – 153.4)	103.7 (63.1 – 129.7)	66.5 (57.0 – 78.4)	61.5 (52.6 – 80.2)	68.9 (54.9 – 83.6)	78.0 (65.0 – 101.7)
ISR (pmol/min/m ²) (nmol/m ²)	Fasting	96.0 (53.8 – 110.6)	73.5 (56.7 – 121.0)	63.7 (59.7 – 90.5)	48.0 (38.4 – 64.2)	52.4 (41.6 – 58.4)	55.7 (47.0 – 74.7)
	Mean	87.8 (63.6 – 125.3)	101.0 (66.6 – 141.8)	78.3 (49.7 – 111.9)	47.0 (40.4 – 56.3)	52.4 (45.3 – 62.4)	43.0 (36.4 – 56.6)

BMI (kg/m ²)	23.3 (18.9 – 27.1)	23.0 (18.6 – 26.7)	23.0 (20.3 – 26.7)	23.3 (22.1 – 26.7)	23.2 (21.2 – 26.0)	23.1 (22.5 – 26.2)
-----------------------------	-----------------------	-----------------------	-----------------------	-----------------------	-------------------------------------	-----------------------

Data shown are median (IQR).

GREEN – different from other group at time-point ($p < 0.05$),

RED – treatment difference from baseline within group, as per paired non-parametric testing.

Green box with **red** text – difference from baseline and between groups.

Appendix 8: Assays

A list of the assays used throughout the course of this thesis:

Lactate

Fluoride oxalate samples were analysed for plasma lactate using a lactate oxidase method on a Siemens ADVIA 2400 Chemistry System (analysed by Biochemical Medicine, Department of Blood Sciences, NHS Tayside).

Glucose

Glucose was measured at the University of Surrey by enzymatic determination, using the ABX Pentra Glucose PAP CP reagent, and the ABX Diagnostics COBAS Mira Plus.

NEFA

NEFA were measured at the University of Surrey by the Acyl-CoA Synthase / Acyl CoA Oxidase (ACS-ACOD) method, on the Roche COBAS Mira Plus (Basel, Switzerland).

Glucagon

Glucagon was measured by the Immunoassay Biomarker Core Laboratory at the University of Dundee, using a radioimmunoassay (RIA, GL-32K) from Millipore (UK) on a Wallac Gamma Counter, which utilises ¹²⁵I-labelled Glucagon and a Glucagon antiserum to determine the level of pancreatic glucagon by the double antibody / PEG (polyethylene glycol) technique.

Total GLP-1

Total GLP-1 was measured by the Immunoassay Biomarker Core Laboratory at the University of Dundee, using an electrochemiluminescence immunoassay

(K150JVC-1) from Meso Scale Discovery (Maryland, USA) on a Quickplex SQ120 reader.

Active GLP-1

Active GLP-1 was also measured by the Immunoassay Biomarker Core Laboratory at the University of Dundee, using an electrochemiluminescence immunoassay (K150JWC-1) from Meso Scale Discovery (Maryland, USA) on a Quickplex SQ120 reader.

Leptin

Leptin was measured by the Immunoassay Biomarker Core Laboratory at the University of Dundee, using an enzyme-linked immunoassay (ELISA, DLP00) from R&D Systems (Minneapolis, USA), on a Thermo Varioskan multimodal plate reader.

Adiponectin

Adiponectin was measured by the Immunoassay Biomarker Core Laboratory at the University of Dundee, using an enzyme-linked immunoassay (ELISA, DRP300) from R&D Systems (Minneapolis, USA), on a Thermo Varioskan multimodal plate reader.

Insulin

Insulin was measured by the Immunoassay Biomarker Core Laboratory at the University of Dundee, using an ELISA (80-INSHU-E01.1) from Alpco (Salem, USA), on a Thermo Varioskan multimodal plate reader.

C-peptide

C-peptide was measured by the Immunoassay Biomarker Core Laboratory at the University of Dundee, using an ELISA (80-CPTHU-E01.1) from Alpco (Salem, USA), on a Thermo Varioskan multimodal plate reader.

Paracetamol

Paracetamol was measured by spectrophotometry in the Department of Blood Sciences in NHS Tayside, using an enzymatic bichromatic endpoint technique on a Siemens Dimension VISTA 1500.

U+E and LFTs

U+E and LFTs were measured by the Department of Blood Sciences in NHS Tayside, using a Siemens ADVIA 2400 Chemistry System.

References

1. IDF Diabetes Atlas Brussels, Belgium: International Diabetes Federation; 2017 [8th Edition]:[Available from: <http://www.diabetesatlas.org>].
2. NICE guideline [NG28]: NICE; 2015 [updated May 2017. Available from: <https://www.nice.org.uk/guidance/ng28/chapter/1-Recommendations#drug-treatment-2>].
3. Inzucchi SE, Bergenstal RM, Buse JB, Diamant M, Ferrannini E, Nauck M, et al. Management of hyperglycaemia in type 2 diabetes, 2015: a patient-centred approach. Update to a Position Statement of the American Diabetes Association and the European Association for the Study of Diabetes. *Diabetologia*. 2015;58(3):429-42.
4. Ibrahim M, Tuomilehto J, Aschner P, Beseler L, Cahn A, Eckel RH, et al. Global status of diabetes prevention and prospects for action: A consensus statement. *Diabetes/metabolism research and reviews*. 2018:e3021.
5. Khetan AK, Rajagopalan S. Prediabetes. *The Canadian journal of cardiology*. 2018;34(5):615-23.
6. Priya G. Management of prediabetes. *JPMA The Journal of the Pakistan Medical Association*. 2018;68(4):669-71.
7. Bailey CJ, Day C. Traditional Plant Medicines as Treatments for Diabetes. *Diabetes Care*. 1989;12(8):553.
8. Bailey CJ, Campbell IW, Chan JCN, Davidson JA, Howlett HCS, Ritz P. *Metformin - The Gold Standard: A Scientific Handbook*. Wiley; 2008. p. 4-8.
9. Sterne J. Du nouveau dans les antidiabetiques. La NN dimethylamine guanyl guanide (NNDG). *Maroc méd*. 1957;36:1295-6.
10. Mc KJ, Kuwayti K, Rado PP. Clinical experience with DBI (phenformin) in the management of diabetes. *Canadian Medical Association journal*. 1959;80(10):773-8.
11. Bloech J, Lenhardt A. [Diabetes therapy with butylbiguanide Silubin. Clinical results in 129 treated patients]. *Die Medizinische Welt*. 1963;3:161-7.
12. Nattrass M, Alberti KG. Biguanides. *Diabetologia*. 1978;14(2):71-4.
13. Bailey CJ. Metformin: historical overview. *Diabetologia*. 2017;60(9):1566-76.
14. Effect of intensive blood-glucose control with metformin on complications in overweight patients with type 2 diabetes (UKPDS 34). UK Prospective Diabetes Study (UKPDS) Group. *Lancet (London, England)*. 1998;352(9131):854-65.
15. Bailey CJ, Campbell IW, Chan JCN, Davidson JA, Howlett HCS, Ritz P. *Metformin - The Gold Standard: A Scientific Handbook*. Wiley; 2008. p. 3-22.

16. Graham GG, Punt J, Arora M, Day RO, Doogue MP, Duong J, et al. Clinical Pharmacokinetics of Metformin. *Clinical pharmacokinetics*. 2011;50(2):81-98.
17. Tucker GT, Casey C, Phillips PJ, Connor H, Ward JD, Woods HF. Metformin kinetics in healthy subjects and in patients with diabetes mellitus. *British journal of clinical pharmacology*. 1981;12(2):235-46.
18. Marathe PH, Wen Y, Norton J, Greene DS, Barbhuiya RH, Wilding IR. Effect of altered gastric emptying and gastrointestinal motility on metformin absorption. *British journal of clinical pharmacology*. 2002;50(4):325-32.
19. Wilcock C, Bailey CJ. Accumulation of metformin by tissues of the normal and diabetic mouse. *Xenobiotica*. 1994;24(1):49-57.
20. Rena G, Hardie DG, Pearson ER. The mechanisms of action of metformin. *Diabetologia*. 2017;60(9):1577-85.
21. Bailey CJ, Wilcock C, Scarpello JH. Metformin and the intestine. *Diabetologia*. 2008;51(8):1552-3.
22. Proctor WR, Bourdet DL, Thakker DR. Mechanisms underlying saturable intestinal absorption of metformin. *Drug Metab Dispos*. 2008;36(8):1650-8.
23. Han TK, Proctor WR, Costales CL, Cai H, Everett RS, Thakker DR. Four cation-selective transporters contribute to apical uptake and accumulation of metformin in Caco-2 cell monolayers. *J Pharmacol Exp Ther*. 2015;352(3):519-28.
24. Koehler MR, Wissinger B, Gorboulev V, Koepsell H, Schmid M. The two human organic cation transporter genes SLC22A1 and SLC22A2 are located on chromosome 6q26. *Cytogenetic and Genome Research*. 1997;79(3-4):198-200.
25. Koepsell H, Endou H. The SLC22 drug transporter family. *Pflügers Archiv*. 2004;447(5):666-76.
26. Müller J, Lips KS, Metzner L, Neubert RHH, Koepsell H, Brandsch M. Drug specificity and intestinal membrane localization of human organic cation transporters (OCT). *Biochemical Pharmacology*. 2005;70(12):1851-60.
27. Han T, Everett RS, Proctor WR, Ng CM, Costales CL, Brouwer KLR, et al. Organic Cation Transporter 1 (OCT1/mOct1) Is Localized in the Apical Membrane of Caco-2 Cell Monolayers and Enterocytes. *Molecular Pharmacology*. 2013;84(2):182.
28. Lee N, Duan H, Hebert MF, Liang CJ, Rice KM, Wang J. Taste of a pill: organic cation transporter-3 (OCT3) mediates metformin accumulation and secretion in salivary glands. *J Biol Chem*. 2014;289(39):27055-64.
29. Dujic T, Zhou K, Donnelly LA, Tavendale R, Palmer CN, Pearson ER. Association of Organic Cation Transporter 1 With Intolerance to Metformin in Type 2 Diabetes: A GoDARTS Study. *Diabetes*. 2015;64(5):1786-93.

30. Stage TB, Brøsen K, Christensen MMH. A Comprehensive Review of Drug–Drug Interactions with Metformin. *Clinical pharmacokinetics*. 2015;54(8):811-24.
31. Christensen MMH, Hojlund K, Hother-Nielsen O, Stage TB, Damkier P, Beck-Nielsen H, et al. Steady-state pharmacokinetics of metformin is independent of the OCT1 genotype in healthy volunteers. *Eur J Clin Pharmacol*. 2015;71(6):691-7.
32. Christensen MM, Brasch-Andersen C, Green H, Nielsen F, Damkier P, Beck-Nielsen H, et al. The pharmacogenetics of metformin and its impact on plasma metformin steady-state levels and glycosylated hemoglobin A1c. *Pharmacogenet Genomics*. 2011;21(12):837-50.
33. Christensen MM, Brasch-Andersen C, Green H, Nielsen F, Damkier P, Beck-Nielsen H, et al. The pharmacogenetics of metformin and its impact on plasma metformin steady-state levels and glycosylated hemoglobin A1c: Corrigendum. *Pharmacogenetics and Genomics*. 2015;25(1).
34. Shu Y, Brown C, Castro RA, Shi RJ, Lin ET, Owen RP, et al. Effect of genetic variation in the organic cation transporter 1, OCT1, on metformin pharmacokinetics. *Clin Pharmacol Ther*. 2008;83(2):273-80.
35. Engel K, Wang J. Interaction of organic cations with a newly identified plasma membrane monoamine transporter. *Mol Pharmacol*. 2005;68(5):1397-407.
36. Engel K, Zhou M, Wang J. Identification and characterization of a novel monoamine transporter in the human brain. *J Biol Chem*. 2004;279(48):50042-9.
37. Zhou M, Xia L, Wang J. Metformin transport by a newly cloned proton-stimulated organic cation transporter (plasma membrane monoamine transporter) expressed in human intestine. *Drug Metab Dispos*. 2007;35(10):1956-62.
38. Murphy DL, Lerner A, Rudnick G, Lesch KP. Serotonin transporter: gene, genetic disorders, and pharmacogenetics. *Molecular interventions*. 2004;4(2):109-23.
39. Murphy DL, Moya PR. Human serotonin transporter gene (SLC6A4) variants: their contributions to understanding pharmacogenomic and other functional GxG and GxE differences in health and disease. *Current opinion in pharmacology*. 2011;11(1):3-10.
40. Mohammad-Zadeh LF, Moses L, Gwaltney-Brant SM. Serotonin: a review. *Journal of veterinary pharmacology and therapeutics*. 2008;31(3):187-99.
41. Zhang ZF, Duan ZJ, Wang LX, Yang D, Zhao G, Zhang L. The serotonin transporter gene polymorphism (5-HTTLPR) and irritable bowel syndrome: a meta-analysis of 25 studies. *BMC gastroenterology*. 2014;14:23.
42. Gill RK, Pant N, Saksena S, Singla A, Nazir TM, Vohwinkel L, et al. Function, expression, and characterization of the serotonin transporter in the

native human intestine. *American journal of physiology Gastrointestinal and liver physiology*. 2008;294(1):G254-62.

43. Heils A, Teufel A, Petri S, Stober G, Riederer P, Bengel D, et al. Allelic variation of human serotonin transporter gene expression. *Journal of neurochemistry*. 1996;66(6):2621-4.

44. Moya PR, Wendland JR, Rubenstein LM, Timpano KR, Heiman GA, Tischfield JA, et al. Common and rare alleles of the serotonin transporter gene, SLC6A4, associated with Tourette's disorder. *Movement disorders : official journal of the Movement Disorder Society*. 2013;28(9):1263-70.

45. Murphy DL, Maile MS, Vogt NM. 5HTTLPR: White Knight or Dark Blight? *ACS chemical neuroscience*. 2013;4(1):13-5.

46. Nakamura M, Ueno S, Sano A, Tanabe H. The human serotonin transporter gene linked polymorphism (5-HTTLPR) shows ten novel allelic variants. *Molecular psychiatry*. 2000;5(1):32-8.

47. Dujic T, Zhou K, Tavendale R, Palmer CN, Pearson ER. Effect of Serotonin Transporter 5-HTTLPR Polymorphism on Gastrointestinal Intolerance to Metformin: A GoDARTS Study. *Diabetes Care*. 2016;39(11):1896-901.

48. Kajiwara M, Terada T, Ogasawara K, Iwano J, Katsura T, Fukatsu A, et al. Identification of multidrug and toxin extrusion (MATE1 and MATE2-K) variants with complete loss of transport activity. *Journal Of Human Genetics*. 2009;54:40.

49. Staud F, Cervený L, Ahmadimoghaddam D, Ceckova M. Multidrug and toxin extrusion proteins (MATE/SLC47); role in pharmacokinetics. *The international journal of biochemistry & cell biology*. 2013;45(9):2007-11.

50. Tanihara Y, Masuda S, Sato T, Katsura T, Ogawa O, Inui K. Substrate specificity of MATE1 and MATE2-K, human multidrug and toxin extrusions/H(+)-organic cation antiporters. *Biochem Pharmacol*. 2007;74(2):359-71.

51. Dujic T, Zhou K, Yee SW, van Leeuwen N, de Keyser CE, Javorsky M, et al. Variants in Pharmacokinetic Transporters and Glycemic Response to Metformin: A Metgen Meta-Analysis. *Clin Pharmacol Ther*. 2017;101(6):763-72.

52. Li Q, Yang H, Guo D, Zhang T, Polli JE, Zhou H, et al. Effect of Ondansetron on Metformin Pharmacokinetics and Response in Healthy Subjects. *Drug Metab Dispos*. 2016;44(4):489-94.

53. Beckmann R. Resorption, Verteilung im Organismus und Ausscheidung von Metformin. *Diabetologia*. 1969;5(5):318-24.

54. Grun B, Kiessling MK, Burhenne J, Riedel KD, Weiss J, Rauch G, et al. Trimethoprim-metformin interaction and its genetic modulation by OCT2 and MATE1 transporters. *British journal of clinical pharmacology*. 2013;76(5):787-96.

55. Hacker K, Maas R, Kornhuber J, Fromm MF, Zolk O. Substrate-Dependent Inhibition of the Human Organic Cation Transporter OCT2: A Comparison of Metformin with Experimental Substrates. *PLoS One*. 2015;10(9):e0136451.

56. Koepsell H. Substrate recognition and translocation by polyspecific organic cation transporters. *Biological chemistry*. 2011;392(1-2):95-101.
57. Gong L, Goswami S, Giacomini KM, Altman RB, Klein TE. Metformin pathways: pharmacokinetics and pharmacodynamics. *Pharmacogenet Genomics*. 2012;22(11):820-7.
58. Stocker SL, Morrissey KM, Yee SW, Castro RA, Xu L, Dahlin A, et al. The effect of novel promoter variants in MATE1 and MATE2 on the pharmacokinetics and pharmacodynamics of metformin. *Clin Pharmacol Ther*. 2013;93(2):186-94.
59. Xia L, Zhou M, Kalhorn TF, Ho HT, Wang J. Podocyte-specific expression of organic cation transporter PMAT: implication in puromycin aminonucleoside nephrotoxicity. *American journal of physiology Renal physiology*. 2009;296(6):F1307-13.
60. Duong JK, Kumar SS, Kirkpatrick CM, Greenup LC, Arora M, Lee TC, et al. Population pharmacokinetics of metformin in healthy subjects and patients with type 2 diabetes mellitus: simulation of doses according to renal function. *Clinical pharmacokinetics*. 2013;52(5):373-84.
61. Xia L, Engel K, Zhou M, Wang J. Membrane localization and pH-dependent transport of a newly cloned organic cation transporter (PMAT) in kidney cells. *American journal of physiology Renal physiology*. 2007;292(2):F682-90.
62. Tzvetkov MV, Vormfelde SV, Balen D, Meineke I, Schmidt T, Sehart D, et al. The effects of genetic polymorphisms in the organic cation transporters OCT1, OCT2, and OCT3 on the renal clearance of metformin. *Clin Pharmacol Ther*. 2009;86(3):299-306.
63. The Diabetes Prevention Program (DPP): description of lifestyle intervention. *Diabetes Care*. 2002;25(12):2165-71.
64. Johnson JA, Majumdar SR, Simpson SH, Toth EL. Decreased Mortality Associated With the Use of Metformin Compared With Sulfonylurea Monotherapy in Type 2 Diabetes. *Diabetes Care*. 2002;25(12):2244.
65. Kao J, Tobis J, McClelland RL, Heaton MR, Davis BR, Holmes DR, et al. Relation of metformin treatment to clinical events in diabetic patients undergoing percutaneous intervention. *The American Journal of Cardiology*. 2004;93(11):1347-50.
66. Knowler WC, Fowler SE, Hamman RF, Christophi CA, Hoffman HJ, Brenneman AT, et al. 10-year follow-up of diabetes incidence and weight loss in the Diabetes Prevention Program Outcomes Study. *Lancet (London, England)*. 2009;374(9702):1677-86.
67. Kooy A, de Jager J, Lehert P, et al. Long-term effects of metformin on metabolism and microvascular and macrovascular disease in patients with type 2 diabetes mellitus. *Archives of Internal Medicine*. 2009;169(6):616-25.

68. Foretz M, Guigas B, Bertrand L, Pollak M, Viollet B. Metformin: from mechanisms of action to therapies. *Cell Metab.* 2014;20(6):953-66.
69. Hur KY, Lee M-S. New mechanisms of metformin action: Focusing on mitochondria and the gut. *Journal of Diabetes Investigation.* 2015;6(6):600-9.
70. Jackson RA, Hawa MI, Jaspan JB, Sim BM, Disilvio L, Featherbe D, et al. Mechanism of metformin action in non-insulin-dependent diabetes. *Diabetes.* 1987;36(5):632-40.
71. Minamii T, Nogami M, Ogawa W. Mechanisms of metformin action: In and out of the gut. *J Diabetes Investig.* 2018;9(4):701-3.
72. Rena G, Pearson ER, Sakamoto K. Molecular mechanism of action of metformin: old or new insights? *Diabetologia.* 2013;56(9):1898-906.
73. Sliwinska A, Drzewoski J. Molecular action of metformin in hepatocytes: an updated insight. *Current diabetes reviews.* 2015;11(3):175-81.
74. Viollet B, Foretz M. Revisiting the mechanisms of metformin action in the liver. *Annales d'endocrinologie.* 2013;74(2):123-9.
75. Viollet B, Guigas B, Sanz Garcia N, Leclerc J, Foretz M, Andreelli F. Cellular and molecular mechanisms of metformin: an overview. *Clinical Science (London, England : 1979).* 2012;122(6):253-70.
76. Wu T, Horowitz M, Rayner CK. New insights into the anti-diabetic actions of metformin: from the liver to the gut. *Expert review of gastroenterology & hepatology.* 2017;11(2):157-66.
77. McCreight LJ, Bailey CJ, Pearson ER. Metformin and the gastrointestinal tract. *Diabetologia.* 2016;59(3):426-35.
78. Owen MR, Doran E, Halestrap AP. Evidence that metformin exerts its anti-diabetic effects through inhibition of complex 1 of the mitochondrial respiratory chain. *The Biochemical journal.* 2000;348 Pt 3:607-14.
79. Jeon S-M. Regulation and function of AMPK in physiology and diseases. *Experimental & Molecular Medicine.* 2016;48(7):e245.
80. Hardie DG. AMPK--sensing energy while talking to other signaling pathways. *Cell Metab.* 2014;20(6):939-52.
81. Hardie DG. The AMP-activated protein kinase pathway--new players upstream and downstream. *Journal of cell science.* 2004;117(Pt 23):5479-87.
82. Madiraju AK, Erion DM, Rahimi Y, Zhang XM, Braddock DT, Albright RA, et al. Metformin suppresses gluconeogenesis by inhibiting mitochondrial glycerophosphate dehydrogenase. *Nature.* 2014;510(7506):542-6.
83. Baptiste CG, Battista M-C, Trottier A, Baillargeon J-P. Insulin and hyperandrogenism in women with polycystic ovary syndrome. *The Journal of steroid biochemistry and molecular biology.* 2010;122(1-3):42-52.

84. Hundal HS, Ramlal T, Reyes R, Leiter LA, Klip A. Cellular mechanism of metformin action involves glucose transporter translocation from an intracellular pool to the plasma membrane in L6 muscle cells. *Endocrinology*. 1992;131(3):1165-73.
85. Lee JO, Lee SK, Jung JH, Kim JH, You GY, Kim SJ, et al. Metformin induces Rab4 through AMPK and modulates GLUT4 translocation in skeletal muscle cells. *Journal of cellular physiology*. 2011;226(4):974-81.
86. Sarabia V, Lam L, Burdett E, Leiter LA, Klip A. Glucose transport in human skeletal muscle cells in culture. Stimulation by insulin and metformin. *J Clin Invest*. 1992;90(4):1386-95.
87. Lee JO, Lee SK, Kim JH, Kim N, You GY, Moon JW, et al. Metformin regulates glucose transporter 4 (GLUT4) translocation through AMP-activated protein kinase (AMPK)-mediated Cbl/CAP signaling in 3T3-L1 preadipocyte cells. *J Biol Chem*. 2012;287(53):44121-9.
88. Yamaguchi S, Katahira H, Ozawa S, Nakamichi Y, Tanaka T, Shimoyama T, et al. Activators of AMP-activated protein kinase enhance GLUT4 translocation and its glucose transport activity in 3T3-L1 adipocytes. *American journal of physiology Endocrinology and metabolism*. 2005;289(4):E643-9.
89. Vincent MF, Marangos PJ, Gruber HE, Van den Berghe G. Inhibition by AICA riboside of gluconeogenesis in isolated rat hepatocytes. *Diabetes*. 1991;40(10):1259-66.
90. Miller RA, Chu Q, Xie J, Foretz M, Viollet B, Birnbaum MJ. Biguanides suppress hepatic glucagon signalling by decreasing production of cyclic AMP. *Nature*. 2013;494(7436):256-60.
91. Hunter RW, Hughey CC, Lantier L, Sundelin EI, Peggie M, Zeqiraj E, et al. Metformin reduces liver glucose production by inhibition of fructose-1-6-bisphosphatase. *Nature Medicine*. 2018;24(9):1395-406.
92. Madiraju AK, Qiu Y, Perry RJ, Rahimi Y, Zhang X-M, Zhang D, et al. Metformin inhibits gluconeogenesis via a redox-dependent mechanism in vivo. *Nature medicine*. 2018;24(9):1384-94.
93. Morales DR, Morris AD. Metformin in cancer treatment and prevention. *Annual review of medicine*. 2015;66:17-29.
94. Rizos CV, Elisaf MS. Metformin and cancer. *European Journal of Pharmacology*. 2013;705(1):96-108.
95. Farmer RE, Ford D, Forbes HJ, Chaturvedi N, Kaplan R, Smeeth L, et al. Metformin and cancer in type 2 diabetes: a systematic review and comprehensive bias evaluation. *Int J Epidemiol*. 2017;46(2):728-44.
96. Li M, Li X, Zhang H, Lu Y. Molecular Mechanisms of Metformin for Diabetes and Cancer Treatment. *Frontiers in physiology*. 2018;9:1039.

97. Ben Sahra I, Le Marchand-Brustel Y, Tanti JF, Bost F. Metformin in cancer therapy: a new perspective for an old antidiabetic drug? *Molecular cancer therapeutics*. 2010;9(5):1092-9.
98. Mallik R, Chowdhury TA. Metformin in cancer. *Diabetes Res Clin Pract*. 2018.
99. Kobiela J, Dobrzycka M, Jedrusik P, Kobiela P, Spsychalski P, Sledzinski Z, et al. Metformin and Colorectal Cancer - A Systematic Review. *Experimental and clinical endocrinology & diabetes : official journal, German Society of Endocrinology [and] German Diabetes Association*. 2018.
100. Ben Sahra I, Laurent K, Loubat A, Giorgetti-Peraldi S, Colosetti P, Auberger P, et al. The antidiabetic drug metformin exerts an antitumoral effect in vitro and in vivo through a decrease of cyclin D1 level. *Oncogene*. 2008;27(25):3576-86.
101. Podhorecka M, Ibanez B, Dmoszynska A. Metformin - its potential anti-cancer and anti-aging effects. *Postepy higieny i medycyny doswiadczonej (Online)*. 2017;71(0):170-5.
102. Anisimov VN. Metformin: Do we finally have an anti-aging drug? *Cell Cycle*. 2013;12(22):3483-9.
103. Algire C, Moiseeva O, Deschenes-Simard X, Amrein L, Petruccelli L, Birman E, et al. Metformin reduces endogenous reactive oxygen species and associated DNA damage. *Cancer prevention research (Philadelphia, Pa)*. 2012;5(4):536-43.
104. Saisho Y. Metformin and Inflammation: Its Potential Beyond Glucose-lowering Effect. *Endocrine, metabolic & immune disorders drug targets*. 2015;15(3):196-205.
105. Haffner S, Tempresa M, Crandall J, Fowler S, Goldberg R, Horton E, et al. Intensive lifestyle intervention or metformin on inflammation and coagulation in participants with impaired glucose tolerance. *Diabetes*. 2005;54(5):1566-72.
106. Krysiak R, Okopien B. The effect of metformin on monocyte secretory function in simvastatin-treated patients with impaired fasting glucose. *Metabolism*. 2013;62(1):39-43.
107. Krysiak R, Okopien B. Lymphocyte-suppressing and systemic anti-inflammatory effects of high-dose metformin in simvastatin-treated patients with impaired fasting glucose. *Atherosclerosis*. 2012;225(2):403-7.
108. Sobel BE, Hardison RM, Genuth S, Brooks MM, McBane RD, 3rd, Schneider DJ, et al. Profibrinolytic, antithrombotic, and antiinflammatory effects of an insulin-sensitizing strategy in patients in the Bypass Angioplasty Revascularization Investigation 2 Diabetes (BARI 2D) trial. *Circulation*. 2011;124(6):695-703.
109. Misso ML, Teede HJ. Metformin in women with PCOS, cons. *Endocrine*. 2015;48(2):428-33.

110. De Leo V, la Marca A, Petraglia F. Insulin-lowering agents in the management of polycystic ovary syndrome. *Endocrine reviews*. 2003;24(5):633-67.
111. Pasquali R. Metformin in women with PCOS, pros. *Endocrine*. 2015;48(2):422-6.
112. Wang YW, He SJ, Feng X, Cheng J, Luo YT, Tian L, et al. Metformin: a review of its potential indications. *Drug design, development and therapy*. 2017;11:2421-9.
113. Buse JB, DeFronzo RA, Rosenstock J, Kim T, Burns C, Skare S, et al. The Primary Glucose-Lowering Effect of Metformin Resides in the Gut, Not the Circulation: Results From Short-term Pharmacokinetic and 12-Week Dose-Ranging Studies. *Diabetes Care*. 2016;39(2):198-205.
114. Gambhir SS. Molecular imaging of cancer with positron emission tomography. *Nature reviews Cancer*. 2002;2(9):683-93.
115. Oh JR, Song HC, Chong A, Ha JM, Jeong SY, Min JJ, et al. Impact of medication discontinuation on increased intestinal FDG accumulation in diabetic patients treated with metformin. *AJR Am J Roentgenol*. 2010;195(6):1404-10.
116. Capitano S, Marini C, Sambuceti G, Morbelli S. Metformin and cancer: Technical and clinical implications for FDG-PET imaging. *World journal of radiology*. 2015;7(3):57-60.
117. Gontier E, Fourme E, Wartski M, Blondet C, Bonardel G, Le Stanc E, et al. High and typical 18F-FDG bowel uptake in patients treated with metformin. *Eur J Nucl Med Mol Imaging*. 2008;35(1):95-9.
118. Röder PV, Geillinger KE, Zietek TS, Thorens B, Koepsell H, Daniel H. The Role of SGLT1 and GLUT2 in Intestinal Glucose Transport and Sensing. *PLOS ONE*. 2014;9(2):e89977.
119. Gorboulev V, Schurmann A, Vallon V, Kipp H, Jaschke A, Klessen D, et al. Na(+)-D-glucose cotransporter SGLT1 is pivotal for intestinal glucose absorption and glucose-dependent incretin secretion. *Diabetes*. 2012;61(1):187-96.
120. Sakar Y, Meddah B, Faouzi MA, Cherrah Y, Bado A, Ducroc R. Metformin-induced regulation of the intestinal D-glucose transporters. *Journal of physiology and pharmacology : an official journal of the Polish Physiological Society*. 2010;61(3):301-7.
121. Walker J, Jijon HB, Diaz H, Salehi P, Churchill T, Madsen KL. 5-aminoimidazole-4-carboxamide riboside (AICAR) enhances GLUT2-dependent jejunal glucose transport: a possible role for AMPK. *The Biochemical journal*. 2005;385(Pt 2):485-91.
122. Naftalin RJ. Does apical membrane GLUT2 have a role in intestinal glucose uptake? *F1000Research*. 2014;3:304.
123. Ait-Omar A, Monteiro-Sepulveda M, Poitou C, Le Gall M, Cotillard A, Gilet J, et al. GLUT2 accumulation in enterocyte apical and intracellular membranes: a

study in morbidly obese human subjects and ob/ob and high fat-fed mice. *Diabetes*. 2011;60(10):2598-607.

124. Davis TM, Jackson D, Davis WA, Bruce DG, Chubb P. The relationship between metformin therapy and the fasting plasma lactate in type 2 diabetes: The Fremantle Diabetes Study. *British journal of clinical pharmacology*. 2001;52(2):137-44.

125. Bailey CJ, Wilcock C, Day C. Effect of metformin on glucose metabolism in the splanchnic bed. *British journal of pharmacology*. 1992;105(4):1009-13.

126. Penicaud L, Hitier Y, Ferre P, Girard J. Hypoglycaemic effect of metformin in genetically obese (fa/fa) rats results from an increased utilization of blood glucose by intestine. *The Biochemical journal*. 1989;262(3):881-5.

127. Bailey CJ, Mynett KJ, Page T. Importance of the intestine as a site of metformin-stimulated glucose utilization. *British journal of pharmacology*. 1994;112(2):671-5.

128. Lalau JD, Lacroix C, Compagnon P, de Cagny B, Rigaud JP, Bleichner G, et al. Role of metformin accumulation in metformin-associated lactic acidosis. *Diabetes Care*. 1995;18(6):779-84.

129. Misbin RI, Green L, Stadel BV, Gueriguian JL, Gubbi A, Fleming GA. Lactic acidosis in patients with diabetes treated with metformin. *The New England journal of medicine*. 1998;338(4):265-6.

130. Mannucci E, Ognibene A, Cremasco F, Bardini G, Mencucci A, Pierazzuoli E, et al. Effect of metformin on glucagon-like peptide 1 (GLP-1) and leptin levels in obese nondiabetic subjects. *Diabetes Care*. 2001;24(3):489-94.

131. Green BD, Irwin N, Duffy NA, Gault VA, O'Harte F P, Flatt PR. Inhibition of dipeptidyl peptidase-IV activity by metformin enhances the antidiabetic effects of glucagon-like peptide-1. *Eur J Pharmacol*. 2006;547(1-3):192-9.

132. Lindsay JR, Duffy NA, McKillop AM, Ardill J, O'Harte FP, Flatt PR, et al. Inhibition of dipeptidyl peptidase IV activity by oral metformin in Type 2 diabetes. *Diabet Med*. 2005;22(5):654-7.

133. Cuthbertson J, Patterson S, O'Harte FP, Bell PM. Investigation of the effect of oral metformin on dipeptidylpeptidase-4 (DPP-4) activity in Type 2 diabetes. *Diabet Med*. 2009;26(6):649-54.

134. Thondam SK, Cross A, Cuthbertson DJ, Wilding JP, Daousi C. Effects of chronic treatment with metformin on dipeptidyl peptidase-4 activity, glucagon-like peptide 1 and ghrelin in obese patients with Type 2 diabetes mellitus. *Diabet Med*. 2012;29(8):e205-10.

135. Vardarli I, Arndt E, Deacon CF, Holst JJ, Nauck MA. Effects of sitagliptin and metformin treatment on incretin hormone and insulin secretory responses to oral and "isoglycemic" intravenous glucose. *Diabetes*. 2014;63(2):663-74.

136. Wu T, Thazhath SS, Bound MJ, Jones KL, Horowitz M, Rayner CK. Mechanism of increase in plasma intact GLP-1 by metformin in type 2 diabetes:

stimulation of GLP-1 secretion or reduction in plasma DPP-4 activity? *Diabetes Res Clin Pract.* 2014;106(1):e3-6.

137. Fadini GP, Albiero M, Menegazzo L, de Kreutzenberg SV, Avogaro A. The increased dipeptidyl peptidase-4 activity is not counteracted by optimized glucose control in type 2 diabetes, but is lower in metformin-treated patients. *Diabetes Obes Metab.* 2012;14(6):518-22.

138. Hinke SA, Kuhn-Wache K, Hoffmann T, Pederson RA, McIntosh CH, Demuth HU. Metformin effects on dipeptidylpeptidase IV degradation of glucagon-like peptide-1. *Biochem Biophys Res Commun.* 2002;291(5):1302-8.

139. Yasuda N, Inoue T, Nagakura T, Yamazaki K, Kira K, Saeki T, et al. Enhanced secretion of glucagon-like peptide 1 by biguanide compounds. *Biochem Biophys Res Commun.* 2002;298(5):779-84.

140. Mulherin AJ, Oh AH, Kim H, Grieco A, Lauffer LM, Brubaker PL. Mechanisms underlying metformin-induced secretion of glucagon-like peptide-1 from the intestinal L cell. *Endocrinology.* 2011;152(12):4610-9.

141. Migoya EM, Bergeron R, Miller JL, Snyder RN, Tanen M, Hilliard D, et al. Dipeptidyl peptidase-4 inhibitors administered in combination with metformin result in an additive increase in the plasma concentration of active GLP-1. *Clin Pharmacol Ther.* 2010;88(6):801-8.

142. Napolitano A, Miller S, Nicholls AW, Baker D, Van Horn S, Thomas E, et al. Novel gut-based pharmacology of metformin in patients with type 2 diabetes mellitus. *PLoS One.* 2014;9(7):e100778.

143. Kim MH, Jee JH, Park S, Lee MS, Kim KW, Lee MK. Metformin enhances glucagon-like peptide 1 via cooperation between insulin and Wnt signaling. *J Endocrinol.* 2014;220(2):117-28.

144. Firneisz G, Varga T, Lengyel G, Feher J, Ghyczy D, Wichmann B, et al. Serum dipeptidyl peptidase-4 activity in insulin resistant patients with non-alcoholic fatty liver disease: a novel liver disease biomarker. *PLoS One.* 2010;5(8):e12226.

145. Yi F, Sun J, Lim GE, Fantus IG, Brubaker PL, Jin T. Cross talk between the insulin and Wnt signaling pathways: evidence from intestinal endocrine L cells. *Endocrinology.* 2008;149(5):2341-51.

146. Lien F, Berthier A, Bouchaert E, Gheeraert C, Alexandre J, Porez G, et al. Metformin interferes with bile acid homeostasis through AMPK-FXR crosstalk. *J Clin Invest.* 2014;124(3):1037-51.

147. Thomas C, Gioiello A, Noriega L, Strehle A, Oury J, Rizzo G, et al. TGR5-mediated bile acid sensing controls glucose homeostasis. *Cell Metab.* 2009;10(3):167-77.

148. Cubeddu LX, Bönisch H, Göthert M, Molderings G, Racké K, Ramadori G, et al. Effects of metformin on intestinal 5-hydroxytryptamine (5-HT) release and

on 5-HT₃ receptors. *Naunyn-Schmiedeberg's Archives of Pharmacology*. 2000;361(1):85-91.

149. Yee SW, Lin L, Merski M, Keiser MJ, Gupta A, Zhang Y, et al. Prediction and validation of enzyme and transporter off-targets for metformin. *Journal of pharmacokinetics and pharmacodynamics*. 2015;42(5):463-75.

150. Duca FA, Cote CD, Rasmussen BA, Zadeh-Tahmasebi M, Rutter GA, Filippi BM, et al. Metformin activates a duodenal Ampk-dependent pathway to lower hepatic glucose production in rats. *Nat Med*. 2015;21(5):506-11.

151. Stepensky D, Friedman M, Raz I, Hoffman A. Pharmacokinetic-pharmacodynamic analysis of the glucose-lowering effect of metformin in diabetic rats reveals first-pass pharmacodynamic effect. *Drug Metab Dispos*. 2002;30(8):861-8.

152. Scarpello JH, Hodgson E, Howlett HC. Effect of metformin on bile salt circulation and intestinal motility in type 2 diabetes mellitus. *Diabet Med*. 1998;15(8):651-6.

153. Carter D, Howlett HC, Wiernsperger NF, Bailey CJ. Differential effects of metformin on bile salt absorption from the jejunum and ileum. *Diabetes Obes Metab*. 2003;5(2):120-5.

154. Caspary WF, Zavada I, Reimold W, Deuticke U, Emrich D, Willms B. Alteration of bile acid metabolism and vitamin-B12-absorption in diabetics on biguanides. *Diabetologia*. 1977;13(3):187-93.

155. Carter D, Howlett HC, Wiernsperger NF, Bailey C. Effects of metformin on bile salt transport by monolayers of human intestinal Caco-2 cells. *Diabetes Obes Metab*. 2002;4(6):424-7.

156. Beysen C, Murphy EJ, Deines K, Chan M, Tsang E, Glass A, et al. Effect of bile acid sequestrants on glucose metabolism, hepatic de novo lipogenesis, and cholesterol and bile acid kinetics in type 2 diabetes: a randomised controlled study. *Diabetologia*. 2012;55(2):432-42.

157. Zema MJ. Colesevelam hydrochloride: evidence for its use in the treatment of hypercholesterolemia and type 2 diabetes mellitus with insights into mechanism of action. *Core evidence*. 2012;7:61-75.

158. Qin J, Li Y, Cai Z, Li S, Zhu J, Zhang F, et al. A metagenome-wide association study of gut microbiota in type 2 diabetes. *Nature*. 2012;490(7418):55-60.

159. Karlsson FH, Tremaroli V, Nookaew I, Bergstrom G, Behre CJ, Fagerberg B, et al. Gut metagenome in European women with normal, impaired and diabetic glucose control. *Nature*. 2013;498(7452):99-103.

160. Hur KY, Lee MS. Gut Microbiota and Metabolic Disorders. *Diabetes Metab J*. 2015;39(3):198-203.

161. Tilg H, Moschen AR. Microbiota and diabetes: an evolving relationship. *Gut*. 2014;63(9):1513-21.

162. Everard A, Belzer C, Geurts L, Ouwerkerk JP, Druart C, Bindels LB, et al. Cross-talk between *Akkermansia muciniphila* and intestinal epithelium controls diet-induced obesity. *Proc Natl Acad Sci U S A*. 2013;110(22):9066-71.
163. Zhang X, Shen D, Fang Z, Jie Z, Qiu X, Zhang C, et al. Human gut microbiota changes reveal the progression of glucose intolerance. *PLoS One*. 2013;8(8):e71108.
164. Forslund K, Hildebrand F, Nielsen T, Falony G, Le Chatelier E, Sunagawa S, et al. Disentangling type 2 diabetes and metformin treatment signatures in the human gut microbiota. *Nature*. 2015;528(7581):262-6.
165. Lee H, Ko G. Effect of metformin on metabolic improvement and gut microbiota. *Appl Environ Microbiol*. 2014;80(19):5935-43.
166. Shin NR, Lee JC, Lee HY, Kim MS, Whon TW, Lee MS, et al. An increase in the *Akkermansia* spp. population induced by metformin treatment improves glucose homeostasis in diet-induced obese mice. *Gut*. 2014;63(5):727-35.
167. Burton JH, Johnson M, Johnson J, Hsia DS, Greenway FL, Heiman ML. Addition of a Gastrointestinal Microbiome Modulator to Metformin Improves Metformin Tolerance and Fasting Glucose Levels. *J Diabetes Sci Technol*. 2015;9(4):808-14.
168. Florez JC. The pharmacogenetics of metformin. *Diabetologia*. 2017;60(9):1648-55.
169. Zhou K, Donnelly L, Yang J, Li M, Deshmukh H, Van Zuydam N, et al. Heritability of variation in glycaemic response to metformin: a genome-wide complex trait analysis. *The lancet Diabetes & endocrinology*. 2014;2(6):481-7.
170. Zhou K, Bellenguez C, Spencer CC, Bennett AJ, Coleman RL, Tavendale R, et al. Common variants near *ATM* are associated with glycemic response to metformin in type 2 diabetes. *Nature genetics*. 2011;43(2):117-20.
171. Pawlyk AC, Giacomini KM, McKeon C, Shuldiner AR, Florez JC. Metformin pharmacogenomics: current status and future directions. *Diabetes*. 2014;63(8):2590-9.
172. Zhou K, Yee SW, Seiser EL, van Leeuwen N, Tavendale R, Bennett AJ, et al. Variation in the glucose transporter gene *SLC2A2* is associated with glycemic response to metformin. *Nature genetics*. 2016;48(9):1055-9.
173. Zhou K, Donnelly LA, Kimber CH, Donnan PT, Doney AS, Leese G, et al. Reduced-function *SLC22A1* polymorphisms encoding organic cation transporter 1 and glycemic response to metformin: a GoDARTS study. *Diabetes*. 2009;58(6):1434-9.
174. Jablonski KA, McAteer JB, de Bakker PI, Franks PW, Pollin TI, Hanson RL, et al. Common variants in 40 genes assessed for diabetes incidence and response to metformin and lifestyle intervention in the diabetes prevention program. *Diabetes*. 2010;59(10):2672-81.
175. DIRECT-IMI. [Available from: <https://www.direct-diabetes.org/index.php>.

176. Hébert HL, Shepherd B, Milburn K, Veluchamy A, Meng W, Carr F, et al. Cohort Profile: Genetics of Diabetes Audit and Research in Tayside Scotland (GoDARTS). *International Journal of Epidemiology*. 2018;47(2):380-1j.
177. (SHARE) SHRR. 2018 [Available from: <https://www.registerforshare.org/index.php>].
178. (GoSHARE) GoS. 2018.
179. Smith BH, Campbell A, Linksted P, Fitzpatrick B, Jackson C, Kerr SM, et al. Cohort Profile: Generation Scotland: Scottish Family Health Study (GS:SFHS). The study, its participants and their potential for genetic research on health and illness. *Int J Epidemiol*. 2013;42(3):689-700.
180. Health Informatics Centre [Available from: <https://www.dundee.ac.uk/hic>].
181. Dhillon S GK. Basic Pharmacokinetics: Dandy Booksellers. Available from: <https://www.dandybooksellers.com/acatalog/test/acatalog/9780853695714.pdf>.
182. Gabrielsson J, Weiner D. Non-compartmental analysis. *Methods in molecular biology* (Clifton, NJ). 2012;929:377-89.
183. Nielsen F, Christensen MMH, Brøsen K. Quantitation of Metformin in Human Plasma and Urine by Hydrophilic Interaction Liquid Chromatography and Application to a Pharmacokinetic Study. *Therapeutic Drug Monitoring*. 2014;36(2):211-7.
184. Acharya C, Hooker AC, Turkyilmaz GY, Jonsson S, Karlsson MO. A diagnostic tool for population models using non-compartmental analysis: The ncappc package for R. *Comput Methods Programs Biomed*. 2016;127(Supplement C):83-93.
185. Budin-Ljosne I, Soye KJ, Tasse AM, Knoppers BM, Harris JR. Genotype-driven recruitment: a strategy whose time has come? *BMC Med Genomics*. 2013;6:19.
186. Beskow LM, Linney KN, Radtke RA, Heinzen EL, Goldstein DB. Ethical challenges in genotype-driven research recruitment. *Genome Research*. 2010;20(6):705-9.
187. Corbin LJ, Tan VY, Hughes DA, Wade KH, Paul DS, Tansey KE, et al. Formalising recall by genotype as an efficient approach to detailed phenotyping and causal inference. *Nature communications*. 2018;9(1):711.
188. Atabaki-Pasdar N, Ohlsson M, Shungin D, Kurbasic A, Ingelsson E, Pearson ER, et al. Statistical power considerations in genotype-based recall randomized controlled trials. *Scientific reports*. 2016;6:37307.
189. Beskow LM. Genotype-Driven Recruitment and the Disclosure of Individual Research Results. *The American journal of bioethics : AJOB*. 2017;17(4):64-5.

190. Beskow LM, Fullerton SM, Namey EE, Nelson DK, Davis AM, Wilfond BS. Recommendations for ethical approaches to genotype-driven research recruitment. *Human genetics*. 2012;131(9):1423-31.
191. Beskow LM, Namey EE, Cadigan RJ, Brazg T, Crouch J, Henderson GE, et al. Research participants' perspectives on genotype-driven research recruitment. *Journal of empirical research on human research ethics : JERHRE*. 2011;6(4):3-20.
192. Beskow LM, Namey EE, Miller PR, Nelson DK, Cooper A. IRB chairs' perspectives on genotype-driven research recruitment. *Irb*. 2012;34(3):1-10.
193. Michie M, Cadigan RJ, Henderson G, Beskow LM. Am I a control?: Genotype-driven research recruitment and self-understandings of study participants. *Genetics in medicine : official journal of the American College of Medical Genetics*. 2012;14(12):983-9.
194. Ossorio P, Mailick M. Genotype-Driven Recruitment Without Deception. *The American journal of bioethics : AJOB*. 2017;17(4):60-1.
195. Tabor HK, Brazg T, Crouch J, Namey EE, Fullerton SM, Beskow LM, et al. Parent perspectives on pediatric genetic research and implications for genotype-driven research recruitment. *Journal of empirical research on human research ethics : JERHRE*. 2011;6(4):41-52.
196. Taylor HA, Morales C, Wilfond BS. Genotype-Driven Recruitment in Population-Based Biomedical Research. *The American journal of bioethics : AJOB*. 2017;17(4):58-9.
197. Olson JE, Bielinski SJ, Ryu E, Winkler EM, Takahashi PY, Pathak J, et al. Biobanks and personalized medicine. *Clinical genetics*. 2014;86(1):50-5.
198. Charidemou E, Ashmore T, Griffin JL. The use of stable isotopes in the study of human pathophysiology. *The international journal of biochemistry & cell biology*. 2017;93:102-9.
199. Steele R. INFLUENCES OF GLUCOSE LOADING AND OF INJECTED INSULIN ON HEPATIC GLUCOSE OUTPUT*. *Annals of the New York Academy of Sciences*. 1959;82(2):420-30.
200. Steele R, Bishop JS, Dunn A, Altszuler N, Rathgeb I, de Bodo RC. Inhibition by insulin of hepatic glucose production in the normal dog. *American Journal of Physiology-Legacy Content*. 1965;208(2):301-6.
201. Ferrannini E, Muscelli E, Frascerra S, Baldi S, Mari A, Heise T, et al. Metabolic response to sodium-glucose cotransporter 2 inhibition in type 2 diabetic patients. *The Journal of clinical investigation*. 2014;124(2):499-508.
202. Polidori D, Sha S, Mudaliar S, Ciaraldi TP, Ghosh A, Vaccaro N, et al. Canagliflozin lowers postprandial glucose and insulin by delaying intestinal glucose absorption in addition to increasing urinary glucose excretion: results of a randomized, placebo-controlled study. *Diabetes Care*. 2013;36(8):2154-61.

203. Gastaldelli A, Casolaro A, Pettiti M, Nannipieri M, Ciociaro D, Frascerra S, et al. Effect of pioglitazone on the metabolic and hormonal response to a mixed meal in type II diabetes. *Clin Pharmacol Ther.* 2007;81(2):205-12.
204. Zierler K. A critique of compartmental analysis. *Annual review of biophysics and bioengineering.* 1981;10:531-62.
205. Radziuk J, Norwich KH, Vranic M. Experimental validation of measurements of glucose turnover in nonsteady state. *American Journal of Physiology-Endocrinology and Metabolism.* 1978;234(1):E84.
206. Mari A. Estimation of the rate of appearance in the non-steady state with a two-compartment model. *The American journal of physiology.* 1992;263(2 Pt 1):E400-15.
207. Katz J, Dunn A, Chenoweth M, Golden S. Determination of synthesis, recycling and body mass of glucose in rats and rabbits in vivo 3H-and 14C-labelled glucose. *The Biochemical journal.* 1974;142(1):171-83.
208. Mari A. Circulatory models of intact-body kinetics and their relationship with compartmental and non-compartmental analysis. *Journal of theoretical biology.* 1993;160(4):509-31.
209. Mari A, Stojanovska L, Proietto J, Thorburn AW. A circulatory model for calculating non-steady-state glucose fluxes. Validation and comparison with compartmental models. *Comput Methods Programs Biomed.* 2003;71(3):269-81.
210. Mari A. Calculation of organ and whole-body uptake and production with the impulse response approach. *Journal of theoretical biology.* 1995;174(3):341-53.
211. McGuinness OP, Mari A. Assessment of insulin action on glucose uptake and production during a euglycemic-hyperinsulinemic clamp in dog: a new kinetic analysis. *Metabolism.* 1997;46(10):1116-27.
212. Mari A, Valerio A. A circulatory model for the estimation of insulin sensitivity. *Control Engineering Practice.* 1997;5(12):1747-52.
213. McCreight L, Stage TB, Connelly P, Lonergan M, Nielsen F, Prehn C, et al. Pharmacokinetics of metformin in patients with gastrointestinal intolerance. *Diabetes Obes Metab.* 2018.
214. Shojaee-Moradie F, Jackson NC, Jones RH, Mallet AI, Hovorka R, Umpleby AM. Quantitative measurement of 3-O-methyl-D-glucose by gas chromatography-mass spectrometry as a measure of glucose transport in vivo. *Journal of mass spectrometry : JMS.* 1996;31(9):961-6.
215. Laine RA, Sweeley CC. Analysis of trimethylsilyl O-methyloximes of carbohydrates by combined gas-liquid chromatography-mass spectrometry. *Analytical biochemistry.* 1971;43(2):533-8.
216. Thorens B. GLUT2, glucose sensing and glucose homeostasis. *Diabetologia.* 2015;58(2):221-32.

217. McCulloch LJ, van de Bunt M, Braun M, Frayn KN, Clark A, Gloyn AL. GLUT2 (SLC2A2) is not the principal glucose transporter in human pancreatic beta cells: implications for understanding genetic association signals at this locus. *Molecular genetics and metabolism*. 2011;104(4):648-53.
218. Sternisha SM, Miller BG. Molecular and cellular regulation of human glucokinase. *Archives of biochemistry and biophysics*. 2019.
219. Koster JC, Permutt MA, Nichols CG. Diabetes and insulin secretion: the ATP-sensitive K⁺ channel (K ATP) connection. *Diabetes*. 2005;54(11):3065-72.
220. Wilcox G. Insulin and insulin resistance. *The Clinical biochemist Reviews*. 2005;26(2):19-39.
221. Natali A DPS, Mari A. Normal β -cell function. In: DeFronzo RA FE, Zimmet P, Alberti G, editor. *International Textbook of Diabetes Mellitus*. 1 John Wiley & Sons, Ltd.; 2015. p. 108 - 24.
222. Mari A, Ferrannini E. Beta-cell function assessment from modelling of oral tests: an effective approach. *Diabetes Obes Metab*. 2008;10 Suppl 4:77-87.
223. Mari A, Schmitz O, Gastaldelli A, Oestergaard T, Nyholm B, Ferrannini E. Meal and oral glucose tests for assessment of beta -cell function: modeling analysis in normal subjects. *American journal of physiology Endocrinology and metabolism*. 2002;283(6):E1159-66.
224. Mari A, Tura A, Gastaldelli A, Ferrannini E. Assessing insulin secretion by modeling in multiple-meal tests: role of potentiation. *Diabetes*. 2002;51 Suppl 1:S221-6.
225. Muscelli E, Mari A, Natali A, Astiarraga BD, Camastra S, Frascerra S, et al. Impact of incretin hormones on beta-cell function in subjects with normal or impaired glucose tolerance. *American journal of physiology Endocrinology and metabolism*. 2006;291(6):E1144-50.
226. Cauter EV, Mestrez F, Sturis J, Polonsky KS. Estimation of Insulin Secretion Rates from C-Peptide Levels: Comparison of Individual and Standard Kinetic Parameters for C-Peptide Clearance. *Diabetes*. 1992;41(3):368.
227. Chap Z, Ishida T, Chou J, Hartley CJ, Entman ML, Brandenburg D, et al. First-pass hepatic extraction and metabolic effects of insulin and insulin analogues. *The American journal of physiology*. 1987;252(2 Pt 1):E209-17.
228. Varghese RT, Dalla Man C, Laurenti MC, Piccinini F, Sharma A, Shah M, et al. Performance of individually measured vs population-based C-peptide kinetics to assess β -cell function in the presence and absence of acute insulin resistance. *Diabetes, Obesity and Metabolism*. 2018;20(3):549-55.
229. Kenny GP, Notley SR, Gagnon D. Direct calorimetry: a brief historical review of its use in the study of human metabolism and thermoregulation. *European journal of applied physiology*. 2017;117(9):1765-85.
230. Kaiyala KJ. What does indirect calorimetry really tell us? *Molecular Metabolism*. 2014;3(4):340-1.

231. Ferrannini E. The theoretical bases of indirect calorimetry: A review. *Metabolism*. 1988;37(3):287-301.
232. Weir JB. New methods for calculating metabolic rate with special reference to protein metabolism. 1949. *Nutrition*. 1990;6(3):213-21.
233. Mouzaki M, Schwartz SM, Mtaweh H, La Rotta G, Mah K, Herridge J, et al. Can Vco₂-Based Estimates of Resting Energy Expenditure Replace the Need for Indirect Calorimetry in Critically Ill Children? *Journal of Parenteral and Enteral Nutrition*. 2016;41(4):619-24.
234. Frayn KN. Calculation of substrate oxidation rates in vivo from gaseous exchange. *Journal of applied physiology: respiratory, environmental and exercise physiology*. 1983;55(2):628-34.
235. Haugen HA, Chan LN, Li F. Indirect calorimetry: a practical guide for clinicians. *Nutrition in clinical practice : official publication of the American Society for Parenteral and Enteral Nutrition*. 2007;22(4):377-88.
236. McClave SA, Snider HL. Invited Review: Use of Indirect Calorimetry in Clinical Nutrition. *Nutrition in Clinical Practice*. 1992;7(5):207-21.
237. Kennedy S, Ryan L, Fraser A, Clegg ME. Comparison of the GEM and the ECAL indirect calorimeters against the Deltatrac for measures of RMR and diet-induced thermogenesis. *Journal of nutritional science*. 2014;3:e52.
238. Takagi M, Uno H, Nishi R, Sugimoto M, Hasegawa S, Piao J, et al. ATM Regulates Adipocyte Differentiation and Contributes to Glucose Homeostasis. *Cell reports*. 2015.
239. Rothblum-Oviatt C, Wright J, Lefton-Greif MA, McGrath-Morrow SA, Crawford TO, Lederman HM. Ataxia telangiectasia: a review. *Orphanet journal of rare diseases*. 2016;11(1):159.
240. Preis SR, Massaro JM, Robins SJ, Hoffmann U, Vasan RS, Irlbeck T, et al. Abdominal subcutaneous and visceral adipose tissue and insulin resistance in the Framingham heart study. *Obesity (Silver Spring, Md)*. 2010;18(11):2191-8.
241. Fox CS, Massaro JM, Hoffmann U, Pou KM, Maurovich-Horvat P, Liu CY, et al. Abdominal visceral and subcutaneous adipose tissue compartments: association with metabolic risk factors in the Framingham Heart Study. *Circulation*. 2007;116(1):39-48.
242. Kaess BM, Pedley A, Massaro JM, Murabito J, Hoffmann U, Fox CS. The ratio of visceral to subcutaneous fat, a metric of body fat distribution, is a unique correlate of cardiometabolic risk. *Diabetologia*. 2012;55(10):2622-30.
243. Marzetti M, Brunton T, McCreight L, Pearson E, Docherty S, Gandy SJ. Quantitative MRI evaluation of whole abdomen adipose tissue volumes in healthy volunteers-validation of technique and implications for clinical studies. *The British journal of radiology*. 2018;91(1087):20180025.

244. Reeder SB, Cruite I, Hamilton G, Sirlin CB. Quantitative Assessment of Liver Fat with Magnetic Resonance Imaging and Spectroscopy. *Journal of magnetic resonance imaging : JMRI*. 2011;34(4):spcone-spcone.
245. Wood JC. Use of magnetic resonance imaging to monitor iron overload. *Hematology/oncology clinics of North America*. 2014;28(4):747-vii.
246. DeFronzo RA, Tobin JD, Andres R. Glucose clamp technique: a method for quantifying insulin secretion and resistance. *The American journal of physiology*. 1979;237(3):E214-23.
247. Selimoglu H, Duran C, Kiyici S, Guclu M, Ersoy C, Ozkaya G, et al. Comparison of composite whole body insulin sensitivity index derived from mixed meal test and oral glucose tolerance test in insulin resistant obese subjects. *Endocrine*. 2009;36(2):299-304.
248. Matthews DR, Hosker JP, Rudenski AS, Naylor BA, Treacher DF, Turner RC. Homeostasis model assessment: insulin resistance and beta-cell function from fasting plasma glucose and insulin concentrations in man. *Diabetologia*. 1985;28(7):412-9.
249. Singh B, Saxena A. Surrogate markers of insulin resistance: A review. *World journal of diabetes*. 2010;1(2):36-47.
250. Wallace TM, Levy JC, Matthews DR. Use and Abuse of HOMA Modeling. *Diabetes Care*. 2004;27(6):1487.
251. Matsuda M, DeFronzo RA. Insulin sensitivity indices obtained from oral glucose tolerance testing: comparison with the euglycemic insulin clamp. *Diabetes Care*. 1999;22(9):1462-70.
252. Goedecke JH, Dave JA, Faulenbach MV, Utzschneider KM, Lambert EV, West S, et al. Insulin response in relation to insulin sensitivity: an appropriate beta-cell response in black South African women. *Diabetes Care*. 2009;32(5):860-5.
253. Mari A, Pacini G, Murphy E, Ludvik B, Nolan JJ. A Model-Based Method for Assessing Insulin Sensitivity From the Oral Glucose Tolerance Test. *Diabetes Care*. 2001;24(3):539.
254. Bergman RN, Ader M, Huecking K, Van Citters G. Accurate assessment of beta-cell function: the hyperbolic correction. *Diabetes*. 2002;51 Suppl 1:S212-20.
255. Bergman RN, Phillips LS, Cobelli C. Physiologic evaluation of factors controlling glucose tolerance in man: measurement of insulin sensitivity and beta-cell glucose sensitivity from the response to intravenous glucose. *J Clin Invest*. 1981;68(6):1456-67.
256. Santos JL, Yevenes I, Cataldo LR, Morales M, Galgani J, Arancibia C, et al. Development and assessment of the disposition index based on the oral glucose tolerance test in subjects with different glycaemic status. *Journal of physiology and biochemistry*. 2016;72(2):121-31.

257. Bacha F, Gungor N, Lee S, de las Heras J, Arslanian S. Indices of insulin secretion during a liquid mixed-meal test in obese youth with diabetes. *The Journal of pediatrics*. 2013;162(5):924-9.
258. Retnakaran R, Qi Y, Goran MI, Hamilton JK. Evaluation of proposed oral disposition index measures in relation to the actual disposition index. *Diabet Med*. 2009;26(12):1198-203.
259. Retnakaran R, Shen S, Hanley AJ, Vuksan V, Hamilton JK, Zinman B. Hyperbolic Relationship Between Insulin Secretion and Sensitivity on Oral Glucose Tolerance Test. *Obesity*. 2012;16(8):1901-7.
260. Kirpichnikov D, McFarlane SI, Sowers JR. Metformin: an update. *Annals of internal medicine*. 2002;137(1):25-33.
261. United Kingdom Prospective Diabetes Study 24: a 6-year, randomized, controlled trial comparing sulfonylurea, insulin, and metformin therapy in patients with newly diagnosed type 2 diabetes that could not be controlled with diet therapy. United Kingdom Prospective Diabetes Study Group. *Annals of internal medicine*. 1998;128(3):165-75.
262. Kooy A, de Jager J, Lehert P, Bets D, Wulffele MG, Donker AJ, et al. Long-term effects of metformin on metabolism and microvascular and macrovascular disease in patients with type 2 diabetes mellitus. *Arch Intern Med*. 2009;169(6):616-25.
263. Sikander A, Rana SV, Prasad KK. Role of serotonin in gastrointestinal motility and irritable bowel syndrome. *Clinica chimica acta; international journal of clinical chemistry*. 2009;403(1-2):47-55.
264. Camilleri M. Serotonin in the gastrointestinal tract. *Current opinion in endocrinology, diabetes, and obesity*. 2009;16(1):53-9.
265. Deiteren A, De Man JG, Pelckmans PA, De Winter BY. Histamine H(4) receptors in the gastrointestinal tract. *British journal of pharmacology*. 2015;172(5):1165-78.
266. Chiang JY. Bile acid metabolism and signaling. *Comprehensive Physiology*. 2013;3(3):1191-212.
267. Takamine F, Imamura T. Isolation and characterization of bile acid 7-dehydroxylating bacteria from human feces. *Microbiology and immunology*. 1995;39(1):11-8.
268. Begley M, Gahan CG, Hill C. The interaction between bacteria and bile. *FEMS microbiology reviews*. 2005;29(4):625-51.
269. Scheen AJ, de Magalhaes AC, Salvatore T, Lefebvre PJ. Reduction of the acute bioavailability of metformin by the alpha-glucosidase inhibitor acarbose in normal man. *European journal of clinical investigation*. 1994;24 Suppl 3:50-4.
270. Jayasagar G, Krishna Kumar M, Chandrasekhar K, Madhusudan Rao C, Madhusudan Rao Y. Effect of cephalixin on the pharmacokinetics of metformin

in healthy human volunteers. *Drug metabolism and drug interactions*. 2002;19(1):41-8.

271. Somogyi A, Stockley C, Keal J, Rolan P, Bochner F. Reduction of metformin renal tubular secretion by cimetidine in man. *British journal of clinical pharmacology*. 1987;23(5):545-51.

272. Song IH, Zong J, Borland J, Jerva F, Wynne B, Zamek-Gliszczynski MJ, et al. The Effect of Dolutegravir on the Pharmacokinetics of Metformin in Healthy Subjects. *Journal of acquired immune deficiency syndromes (1999)*. 2016;72(4):400-7.

273. Kusuhara H, Ito S, Kumagai Y, Jiang M, Shiroshita T, Moriyama Y, et al. Effects of a MATE protein inhibitor, pyrimethamine, on the renal elimination of metformin at oral microdose and at therapeutic dose in healthy subjects. *Clin Pharmacol Ther*. 2011;89(6):837-44.

274. Zack J, Berg J, Juan A, Pannacciulli N, Allard M, Gottwald M, et al. Pharmacokinetic drug-drug interaction study of ranolazine and metformin in subjects with type 2 diabetes mellitus. *Clinical pharmacology in drug development*. 2015;4(2):121-9.

275. Muller F, Pontones CA, Renner B, Mieth M, Hoier E, Auge D, et al. N(1)-methylnicotinamide as an endogenous probe for drug interactions by renal cation transporters: studies on the metformin-trimethoprim interaction. *Eur J Clin Pharmacol*. 2015;71(1):85-94.

276. Johansson S, Read J, Oliver S, Steinberg M, Li Y, Lisbon E, et al. Pharmacokinetic evaluations of the co-administrations of vandetanib and metformin, digoxin, midazolam, omeprazole or ranitidine. *Clinical pharmacokinetics*. 2014;53(9):837-47.

277. Najib N, Idkaidek N, Beshtawi M, Bader M, Admour I, Alam SM, et al. Bioequivalence evaluation of two brands of metformin 500 mg tablets (Dialon & Glucophage)--in healthy human volunteers. *Biopharmaceutics & drug disposition*. 2002;23(7):301-6.

278. Robert F, Fendri S, Hary L, Lacroix C, Andrejak M, Lalau JD. Kinetics of plasma and erythrocyte metformin after acute administration in healthy subjects. *Diabetes Metab*. 2003;29(3):279-83.

279. Woerle HJ, Meyer C, Dostou JM, Gosmanov NR, Islam N, Popa E, et al. Pathways for glucose disposal after meal ingestion in humans. *American journal of physiology Endocrinology and metabolism*. 2003;284(4):E716-25.

280. Koepsell H. Role of organic cation transporters in drug-drug interaction. *Expert opinion on drug metabolism & toxicology*. 2015;11(10):1619-33.

281. Shu Y, Sheardown SA, Brown C, Owen RP, Zhang S, Castro RA, et al. Effect of genetic variation in the organic cation transporter 1 (OCT1) on metformin action. *J Clin Invest*. 2007;117(5):1422-31.

282. Shikata E, Yamamoto R, Takane H, Shigemasa C, Ikeda T, Otsubo K, et al. Human organic cation transporter (OCT1 and OCT2) gene polymorphisms and therapeutic effects of metformin. *J Hum Genet.* 2007;52(2):117-22.
283. Koepsell H, Lips K, Volk C. Polyspecific organic cation transporters: structure, function, physiological roles, and biopharmaceutical implications. *Pharm Res.* 2007;24(7):1227-51.
284. Kim A, Chung I, Yoon SH, Yu KS, Lim KS, Cho JY, et al. Effects of proton pump inhibitors on metformin pharmacokinetics and pharmacodynamics. *Drug Metab Dispos.* 2014;42(7):1174-9.
285. Nies AT, Hofmann U, Resch C, Schaeffeler E, Rius M, Schwab M. Proton pump inhibitors inhibit metformin uptake by organic cation transporters (OCTs). *PLoS One.* 2011;6(7):e22163.
286. Oefelein MG, Tong W, Kerr S, Bhasi K, Patel RK, Yu D. Effect of concomitant administration of trospium chloride extended release on the steady-state pharmacokinetics of metformin in healthy adults. *Clinical drug investigation.* 2013;33(2):123-31.
287. Cho SK, Yoon JS, Lee MG, Lee DH, Lim LA, Park K, et al. Rifampin enhances the glucose-lowering effect of metformin and increases OCT1 mRNA levels in healthy participants. *Clin Pharmacol Ther.* 2011;89(3):416-21.
288. Cho SK, Kim CO, Park ES, Chung JY. Verapamil decreases the glucose-lowering effect of metformin in healthy volunteers. *British journal of clinical pharmacology.* 2014;78(6):1426-32.
289. Kwon M, Choi YA, Choi MK, Song IS. Organic cation transporter-mediated drug-drug interaction potential between berberine and metformin. *Archives of pharmacal research.* 2015;38(5):849-56.
290. Li L, Song F, Tu M, Wang K, Zhao L, Wu X, et al. In vitro interaction of clopidogrel and its hydrolysate with OCT1, OCT2 and OAT1. *International journal of pharmaceutics.* 2014;465(1-2):5-10.
291. Bachmakov I, Glaeser H, Fromm MF, König J. Interaction of oral antidiabetic drugs with hepatic uptake transporters: focus on organic anion transporting polypeptides and organic cation transporter 1. *Diabetes.* 2008;57(6):1463-9.
292. Minematsu T, Giacomini KM. Interactions of tyrosine kinase inhibitors with organic cation transporters and multidrug and toxic compound extrusion proteins. *Molecular cancer therapeutics.* 2011;10(3):531-9.
293. Leabman MK, Huang CC, DeYoung J, Carlson EJ, Taylor TR, de la Cruz M, et al. Natural variation in human membrane transporter genes reveals evolutionary and functional constraints. *Proc Natl Acad Sci U S A.* 2003;100(10):5896-901.

294. Seitz T, Stalmann R, Dalila N, Chen J, Pojar S, Dos Santos Pereira JN, et al. Global genetic analyses reveal strong inter-ethnic variability in the loss of activity of the organic cation transporter OCT1. *Genome medicine*. 2015;7(1):56.
295. Mofo Mato EP, Guewo-Fokeng M, Essop MF, Owira PMO. Genetic polymorphisms of organic cation transporter 1 (OCT1) and responses to metformin therapy in individuals with type 2 diabetes: A systematic review. *Medicine*. 2018;97(27):e11349.
296. Shu Y, Leabman MK, Feng B, Mangravite LM, Huang CC, Stryke D, et al. Evolutionary conservation predicts function of variants of the human organic cation transporter, OCT1. *Proc Natl Acad Sci U S A*. 2003;100(10):5902-7.
297. Becker ML, Visser LE, van Schaik RH, Hofman A, Uitterlinden AG, Stricker BH. Genetic variation in the organic cation transporter 1 is associated with metformin response in patients with diabetes mellitus. *The pharmacogenomics journal*. 2009;9(4):242-7.
298. Dujic T, Causevic A, Bego T, Malenica M, Velija-Asimi Z, Pearson ER, et al. Organic cation transporter 1 variants and gastrointestinal side effects of metformin in patients with Type 2 diabetes. *Diabet Med*. 2016;33(4):511-4.
299. Francis CY, Morris J, Whorwell PJ. The irritable bowel severity scoring system: a simple method of monitoring irritable bowel syndrome and its progress. *Alimentary pharmacology & therapeutics*. 1997;11(2):395-402.
300. Rabeneck L. Measuring dyspepsia-related health in randomized trials: the Severity of Dyspepsia Assessment (SODA) and its use in treatment with NSAIDs and COX-2-specific inhibitors. *Rheumatology (Oxford, England)*. 2003;42 Suppl 3:iii32-9.
301. Christensen RHB. Regression Models for Ordinal Data CRAN2018 [updated 25/08/2018. Available from: <https://cran.r-project.org/web/packages/ordinal/ordinal.pdf>.
302. Liang X, Yee SW, Chien H-C, Chen EC, Luo Q, Zou L, et al. Organic cation transporter 1 (OCT1) modulates multiple cardiometabolic traits through effects on hepatic thiamine content. *PLoS biology*. 2018;16(4):e2002907-e.
303. Boyko EJ. Observational Research Opportunities and Limitations. *Journal of diabetes and its complications*. 2013;27(6):10.1016/j.jdiacomp.2013.07.007.
304. van Leeuwen N, Nijpels G, Becker ML, Deshmukh H, Zhou K, Stricker BH, et al. A gene variant near ATM is significantly associated with metformin treatment response in type 2 diabetes: a replication and meta-analysis of five cohorts. *Diabetologia*. 2012;55(7):1971-7.
305. Gatti RA, Berkel I, Boder E, Braedt G, Charmley P, Concannon P, et al. Localization of an ataxia-telangiectasia gene to chromosome 11q22-23. *Nature*. 1988;336(6199):577-80.

306. Ditch S, Paull TT. The ATM protein kinase and cellular redox signaling: beyond the DNA damage response. *Trends in biochemical sciences*. 2012;37(1):15-22.
307. Sun Y, Connors KE, Yang DQ. AICAR induces phosphorylation of AMPK in an ATM-dependent, LKB1-independent manner. *Molecular and cellular biochemistry*. 2007;306(1-2):239-45.
308. Spears LD, Qin C, Zhang Z, Ralston L, Fisher JS. The ATM activator chloroquine stimulates phosphorylation of AMP activated protein kinase (AMPK) and acetyl CoA-carboxylase (ACC) independent of ATM. *The FASEB Journal*. 2010;24(1_supplement):lb674-lb.
309. Shaw RJ, Lamia KA, Vasquez D, Koo SH, Bardeesy N, Depinho RA, et al. The kinase LKB1 mediates glucose homeostasis in liver and therapeutic effects of metformin. *Science*. 2005;310(5754):1642-6.
310. Shackelford DB, Shaw RJ. The LKB1-AMPK pathway: metabolism and growth control in tumour suppression. *Nature reviews Cancer*. 2009;9(8):563-75.
311. Suzuki A, Kusakai G, Kishimoto A, Shimojo Y, Ogura T, Lavin MF, et al. IGF-1 phosphorylates AMPK-alpha subunit in ATM-dependent and LKB1-independent manner. *Biochem Biophys Res Commun*. 2004;324(3):986-92.
312. Ambrose M, Goldstine JV, Gatti RA. Intrinsic mitochondrial dysfunction in ATM-deficient lymphoblastoid cells. *Human molecular genetics*. 2007;16(18):2154-64.
313. Yang D-Q, Kastan MB. Participation of ATM in insulin signalling through phosphorylation of eIF-4E-binding protein 1. *Nature Cell Biology*. 2000;2:893.
314. Armata HL, Golebiowski D, Jung DY, Ko HJ, Kim JK, Sluss HK. Requirement of the ATM/p53 tumor suppressor pathway for glucose homeostasis. *Molecular and cellular biology*. 2010;30(24):5787-94.
315. Schneider JG, Finck BN, Ren J, Standley KN, Takagi M, Maclean KH, et al. ATM-dependent suppression of stress signaling reduces vascular disease in metabolic syndrome. *Cell Metab*. 2006;4(5):377-89.
316. Miles PD, Treuner K, Latronica M, Olefsky JM, Barlow C. Impaired insulin secretion in a mouse model of ataxia telangiectasia. *American journal of physiology Endocrinology and metabolism*. 2007;293(1):E70-4.
317. Sun XJ, Wang L-M, Zhang Y, Yenush L, Myers Jr MG, Glasheen E, et al. Role of IRS-2 in insulin and cytokine signalling. *Nature*. 1995;377:173.
318. Viniestra JG, Martínez N, Modirassari P, Losa JH, Cobo CP, Lobo VJS-A, et al. Full Activation of PKB/Akt in Response to Insulin or Ionizing Radiation Is Mediated through ATM. *Journal of Biological Chemistry*. 2005;280(6):4029-36.
319. Halaby MJ, Hibma JC, He J, Yang DQ. ATM protein kinase mediates full activation of Akt and regulates glucose transporter 4 translocation by insulin in muscle cells. *Cellular signalling*. 2008;20(8):1555-63.

320. Zisman A, Peroni OD, Abel ED, Michael MD, Mauvais-Jarvis F, Lowell BB, et al. Targeted disruption of the glucose transporter 4 selectively in muscle causes insulin resistance and glucose intolerance. *Nat Med*. 2000;6(8):924-8.
321. Medicine NUSNLo. Ataxia-telangiectasia: NIH; 2018 [updated 7/11/18. Available from: <https://ghr.nlm.nih.gov/condition/ataxia-telangiectasia>
322. Mavrou A, Tsangaris GT, Roma E, Kolialexi A. The ATM gene and ataxia telangiectasia. *Anticancer research*. 2008;28(1b):401-5.
323. Teive HA, Moro A, Moscovich M, Arruda WO, Munhoz RP, Raskin S, et al. Ataxia-telangiectasia - A historical review and a proposal for a new designation: ATM syndrome. *J Neurol Sci*. 2015;355(1-2):3-6.
324. Thompson D, Duedal S, Kirner J, McGuffog L, Last J, Reiman A, et al. Cancer risks and mortality in heterozygous ATM mutation carriers. *Journal of the National Cancer Institute*. 2005;97(11):813-22.
325. van Os NJ, Roeleveld N, Weemaes CM, Jongmans MC, Janssens GO, Taylor AM, et al. Health risks for ataxia-telangiectasia mutated heterozygotes: a systematic review, meta-analysis and evidence-based guideline. *Clinical genetics*. 2016;90(2):105-17.
326. Stewart GS, Last JI, Stankovic T, Haites N, Kidd AM, Byrd PJ, et al. Residual ataxia telangiectasia mutated protein function in cells from ataxia telangiectasia patients, with 5762ins137 and 7271T-->G mutations, showing a less severe phenotype. *J Biol Chem*. 2001;276(32):30133-41.
327. Verhagen MM, Last JI, Hogervorst FB, Smeets DF, Roeleveld N, Verheijen F, et al. Presence of ATM protein and residual kinase activity correlates with the phenotype in ataxia-telangiectasia: a genotype-phenotype study. *Human mutation*. 2012;33(3):561-71.
328. Schalch DS, McFarlin DE, Barlow MH. An unusual form of diabetes mellitus in ataxia telangiectasia. *The New England journal of medicine*. 1970;282(25):1396-402.
329. Bar RS, Levis WR, Rechler MM, Harrison LC, Siebert C, Podskalny J, et al. Extreme Insulin Resistance in Ataxia Telangiectasia. *New England Journal of Medicine*. 1978;298(21):1164-71.
330. Connelly PJ, Smith N, Chadwick R, Exley AR, Shneerson JM, Pearson ER. Recessive mutations in the cancer gene Ataxia Telangiectasia Mutated (ATM), at a locus previously associated with metformin response, cause dysglycaemia and insulin resistance. *Diabet Med*. 2016;33(3):371-5.
331. Matsuzawa Y. The metabolic syndrome and adipocytokines. *FEBS Letters*. 2006;580(12):2917-21.
332. Yadav A, Kataria MA, Saini V, Yadav A. Role of leptin and adiponectin in insulin resistance. *Clinica chimica acta; international journal of clinical chemistry*. 2013;417:80-4.

333. Farooqi IS, Matarese G, Lord GM, Keogh JM, Lawrence E, Agwu C, et al. Beneficial effects of leptin on obesity, T cell hyporesponsiveness, and neuroendocrine/metabolic dysfunction of human congenital leptin deficiency. *The Journal of Clinical Investigation*. 2002;110(8):1093-103.
334. Hulin B, McCarthy PA, Michael Gibbs E. The glitazone family of antidiabetic agents 1996. 85-102 p.
335. Miller JL. FDA approves pioglitazone for diabetes. *American journal of health-system pharmacy : AJHP : official journal of the American Society of Health-System Pharmacists*. 1999;56(17):1698.
336. Pioglitazone and rosiglitazone for diabetes. *Drug and therapeutics bulletin*. 2001;39(9):65-8.
337. Miller JL. Rosiglitazone approved for treatment of type 2 diabetes. *American journal of health-system pharmacy : AJHP : official journal of the American Society of Health-System Pharmacists*. 1999;56(13):1292, 4.
338. Lee YH, Kim JH, Kim SR, Jin HY, Rhee EJ, Cho YM, et al. Lobeglitazone, a Novel Thiazolidinedione, Improves Non-Alcoholic Fatty Liver Disease in Type 2 Diabetes: Its Efficacy and Predictive Factors Related to Responsiveness. *Journal of Korean medical science*. 2017;32(1):60-9.
339. Cohen D. European regulatory body recommends suspension of rosiglitazone. *BMJ (Clinical research ed)*. 2010;341:c5291.
340. NICE. Pioglitazone: BNF; 2018 [Available from: <https://bnf.nice.org.uk/drug/pioglitazone.html#indicationsAndDoses>].
341. Belfort R, Harrison SA, Brown K, Darland C, Finch J, Hardies J, et al. A Placebo-Controlled Trial of Pioglitazone in Subjects with Nonalcoholic Steatohepatitis. *New England Journal of Medicine*. 2006;355(22):2297-307.
342. Iogna Prat L, Tsochatzis EA. The effect of antidiabetic medications on non-alcoholic fatty liver disease (NAFLD). *Hormones (Athens, Greece)*. 2018;17(2):219-29.
343. Singh S, Loke YK, Furberg CD. Long-term use of thiazolidinediones and the associated risk of pneumonia or lower respiratory tract infection: systematic review and meta-analysis. *Thorax*. 2011;66(5):383-8.
344. Wood JC, Enriquez C, Ghugre N, Tyzka JM, Carson S, Nelson MD, et al. MRI R2 and R2* mapping accurately estimates hepatic iron concentration in transfusion-dependent thalassemia and sickle cell disease patients. *Blood*. 2005;106(4):1460-5.
345. Hundal RS, Krssak M, Dufour S, Laurent D, Lebon V, Chandramouli V, et al. Mechanism by which metformin reduces glucose production in type 2 diabetes. *Diabetes*. 2000;49(12):2063-9.
346. Mari A, Ahren B, Pacini G. Assessment of insulin secretion in relation to insulin resistance. *Current opinion in clinical nutrition and metabolic care*. 2005;8(5):529-33.

347. Tura A, Muscelli E, Gastaldelli A, Ferrannini E, Mari A. Altered pattern of the incretin effect as assessed by modelling in individuals with glucose tolerance ranging from normal to diabetic. *Diabetologia*. 2014;57(6):1199-203.
348. Cnop M, Havel PJ, Utzschneider KM, Carr DB, Sinha MK, Boyko EJ, et al. Relationship of adiponectin to body fat distribution, insulin sensitivity and plasma lipoproteins: evidence for independent roles of age and sex. *Diabetologia*. 2003;46(4):459-69.
349. Stich V, Berlan M. Physiological regulation of NEFA availability: lipolysis pathway. *The Proceedings of the Nutrition Society*. 2004;63(2):369-74.
350. McIntyre HD, Ma A, Bird DM, Paterson CA, Ravenscroft PJ, Cameron DP. Metformin increases insulin sensitivity and basal glucose clearance in type 2 (non-insulin dependent) diabetes mellitus. *Australian and New Zealand journal of medicine*. 1991;21(5):714-9.
351. Ole H-N, Ole S, Per HA, Henning B-N, Oluf P. Metformin improves peripheral but not hepatic insulin action in obese patients with type II diabetes. *Acta Endocrinologica*. 1989;120(3):257-65.
352. Zarrinpar A, Chaix A, Xu ZZ, Chang MW, Marotz CA, Saghatelian A, et al. Antibiotic-induced microbiome depletion alters metabolic homeostasis by affecting gut signaling and colonic metabolism. *Nature communications*. 2018;9(1):2872.
353. Koffert JP, Mikkola K, Virtanen KA, Andersson A-MD, Faxius L, Hällsten K, et al. Metformin treatment significantly enhances intestinal glucose uptake in patients with type 2 diabetes: Results from a randomized clinical trial. *Diabetes Research and Clinical Practice*. 2017;131:208-16.
354. Christensen MM, Hojlund K, Hother-Nielsen O, Stage TB, Damkier P, Beck-Nielsen H, et al. Endogenous glucose production increases in response to metformin treatment in the glycogen-depleted state in humans: a randomised trial. *Diabetologia*. 2015;58(11):2494-502.
355. Gastaldelli A, Harrison S, Belfort-Aguiar R, Hardies J, Balas B, Schenker S, et al. Pioglitazone in the treatment of NASH: the role of adiponectin. *Alimentary pharmacology & therapeutics*. 2010;32(6):769-75.
356. Lihn AS, Pedersen SB, Richelsen B. Adiponectin: action, regulation and association to insulin sensitivity. *Obesity reviews : an official journal of the International Association for the Study of Obesity*. 2005;6(1):13-21.
357. Blumer RM, van Roomen CP, Meijer AJ, Houben-Weerts JH, Sauerwein HP, Dubbelhuis PF. Regulation of adiponectin secretion by insulin and amino acids in 3T3-L1 adipocytes. *Metabolism*. 2008;57(12):1655-62.
358. Guo M, Li C, Lei Y, Xu S, Zhao D, Lu XY. Role of the adipose PPARgamma-adiponectin axis in susceptibility to stress and depression/anxiety-related behaviors. *Molecular psychiatry*. 2017;22(7):1056-68.

359. Ikeda Y, Takata H, Inoue K, Shinahara M, Inada S, Maruyama H, et al. Pioglitazone Rapidly Increases Serum Adiponectin Levels in Men With Normal Glucose Tolerance. *Diabetes Care*. 2007;30(6):e48.
360. Polyzos SA, Mantzoros CS. Adiponectin as a target for the treatment of nonalcoholic steatohepatitis with thiazolidinediones: A systematic review. *Metabolism - Clinical and Experimental*. 2016;65(9):1297-306.
361. Zeigerer A, Rodeheffer MS, McGraw TE, Friedman JM. Insulin regulates leptin secretion from 3T3-L1 adipocytes by a PI 3 kinase independent mechanism. *Experimental cell research*. 2008;314(11-12):2249-56.
362. Tsai M, Asakawa A, Amitani H, Inui A. Stimulation of leptin secretion by insulin. *Indian journal of endocrinology and metabolism*. 2012;16(Suppl 3):S543-S8.
363. Zukunft S, Sorgenfrei M, Prehn C, Möller G, Adamski J. Targeted Metabolomics of Dried Blood Spot Extracts. *Chromatographia*. 2013;76(19):1295-305.
364. Pham HT, Arnhard K, Asad YJ, Deng L, Felder TK, St. John-Williams L, et al. Inter-Laboratory Robustness of Next-Generation Bile Acid Study in Mice and Humans: International Ring Trial Involving 12 Laboratories. *The Journal of Applied Laboratory Medicine: An AACC Publication*. 2016.
365. (CHMP) CfMPfHU. Guideline on bioanalytical method validation. European Medicines Agency; 2011.